Louvain Drug Research Institute

Pharmaceutics and Drug Delivery

TARGETING OF SMALL OR BIOPHARMACEUTICAL ANTI-INFLAMMATORY DRUGS TO INFLAMMATORY BOWEL DISEASES BY NANOCARRIERS

Régis COCO

Thèse présentée en vue de l'obtention du grade de
Docteur en Sciences Biomédicales et Pharmaceutiques

Promoteur : Véronique Préat

2013

ACKNOWLEDGEMENTS

Au terme de ce doctorat, je tiens à remercier l'ensemble des personnes ayant, de près ou de loin, participer à l'élaboration et la finalisation de ce projet.

J'aimerais d'abord remercier le Professeur Véronique Préat pour m'avoir accueilli au sein de son laboratoire et supervisé pendant quatre ans, me permettant ainsi de réaliser cette thèse. Je la remercie aussi personnellement pour la flexibilité et le suivi dont elle a fait preuve durant la période suivant ma fracture et mon rééducation.

Je voudrais remercier les professeurs Yves-jacques Schneider et Patrice Cani, membres du jury, pour leurs précieux conseils. Leurs conseils ont été précieux dans l'élaboration d'expériences primordiales. I would like to thanks Pr. David Brayden, committee member also, to allow me to learn new techniques in his laboratory. Je remercie les Professeurs Nathalie Delzenne, Marie-Paule Mingeot, Brigitte Evrard et Philippe Maincent, d'avoir accepté de faire partie de mon jury de thèse. Merci pour les discussions et remarques qui ont permis d'enrichir ce travail.

Je tiens bien sur à remercier l'équipe de Pharmaceutics & Drug Delivery Unit. Merci pour l'ambiance à la fois studieuse et conviviale qui a régné dans ce laboratoire. En particulier, je voudrais remercier Nicolas, un collègue devenu au fil de ce doctorat un frère, pour m'avoir soutenu et aidé durant cette formation doctorale mais aussi durant le MCC en Gestion de la Solvay Business School; Bernard pour son aide immesurable, sa bonne humeur permanente et pour m'avoir fait découvrir le squash; Patrick et Kiran pour les réunions au sommet du "Pole Curcumin" qui ont été à l'origine de 2 articles dans JCR; mes collègues de bureau Héloïse et Gaëlle pour leur bonne humeur, la bonne ambiance qu'elles ont mis dans le bureau ainsi que pour la permanente aide scientifique; Salomé, Julie et Nathalie L. pour la franche camaraderie et leur aide à différentes étapes du doctorat. A special thanks goes to Ana « Speedy » Beloqui. Working with her was a great and major event in my PhD. Merci aussi à Murielle pour sa bonne humeur, la mise en page de ma thèse et surtout pour les "cahiers de labo". Je tiens vivement aussi à remercier Mireille AlHouayek et le Pr. Giulio Muccioli pour m'avoir appris des techniques de 1ère ordre. Je voudrais aussi remercier le Pr. Poupaert pour m'avoir fait découvrir le monde des nanomédicaments.

Je tiens particulièrement à remercier ces amis rencontrés en Belgique c'est-à-dire Gilles, Benoit, Maité, Cédric-Antoine, Alex, Eric, Clémence, Cyrielle et Djibril ainsi que tous les autres qui ont toujours cru en moi et m'ont soutenu depuis mon arrivée et spécialement

durant ce doctorat (ils sont nombreux et j'en oublie surement beaucoup!). Je remercie aussi Florence et Aicha ainsi que leurs familles respectives pour le soutien durant ces quatre dernières années.

Finalement, je ne serais jamais arrivé à ce stade sans ma famille. Mes parents, ma petite soeur Priscilia, mon grand-père Marcellin, ma tante Evelyne, ma marraine Gutane ainsi que le reste de ma famille m'ont donné la force de tenir tous les jours et m'ont insufflé ambition, abnégation et rigueur. Tchimbé rèd pa moli sé moli la ki rèd! Je remercie aussi mon oncle Guy pour le temps passé à relire mon introduction de thèse.

Je tiens tout particulièrement à dédier cette thèse à une personne qui, à ne pas douter, aurait été fier de son petit fils aujourd'hui, ma mamie Cornélie. Merci d'avoir fait de moi l'homme que je suis à présent. Mon dernier remerciement va à mon île, la Guadeloupe.

ABBREVIATIONS

5-ASA	5-aminosalicylic acid
BDS	Budesonide
CC	Curcumin
CD	Crohn's disease
DSS	Dextran sodium sulfate
ES100	Eudragit S 100
Fab	Fragment antibody
GIT	Gastro-intestinal tract
IBD	Inflammatory bowel disease
IgG	Immunoglobulin G
IL	Interleukin
IFN-γ	Interferon gamma
LPS	Lipopolysaccharide
Man	Mannose
MDP	Muramyl dipeptide
MPO	Myeloperoxidase activity
NF-κB	Nuclear factor kappa B
NK	Natural killer cells
NLC	Nanostructured lipid carriers
NOD2	Nucleotide binding oligomerization domain protein 2
NPs	Polymeric nanoparticles
OVA	Ovalbumin
PBS	Phosphate buffer saline
PCL	Poly-ε-caprolactone
PdI	Polydispersity Index
PEG	Polyethyleneglycol
PLA	Poly(lactic acid)
PLGA	Poly(lactic-co-glycolic) acid
RES	Reticulo-endothelial system
ROS	Reactive oxygen species
SLN	Solid lipid nanoparticles
SNEDDS	Self-(nano)emulsifying drug delivery systems
TEER	Transepithelial electric resistance
TLR	Toll-like receptors
TMC	N,N,N-trimethylchitosan chloride

TPP	Tripolyphosphate
TNF-α	Tumor necrosis factor alpha
UC	Ulcerative colitis

FOREWORD

Inflammatory bowel diseases are relapsing and chronic inflammatory disorders of the gut. Although most of the conventional anti-inflammatory agents can be administered orally, non-specific delivery of these drugs is observed, leading to systemic toxicity associated with serious adverse effects. The development of drug delivery systems able to specifically target and to deliver anti-inflammatory drugs to inflamed colonic areas of the colon is of great interest. It should lead to higher local concentrations and maintain therapeutic efficacy while enhancing safety by decreasing non-specific delivery. Use of nanocarriers for this purpose seems promising as they showed a preferential uptake in inflamed areas.

Hence, the aim of this thesis was to encapsulate small drugs (budesonide and curcumin) and biopharmaceutics (ovalbumin as model drug and anti-TNF-α fragment antibody) in various nanocarriers: polymeric nanoparticles, nano-structured lipid carriers and self-nanoemulsifying drug delivery systems. Various delivery strategies were assessed: pH-sensitivity, mucoadhesion, sustained release, active targeting and lipid-based delivery. The potential of these nanoparticulate drug delivery systems for inflamed colon-specific topical targeting and delivery was evaluated in in vitro, ex vivo and in vivo models.

Firstly, we have demonstrated the efficacy of nanostructured lipid carriers for the topical delivery of budesonide in inflamed colon using. Secondly, we compared the topical delivery of curcumin, showing that a nanoscale delivery strategy using pH-sensitive and sustained release nanoparticles gives better in vivo results than the other nanoscale delivery strategy using self-nanoemulsifying drug delivery systems. Thirdly, using ovalbumin as model drug, we have compared several strategies to target the inflamed colon using polymeric nanoparticles as biopharmaceutical drug carrier. Exploiting the ability of design of polymeric nanoparticles, we have demonstrated that active targeting of macrophages and dendritic cells leads to a preferential accumulation in inflamed areas. Finally, we formulated 2 types of polymeric nanoparticles encapsulating an active biopharmaceutical agent possessing features suitable for the inflamed colon delivery.

TABLE OF CONTENTS

CHAPTER I. INTRODUCTION 1

CHAPTER II. AIM OF THE THESIS 87

CHAPTER III. BUDESONIDE-LOADED NLC REDUCE INFLAMMATION IN MURINE COLITIS..... 91

CHAPTER IV. DESIGN OF CURCUMIN-LOADED NANOCARRIERS FOR THE TREATMENT OF INFLAMMATORY BOWEL DISEASE 119

CHAPTER V. PROTEIN DELIVERY TO INFLAMED COLON BY NANOPARTICLES..... 151

CHAPTER VI. DESIGN OF ANTI-TNF-α FAB LOADED NANOPARTICLES FOR IBD TREATMENT.. 181

CHAPTER VII. DISCUSSION AND PERSPECTIVES 195

CHAPTER I.

Introduction

TABLE OF CONTENTS

I. INFLAMMATORY BOWEL DISEASES 5

I.1 Epidemiology 5

I.1.1 Descriptive Epidemiology 5

I.1.2 Analytic Epidemiology 7

I.2 Etiology 8

I.2.1 Genetic susceptibility 9

I.2.2 Luminal microbial antigens and adjuvants 11

I.2.3 Mucosal Immune Response 13

I.3 Physiopathology 16

I.3.1 Crohn's Disease 17

I.3.2 Ulcerative colitis 19

I.3.3 Complications associated with IBD 19

I.4 Conventional IBD therapy 20

I.4.1 Aim 20

I.4.2 Management of CD 21

I.4.3 Management of UC 23

I.4.4 Corticosteroids 24

I.4.5 Biopharmaceutics 25

I.4.6 Curcumin 28

II. NANOMEDICINES FOR TOPICAL IBD TREATMENT 30

II.1 Generalities on topical IBD treatment with nanocarriers 31

II.1.1 Achieving a topical delivery in IBD-inflamed colonic mucosa: The state-of-the-art 31

II.1.2 Models of IBD 36

II.1.3 The purpose of nanocarriers for IBD treatment 42

II.1.4 Nano-sized delivery strategies for IBD treatment 43

II.1.5 The perfect nanocarrier for IBD 48

II.1.6 IBD drugs in nanoformulations 49

II.2 Polymeric nanocarriers of interest 52

II.2.1 Eudragit®: A pH-sensitive polymer 53

II.2.2 PLGA: From the sustained release to the active targeting 58

II.2.3 Trimethylchitosan: A mucoadhesive polymer 63

II.3 Lipid-based nanocarriers of interest 70

II.3.1 Self-nanoemulsifying drug delivery systems 70

II.3.2 Nano-structured Lipid Carriers (NLC) 71

III. REFERENCES 73

I. INFLAMMATORY BOWEL DISEASES

Inflammatory bowel diseases (IBD) are relapsing and chronic inflammatory disorders of the gastro-intestinal mucosa with a tropism for the colon. Infection, ischemia or drug reactions can cause inflammation in the gut mucosa and constitute non-idiopathic inflammatory diseases. Idiopathic IBD group consists of Crohn's disease (CD) and Ulcerative Colitis (UC). They are commonly referred as IBD [1]. These chronic diseases start generally during the young adulthood, with a peak age of 20-30 years for CD and 30-40 years for UC [2]. IBD are characterized by a shift between periods of active disease (flares) and periods of little or no disease activity (remissions). As chronic diseases, idiopathic IBD are disabling, lead to significant health care costs and cause patients to suffer mainly from decrease in quality of life and capacity in work. They remain incurable even if their physiopathology is better understood and effective treatments have been developed.

I.1 EPIDEMIOLOGY

I.1.1 Descriptive Epidemiology

Table 1: External factors linked to IBD [3-5]

External Factors	Crohn's disease (CD)	Ulcerative Colitis (UC)
Westernization of the lifestyle behaviors	↗Northern America, Europe, Asia, Latin America, North Africa	↗Northern America, Europe, Asia, Latin America, North Africa
Ethnic origin	↗ Afro-American, Caucasian ↘ Hispanic; Asian	↗ Afro-American, Caucasian ↘ Hispanic; Asian
Migration of ethnic groups	↗: Afro-American, Caucasian	↗: Hispanic
Gender	↗: Women	↗: Men
Infancy	↗: Boy	↗: Girl
Smoking cigarettes	↗	↘
Appendectomy	↗	↘
Monozygotic twins concordance (%)	50	5-15

The descriptive epidemiology of IBD i.e. the variations of IBD incidence, the prevalence and demographic factors enable us to establish the profiles of these diseases providing us with data on etiology, typical patient and the geographical distribution of IBD diseases (Table 1). However, epidemiologic studies for IBD are difficult to process due to the fact that there is no

gold standard to diagnose them. Indeed, these diseases settle gradually and their differential diagnosis is wide. Furthermore, physicians may diagnose, verify and classify IBD differently depending on the geographical location, resulting in difficult comparison of studies.

IBD are part from the five most prevalent gastrointestinal diseases in the United States of America with a prevalence between 44 to 201/100,000, and 37.5 to 238/100,000, respectively for CD and UC [6]. Western countries including North American countries, the United Kingdom and Northern European countries present the highest incidence and prevalence rates of IBD. In Europe, the prevalence of CD and UC varies respectively from 1.5 to 213 cases per 100,000 persons and from 2.4 to 294 cases per 100,000 persons. An extrapolation made for the total European population indicates that there may be up to 1.6 million persons with CD and 2.1 million persons with UC, meaning a combined total of 3.7 million persons with IBD [7]. However, these rates are stabilizing in these countries whereas they are increasing in rapidly westernizing countries such as ones found in southern Europe, Asia, Latin America and North Africa, demonstrating the dynamics of the IBD diseases (Figure 1) [4]. By examining the geographical and temporal trends as well as the distribution patterns of IBD, high correlations with the industrialization of the countries and the attendant lifestyle and behaviors changes become apparent.

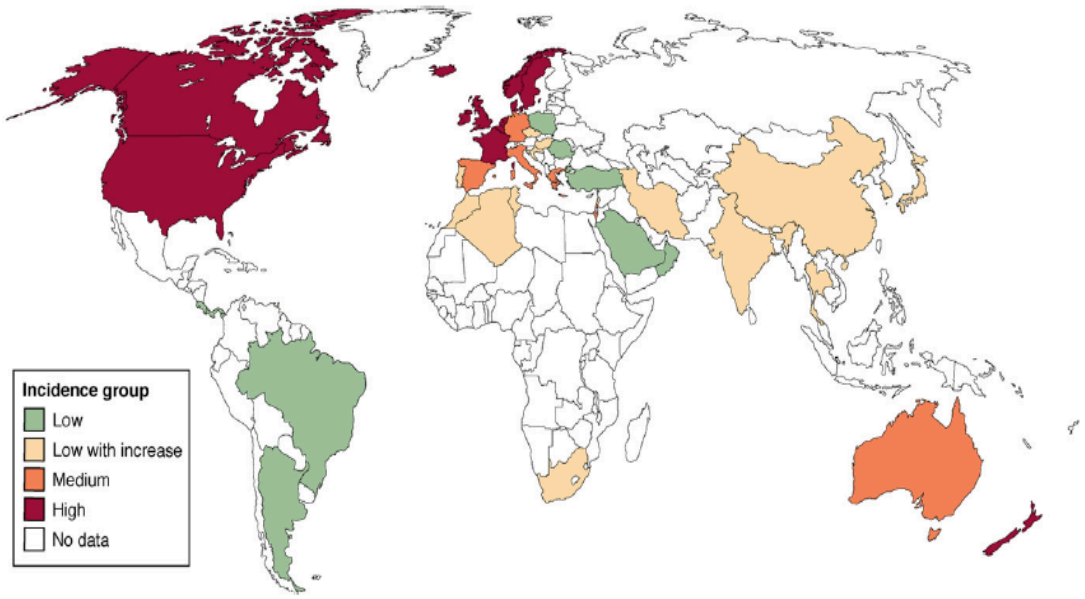


Figure 1: The global map of inflammatory bowel disease: *red* refers to annual incidence greater than $10/10^5$, *orange* to incidence of $5–10/10^5$, *green* to incidence less than $4/10^5$, *yellow* to low incidence that is continuously increasing. Absence of color indicates absence of data [2].

Furthermore, ethnic origin is a risk factor for IBD. African-American (29.8 per 100 000 person-years) and Caucasian population (43.6 per 100 000) present higher prevalence rates

of CD than Hispanic (4.1 per 100 000) and Asian individuals (5.6 per 100 000). UC is more frequently present in Hispanic population whereas African-American and Caucasian populations are diagnosed more frequently with CD [8]. The study of the correlation between IBD and migration of ethnic groups (eg, Chinese people living in Hong Kong compared with mainland China or Jewish people living in Israel compared with elsewhere) shows that genetic, environmental and lifestyle factors interact to determine risk for IBD [9].

Specific population-based evidence, such as variance of IBD occurrences in monozygotic twins, has highlighted that environmental and genetic factors are primordial in IBD pathogenesis, even if the association between them is not clearly elucidated (Table 1) [10, 11].

Gender is a risk factor in high-incidence areas. Indeed, CD occurs 20-30 % more frequently in women whereas there is a male tendency of predominance (60%) for UC [12]. Children are also affected by IBD and present a particular profile towards these diseases [13, 14]. Pediatric patients present a distribution of CD and UC for male and female opposite to that of adults [15]. The peak age of diagnosis is about 12 which implies an increased incidence around puberty [16].

I.1.2 Analytic Epidemiology

Even if UC and CD present similarities in their symptoms and their macroscopic similarities, analytic epidemiology showed that these diseases present behavioral differences concerning associated risk factors such as smoking and appendectomy. Others factors such as breastfeeding, childhood vaccinations, childhood infections, and dietary intake of fibers are more controversial [3, 17-19].

An unusual association has been put forward between smoking and IBD. Indeed, less frequent exacerbations of UC have been observed with smoking. It seems that nicotine, one of the main components of cigarettes, may modify favorably intestinal mucus production, cytokine synthesis, macrophage function and microvasculature. The mechanism of action is unclear but nicotine effect is strongly linked to a reduction of IL-8 mucosal level. However, nicotine should not to be considered as a therapy for UC as nicotine patches or enemas have failed to show efficacy in the management of UC. Furthermore, smoking may increase risks of neoplasia and vascular disease [20, 21]. Appendectomy has a protective role against UC because it leads to the suppression of a key site of activation of autoreactive T cells involved in colonic inflammation [22]. The association between oral contraceptives and

disease localization of UC to rectum/left-sided colon suggests a hypothetical prophylactic role of these drugs.

In contrast, CD presents opposite associations with these factors. Smoking increases the onset of CD [22]. It promotes the formation of fistulas and strictures and increases the rates of aggravations and the need for corticosteroids. It accelerates also the need for surgery after surgically induced remissions. These deleterious effects of smoking in CD are explained by the decrease of total radical-trapping antioxidant potential and abnormalities of the microvasculature. Smoking cessation should provide a better control of the disease activity in CD. Appendectomy has a damaging role in CD [23, 24].

I.2 ETIOLOGY

The now widely accepted etiology of inflammatory bowel diseases is that in genetically predisposed people, luminal antigens stimulate an inappropriate and aggressive immune response. Environmental triggers may activate or reactivate the inflammation. Even if various in vitro and in vivo experiments have been made in order to fully understand the etiology of IBD, it remains unclear. It seems though, that different initiating pathways may lead to the inflamed state of the gut (Figure 2). However, these initial events are not mutually exclusive but concomitant actions of some of them are likely to perpetuate the disease exacerbation [25-28].

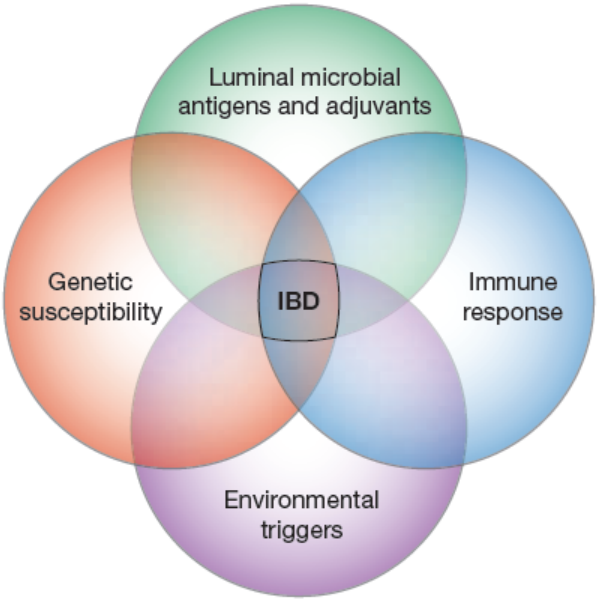


Figure 2: Multifactorial etiology of inflammatory bowel diseases. The four key factors of pathogenesis of IBD are: genetic susceptibility, commensal microflora, immune response and environmental triggers [27].

I.2.1 Genetic susceptibility

Genetic factors play a central role in pathogenesis of IBD. For instance, Ashkenazi Jews present an increased risk for IBD and there is a significant disease concordance in monozygotic twins, which is higher for CD than UC. Currently, more than 100 loci have been identified to contribute modestly to increase IBD risk of 1.5-fold and are associated with various pathophysiological and intestinal processes such as microbe recognition, lymphocyte activation, cytokine signaling, or intestinal epithelial defense [29, 30].

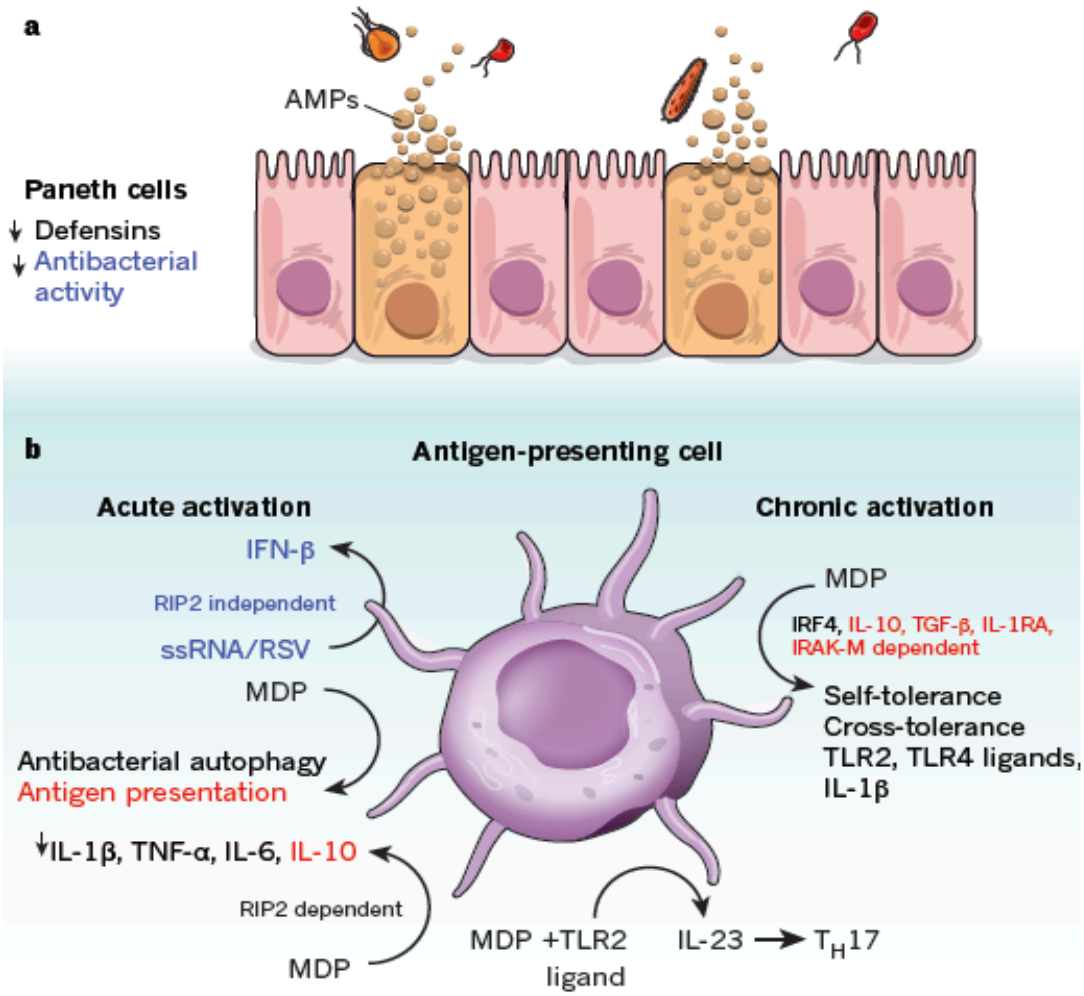


Figure 3: Cell-intrinsic functions of NOD2. NOD2 is activated by the bacterial peptidoglycan muramyl dipeptide (MDP), part of the antimicrobial peptides (AMPs) class. a. In Paneth cells, *Nod2* deficiency leads to attenuated antibacterial activity in the intestinal crypts and decreased expression of defensins. b. MDP-stimulated release of pro-inflammatory NF-κB-dependent cytokines (such as IL-1β, TNF-α and IL-6) is decreased in antigen-presenting cells from *Nod2*-deficient patients [29].

However, only nucleotide binding oligomerization domain protein 2 (NOD2) has been widely accepted and classified as a meaningful and specific susceptibility gene to CD (Figure 3) with a 17.1-fold increase in risk for homozygous or heterozygous carriage [29, 30]. Located in chromosome 15, NOD2 takes part in the bacterial recognition by the gut innate immune system, and its polymorphisms are also associated with epithelial defects leading to inappropriate cytokine activation. Intracellular NOD2 proteins are preferentially expressed in Paneth cells. These specialized epithelial cells, present in the small intestine, produce antimicrobial proteins, such as defensins, playing a key role in the gut innate immunity. NOD2 proteins can also be found in leukocytes, epithelial cells and fibroblasts. Their mutation results in an impaired regulatory activity due to a reduction in its ability to activate

nuclear factor κB (NF-κB) in response to muramyl dipeptide (MDP), a bacterial component. NOD2-defective patients present attenuated antibacterial activity in their intestinal crypts and decreased expression of defensins [25]. Thereby, they are more susceptible to develop CD early associated with stricturing and fistulating complications [31].

Intracellular homeostasis, consisting in the degradation and clearance of cytosolic components and organelles occurs in the cells by an intracellular processing called autophagy. Autophagy is involved in the resistance against infection and the removal of intracellular pathogens. Mutations with genes that regulate autophagy have also been found to be associated with pathogenesis of CD. ATG16L1, the autophagy gene, encodes for a peptidic component of the autophagy complex mainly found in the small intestinal Paneth cells. Its mutation was associated with a reduced activity in exocytosis of secretory granules that contain antimicrobial peptides. *Immunity-related GTPase M* and *Leucine-rich repeat kinase 2* related-genes were also found to be associated with CD. Autophagy seems to play a key role in CD due to the fact that microbial components deposit in successive layers in the thickness of the cellular walls of the intestinal epithelial cells, which present a high cellular turnover [26].

Mutations in genes that regulate IL-7 and IL-2 signaling, cytokines regulating T-cell survival and proliferation were associated with IBD. Defective pathways of lymphocyte activation were also found to be associated with extra-intestinal complications of IBD with polymorphisms in HLA class I and II genes [30]. At the opposite, mutations in the IL23R gene might protect against CD [25]. It seems that most of the genes involved in IBD pathogenesis are part of the interaction between bacteria and the immune system.

I.2.2 Luminal microbial antigens and adjuvants

Ileus terminal and colon, the most susceptible organs for IBD location, present the highest concentrations of bacteria (10^{11} to 10^{12} bacteria/g of material). IBD patients present higher bacterial number in their mucosa compared to healthy people, with a link between disease severity in the colon and mucosal concentrations of bacteria. And yet, it has been related that activation of IBD is more frequent after gastrointestinal infections. The paradigm of “no bacteria, no IBD” was based on several IBD animal models. Colitis did not develop in mice kept in germ-free environment as no luminal microbial antigens could activate the unbalanced immune response. IL-10 deficient mice present spontaneously colitis except under germ free conditions [25, 32].

Two hypotheses have been pushed forward to explain the causal and aggravating role of gut microbiota in IBD: the existence of a candidate pathogen microorganism and the role of dysbiosis in IBD, an imbalance between harmful and protective bacteria [32].

No bacteria species has been identified yet to be indispensable in the pathogenesis of IBD. Different types of bacteria species such as *Clostridium* and or *Mycobacterium paratuberculosis* have been investigated in order to find a candidate pathogen microorganism. Relevant data made on adherent-invasive *Escherichia coli* suggest that, in patients with CD, these bacteria would pass through the leaky intestinal barrier, infect the macrophages of the lamina propria and multiply inside of them, making them secrete high amounts of TNF-α. Adherent-invasive *Escherichia coli* induces also an overexpression of the CEACAM6 host receptor, which helps it to adhere to the brush border of the ileal enterocytes. The entire mechanism clearly represents a colonization/inflammation sequence in CD patients [33, 34]. Nevertheless, the debate remains unresolved and some authors think that there is more of an influence of endogenous bacteria than a specific pathogen in the pathophysiological process of IBD [28].

The diversity of gut microbiota has only recently been studied, due to the fact that 70% of gut microbiota was uncultivable, and that most of the techniques were based on bacterial culture [35]. With the recent possibility to study fecal and mucosa-associated microbiota, dysbiosis was investigated from patients with IBD, by comparing them to healthy subjects. Most of the studies were done in CD patients compared to UC patients and concluded for a restricted bacterial biodiversity and the presence of unusual bacteria. Bacterial biodiversity was found affected, quantitatively and qualitatively. Bacteria of *C. leptum* group such as *Faecalibacterium prausnitzii* and other bacteria considered “beneficial” as *Lactobacillus* and *Bifidobacteria* were decreased in fecal material of patients with CD. In particular, the experimental restitution of *Faecalibacterium prausnitzii* provided anti-inflammatory effects in CD [32]. Other bacteria were also found in reduced concentrations in feces of CD patients but data remain controversial [36-40]. Mucus-associated microbiota of CD patients shows higher bacterial concentrations than healthy patients. This result could be related to a lack of protection of the intestinal barrier particularly by the dysfunction of the antibacterial defensins, which could promote the bacterial colonization of the mucosa, leading to CD lesions. Reduction of *Firmicutes* and overrepresentation of *Enterobacteriaceae* confirmed the reduced biodiversity found in CD patients [32].

I.2.3 Mucosal Immune Response

Lipopolysaccharides, peptidoglycan, lipoteichoic acid, single-stranded RNA, double-stranded RNA, and methylated DNA are common luminal microbial components. Their recognition and processing into antigens begins at the epithelial level, first point of contact with luminal microbes. Patients with IBD suffered from a continuum of disturbed mechanisms of both innate and adaptive immune responses. Through several pathways, the resulting antigens lead to the inflammatory cascades.

Increased intestinal permeability is known as a causative factor in IBD pathogenesis. Patients with IBD present a lowered epithelial resistance on inflamed and non-inflamed mucosa [41]. Individuals with a family risk present a damaged epithelial barrier before the clinical onset of the disease, involving a genetic part [42, 43]. As an evidence, IL-10-/- mice, which spontaneously develop colitis with IBD-like symptoms, present an increased intestinal permeability, which was present before the clinical appearance of the disease [44]. Epithelial gap densities of patients with IBD were shown by confocal laser endoscopy to be significantly higher than in controls patients. However, they were not correlated to the disease activity, implying that other effects are responsible [45]. Various mechanisms were proposed such as increased epithelial apoptosis, T-cell mediated disruption of tight-junction proteins or enteric neuron dysfunction.

In a healthy state, toll-like receptors (TLR) recognize almost all microbe-associated molecular patterns and contribute to the equilibrium between intact epithelial barrier and commensal flora. Interactions between the TLR and the microbial antigens trigger intracellular processing leading to antimicrobial responses via the induction of the inflammatory cytokine cascade and the activation of the NF-κB [25, 46]. In an inflamed context, immune-related cells from inflamed mucosa present a pattern of TLR expression different from those from healthy mucosa (Figure 5). Thus, whereas TLR5, expressed at the basolateral side, has generally no signal in a healthy mucosa, flagellin, a bacterial component, can interact as a ligand with TLR5 on the inflamed mucosa, leading to disease exacerbation [47, 48]. These cells also acquire an atypical antigen-presenting activity in the presence of inflammatory cytokines such as IFN-γ and TNF-α. They acquire the ability to activate effector-T-cells by expression of lectins but also overexpression of classical and non-classical histocompatibility molecules [49, 50]. In addition to TLR, mutated cytosolic NOD proteins may be responsible for defects in innate bacterial elimination, causing deregulation in the inflammatory response [51].

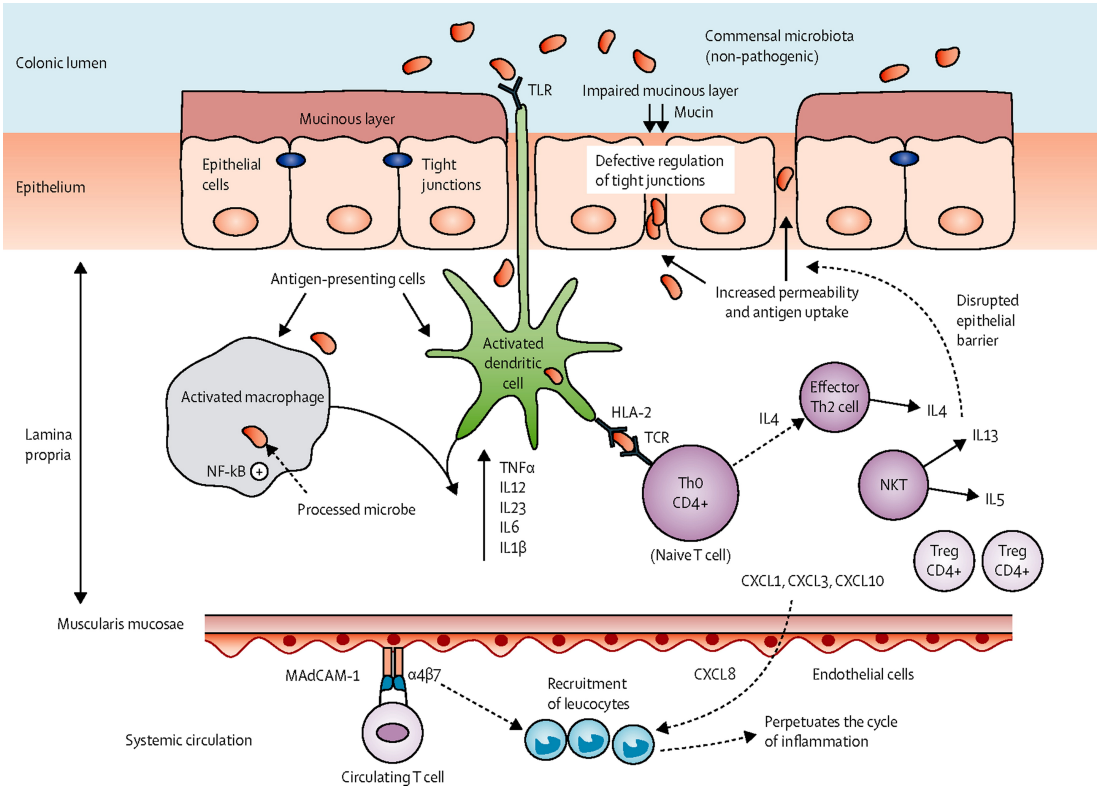


Figure 4: Pathogenesis of IBD in the inflamed mucosa**.** Enhanced permeability of the intestinal epithelium results in an increased uptake of luminal antigens. Exacerbated recognition activity of macrophages and DC by their altered toll-like receptors (TLR) pattern activates them even if the trigger antigen is commensal. Macrophages and DC process the antigens and present them to naive CD4 T-cells, promoting differentiation into Th2 effector cells. Circulating T cells bind to colonic endothelial cells via the overexpressed mucosal addressin-cell adhesion molecule 1 (MAdCAM-1), leading to gut-specific T cells infiltration into the lamina propria. Upregulation of inflammatory chemokines (CXCL), such CXCL1, CXCL3, and CXCL8, leads to recruitment of circulating leucocytes which perpetuates the cycle of inflammation [52].

T cells, B cells, granulocytes, mast cells and natural killer (NK) cells are aggregated in lymphoid follicles, located in the loose connective tissue of the lamina propria of the colon. Professional antigen-presenting cells such as dendritic cells and macrophages serve as an interface between the epithelial enterocytes receiving the luminal antigens and the underlying lymphoid tissue containing the effector cells of the immune response. These cells of the innate and adaptive immune system retain a tolerance against luminal antigens from dietary and commensal flora, and provoke immune responses to pathogens. In the IBD-induced mucosal inflammation, the antigen-presenting cells play a deleterious role due to disturbed antigen recognition and processing [48]. As dendritic cells can express tight junctions such as occluding or claudin, they can open the tight junction structures like a zip, send their dendrites between epithelial cells and sample luminal bacteria, while preserving the intestinal barrier function [53]. Dendritic cells maintain tolerance of the commensal microflora by displaying an immature phenotype, and once activated, by inducing the differentiation of

naïve T cells into T helper (Th) cells via cytokines and co-stimulatory signals. At the opposite, in patients with IBD, activated dendritic cells present aberrant responses to microbial stimuli and lack their regulatory activity, contributing to permanent homing to inflamed mucosa and depressed clearance of overactive T-cell populations (Figure 5) [25, 51].

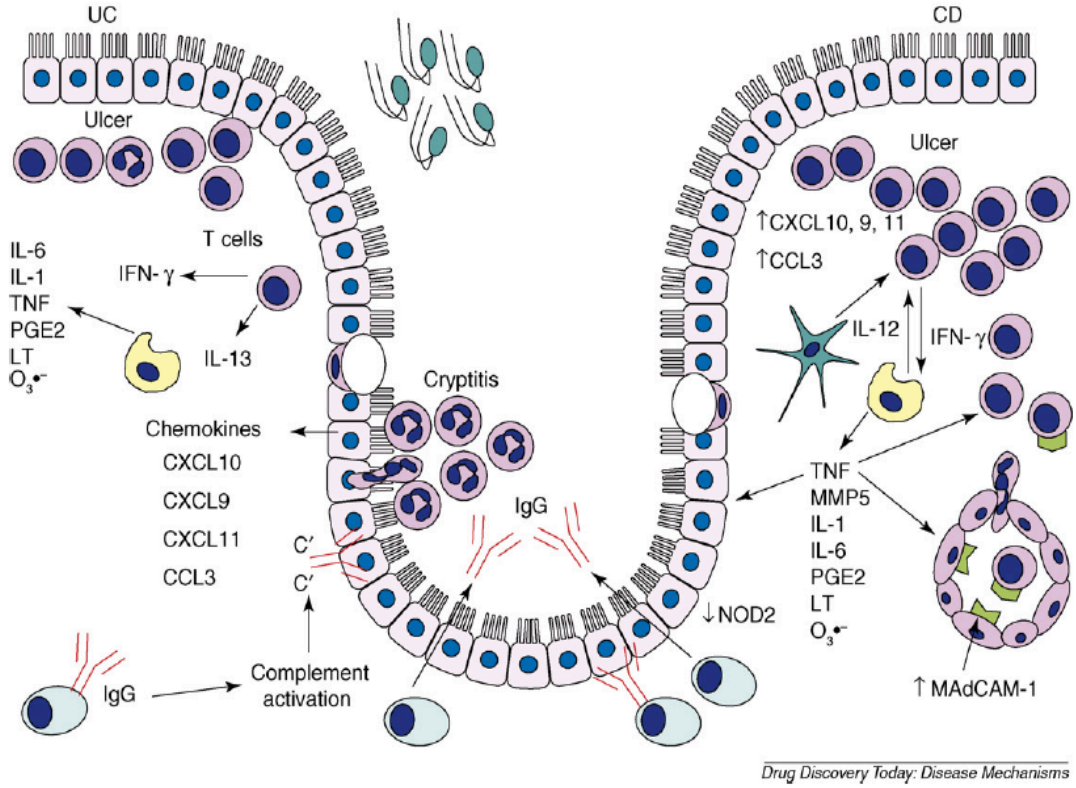


Figure 5: Impairment of the immune response in IBD. Mucosal inflammation in IBD is the result of the interactions of mucosal immune cells with a variety of inflammatory mediators. As luminal antigens trigger the immune response, cytokines (IL-12, IFN-γ) secreted by activated T cells recruit and stimulate additional immune cells, eventually leading to mucosal damage. At the same time, there is an increased expression of adhesion molecules (MadCAM-1) and chemokines (CXCL10, CXCL9 and CXCL11), resulting in the recruitment of additional inflammatory cells to the inflamed sites, setting up a self-perpetuating inflammatory reaction [28].

Gut is the primary location where naïve T cells can be differentiated in different subsets of activated CD4+ Th cells. Each subset of Th cells presents unique effector functions against pathogens [54]. For instance, in healthy people, constitutive activity of Treg cells protects against autoimmunity while inducible activity mainly suppresses immune responses against commensal antigens. In the pathogenesis of IBD, inappropriate regulatory and effector activities of CD4+ T cells are thought to play a key role even if the exact mechanism remains unclear. It is, however, clearly assumed that CD presented an altered Th1 and/or Th17 response whereas UC is associated with disturbed Th2 T cells. Furthermore, both diseases present also a Treg dysfunction, which usually inhibit deleterious T cell responses. It seems

now that the current consensus is that Treg do not present intrinsic drawbacks, but their suppressive activity is rather diminished by a loss of sensitivity from their target cells [48].

Psychosocial stress might activate or exacerbate the inflamed state of the mucosa. *In vivo* and *in vitro* studies show that disturbed neuro-immunological interaction altered by adrenergic regulation of IL-10 may be one of the mechanisms responsible for this trigger [55].

Finally, all the previously mentioned events lead to the antigen recognition and migration of activated inflammatory cells from the vasculature into the intestinal mucosa, the accumulation of aggressive luminal antigens and pro-inflammatory mediators in the mucosa, resulting in tissue damage and self-perpetuating cycle of mucosal inflammation [56].

I.3 PHYSIOPATHOLOGY

Even if UC and CD, the two idiopathic IBD, present similar clinical symptoms such as fever, diarrhea, abdominal pain, rectal bleeding and weight loss, they distinguish themselves with clinical, pathological, and endoscopic features. Biopsies taken from multiples sites (rectum above all) allow differentiating UC from CD but also idiopathic from non-idiopathic IBD. The classical features of inflammatory intestinal process such as crypt architectural distortion, the loss of normal inflammatory cell gradient or increased inflammatory cells in the lamina propria are not always present in the acute disease but are representative of the chronicity of these pathologies. The distinction between UC and CD is not always easy to make and depends strongly on the correlation between the endoscopic findings and the clinical history (Table 2). However, inside the colon, colon inflammation from UC or CD does not occur in the same areas. Thereby, UC present a proximal distribution whereas CD-related inflamed areas are spread all over the colon [1, 27, 31, 57].

Table 2: Differentiation in the inflammatory process of UC and CD [1, 27, 31, 57, 58]

	CD	UC
Gastro-intestinal sites	All (ileo-colonic)	Colon
Rectum	Involved or spared	Involved 95%
Distribution	Skip areas	Continuous
Inflammation	Transmural	Mucosal
Granulomas	May be present	Absent
Crypt abscesses	Usually absent	Usually present
Blood in stool	Occasionally	No
Mucus	Occasionally	Yes
Systemic symptoms	Frequently	Occasionally
Pain	Frequently	Occasionally
Significant perianal disease	Frequently	Yes
Fistulas	Yes	No
Small-intestinal obstruction	Frequently	No
Colonic obstruction	Frequently	Rarely
Response to antibiotics	Yes	No
Recurrence after surgery	Yes	No
Rectal sparing	Frequently	Rarely
Continuous disease	Occasionally	Yes
"Cobblestoning"	Yes	No

I.3.1 Crohn's Disease

CD affects the entire length of the gastro-intestinal tract (GIT), from the oral mucosa to the anus, even if 90 % of cases present the terminal ileum as the most affected part. Among these 90%, one-third of these patients have a colonic distribution. Macroscopic and microscopic clinical aspects of CD strongly depend on the location of inflamed mucosa and the severity of the disease. Clinical manifestations of patients with active clinically CD are loose stools, rectal loss of mucus, rectal bleeding associated with fever, abdominal pain and weight loss. Most of the time, CD-related inflammation is non-stricturing or non-penetrating [59]. Inflammatory lesions from patients with CD have a characteristic patchy distribution, namely that healthy mucosa is overlapping by abruptly inflamed areas. CD-induced inflammation is transmural and the inflammatory process can touch all layers of bowel wall,

resulting in oedema. The aphthous ulcers are the first characteristic of CD that can be seen in the lumen. These ulcers are erythematous areas, which grow from lymphoid aggregates within the lamina propria. Even if it is not always present, the non-caseating granuloma is typically a CD feature and can be found at this stage. The deep ulcers can merge by enlargement and can reach the epithelium, leading to the infiltration of neutrophils polymorphs. These immune cells modified the epithelial architecture with cryptitis (Figure 6). Regeneration of the epithelium appears close to the deep ulcers, which make their way in the mucosa by lining the lumen. Transversal merges can also occur and lead to a persistent mucosal 'cobblestoning' appearance with the alternation of ulcers and healthy or oedematous regenerative mucosa. When CD is active, inflamed areas are red and inflamed. Active CD-related changes are persistent and can be observed even in the quiescent stage, leading, during this steady state of the inflamed mucosa, to fibrosis and to the formation of fistulas and wall abscess [1, 31].

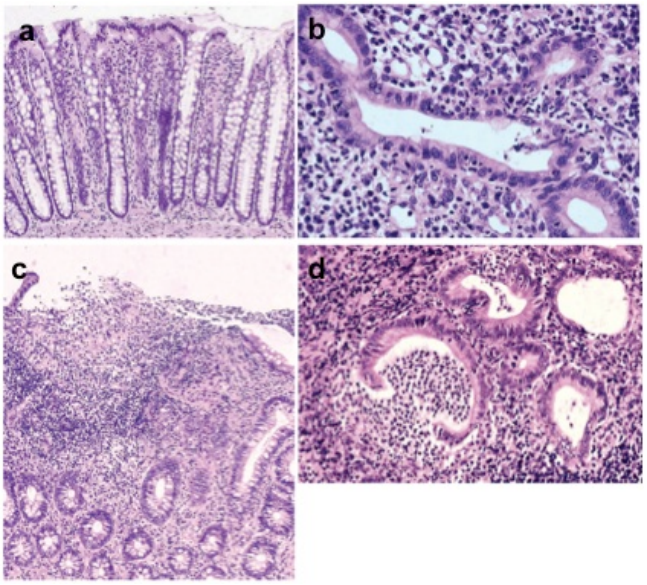


Figure 6: a) Normal colonic mucosa with parallel straight crypts or inflamed state; **b**) Cryptitis; **c**) Aphthous ulcer; **d**) Cryptic abscess (Adapted from [1])

I.3.2 Ulcerative colitis

Besides the common symptoms of IBD, patients with UC suffer from frequency and urgency of defecation. Unlike CD, UC has an exclusively colonic localization. UC always starts in the rectum and extends continuously to the proximal part of the colon with occasionally a tropism for the appendix in severe cases. Classification of the UC depends on the severity and the proximal progression [60]. Microscopic features of active UC include oedema that obscures the normal vascular appearance, granular erythema and mucopurulent exudate, areas of extensive superficial ulceration, the presence of inflammatory pseudopolyps, cryptitis, crypt abscess and mucosal destruction (Figure 6). Counter to CD, UC-induced inflammation is superficial, does not invade the muscularis mucosae and does not lead to stenosis and obstruction. Distribution of ulcerous areas and residual intact mucosa broadens longitudinally along the colon. Patient with UC may suffer from toxic mega colon. This severe complication is due to a loss of colonic contractility and is life-threatening [1, 31].

I.3.3 Complications associated with IBD

Colorectal cancer is the most common complication of IBD. The risk is even worse for the patients with UC and is correlated to the extent and the age of the clinical activity. Patients with more extensive UC are 4 times more likely to develop colorectal adenocarcinoma than patients with left-sided disease. 23 % of patients with 25 years of diagnosed UC will develop colorectal cancer [31]. Colitis-associated cancer is difficult to treat and is associated to high mortality [61]. Perianal fistulas occurs 22 % of patients with IBD. Their presence increases with disease time, varies with disease location with the highest frequency associated to the colonic disease location and often appears before or simultaneously with intestinal symptoms [59].

Extra-intestinal manifestations are common in IBD and may occur before or after onset of the active inflammation. At least 36 % of IBD patients will suffer from one of them [59]. Hepatobiliary, musculoskeletal, dermatological and ocular organs systems are commonly affected in patients with IBD and should be regularly screened for diseases [31]. More than 80 % of patients with primary sclerosing cholangitis, a chronic liver disease, have already UC [62]. Extra-intestinal diseases such as erythema nodusum, a cutaneous manifestation affecting the extensor surfaces of the extremities, will follow clinical activity of colonic inflammation. Arthropathies such ankylosing spondylitis have a reported incidence of 4-23% [59, 63]. Pyostomatitis vegetans is a stomatitis consisting in multiple friable pustules and ulcerations of oral mucosa. Its manifestation means that the disease is in an active state and is visible often before the diagnosis of UC. So pyostomatitis vegetans is considered as a

specific marker of active IBD, in particular UC [60]. Ophthalmic complications such as uveitis, episcleritis and scleritis are common in IBD. Approximately 50 % of IBD patients will be affected by a ocular complication [64]. Bronchiolitis obliterans organizing pneumonia and bronchiectasis are the most common pulmonary manifestations of IBD [65]. All these extra-intestinal complications are associated with pain and depression for the patients and are treated with the same therapeutic arsenal as IBD [66].

I.4 CONVENTIONAL IBD THERAPY

I.4.1 Aim

As incurable diseases, the actual aim of the therapy of both UC and CD is to treat symptoms and restore the well being of the patient. For this purpose, three essential steps have been put forward: induction of remission during the acute episodes, maintain of this remission and prevention of the relapses.

Although the conventional therapy has focused on the mere cure of the symptoms, the emergence of the first biological agents against IBD, the anti-TNF-α antibodies, clearly shows that mucosal healing, that is to say complete endoscopic healing of all the inflammatory lesions and ulcerations in the gut mucosa of a patient with diagnosed IBD, should be a more reliable objective [67, 68].

Conventional drugs, including aminosalicylates, corticosteroids, thiopurines and methotrexate have been used for over four decades. For two decade, anti-TNFα agents have made their entrance in the management of IBD and are now considered as 2nd line drugs. Physicians consider that the choice of therapy depends on several factors, including external factors (drug intolerance, patient preferences, also pharmaceutical regulation, therapy cost…) but also individual factors (disease extent and activity, patient acceptability or mode of drug delivery) and must be reliably analyzed before the start of the treatment [69].

I.4.2 Management of CD

I.4.2.1 Induction of the remission of patients with CD

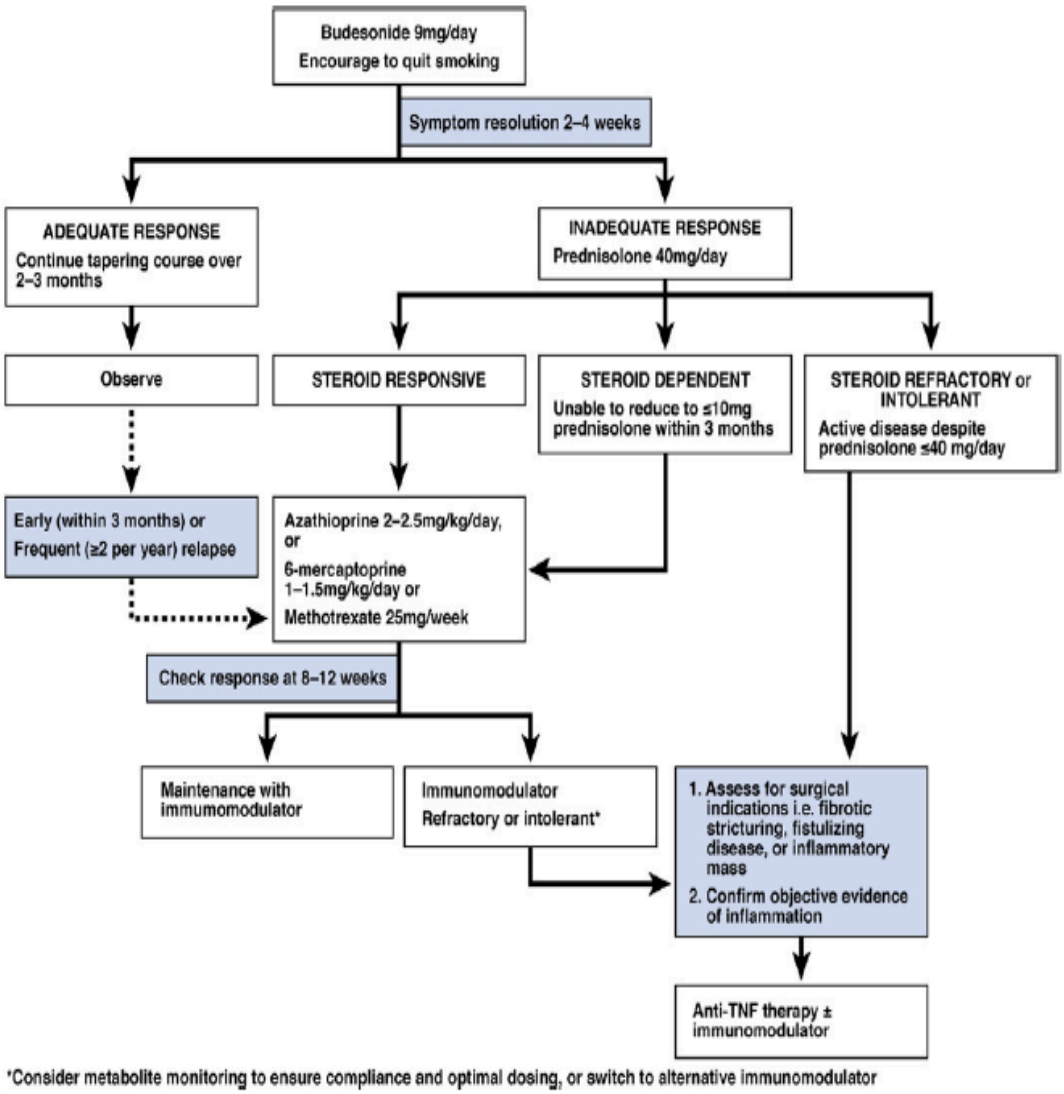


Figure 7: Management algorithm for mild-to-moderate ileal Crohn's disease [69].

When CD activity is defined as mild-to-moderate, it means that patients suffers from an intestinal inflammation without obstruction, painful mass, systemic symptoms (fevers, dehydration, and rigors) or more than 10% weight loss. With these patients, some basic principles have to be followed (Figure 7) [10]:

- Aminosalicylates are likely to present a lack of response so they are not used for CD. Indeed, aminosalicylates have been found less effective than budesonide or conventional steroids in large controlled clinical trials [70].
- Surgery may be more needed than for UC
- Nutritional therapy is highly recommended in first-line therapy for children with CD
- Budesonide is generally the first choice for patients with mild-to-moderately active ileo-colonic CD.

Corticosteroids have been recognized as effective at inducing remission. However, this therapeutic class presents a well-known serious side effects profile such as include increased risk of infection, decreased bone density, Cushingoid sequelae, hyperlipidaemia skin changes, psychological changes and sleep disturbances, myopathy, cataracts and hyperglycemia. It is reported that most of these adverse effects are mainly related to their systemic administration. Their adverse effects spare no tissues and organs and depend on various factors, including dosage tapering regimen, way of administration, gender, and individual sensibility to corticosteroids.

When the CD is severe, oral or intravenous corticosteroids represent the first-line treatment. If patients do not respond, anti-TNF therapy is then initiated. In any cases, nutritional support, assessment of surgery and treatment of iron deficiency and psychological consequences are collateral but significant worries in the management of severe CD [69].

I.4.2.2 Maintenance of remission of patients with CD

Even if the use of steroids is discouraged to maintain remission of patients with CD, budesonide is approved by the FDA and used in a short-term maintaining therapy (2 months at 6 mg a day). Thiopurines and methotrexate maintain remission and anti-TNF-α therapy is effective only if associated with an immunosuppressive drug (Figure 7). If the patient is part of the 50 % of patients who will have a surgery within the 10 years of diagnosis, anti-TNF-α therapy is declared as very useful to prevent endoscopic recurrence. Furthermore, the patient has to stop smoking cigarettes [69].

I.4.3 Management of UC

I.4.3.1 Induction of the remission of patients with UC

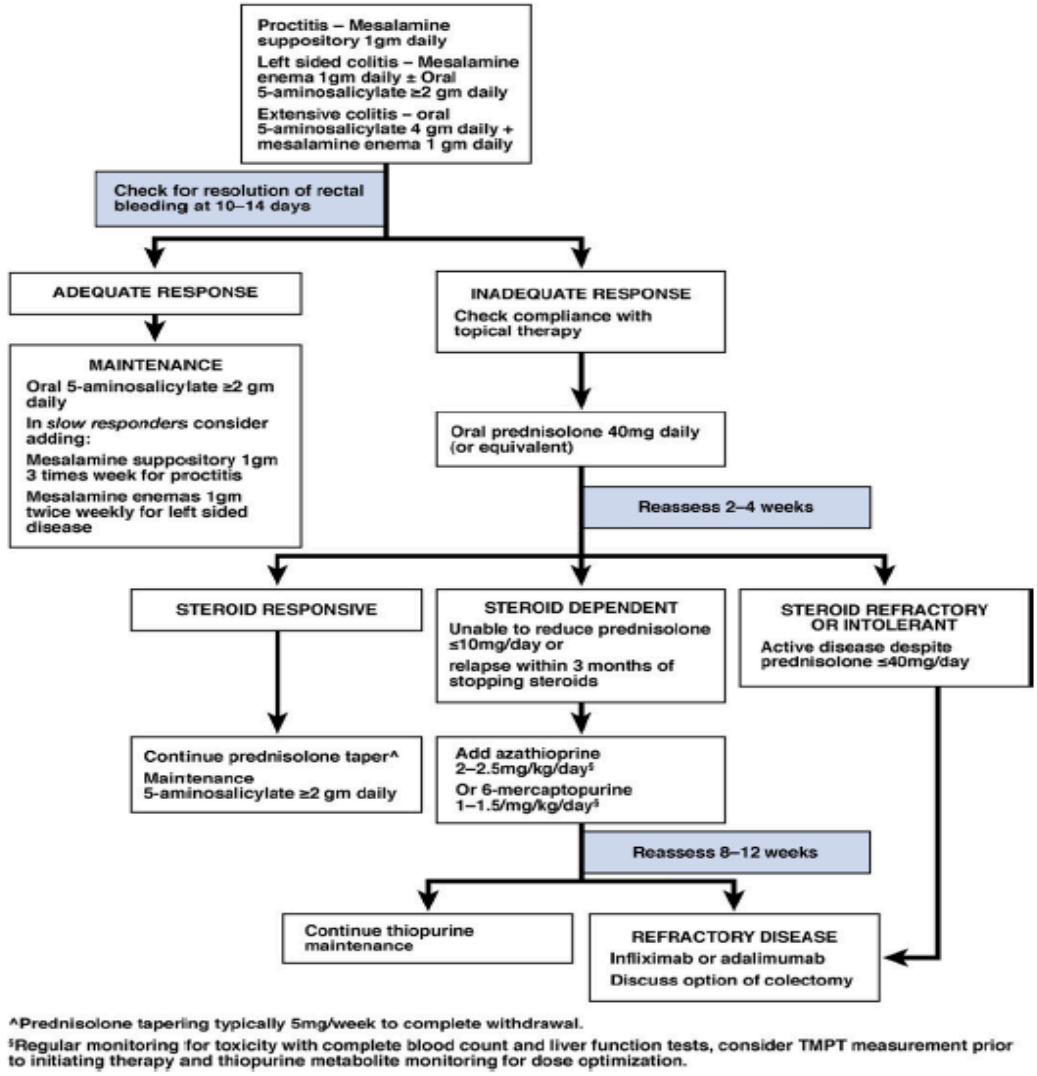


Figure 8: Management algorithm for mild-to-moderately active UC [69].

UC activity can be referred as mild or moderate when there are respectively <4 motions/day or >4 bloody motions/day and there are in any cases no signs of systemic toxicity (pulse <90 beats per minute, temperature <37.5°C, hemoglobin >10.5 g/dL or erythrocyte sedimentation rate <30 mm/hour). Unlike CD, 5-aminosalicylates are the most common treatment for patients with mild or moderately active UC (Figure 8). In order to achieve efficient mucosal concentrations of mesalamine, delivery of the active substance mesalamine be achieved by enemas, suppositories (if the localization of the disease is mainly distal), gastroresistant and

pH-dependent coated compound (eg, Asacol® or Salofalk®) or prodrugs (balsalazide, olsalazine, or sulfasalazine).

Patients with acute severe UC suffer from symptoms such as bloody stool frequency (> 6/day), tachycardia (>90 beats per minute), temperature >37.8°C, anemia (hemoglobin <10.5 g/dL) or an increased erythrocyte sedimentation rate (>30 mm/hour). 5-days administration of intravenous corticosteroids (methylprednisolone 60 mg or equivalent) is the first choice. Collateral treatments such as fluid and electrolyte replacement, with heparin thromboprophylaxis are really helpful and strongly advised. As patients with UC presenting *Clostridium difficile* infection are associated with higher mortality, oral dosages of vancomycin should be given to these patients. In case of inadequate response, surgery is not the only final option. A "rescue therapy" based on the use of immunosuppressive drugs such as cyclosporin or antagonists of TNF-α can be considered [69].

I.4.3.2 Maintenance of remission of patients with UC

By reducing the risk of relapse by 50 %, oral mesalamine is considered as the first-line maintenance therapy. If relapses occurred, infliximab, or to a lesser extent, thiopurines can be given to the patients with treatment-refractory UC [69].

I.4.4 Corticosteroids

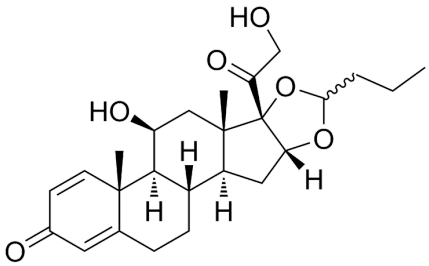


Figure 9: Chemical structure of budesonide (BDS)

Budesonide (BDS) is a topically active steroid, which offers the possibility of keeping the steroid-related activity while minimizing the related systemic side effects (Figure 9). This latter property is due to the fact that this compound undergoes extensive first-pass hepatic metabolism by cytochrome P450, as only about 10–15% of the drug reaches systemic circulation and the majority of the drugs is transformed into inactive metabolites. BDS possessed a very high affinity for corticosteroid receptors (15 times that of prednisolone and 195 times that of hydrocortisone) [71]. BDS is used in clinical practice for several diseases: IBD, asthma, allergic rhinitis or chronic obstructive pulmonary disease. Depending on the

target organ, topical delivery of BDS can be obtained by aerosol, nebulizer, tablets, enemas or rectal foams.

BDS downregulates activated macrophage cytokine production. It suppresses the production of the regulatory factor NF-κB that is important for the activation of proinflammatory agents in the case of IBD. BDS regulates immune responses by inducing monocytes apoptosis. The immunomodulatory effects of BDS consist in suppressing pro-inflammatory cytokines and T cell proliferation. BDS suppresses DNA synthesis and TNF-α secretion in normal human intestinal lamina propria lymphocytes. In vitro administration of steroids disturbs permeability changes of intestinal epithelial cells induced by proinflammatory cytokines or inflammatory activated cells [72]. Oral budesonide may have been found nearly as efficacious as systemic steroids for induction in mild to moderate CD. So budesonide at of 9 mg/day is recommended for induction in patients with mild to moderate disease involving the ileum and/or proximal colon. Budesonide has even been found to be effective in maintaining a short 3–6 month remission period. However, a large group of patients called “steroid-dependent” suffer from relapse after steroid therapy. So most specialists in IBD recommend minimizing the use of steroids at all costs and avoid them entirely if possible [73].

I.4.5 Biopharmaceutics

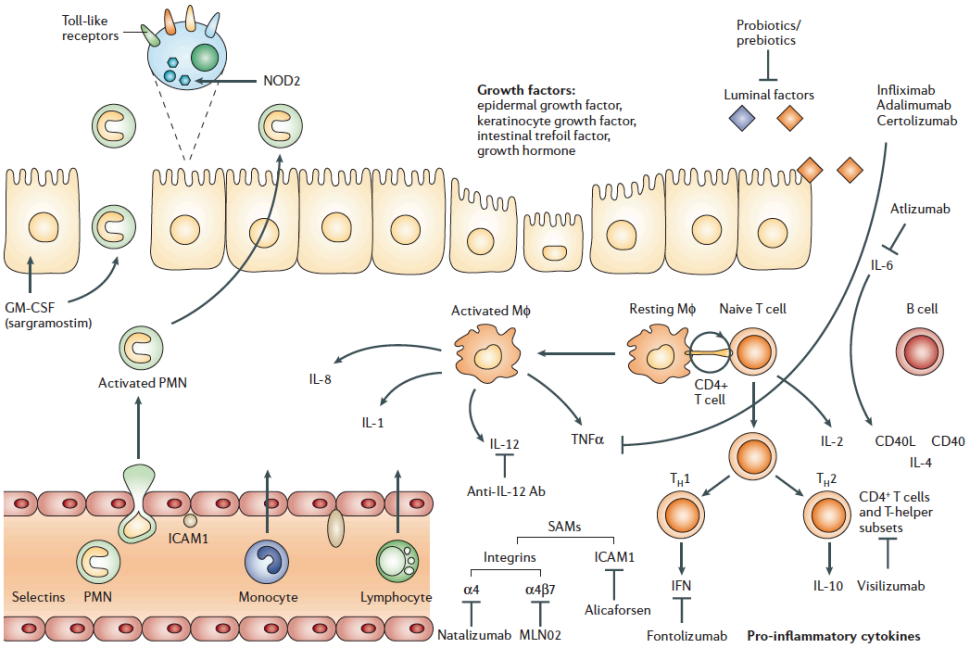


Figure 10: Novel therapeutic targets in IBD. Concerning TNF-α, 3 antibodies are available on the market [74].

TNF-α antagonist therapy has emerged as an alternative therapy for two decades, mainly because of a better understanding of the pathophysiological process of IBD and improvement in biotechnology (Figure 10). The proinflammatory cytokine TNF-α presents a pivotal role in the pathogenesis of IBD. During the acute phase, TNF-α secretion is crucial for the innate immunity and the initial response to pathogens. Binding of TNF-α leads to apoptosis of T cells. And so CD suffers from an inappropriate production and available amount of TNF-α, leading, inter alia, in the dysregulation of T cell populations.

For this purpose, three TNF-α monoclonal antibodies (i) infliximab, a murine monoclonal antibody (mAb), (ii) adalimumab, a humanized mAb and then (iii) certolizumab pegol, a PEGylated Fab' fragment of a humanized anti-TNF-α mAb, have shown significant efficacy in patients with severe CD refractory to conventional treatments [75]. Their use is also associated with a reduction in hospitalization and surgeries, an improvement in the quality of life and mucosal healing [76]. Systemic administration of these agents is achieved by intravenous (infliximab) or subcutaneous (certolizumab pegol and adalimumab) injection.

These antibodies bind to transmembrane and soluble TNF-α and thus block the forward interaction between TNF-α and its receptor. This blockade withdraws the resulting forward signaling pathway and/or triggers the reverse signaling (Figure 11) [77].

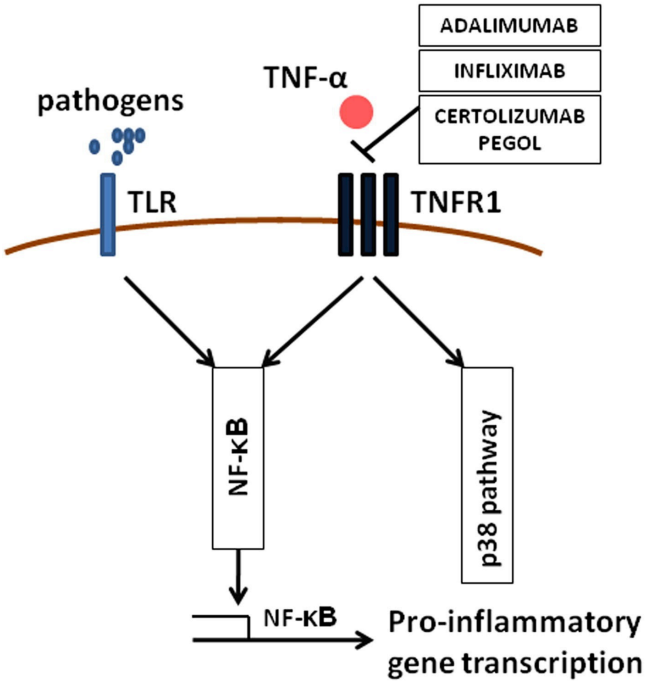


Figure 11: Two main TNF-α inflammatory signaling pathways NF-κB and p38 mitogen-activated protein kinase pathways) Adapted from [78]

Certolizumab pegol (Cimzia®; UCB) is the Fab' fragment of a humanized anti-TNF-α, linked to two crosslinked chains of 20 kDa-weighted PEG. Compared to other antibodies, certolizumab pegol may provide advantages. First, the reduced size of antibody fragment Fab compared to an IgG molecule allows faster penetration into body tissues. Then, the absence of Fc region prevents fixing to the complement, reducing undesirable side effects, such as cytokine release syndrome. PEGylation reduces requirement for frequent dosing, toxicity, antigenicity and immunogenicity and increases plasmatic half-life, bioavailability and proteolytic resistance as well. Subcutaneous administration may provide good tolerability, as peak serum concentrations are lower than would be achieved after intravenous delivery. Furthermore, a lower immunogenicity has been found compared with infliximab. Subcutaneous injections of 400 mg of certolizumab pegol, are administered every 2 weeks for the first three doses and then every 4 weeks for maintenance. Phase III trials have shown clinical efficacy with good tolerability in patients with moderate-to-severe Crohn's disease and rheumatoid arthritis [79]. As they do not possess a Fc region, they can be prepared via bacteria, which is a cheaper industrial production.

However, these biologics present a high-risk profile of side effects, which is worse when they are in combination with other IBD drugs. Serious and life threatening opportunistic infections such as reactivated tuberculosis or pneumocystosis profit from the treatment-induced dysregulation of the immune system. Malignancies such as lymphomas, colorectal carcinoma or autoimmune diseases such as cutaneous vasculitis and sarcoidosis are also associated with the use of biologic agents in IBD patients. Anti-TNF-α antibodies are also responsible for acute and delayed infusion reactions and injection site reactions. Demyelization of peripheral nerve bundles and optic neuritis are one of the neurological side effects associated with anti-TNF-α agents. Furthermore, heart failure and severe acute infectious diseases are serious contraindications to the use of anti-TNF-α agents [80, 81].

Even if the emergence of anti-TNF-α antibodies has improved the therapy for IBD, it appears in clinical practice that some patients respond amiss or do not respond at all. Furthermore, a significant proportion of responders seem to lose response over time. Different hypothesis have been put forward. Paradoxical inflammation may occur in IBD patients, contributing to the loss of response. TNF-α blockade leads to shifts of inflammatory and regulatory TNF-α mediated but also non-TNFα mediated cell populations and differentially regulates cells secreting other specific cytokines. Anti-TNF-α therapy may interfere with these non-TNF-α mediated inflammatory pathways [77]. From a practical point of view, anti-TNF-α therapy also

suffers from its inappropriate and abusive use. Besides, paradoxically, this therapeutic option is too often considered late in the disease progression [69].

I.4.6 Curcumin

Among these IBD therapeutic candidates, curcumin offers an interesting and promising profile as it has been shown good efficacy, tolerability and safety. Curcumin is the most active component of the rhizome of the turmeric (*Curcuma longa*) plant. The turmeric is used as a dietary spice, coloring agent in foods and textiles, and a treatment for a wide variety of ailments. The characteristic orange–yellow color of this crystalline powder is given by the curcuminoids.

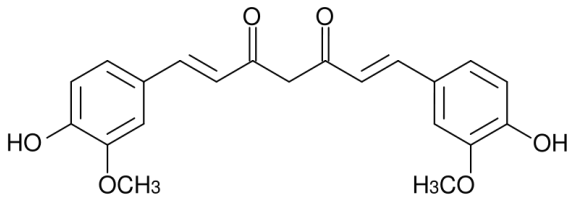


Figure 12: Chemical structure of curcumin

Curcumin is a pleiotropic natural diphenolic compound (Figure 12). It is a modulator of intracellular signaling pathways that control numerous targets including growth factors, growth factor receptors, transcription factors, cytokines, enzymes and genes regulating apoptosis. Curcumin possesses anti-inflammatory effects and has been used in various chronic inflammatory disorders (Alzheimer's disease, Parkinson's disease, multiple sclerosis, epilepsy, cerebral injury, cancer, allergy, asthma, bronchitis, colitis, rheumatoid arthritis, renal ischemia, psoriasis, diabetes, obesity, depression, fatigue and AIDS) [82].

Prophylactic treatment using curcumin shown protective effects on dinitrobenzene sulfonic acid–induced murine colitis and in 2,4,6- trinitrobenzene sulphonic acid–induced murine colitis and in dextran sulfate-induced murine colitis. Minimum doses of curcumin at 50 mg/kg daily for 10 days have been shown to significantly ameliorate diarrhea and the disruption of colonic architecture, reduce both neutrophil infiltration, lipid peroxidation and serine protease activity in the inflamed colon and suppress NF-κB activation in colonic mucosa [83-85].

In a randomized trial containing a total of 89 participants, patients were given aminosalicylates as treatment. Compared to the control group, curcumin group presented a lower but not statistically significant six months relapse rate. Nevertheless, the curcumin group presents significantly lower disease activity index and endoscopic index scores at six

months, suggesting that curcumin may be a safe and effective additional therapy for maintenance of remission in UC [86].

However, curcumin presents poor ADME profile. As a drawback, curcumin presents a very low solubility in water (i.e. 0.0004 mg/ml at pH 7.3) but is soluble in ethanol, dimethylsulfoxide and acetone. Curcumin is really sensitive to light and decomposition of curcumin is pH-dependent and occurs faster at neutral to basic conditions. Curcumin is known to be metabolized fast, conjugated in the liver, and excreted in the feces with minimal amounts found in urine [58]. These physicochemical characteristics result in low bioavaibility in the body. A solution against the limiting factors of curcumin should be to improve its bioavailability, protect it from degradation and metabolism and increase its capacity to target specific cells [87].

II. NANOMEDICINES FOR TOPICAL IBD TREATMENT

According to the European Science Foundation, nanocarriers are defined as nanometer size scale complex systems, consisting of at least two components, one of which being the active ingredient [88]. Nanoscale is usually defined as smaller than one tenth of micrometer in at least one dimension. However, nanoparticulate delivery systems tested for drug delivery of therapeutic and imaging agents are included in a range from 2 to 1000 nm [89]. Their small size gives them unique characteristics for the oral delivery of drugs, biopharmaceuticals and vaccines.

Among the various applications available, the use of nanoparticulate drug delivery systems in oral drug delivery may overcome several weaknesses inherent to the oral administration of drugs such as poor solubility, poor permeability and poor gastro-intestinal stability [90]. In IBD therapy, various nanomedicines have been tested including liposomes, nanocrystals, polymeric nanoparticles, solid lipid nanoparticles [91].

Polymeric nanoparticles are defined as solid and spherical structures with submicronic size and prepared from natural or synthetic polymers. A wide variety of drugs can be delivered using nanoparticles such as hydrophilic small and hydrophobic small drugs. Vaccines and biological macromolecules can also be encapsulated, even if the oral administration of these formulations is still not enabled orally. Nanoparticles also allow targeted administration to specific organs or cells or controlled drug delivery [92]. However, their administration is route dependent and few are marketed.

Lipid-based nanocarriers class includes inter alia liposomes, lipid micelles, solid lipid nanoparticles, nanoemulsions and nanosuspensions. They offer a major advantage compared to polymeric nanoparticles: most of their components (phospholipids, cholesterol and triglycerides) are recognized as biocompatible and biodegradable by the FDA and are used in pharmaceutical products. Lipid-based nanocarriers are promising vehicle for poorly water-soluble drugs but also for peptide and protein drugs [93].

II.1 GENERALITIES ON TOPICAL IBD TREATMENT WITH NANOCARRIERS

II.1.1 Achieving a topical delivery in IBD-inflamed colonic mucosa: The state-of-the-art

Topical administration of therapeutic compounds in the colon has received considerable interest in recent years. Colonic drug delivery, as it is called, consists in the targeted delivery of drugs into the last part of the GIT. It can be useful for the localized treatment of several colonic diseases such as IBD, irritable bowel syndrome or colon cancer. The colonic environment has also been found to be a more favorable area for systemic delivery of therapeutic proteins and peptides or applications such as chronotherapy for asthma or angina, or treatment of nicotine addiction, considering the harsher environment of the upper parts of the GI (acidity, mucosal and luminal digestive enzymes, etc…) [94]. However, in order to reach the colon and achieve efficient topical delivery, drug delivery systems have to pass through several hurdles: ways of administration, harsh and complex luminal content, mucosal barrier or pathophysiological changes related to the inflamed state. Topical delivery of IBD drugs would ensure a direct treatment at the inflamed sites and, thus, a decrease in doses and side effects. Eventually, it will provide significant clinical benefits to the patients [95].

One of the main differences between CD and UC is the localization of the inflamed area. As inflammation of UC is strictly localized in the colon, inflammation from CD can be found from the mouth to the rectum [29]. However, the colon remains the organ of interest in the case of IBD. So reaching the inflamed colon is of great interest when trying to deliver topically active anti-inflammatory drugs.

II.1.1.1 Reaching topically the colon

Characterized by a small surface area (1.3 m^2), the colon is the second part of the large intestine between the caecum and the rectum. The main functions of the colon (fermentation of polysaccharides and proteins, absorption of water and electrolytes, and the formation, storage and elimination of faecal material) make it a poor site for drug delivery and absorption. However, with longer residence time in the colon and lower activity of the drug-metabolizing cytochrome P450 3A class or proteases present in the mucosa of the distal bowel, colon may be considered as a promising target organ for drug delivery [94].

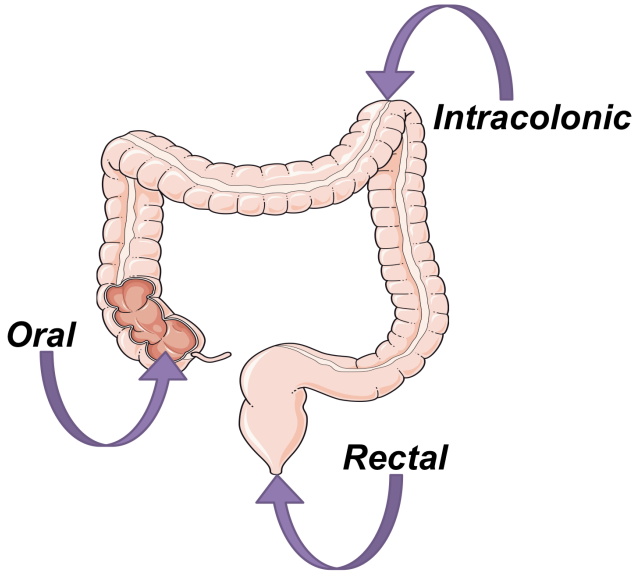


Figure 13: Reaching topically the colon: 3 available ways of administration

Achieving a topical delivery in the colon means to reach the most distal segment of the GIT (Figure 13). Oral route, the preferred mode of administration, presents the advantage of superior patient compliance. The drug delivery system must avoid drug release in the stomach and small intestine and must release the content in the colon. Nonetheless, when travelling all over the GIT, the formulations have to face harsh conditions (pH, enzymes, electrolytes, transit time, pressure, etc…). Oral drug delivery systems can be absorbed systematically and be inactivated by first pass metabolism so only a part of the delivered amount of drug reaches the inflamed areas. Furthermore, inter- and intraindividual variations are significant and the inflamed state affect the parameters [95].

Rectal administration is one of the alternatives to reach the colon. Formulations such as suppositories, foams or enemas allow drugs to reach the rectum and distal part of the descending colon. However, when more proximal parts of the GIT are inflamed, such formulations are inefficient to deliver the anti-inflammatory drug [96]. Furthermore, due to their composition and likely viscosity, rectal formulations may change the deposition of the formulation drug on the mucosa.

Intracolonic administration is the administration of the drug delivery system directly inside the colon. It allows bypassing all the unfriendly environment of the GIT. Some murine models such as DNBS, TNBS or acetic acid use this type of administration to induce colitis [97-99].

However, this invasive administration is really complicated in clinical practice and has been performed only in animal models.

II.1.1.2 Colonic Barriers

Once arrived in the colon, the drug delivery system has to face three main interconnected barriers in order to deliver topically its content into the inflamed colonic mucosa: the lumen and its complex composition, the viscous mucus and the dysregulated inflamed epithelium. As these barrier components are strongly disrupted by the IBD-related pathophysiological changes (Table 3), specific characteristics of the inflamed colon have to be highlighted.

Mainly due to its main functions, the colon presents viscous luminal content by nature.

Table 3: Pathophysiological changes in the GIT in IBD (Adapted from [96])

	Healthy	**UC**	**CD**
Luminal colonic pH	6.2-7.4	2.7-5.5	5-7
Colonic transit time	41.1-62.3 h	9.5-39.1 h	---
Colonic bacterial flora	10^{11} – 10^{12} CFU/ml	Decreased	Decreased
Intestinal barrier function	---	Inadequate tight junctions, reduced phosphatidylcholine levels	Reduced numbers of tight junctions, increased intestinal permeability, reduced defensin levels
Mucus	---	Decreased	Increased
Presence of ROS	---	Increased	Increased
Lipid content	---	Decreased	Decreased

Intraluminal pH varies through the GIT. From acidic values in the stomach, pH increases to reach more neutral values in the large intestine. However, data suggested that IBD patients present lower colonic pH than normal patients. Mucosal disease and changes in diet associated with the IBD drive to alterations of normal determinants of colonic pH: mucosal bicarbonate and lactate production, bacterial fermentation of carbohydrates, mucosal absorption of short chain fatty acids, and possibly intestinal transit [100]. Thus, while healthy patients present a proximal and distal colonic pH of respectively 6.8 and 7.2, proximal and distal colonic pH of patients with active or inactive CD was found to be more acidic with a mean value of 5.3 [101]. Even lower values (2.3-3.4) were found in UC patients. However, intraluminal pH of the inflamed colon is subject to inter- and intra-variability between IBD patients, but also depends on the disease state of the patient. All these characteristics can

lead to incomplete drug delivery and release from pH-dependent releasing colonic formulations [96].

Colonic luminal material flow is slower than the one in the other parts of the colon. For a colonic-specific time dependent delivery, a normal lag time of 5 or 6 hours is usually considered as suitable [94]. In a healthy state, colonic transit time varies between 41.1 and 62.3 h. This high variability is mainly due to factors such as diet quantity and composition, mobility, stress, drugs and of course disease. In active IBD, colonic passage time seems to be inversely correlated to the size of the drug delivery system. Diarrhea, the most frequent symptom of IBD, decreases colonic transit times and has been found to disturb the release profile of drug carriers with a size larger than 200 µm [102]. Furthermore, motor disorders happen even in CD patients in remission phase. IBD-related pathophysiological changes such as inflamed epithelium, reduction in reabsorption of fluid and electrolytes and increased mucus secretion create more content, resulting in an increase in stool weight [103].

Colonic lumen is the residence of bacterial microflora and their products, responsible for a weak but non-negligible metabolic activity and thus the metabolization of drugs. As its bacterial concentration is dramatically higher than those of the other parts of the GIT, colonic microflora possesses unique metabolic functions such as the ability to intervene in the future of the drug delivery system and the drug itself [104].

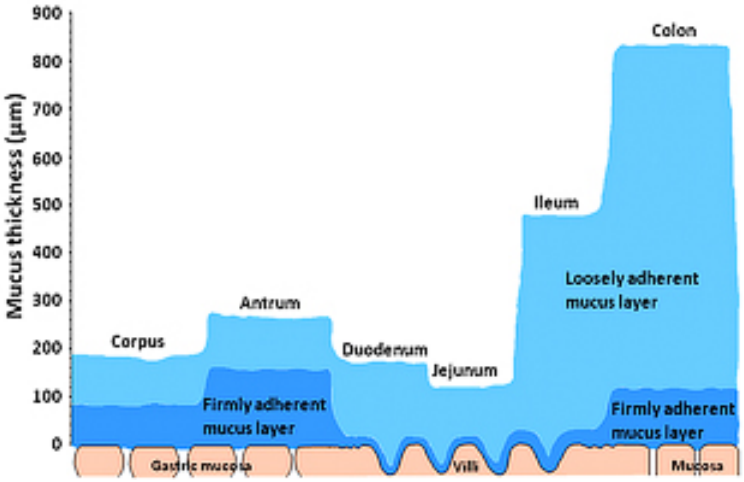


Figure 14: The mucus layers in different parts of the GIT [105]

Mucus is a complex viscoelastic and adhesive hydrogel composed of proteins, carbohydrates, lipids, salts, antibodies, bacteria, secreted antimicrobial molecules and cellular debris. Its main and vital function is the protection of the underlying epithelium. For this purpose, the mucus i) lubricates the epithelial surface and ii) traps and facilitates the

removal of foreign particles such as pathogens or conventional particulate drug delivery systems. Mucin monomers, the main component of the mucus, entangle and crosslink together adhesively and reversibly via disulfide bonds, forming a 'sieve' that can sterically block particulates that are too large to penetrate the mucus mesh spacing [106]. The adhesive properties of mucus are due to the hydrophobic, electrostatic and hydrogen bonding interactions available. Representing 20% of the mucus dry weight, lipids enhance the surface hydrophobicity on the luminal surface of the GIT, resulting in better protection against luminal pathogens [107]. For the efficient transport of the bolus through the GIT, loosely adherent mucus layer overlies a firmly adherent one. Because it must protect the epithelium against abundant bacteria, colonic mucus is the thickest in the GIT (Figure 14). To protect the mucosal epithelium, the turnover of the mucus must be constant. In the inflamed state of IBD colon, changes occur in terms of viscoelastic properties, resistance to bacterial degradation and adhesion. UC pathophysiology diminishes the barrier properties of the mucus layer by several ways. Due to overall depletion of goblet cells and the reduced expression of the protective trefoil peptides [108], the whole mucus layer in the colorectum is less thick. Additionally, clinical evidence of absence of phosphatidylcholine in mucus of UC patients associated with alleviating effects of a therapeutic supplement of phosphatidylcholine has emphasized the modulator role of lipids in IBD-induced inflammation. Inter alia, this phospholipid has been shown to inhibit TNF-α dependent proinflammatory responses [107]. Lipid depletion may also decrease the surface tension and hydrophobicity [106]. In Crohn's disease, thicker mucus layer can be observed especially in ulcerated areas, as there is an increased mucus production [96, 109].

At the interface between the lumen and the lamina propria, intestinal epithelial cells have a strategic position. Organized as a monolayer with tight junctions called epithelium, they have a relevant barrier function in addition to the absorption of the nutrients, signal-transduction or regulatory products secretion. They actively intervene in immune processes such as mucosal defense, tolerance to resident flora and barrier repair. In case of inflammation, by establishing bidirectional interactions with the underlying immune cells, they can selectively modulate the permeability of the epithelial monolayer and synthesize and secrete inflammatory mediators themselves, allow them to trigger immune cells and initiate the inflammatory process [110]. Characterized by a tight paracellular pathway and elevated levels of the efflux transporter P-glycoprotein, normal colonic epithelium is not considered as the first choice for drug delivery and absorption. However, in IBD patients, inflamed as well as non-inflamed intestinal areas present abnormal permeability [41]. In consequence, underlying immune-related cells are more exposed to luminal antigens levels. There is also a clear correlation between disease activity and permeability enhancement. There is still

debate as to the origin of this enhanced permeability: is it an initiating event in the pathogenesis or a consequence of repeated inflammatory cycles [96]? Furthermore, colonic epithelial structure is disrupted in the inflamed areas. In particular, the vicious cycle of inflammation and barrier damage is maintained, as permeability of the mucosa for pathogens and loss of water and electrolytes via the epithelium are increased. However, these pathophysiological changes offer the possibility to nano-sized drug delivery systems to accumulate in the gaps between the cells, mimicking the enhanced permeability and retention effect observed in tumor vasculature. Furthermore, a loss of polarity has been associated with these damaged intestinal epithelial cells. As a result, basolateral membrane proteins also display apical expression. For instance, the expression of transferrin receptor was enhanced both on the apical and the basolateral sides of enterocytes in the inflamed colonic mucosa of IBD patients [96].

All these IBD-related pathophysiological changes may limit the potential of established colon targeting strategies based on the features of the colon in a normal state. However, it may also present new openings to exploit for localized drug delivery in IBD therapy.

II.1.2 Models of IBD

These IBD models are used to evaluate new therapeutic agents for IBD. They provide a routine way to analyze and harvest data on the interaction between the drug delivery systems and IBD-related processes. Concerning nano-sized drug delivery systems, *in vitro*, *ex vivo* and *in vivo* models have been used. Encapsulation and release of IBD drugs, targeting of the inflamed tissue and evaluation of their efficacy are some of the studied criteria. In preclinical studies of IBD drug delivery, animal models are mostly preferred. However, some questions still need to be addressed. For instance, the translation of the obtained data between the types of models is questioned. Another drawback related to the use of these models is the linkage to human disease, which often lacks consistency [111].

II.1.2.1 Simulated colonic fluids

Simulated fluids allow evaluating profile of drug delivery systems in terms of stability, drug release and solubility. Most of the publications studying the behavior of colon-targeted drug delivery systems on simulated fluids simply use buffers with pH between 6.8 and 7 [99, 112], USP or European pharmacopeia-related artificial intestinal fluids [113] or more complex simulated fasted or fed intestinal fluids. Release of budesonide from pH-sensitive nanospheres was assayed in a pH-changing buffer with the purpose to evaluate them in terms of drug release throughout the pH range of the GIT [114].

Recent improvement of knowledge about the colonic lumen of healthy adults has allowed more precise simulations of fluids in ascending colon. Media simulating the ascending colonic lumen in fast and fed states have been developed to predict intracolonic drug solubility [115]. Bovine serum albumin and glucose were selected to simulate colonic content in protein and carbohydrates respectively where bile salt extract and palmitic acid were also added to the composition of these fluids.

However, as inflammation changes all colonic parameters, these simulated artificial media cannot reflect the inflammatory lumen specifically. For instance, in the inflamed ileum of CD patients, due to lower bile acid reabsorption, increased enteral bile acid loss may occur with subsequent cholegenic diarrhea. When comparing healthy and UC colonic lumens, differences were observed in terms of pH, buffer capacity, osmolality, soluble protein, isobutyric acid levels and valeric acid levels. Taken together, these modifications of the environment could change the release profile of the drug delivery system [116].

II.1.2.2 In vitro cellular models

In vitro models have gained interest in drug delivery in IBD, as they can help to study and understand in more details the behavior of drugs and nano-sized delivery systems in the inflamed tissue. Therefore, various cell monolayer models have been widely developed. Briefly, these models consist of human immortalized cells, which grow rapidly into confluent monolayers followed by spontaneous differentiation. Human origin is preferred.

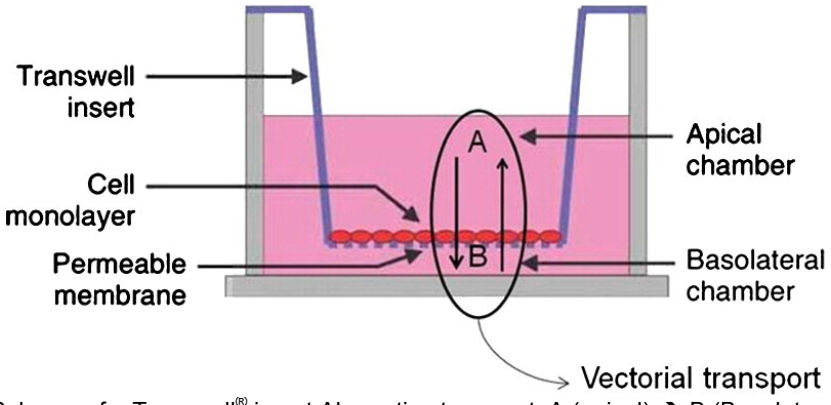


Figure 15: Scheme of a Transwell® insert Absorptive transport: A (apical) ➔ B (Basolateral) [117]

Intestinal epithelial cells possess a very important role in the mucosa. To mimic these *in vivo* human enterocytes, cellular cultures such as Caco-2, T84 or HT29 cell lines have been widely used as *in vitro* models [99, 118]. For instance, Caco-2 is a human colon adenocarcinoma derived cell line. Grown on a Transwell® configuration (Figure 15), they differentiate over 3 weeks to form a monolayer of cells that resemble like mature enterocytes:

highly polarized cells with tight junctions, a glycocalyx and apical microvilli [119, 120]. As apical and basolateral compartments are separated, this Caco-2 cell Transwell® system provide a model of healthy epithelial barrier and can assess the absorption of compounds [120, 121].

However, in an inflamed state, the intestinal barrier presents an increased permeability due mainly to the opening of tight junctions. Furthermore, the whole bacteria recognition process is impaired. All these alterations result in the absence of defensive reactions until the commensal or pathogenic bacteria reaches the lamina propria. Mediators such as bacterial components or pro-inflammatory cytokines are overexpressed in the mucosa and contribute strongly to the pathophysiological changes happening in the inflamed region of IBD. To mimic this inflamed state, a Caco-2 cell Transwell® system was incubated with a cocktail of pro-inflammatory substances (interleukin-1ß, TNF-α, interferon-γ and lipopolysaccharide). Incubation of the cocktail resulted in an *in vitro* inflamed epithelial barrier model, characterized by a reduction of the monolayer integrity and an overexpression of well-known pro-inflammatory markers such as IL-6 or IL-8 [110].

However, a specific IBD model requires the presence and action of different cell types and pro-inflammatory mediators (cytokines, growth factors, eicosanoids, etc…) in order to represent the complexity of an IBD inflamed intestinal epithelium. Indeed, enterocytes are not the only cell species present in the inflamed mucosa. The crucial role of immune-related cells such as macrophages and dendritic cells in the pathogenesis of IBD cannot be denied. Depending on the type of the IBD, mucus secretion varies. An *in vitro* IBD model consisting of the coculture of primary blood cells from IBD patients and Caco-2 or primary colonic crypt cells failed to give any pathophysiological changes, although cells from IBD patients were found producing more IFN-γ than the healthy model [122]. Leonard et al. developed a “three-dimensional” *in vitro* model, consisting of intestinal epithelial cells, human blood-derived macrophages and dendritic cells that were stimulated by the pro-inflammatory interleukin-1β. The main goal of this model was to provide more data than the monoculture model, as it includes immunocompetent cells and related pathophysiological changes [123]. A preferential uptake of 50 nm-sized polystyrene nanoparticles by immunocompetent cells in the 3D model was found in contrast with the stimulated Caco-2 monoculture. Thanks to this model, budesonide nanoformulations (PLGA nanoparticles and liposomes) were screened in terms of therapeutic efficacy and mechanism of uptake and action. Compared to the free solution and the loaded liposomes, budesonide-loaded PLGA nanoparticles presented better characteristics for IBD targeting: higher encapsulation efficiency avoiding a higher loss of budesonide in the generation of the formulation, good recovery from inflammation, depot

effect, no interaction with the healthy model mimicking the non-affected parts of the gut, specific adhesion to the more mucus-rich and acidic inflamed model tissue [124].

II.1.2.3 Ex vivo models

Ex vivo defines assays done with living tissue samples or cellular culture systems outside the organism during maximum 24 hours and kept alive in an artificial and generally sterile environment. With *ex vivo* tissue, the experimenter has the possibility to establish highly controlled conditions and to achieve assays ethically and/or physically impossible in the intact animal or the human body. Cost and number of animal experiments are reduced, as low amount of tissue is needed. However, as different types of cells can be found in the same sample and *ex vivo* conditions cannot mimic all the mucosal responses, caution must be taken in the choice of the model.

Ex vivo models may consist also of tissue samples. In order to study the anti-inflammatory properties of short-chain fatty acids, sections of colon from mice with DSS-induced colitis were cultured during 24 h and mounted in Transwell® inserts in the presence or not of these fatty acids [125].

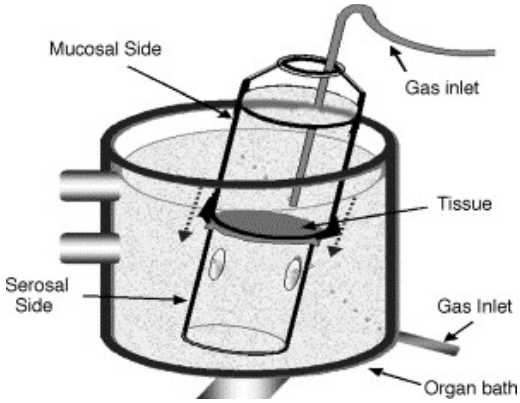


Figure 16: Schematic of horizontal diffusion chamber. Apical and serosal sides of tissue compartment are separated. Fluid levels were maintained at equal levels during experiments to avoid gradient effect [126].

Tissue samples can also be mounted in experimental devices capable of sustaining the tissue in viable conditions. First designed to assess drug transport under conditions simulating the air–mucosa interface, horizontal diffusion chambers were designed similar to classical Ussing chambers (Figure 16). These diffusion chambers mount mucosal sheets horizontally, allowing a separation between the apical and the serosal side. Intestinal tissue from animals (rodent, rabbit or ruminants) can be trapped between the two halves, permitting drug uptake and/or transport. For instance, due to the thinness of their intestine, sub-mucosal muscle from mice intestine samples cannot be removed and thus, only drug uptake

experiments can be performed. In this design, no chemical, osmotic, hydraulic or hydrostatic gradients can modify particle deposition on the mucosal tissue. Briefly, after excision and sampling of the intestine from the mice, Peyer's patches were mounted in the horizontal diffusion chambers. The whole system is put in a bath containing Krebs-Ringer solution gassed with 95% O_2:5% CO_2 at 37°C. By adding small volumes of drug formulations on the apical side of the mucosal samples, uptake and localization of FITC-labeled carboxylated latex particles in the colonic tissue samples have been studied [126].

For instance, when comparing inflammatory gene profiles of two *ex vivo* murine models (dextran sodium sulphate (DSS)-induced colitis and Gαi2-deficient mice), an innate cytokine/chemokine profile was found in the chemically induced DSS colitis whereas a T cell related markers profile was found in Gαi2-deficient mice, reflecting the different phases of colitis that represent these murine models [127]. In order to evaluate the translation of the findings between *ex vivo* and *in vivo* murine models of colitis, the anti-inflammatory effects of methyl-prednisolone were compared in *ex vivo* and *in vivo* colonic tissues from two murine models: (DSS)-induced colitis and Gαi2-deficient mice. After steroid treatment, was similar inflammatory gene profiles were evaluated by quantitative RT-PCR and found suppressed in both mouse models, comparing the *in vivo* studies with the *ex vivo* cultures, suggesting that these murine culture systems reflect *in vivo* responses [127].

II.1.2.4 In vivo models

Animal models are generally designed to mimic a set of signs and symptoms resembling as much as possible human disease features. The design of animal models of IBD is complex. The colon is an organ exposed to external factors (food intake, microflora) and dependent on physiological characteristics (immunological features, nervous irrigation), which influence strongly its behavior. Furthermore, numerous biochemical factors and pleiotropic as well as redundant interactions are involved in pathogenesis of IBD, making chronic inflammation hardly reproducible *in toto* [128].

Despite all these reasons, several and different *in vivo* models of colitis have been developed during the last decades. However, as animal species present differences, animal models of IBD deal with different aspects of the disease and choice of the animal model should be done with caution [128]. It should be similar or identical to human IBD in terms of morphological alterations, inflammation, symptoms and signs, pathophysiology, and time course [129]. For instance, when analyzing expression of some inflammatory genes and some metabolic markers that are known to change transcriptional activity in IBD (32 in total),

2/32 are upregulated in TNBS, 15/32 are upregulated or downregulated in DSS and 30/32 are upregulated or downregulated in the CD45RB transfer colitis [130].

To evaluate the efficacy of a test compound, the choice of the optimal IBD animal model should depend on the reproduced IBD features and the therapeutic strategy tested. It must also provide multiple biomarkers and endpoints. These latter may vary from the general one (amelioration of the inflammatory conditions for instance) to more specific one (cytokine expression patterns) [128].

Based on what the colitis trigger is, several categories of animal models of IBD can be defined: gene knockout models (IL-10, IL-2 or IL-2 receptor KO mice), transgenic mice (IL-7 transgenic mice) and rat (HLA B27 transgenic) models, spontaneous colitis models, adoptive transfer (CD45B) models, inducible colitis models. This latter includes several widely used models including the acid acetic, oxazolone, indomethacin, TNBS and dextran sulphate sodium (DSS) murine models [129].

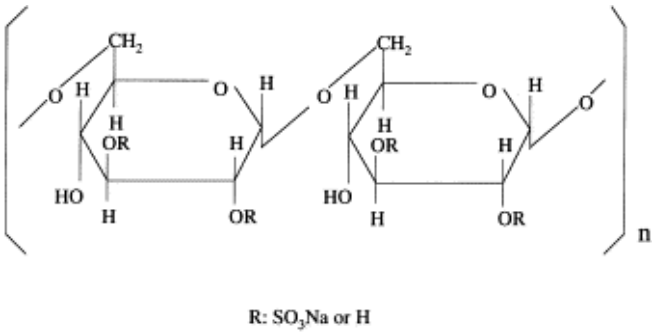


Figure 17: Structure of DSS [131]

DSS is a heparin-like polysaccharide (Figure 17), when administered in drinking water to mice, induces experimental colitis. High reproducibility and simplicity of DSS-induced colitis are mainly responsible of the widespread use of this model for evaluating nanomedicines [118, 132-134]. DSS administration may vary depending on the period of exposition (± 5 days) and the concentration in the drinking water (± 5%). DSS-induced inflammation mimics clinical and histological characteristics of IBD with UC characteristics [135]. Indeed, administration to the rodents of water containing DSS results in the apparition of body weight loss, bloody diarrhea, shortening of the intestine, mucosal ulcers, and infiltration of neutrophils [44, 129].

DSS administration causes acute and chronic colitis. Acute colitis, which occurs during the administration, seems to be induced only by innate immunity. Meanwhile, chronic colitis is

considered to be induced by acquired immunity and occurs a little later [129]. The mechanism of DSS-induced colitis is not fully understood, but it seems that the presence of DSS leads to two consecutive events. Hyperosmolarity caused by DSS is the primary effect. It increases the permeability of intestinal cells and damages crypts. This leads to the deregulation of the intestinal epithelial cell barrier function and to diarrhea, the most common symptom of IBD. As a result, massive quantities of immune-related cells such as T and B lymphocytes, macrophages and neutrophils infiltrate massively and are responsible of mucosal inflammatory responses. The second phase consists in enhanced production of both Th1 and Th2 cytokines by activated macrophages. Indeed, correlation between profile of relevant cytokines as TNF-α and IL-6, with clinical and histological parameters as well as barrier properties has been demonstrated [135]. Inflammation-induced changes of histological, biochemical and macroscopic characters have been used as markers to screen drugs: clinical activity score, myeloperoxidase activity, colon body/weight ratio or cytokine levels.

Usually used as acute colitis model, DSS-induced colitis may become chronic. For instance, 5% DSS given to Swiss-Webster mice by cycles of 7 days of DSS followed by 7 days of water for 5-7 cycles may result in chronicity to the colitis [136]. Continuous administration of 5% DSS during 5 days to C57Bl/6 mice showed chronic characters [137]. Chronic lesions were characterized by enhanced infiltration of cells such as plasma cells, lymphocytes, foamy macrophages, prominent lymphoid aggregates in the lamina propria and serosa, a patchy distribution of inflammation, and fissuring ulcers [138].

Although well established, the DSS-induced colitis model has been criticized. Most of all, DSS model is considered as an acute injury to the epithelial barrier and its subsequent immune reaction. The model fails to mimic the disregulation of the innate or adaptive immune responses, an inner mechanism of pathogenesis of IBD, possibly leading to a misinterpretation of the interaction between nanocarriers and immune-related cells [44].

II.1.3 The purpose of nanocarriers for IBD treatment

Drug targeting consists in the identification and management of a feature that is unique in the target organ. The optimal vehicle should, after oral administration, ensure the topical delivery in the inflamed colon, while avoiding systemic absorption. Several approaches have been proposed for drug delivery to the colon, whatever its state: prodrugs, pH- and time-dependent systems, microflora-activated systems, pressure, etc [139]. However, even if the topic has been extensively studied, very few IBD specific drug delivery systems have given

clinical solutions [95]. This may be due to the fact that these delivery strategies are not strongly related to the inflammation and barely to its location, and then do not constitute real targeting.

Size reduction has become a key characteristic in the formulation of drug delivery systems. Pellet based systems successfully used the reduction of drug carrier size property to increase of the residence time in the large intestine [96]. In IBD patients, an enhanced accumulation of microparticles of 3 µm in size was observed in ulcerous lesions [140]. Compared to 10 µm- and 1 µm-sized particles, 100 nm-sized particles showed the highest binding to inflamed areas of colonic mucosa in a rat TNBS-induced colitis model [141].

Another important factor is the net surface charge of nanoparticles: negatively charged particles are attracted by high concentrations of positively charged proteins in ulcerated tissues as eosinophil cationic proteins. In *ex vivo* colon sacs of dinitrobenzene sulfonic acid treated rats, cationic, anionic and neutral multilamellar liposomes (800±50 nm) were compared in terms of adherence to inflamed tissue. In the inflamed tissue, anionic liposomes preferentially adhered to the inflamed tissue, while cationic liposomes only showed a weak binding. The situation was inverted in the healthy epithelium [142]. Moreover, a study with confocal laser endomicroscopy revealed mucosal accumulation of negatively charged PLGA nanoparticles in ulcerous lesions of human patients with IBD [140]. However, interaction between mucus and nanoparticles is also a key factor. Indeed, positively charged nanoparticles will more adhere to the mucus, mainly due to their main anionic protein components, called mucins. In this context, negatively charged nanoparticles present an opposite behavior and adhere less to the mucus [96]. Furthermore, engineering nanoparticles able to avoid rapid mucus clearance and to cross mucus barrier is a major concern. By mimicking the densely charged net neutral surface of viruses, the concept of mucus-penetrating particles has been investigated. PEG coating of the nanoparticles improved their transport through the mucus by up to 3 orders of magnitude [108, 143]"

II.1.4 Nano-sized delivery strategies for IBD treatment

Nevertheless, size is not sufficient to design the optimal drug delivery system able to target efficiently the inflamed regions of the colon and deliver its content. As discussed earlier, the inflamed colon presents specific and disrupting characteristics, which can dissociate it from the rest of the GIT. The triggering mechanism of the drug delivery system must respond to the pathophysiological conditions particular to the environment of the inflamed colon such as

mucus overproduction or disrupted epithelium. Likewise, conflicts may appear when designing nanoparticles.

II.1.4.1 Passive Targeting

In cancer research, passive targeting takes advantage of the size of nanoparticles and exploits the unique anatomical and pathological abnormalities of the tumor vasculature. The structure of ulcerated regions of inflamed colonic tissue presents similarities with the tumor vasculature such as a disrupted barrier and an exacerbated presence of immune-related cells in areas of active inflammation (Figure 18). So colon specific drug delivery systems can also benefit from the “enhanced permeability” effect. Smaller particles were found to accumulate more easily in the inflamed mucosa and particle adhesion to inflamed area is found enhanced due to strongly increased mucus production leading to a thicker mucus layer [92]. To a lesser extent, neutrophils, mast cells, natural killer cells or T helper cells are some of the immune-related cells, which are highly present in inflamed areas of active IBD colon. Above all, macrophages and dendritic cells play also a significant role in this “enhanced accumulation” phenomenon. As they are able to take up small particles (≈ 4 µm) or bacteria by phagocytosis, their increased presence will also lead to preferential uptake of nanoparticles and small microparticles into inflamed intestinal areas [96].

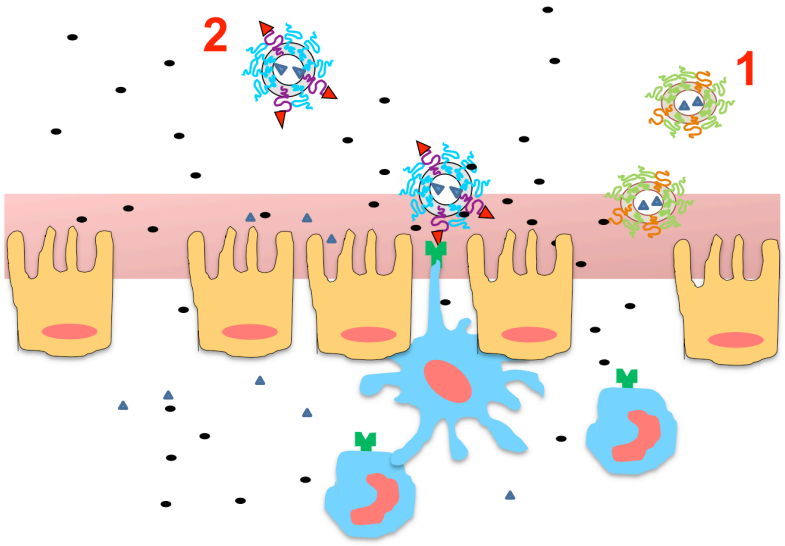


Figure 18: Passive & active targeting in the context of IBD-related inflamed mucosa. Black dots represent antigens.

II.1.4.2 Active targeting

In active targeting, ligands are grafted at the nanoparticles' surface. The ligand is chosen to bind specific receptors overexpressed by the targeted tissue. In the case of IBD, this ligand has to be overexpressed in the inflamed tissue and less or non-expressed by the healthy tissue (Figure 18). In inflamed areas and ulcerated regions of colonic mucosa, there is a higher presence of immune-related cells compared to healthy tissue. As these cells present specific receptors, they can act as targets for nano-sized drug delivery systems. For instance, macrophages and dendritic cells expressed on their membrane mannose receptors. The grafting of mannose on the surface of the nanoparticles will lead to their preferential uptake by mannose receptor presenting cells such as macrophages and dendritic cells [144]. Other ligands such as antibodies for the human transferrin receptor have successfully decorated liposomes to target inflamed intestinal epithelial cells. Indeed, in a healthy state, this receptor is only expressed in the basolateral membrane of the intestinal epithelial cells. In an inflamed state, this transferrin receptor is also expressed in the apical

part of the epithelial monolayer [145]. However, as far as we know, no relevant active targeted polymeric nanoparticulate formulations have been shown yet to have *in vivo* efficacy.

II.1.4.3 pH-sensitivity

As luminal pH is dependent on the part of the GIT, it is possible to target the colon by using a pH-dependent nanoformulation. As colon presents a luminal pH close to 7, an efficient colon specific drug delivery strategy should withstand low pH values of the upper part of the GIT and dissolve itself in more neutral pH, leading to a release of its content in the targeted colon. On this purpose, several pH-sensitive nanoformulations have been reported. Some polymers of Eudragit family possess a pH-sensitive profile. Depending on the ratio of methacrylic acid and methacrylate, these copolymers can withstand acidic environment and dissolve at the desired pH. Eudragit P-4135F- or Eudragit S100 nanoparticles present therapeutic efficacy in experimental colitis [114, 133]. However, the pH-sensitive targeting method has been questioned. As previously said, in active IBD, intraluminal colonic pH has been found lower than expected. This feature can lead to unspecific colon delivery and incomplete drug delivery and release.

II.1.4.4 Mucoadhesion and mucopenetration

Topical delivery in the inflamed colon may lead to consider the mucus as a target and a barrier at the same time. In other terms, difference must be done between adhesion and penetration of particles. Mucus possesses superficial layers on the luminal side, which are faster cleared than the ones close to the epithelium. So if the nanocarriers just adhere to the luminal layers, they will be easily washed and cleared from the stream. Mucus penetrating nanoparticles must be small enough to penetrate the mucus and must avoid steric obstruction and adhesion to deliver properly the content in the mucosa. A preferential adherence to the mucosal tissue has been found for 100 nm-sized fluorescent nanobeads compared to 1 µm and 10 µm-sized beads, as removing the mucus from the inflamed tissue leads to a reduction of the total fluorescence by respectively 39, 31 and 14 % [146]. As the mucus is full of negatively charged proteins, the mucins, positively charged particles present intrinsic mucoadhesive properties. For this purpose, polymers such as chitosan and its derivatives have been used extensively in the formulation of mucosal drug delivery systems with little success [147].

II.1.4.5 Enzymatic-triggered nanosystems

Sulfasalazine, azo-prodrug of 5-aminosalicylic acid (5-ASA), has been the first drug delivery system to use colon specific enzymatic cleavage. In the same vein, focus must be placed on

in the use of drug delivery systems especially biodegradable by colonic bacteria [148]. This strategy is based on the presence of bacterial enzymes such as polysaccharidases, which are available in sufficient quantities to be exploited in colon targeting of drugs. Synthetic polymers or natural polysaccharides including pectin, guar gum, amylose, inulin, dextran, chitosan or chondroitin sulphate are their substrates and can be used as drug carriers. For instance, even if three chitinases have shown enzymatic activity in the human body, chitosan and its derivatives are thought to be degraded in vertebrates mainly by bacterial enzymes in the colon [149]. Cleavage of linking functions such as amino acid, glycoside, glucuronide and sulphate are generally the targeted ones. However, one of the main drawbacks of this strategy is its dependency on the colonic bacterial enzymatic activity, which is modified depending on the type of IBD and the stage of the disease. Thus, the colonic microflora of CD patients is subject to intervariability. These two phenomena lead to variability in drug release for enzymatic-triggered nanosystems [96, 150].

II.1.4.6 Time-dependent drug delivery

This delivery strategy is based on the transit time parameter of the GIT. After oral administration, time-dependent colonic delivery systems are designed to present a lag phase in drug release, resulting in the exclusion or at least the reduction of the drug release in the upper part of the GIT. This property can be ascribed to the use of swellable, erodible, or rupturable hydrophilic polymers. Biodegradable polymers such as PLGA can allow this sustained release and have been used in nanoformulations [124, 133]. Pathophysiological IBD changes such as diarrhea and motor disorders disturb transit times, resulting in ineffective colonic targeting and incomplete drug release [96].

II.1.4.7 Reduction-responsiveness

IBD-induced ROS represent a promising therapy. A way of action should be to use this high level of ROS as a targeting way. For this purpose, siRNA TNF-α loaded thioketal nanoparticles were designed via a new polymer able to degrade in response to ROS, the poly-(1,4-phenyleneacetone dimethylene thioketal) (PPDAT). In a DSS-induced colitis mice model, these orally administered nanoparticles decreased the TNF-α mRNA levels and protect mice from UC [134].

II.1.4.8 Lipid-based therapy

As said earlier, data about the relation between lipid depletion and IBD-induced inflammation suggest that the use of lipid-based nano-sized drug delivery systems as carriers but also as active immunomodulators may be of good interest [107].

Self-emulsifying drug delivery systems emulsify forming oil-in-water emulsions due to mild agitation. This phenomenon also occurs in the GIT [151]. Formulated with PEG6000, castor oil, Tween 80 and Span 80, SEDDS loaded with the poorly water-soluble curcumin was evaluated successfully as IBD therapeutic alternative [152].
Nanostructured lipid carriers are a subclass of solid lipid nanoparticles composed of biocompatible and biodegradable lipids. Their high consistency property makes them suitable for topical applications [153]. However, as far as we know, no IBD-related studies using nano-structured carriers (NLC) as drug delivery systems have been published for IBD treatment.

II.1.4.9 Microencapsulation

Once delivered orally, nanoparticles have to face the harsh conditions of the upper part of the GIT before reaching the inflamed colon where they can be subject to premature uptake or simple enzymatic particle degradation. In order to avoid these negative side effects, the idea of a two-phase release system containing the nanoparticles has emerged.

Hydrogels, hydrophilic networks of polymer chains containing 99% of water, can protect the drug delivery system until it reaches its area of action. Laroui et al. created a hydrogel-encapsulated nanoparticles system. Based on the association of two biocompatible and biodegradable polysaccharides, alginate and chitosan, the system was able to collapse in the colon and deliver their content in the desired area. A specific method of gavage called the double-gavage procedure was used to prevent early degradation in the upper tract. This system was able to load bioactive compounds such as peptides, proteins and siRNA and to treat DSS-induced colitis mice [132, 154].

Another strategy to deliver nanosized systems to the inflamed colon is the loading of nanoparticles into pH-sensitive microspheres (NPMS) [155, 156]. Eudragit P-4135F was chosen as microsphere polymer, as it is defined by a higher dissolution pH. Tacrolimus loaded PLGA nanoparticles were successfully entrapped into microspheres. In vitro, NPMS showed strong pH-sensitive release kinetics, resulting in a likely retention of drug release during intestinal passage. During the *in vivo* colitis in rats, severity of inflammation was assessed and significant mitigating effects of NPMS were observed in terms of clinical activity or myeloperoxidase activity.

II.1.5 The perfect nanocarrier for IBD

Table 4 resumes the key characteristics that should have this “perfect nano-sized drug delivery system”.

Table 4: Key characteristics of the "perfect nano-sized drug delivery system" Adapted from [96]

Characteristics of IBD colon targeting	Objectives	Nanoparticle mechanisms for colonic drug release
Last part of the GIT	- Protection against acidity of the stomach - Avoid high intestinal enzymatic metabolism	- Resistance to low pH - Controlled release
Transit time	- Take account of the decrease of the transit time	- Biodegradable - Sustained release
pH	- Use pH profile of the GIT as a trigger	- pH-sensitive release (6.8<pH7.4)
Microflora	- Use colonic microflora specificity as a trigger	- Prodrug or polysaccharide-based polymers bacterially triggered only by colonic microflora
Mucus	- Avoid adhesion to the superficial layers and thus rapid clearance - Avoid steric obstruction and thus promote mucus penetration	- Mucoadhesivity (Net surface charge > 0) - Nano-range (100-500 nm) - Hydrophilic, net-neutral surface (PEG-coating)
Inflamed epithelium	- Take advantage of disrupted epithelium - Use overexpression of immune-related cells (macrophages and dendritic cells) as a target	- "Enhanced permeability" effect for small particles (size ≈ 100 nm) - Net surface charge < 0 - Active targeting (mannose ligand, etc…)
Systemic absorption	- Enhance topical delivery in the mucosa - Increase the local drug concentration in the inflamed tissue	

Mixing the strategies may appear as a necessity to obtain efficient IBD-specific drug delivery systems. For example, reducible sodium alginate nanospheres cross-linked with disulfide linkages were synthesized for IBD, with pH-sensitivity and reduction-responsiveness as strategies [157].

II.1.6 IBD drugs in nanoformulations

II.1.6.1 Conventional drugs

Common anti-IBD approaches include 5-aminosalicylates, antibiotics, corticosteroids, immunosuppressants or anti-TNF antibodies. They are documented and described in terms of solubility, oral biodisponibility, pharmacokinetics, ADME properties, safety and clinical efficacy [67].

Used for more than 30 years in clinical practice for IBD, 5-aminosalicylic acid (5-ASA) is the pharmacophore moiety of the class of aminosalicylates. Once orally delivered, very low amounts of 5-ASA arrive in the colon and are absorbed. Besides, metabolization results in the predominance of the inactive metabolite, N-acetyl-5-ASA, responsible for significant side

effects. As 5-ASA has a topical activity, its clinical efficacy depends on the local concentration present in the inflamed mucosa. Therefore, it is preferable to deliver the 5-ASA specifically to the colon. For this purpose, 5-ASA was efficiently encapsulated in pH-sensitive nanoparticles using the solution enhanced dispersion by supercritical fluids technique [158]. 5-ASA loaded nanoparticles with a size of 200-350 nm were formulated using methods of oil/water emulsification or nanoprecipitation. To reduce early drug loss and considerable delay the drug release, 5ASA was covalently bound to the matrix polymer poly(ε-caprolactone). The advantages of the encapsulation were to lower significantly the active dose of 5ASA while giving *in vivo* efficacy with a decrease in clinical activity score and myeloperoxidase activity (MPO) [99].

Budesonide, the current ideal corticosteroid against IBD (see I.4.4), was encapsulated in two different nanocarriers, PLGA nanoparticles and liposomes. With a size range of 190 to 220 nm, these nanocarriers provide efficient anti-inflammatory *in vitro* activity and good recovery effects in function of the *in vitro* barrier model [124]. In another study, a budesonide-loaded pH-sensitive nanoformulation using polymeric mixture of PLGA and Eudragit S100 was formulated. They retained their content in acidic and neutral pH values followed by a sustained release phase at pH 7.4. In a TNBS-induced colitis model, superior therapeutic activity of these nanospheres was demonstrated [114].

Immunosuppressive drugs demonstrated to be a very potent drug in the treatment of severe cases of IBD where steroid treatment failed. As they are administered systemically by intravenous injection, one of their main drawbacks is their non-selectivity to inflamed tissue, which is the cause for nephrotoxicity. A selective delivery in the inflamed colonic mucosa is of high interest, as it should ameliorate their side effects profile, their tolerability and their therapeutic activity. Tacrolimus-loaded nanoparticles were prepared from either biodegradable PLGA or pH-sensitive Eudragit P-4135F polymers, using a simple oil/water emulsification method. In a DSS-induced colitis model, both nanoformulations showed similar alleviating effects while nephrotoxic adverse effects were slightly less expressed with pH-sensitive nanoparticles [133]. In another study, more focus was placed on nanoparticle deposition and penetration in the inflamed tissue of two different murine colitis models. Tacrolimus-loaded PLGA nanoparticles showed enhanced and selective drug penetration into the inflamed areas of the colon as opposed to surrounding healthy tissue. They acted as some kind of drug reservoir with reduced drug availability in the healthy areas and provide selectively enhanced drug penetration into the inflamed tissue compared with free drug, whereas in healthy tissue, this phenomenon was reversed [159].

II.1.6.2 Potential drugs

Drugs used normally as therapy options of other diseases can become IBD therapeutic compounds as long as their topical delivery in the inflamed colon allows for efficient use of their therapeutic effects. In this case, an efficient colon-specific drug delivery system may offer new therapeutic perspectives to a drug.

Rolipram, a selective phosphodiesterase inhibitor used normally as an antidepressant, present anti-inflammary effect due to its inhibitive activity on TNF-α production. In a TNBS murine model, rolipram-loaded PLGA nanoparticles provided significantly better inflammation control and less adverse effects than rolipram solution [160]. Due to its suppressive effect on macrophage activity and its low oral bioavailability, clodronate, a bisphosphonate normally used for osteoporosis, was used in experimental colitis. Obtained by a modified solvent displacement method, 120 nm-sized clodronate loaded Eudragit RL-based nanoparticles showed a dissolution medium- and mucin-dependent drug release. In *in vitro* activated macrophages, only these nanoformulations led to a decrease in TNF-α and IL-6 secretion compared to clodronate solution. In 2 murine colitis models, MPO decreased significantly after treatment with clodronate loaded nanoparticles compared to free solution [161].

Successful use of anti-TNF-α antibodies infliximab or certolizumab pegol in IBD therapy has highlighted biopharmaceutical drugs as alternative IBD armamentarium. However, most of these biopharmaceutics (proteins, peptides or nucleic acids) possess bad profile for oral administration: degradation by acidic pH of the stomach, sensitivity to nucleases, lipases, and peptidases overexpressed in the GIT or poor permeability across the mucus or the intestinal epithelium. Encapsulation of these biopharmaceutics in nano-sized drug delivery systems should help improve their physicochemical profile in order to target specifically the inflamed colon.

The central pro-inflammatory cytokine TNF-α is secreted mainly in the inflamed colon by macrophages and dendritic cells. Direct and local inhibition of TNF-α secretion from these cells should reduce IBD inflammation and systemic side effects. Following this idea, TNF-α siRNA/polyethyleneimine was loaded into 380 nm-sized poly(lactic acid) (PLA) nanoparticles. They showed a high encapsulation rate of TNF-α siRNA and *in vitro* and *in vivo* significant anti-inflammatory effects in LPS-treated mice [162].
An efficient strategy should be the inhibition of the transcription of the proinflammatory mediators such as IL-1β, IL-6 or TNF-α. Encapsulated in oral chitosan-modified PLGA nanospheres, a double-stranded decoy oligonucleotide synthetized to bind NF-κB

demonstrated effective results in *in vitro* model and mitigating effects on DSS-induced colitis model [118].

By inhibiting MAPK and NF-κB, the 2 key intracellular signaling pathways of intestinal inflammation, the tripeptide KPV (Lys-Pro-Val) present an anti-inflammatory effect. Once added to drinking water or by intraperitoneal administration, decreased inflammation in experimental colitis. In order to avoid the harsh conditions of the upper part of the gut and target the colon specifically, KPV was first encapsulated in biodegradable PVA-covered PLA nanoparticles then loaded in a colonic-triggered polysaccharide gel containing 2 polymers, alginate and chitosan. Once delivered in the colon by the gel, these nanoparticles delivered extracellularly the peptide close to the epithelial layer and ameliorate inflammatory parameters in a DSS-induced colitis model [132].

Probiotics are living microorganisms with a desired and beneficial effect on human health [163]. In IBD therapy, their consumption may provide anti-colitis, anti-inflammatory and immunomodulatory effects even it remains controversial [164]. Several interrelated mechanisms of action of probiotics in IBD therapy have been proposed: (1) competitive exclusion with microbial pathogens on the surface epithelium, (2) immunomodulation, (3) antimicrobial activity, (4) enhancement of barrier activity through mucin production and secretion; and (5) induction of T-cell apoptosis [165]. However, in immunodeficient patients, high doses can be responsible for severe infection. One solution may be the use of cell-free probiotic extract. So lyophilized probiotic extract was efficiently encapsulated in 200 nm-sized chitosan-coated PLGA nanoparticles in order to use mucoadhesion and uptake into immune-related cells as targeting strategies. In a TNBS-induced colitis model, these nanoparticles provide mitigating effects in control of colitis [166].

II.2 POLYMERIC NANOCARRIERS OF INTEREST

In addition to the submicronic size responsible of the preferential uptake in the inflamed colonic areas, polymeric nanoparticles present the ability to design their surface, resulting in the possibility to use several inflamed colon specific drug delivery strategies. Based on the literature, the selection of 3 different polymers make it possible to create several nano-sized drug delivery systems using different delivery strategies: (i) pH-sensitivity; (ii) mucoadhesivity; (iii) sustained release; (iv) passive or active targeting.

II.2.1 Eudragit®: A pH-sensitive polymer

It is a generally accepted fact that pH increases progressively in the GIT, from low pH values in the upper part (stomach and proximal part of the intestine) to neutral of slightly alkaline pH values in the lower part (ileum and colon). So a pH-sensitive approach consists in the use of polymers able to withstand low pH values of the gastric fluid and disintegrate in the colon. Several polymers (polyvinylacetate phthalate, hydroxypropylmethylcellulose phthalate, cellulose acetate trimelliate and cellulose acetate phthalate) have been used for this purpose but most commonly used pH-sensitive polymers are coming from the Eudragit® family [103].

Developed by Rohm & Haas Gmbh, Eudragit® polymethacrylates are a class of vinyl copolymers made from 2 monomeric species, ester of acrylic and methacrylic acid. These biocompatible acrylic resins are pharmacologically inactive. They possess excellent film-forming characteristics, which make them widely accepted excipients. Physicochemical properties of the Eudragit polymethacrylates can be customized by the presence and the proportion of acid, neutral or alkaline functional groups. Thereby, the mixing of different Eudragit polymers allows unlimited choice of controlled drug release profiles and this in various applications. Eudragit® polymeric family can be divided in 2 types: pH-dependent and pH-independent [167].

For colonic targeting, the characteristic of interest of the Eudragit polymers is the pH-dependent dissolution in aqueous solution. The pH-sensitive property of Eudragit® L, S and E is due to the presence of ionisable functional groups, which provokes their controlled dissolution in one of the compartment of the GIT. For example, anionic Eudragit® L and S possessed ionizable -COOH groups. Thus, insoluble in the stomach due to the acidic pH, the ionization of the carboxylic group occurs, as the dosage form reaches the intestine and the pH increases. This leads to a structural change in the polymer and thus its solubilization [168]. An optimal pH-sensitive drug delivery system should protect its content from the acidic pH of the stomach but release it in the colon, where luminal pH is more neutral. Based on this hypothesis, three Eudragit® polymers are available for formulations of colon drug carriers: Eudragit® FS 30 D, Eudragit® S 100 and Eudragit® S 12.5. This latter was not studied.

Eudragit® FS 30 D, a 30 % (w/w) aqueous dispersion of a copolymer derived from methacrylic acid, methyl acrylate and methyl methacrylate was the first pH-sensitive polymer of interest. With a 1:10 acid to ester ratio, its dissolution pH was above 7. As pH increases, release from Eudragit® FS 30 D is increasing. Furthermore, the release rate of mesalamine

from pellets coated with Eudragit® FS 30 D (Asamax®) was found slower than the one with Eudragit® S. With Eudragit® FS 30 D, action of mesalamine on the targeted area is supposed to last longer [169]. Average molecular weight is approximately 220,000 Da. However, when aqueous dispersions such as Eudragit® FS 30 D are used for coating applications, stickiness appears. Adding of glidants (talc) and plasticizers (triethylcitrate) is supposed to improve the coating [170].

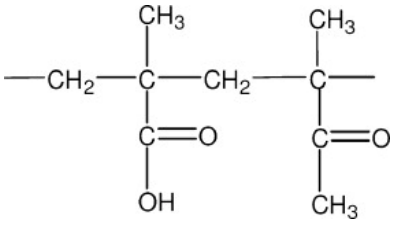


Figure 19: Chemical structure of Eudragit S 100. The ratio of the free carboxyl groups to the ester groups is 1:2

Available as a powder, the second polymer of interest, Eudragit® S100 (ES100), is an anionic mixture of methacrylic acid and methacrylates with ionizable -COOH groups and a methacrylic acid content of 27-30.6 %, corresponding to an acid to ester ratio of 1:2 (Figure 19). Because of this structure, the polymer is insoluble at low pH values, dissolves at pH > 7 and is used for colon drug release. The average molecular weight of this polymer is approximately 135 kDa. ES100 is soluble in organic solvents such as ethanol, acetone or aqueous isopropyl alcohol. Asacol®, an ES100-coated tablet loaded with mesalamine is available for clinical practice.

Eudragit® FS 30 D was used as a film coating for several carriers available for targeting and delivery in the colon: multiple-unit dosage system loaded with the drug model caffeine [171], multiparticulate tablets containing enteric pellets [172], tablets loaded with budesonide, piroxicam or diclofenac [173, 174] or 800 µm-sized meloxicam-loaded colon-specific pellets [175]. However, as far as we know, no nanosized drug delivery system was developed and/or *in vitro* or *in vivo* evaluated.

II.2.1.1 Eudragit® based nanosized drug delivery systems

Several methods of formulation have been listed in the literature to encapsulate various drugs ES100 based nanoparticles (Table 5).

The emulsification solvent evaporation method is widely used to encapsulate poor water-soluble drugs. Briefly, drug and polymer are dissolved in an organic solvent such as acetone

and/or methanol, then an aqueous solution made of water and a surfactant (e.g. polyvinyl alcohol) is added to the polymer solution, resulting in an emulsion of oil (O) in water (W) i.e. O/W. The nanosizing of the emulsion is energetically induced by homogenization or sonication. The elimination of the solvent occurs by evaporation or extraction and the nanoparticles are then washed several times with distilled water by centrifugation to remove the non-entrapped drug and the non-participating polymer or surfactants [176]. This technique has been slightly modified in order to encapsulate hydrophilic drugs. Thus, nucleic acids, peptides or proteins can be contained by ES100 based carriers via a double emulsification W/O/W solvent evaporation technique [177].

Also known as interfacial deposition, the nanoprecipitation method consists of the combined dissolution in the organic phase of ES100 polymer and hydrophobic drug prior to the dropwise addition to the aqueous phase. After the organic solvent evaporation, nanoparticles are washed by centrifugation [178, 179].

A modified quasi-emulsion solvent diffusion (QESD) technique has also been used to provide ES100 based nanocarriers [180, 181]. In brief, the drug is first dissolved in an organic phase containing ES100 polymer. Then, the whole solution is added slowly in the aqueous phase containing some surfactant under agitation. At this stage, a biphasic solution appears immediately with a polymer-organic solvent solution in the external phase and a drug-containing pseudo-emulsion in the internal phase. After evaporation of the organic solvent, the ES100 nanoparticles are separated from the polymer sediments, centrifuged and washed.

Other methods exist such as the solvent displacement or solution enhanced dispersion by supercritical fluids methods [158, 182]. For a combined delivery strategy, the ES100 polymer can be associated with other polymers. For instance, by modified spontaneous emulsification solvent diffusion, a mixture of ES100 and poly(lactic-co-glycolic) acid have been successfully proposed to provide a more sustained pH-sensitive release of the content in the colon [114]. ES100 has also been used as simple coating for mucoadhesive nanoparticles made with chitosan and tripolyphosphate [183].

II.2.1.2 Mechanism of drug release from ES100 nanoparticles

At low pH, the carbonyl oxygen of ester group and the hydroxyl groups of the carboxylic moiety form intra- and intermolecular hydrogen bonds, leading to a compact structure of the polymer. Consequently, in the stomach, the polymer is characterized by low porosity and permeability. The pH-dependent release of the encapsulated drug from ES100 nanoparticles

is due to the mixing between dissolution and swelling. The dissolution of ES100 polymer occurs gradually, as pH of the surrounding medium is moving closer to 7, the theoretical dissolution trigger pH. Furthermore, swelling is supposed to appear at pH above 6.5, contributing also to the release to the content [184].

II.2.1.3 Colon delivery of drug loaded-Eudragit based nanoparticles

Several colon specific drug delivery systems have been developed, with Eudragit S100 as polymer. These nanocarriers may provide an effective colon specific delivery system, as they offer a pH-dependent release, providing protection from the harsh conditions of the upper part of the GIT and specific colonic release of the encapsulated drug. Prednisolone encapsulated in 550 nm-sized ES100 nanocapsules was liberated after 3-h lag time in rat, corresponding to arrival in colon [179].

Budesonide was loaded in a polymeric nanoformulation made with a mixture of ES100 and poly(lactic-co-glycolic) acid (PLGA). *In vitro* drug release studies showed a pH-dependent release profile of the nanoformulation. Indeed, a few amount of budesonide was released in acidic pH values whereas an important and sustained release of budesonide was observed at pH 7.4. In a TNBS-induced murine colitis model, *in vivo* localization of coumarin-6-loaded nanospheres demonstrated a specific accumulation in inflamed colon. In the same *in vivo* colitis model, anti-inflammatory activity of budesonide-loaded nanoparticles displayed a better anti-inflammatory activity than budesonide in suspension [114].

Table 5 lists some examples of Eudragit-based nanoparticles and explains the process of drug encapsulation and potential applications.

Table 5: Examples of Eudragit S100 based nanoparticles

Processes	Encapsulated Drug	Size (nm)	Polydispersity index	Entrapment Efficiency (%)	Applications/Models	Ref
Simple emulsification solvent evaporation	Curcumin	97 ± 2.47	0.14 ± 0.01	72.81 ± 0.13	Colon (Colon cancer) HT-29 human colon adenocarcinoma cell line	[176]
Double emulsification solvent evaporation	Papain	676.4 ± 66		82.35 ± 3.10	Gastrointestinal In vitro release, digestion and stability	[177]
Nanoprecipitation	Diclofenac	172	0.14		Ophthalmic PGE(2)-induced ocular inflammation in rabbit model	[178]
	Prednisolone	567.87	- - -	90.21	Colonic (IBD) in vitro & in vivo release studies	[179]
Modified quasi-emulsion solvent diffusion	Model compounds				Vaginal	[180]
	- Sodium fluorescein	241.9 ± 8.2	0.09 ± 0.04	26.2 ± 2.7	In vitro studies (VK2/E6E7 vaginal epithelial cell line)	
	- Nile red	331.7 ± 25.0	0.23 ± 0.06	71.4 ± 3.8		
	Cyclosporine A	37.4 ± 5.6	- - -	99.9 ± 0.05	Oral bioavailability improvement In vitro & in vivo studies	[181]
Modified spontaneous emulsification solvent diffusion (mixed with PLGA 1:1)	Budesonide	282.8 ± 23.4	0.197 ± 0.08	92.68 ± 0.53%	Colonic (IBD) TNBS colitis rat model	[114]
	Coumarin-6	240	- - -	85.9 ± 1.05%	In vivo localization	
Solution enhanced dispersion by supercritical fluids	5-Aminosalicylic Acid	147 ± 16	0.62 ± 0.05	51.12 ± 1.85	Colonic (IBD) Influence of processus parameters Physico-chemical Characterization	[158]
Solvent displacement method	Sorafenib	64.6	- - -			[182]
Ionic gelation/complexation TPP & coating with ES100	Thymopentin	175.6 +/- 17	- - -	76.70 +/- 2.6%	Oral administration *in vitro* lymphocyte proliferation test *in vivo* immune function (CD4+/CD8+) of irradiated rat	[183]

II.2.2 PLGA: From the sustained release to the active targeting[1]

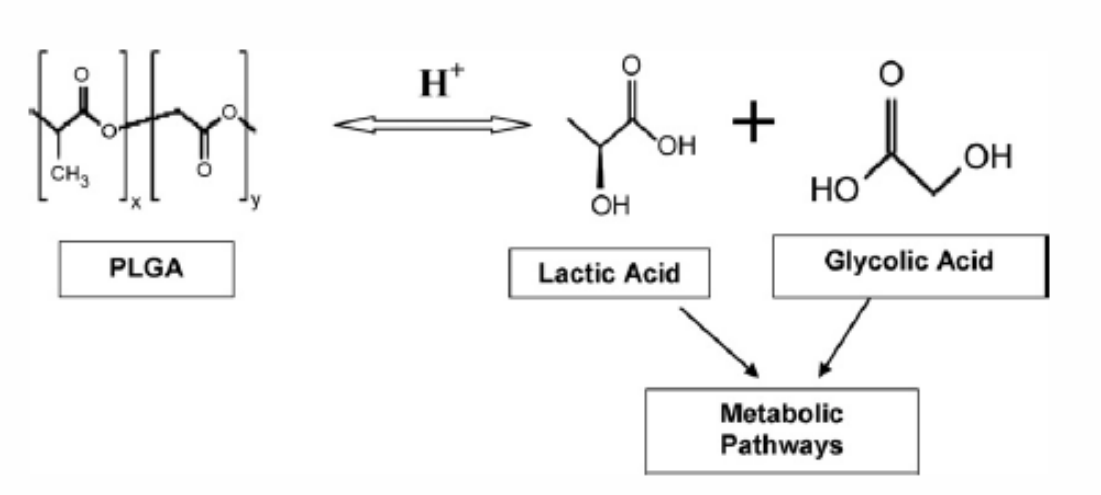


Figure 20: Scheme of the hydrolysis of PLGA [185]

Poly(lactic-co-glycolic acid) (PLGA) is one of the most successfully used biodegradable polymers because its hydrolysis leads to metabolite monomers, lactic acid and glycolic acid (Figure 20). Because these two monomers are endogenous and easily metabolized by the body via the Krebs cycle, a minimal systemic toxicity is associated with the use of PLGA for drug delivery or biomaterial applications [185]. The US FDA and the European Medicines Agency have approved PLGA for the formulations of various drug delivery systems in humans. The polymers are commercially available with different molecular weights and copolymers composition. The degradation time can vary from several months to several years, depending on the molecular weights and copolymer ratio [186, 187]. The forms of PLGA are usually identified by the monomers ratio used. For example, PLGA 50:50 identifies a copolymer whose composition is 50 % lactic acid and 50 % glycolic acid. PLA has also been used to a lesser extent than PLGA due to the lower degradation rate.

[1] This chapter was adapted from Danhier F., Ansorena E., Coco R., Silva J., Le Breton A., Préat V. PLGA-based nanoparticles: an overview of biomedical applications. *J Control Release* **161**, 505-522

II.2.2.1 Optimization of PLGA-based nanoparticles

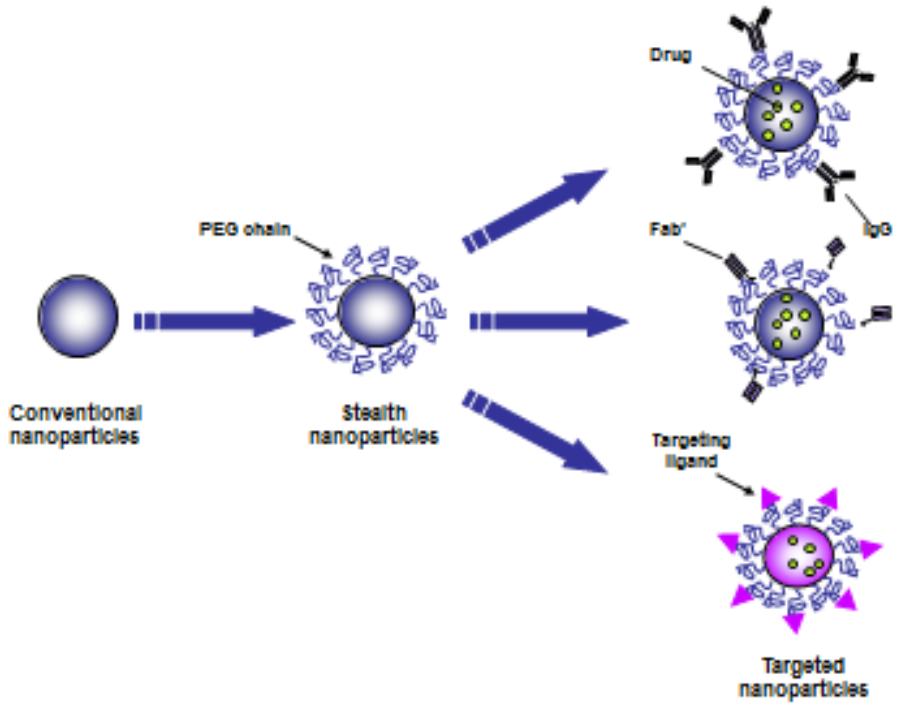


Figure 21: Schematic representation of nanoparticles [92]

PLGA-based nanoparticles have been widely used to encapsulate various compounds. However, once in the bloodstream, it is noteworthy that the body recognizes hydrophobic particles as foreign. The reticulo-endothelial system (RES) eliminates them from the blood stream and takes them up in the liver or the spleen. Briefly, the recognition and the binding of opsonin proteins present in the blood serum to injected nanoparticles leads to attachment of opsonized particles to macrophages and subsequently to their internalization by phagocytosis [188]. To address these limitations, several methods of surface modifications have been developed to produce nanoparticles not recognized by the RES. Nanoparticles can be coated with molecules that hide the hydrophobicity by providing a hydrophilic layer at the surface. The most common moiety for surface modification is the hydrophilic and non-ionic polymer polyethylene glycol (PEG) (Figure 21). It has been largely demonstrated that the "PEGylation" increases their blood circulation half-life by several orders of magnitude [188]. As a matter of fact, PEG presents repulsive properties, as they can block the electrostatic and hydrophobic interactions that help opsonins to bind to particles surfaces. PEGylation of the surface of the particles leads to a decrease in the steric effect and thus a higher stability of nanoparticles in biological fluids. Moreover, PEG exhibits an excellent biocompatibility. So PLGA-PEG has been widely used instead of or in combination of PLGA

to formulate “stealth nanoparticles”. Poloxamer, poloxamines or chitosan have been also studied for surface modification [185, 189].

Another application of surface modification is the targeting of specific organs or areas to increase selective cellular binding and internalization through receptor-mediated endocytosis. Targeting ligands are often grafted at the nanoparticles surface via a linkage on PEG chains [190]. Ligands need to be optimally conjugated on nanoparticles to maintain their affinity for receptors binding. As a sufficient PEG coating is essential for avoiding recognition by the RES, ligands should be extended away from nanoparticle surfaces for avoiding shielding by the PEG chains [191]. Different types of ligands can be grafted: IgG, Fab, peptide, peptidomimetic, etc. However, the grafting of ligands on the PEG part of the PLGA may not be possible. Thus, amphiphilic copolymers such as poly(ε-caprolactone-co-ethylene glycol) (PCL–PEG), can be added to the polymer composition as graft carriers.

These surface modifications allow the naturally negatively charged PLGA nanoparticles to shift to neutral or positive charges profiles. For example, PEGylation of the PLGA polymer [192] or chitosan coating [193], could lead to these shifts.

One of the major pitfalls of PLGA-based nanoparticles relates to the poor loading. Indeed, while PLGA-based nanoparticles often present high encapsulation efficiencies, the drug loading is generally poor (around 1%, which means that nanoparticles content 1 mg active ingredient per 100 mg polymers of nanoparticles). This low drug loading constitutes a major problem for some drugs in the design of PLGA-based nanoparticles.

A second important pitfall is in the high burst release of drug from nanoparticles. This phenomenon is described for most PLGA-based nanoparticles. Consequently, the drug might not be able to reach the target tissue or cells, leading to a loss of efficacy. Because of the application of nanoparticles in sustained release drug delivery, the drug release mechanisms are also important to understand. According to Kumari and colleagues, five mechanisms of drug release exist: (i) desorption of drug bound to the surface, (ii) diffusion through the polymer matrix, (iii) diffusion through the polymer wall of nanocapsules, (iv) nanoparticles matrix erosion and (v) a combined erosion-diffusion process. Drug release mechanisms depend on the polymer used and on the loading efficiency. Generally, the rapid initial, or burst release is attributed to adsorbed drug to the nanoparticles surface [185].

II.2.2.2 Methods of formulation

The most commonly used technique for the preparation of PLGA nanoparticles is the emulsification-solvent evaporation technique. This technique allows the encapsulation of hydrophobic drugs and consists in dissolving the polymer and the compound in an organic solvent (e.g., dichloromethane). The emulsion oil (O) in water (W) i.e. O/W is prepared by adding water and a surfactant (e.g., polysorbate-80, poloxamer-188) to the polymer solution. The nanosized droplets are induced by sonication or homogenization. The solvent is then evaporated or extracted and the nanoparticles collected after centrifugation [189, 194]. A modification of this technique, the double emulsion W/O/W, was used to encapsulate hydrophilic drugs, such as peptides, proteins and nucleic acids. Nanoparticles can also be formed by the nanoprecipitation method also called the interfacial deposition method [195]. Briefly, the polymer and the drug are dissolved in an organic solvent (such as acetone) and added dropwise to water. The organic solvent is evaporated and the pellets are collected after centrifugation. Other techniques exist such as the spray-drying method [187]. Drug loading into nanoparticles is achieved by two methods: (i) the incorporation of the drug during the nanoparticles production and (ii) the adsorption of the drug on nanoparticles after their production.

II.2.2.3 Encapsulation of proteins in PLGA-based nanoparticles

The encapsulation of proteins into PLGA nanoparticles presents challenges such as instability [196]. For example, in the first step of the W/O/W formulation procedure the protein dissolved in the aqueous phase may aggregate or be denatured at the water/organic solvent interface, adsorbed to the hydrophobic polymer or unfold because of the shear stress used for the formation of the primary emulsion [197]. Denatured or aggregated protein species will not only be therapeutically inactive, but also may induce unpredictable side effects, such as toxicity or immunogenicity [198]. To overcome these problems, many studies have focused on optimizing the formulation process in order to improve protein stability during classical W/O/W procedure.

Another factor to be considered is the acidification of the environment induced by the degradation products (lactic acid and glycolic acid), as well as the presence of PLGA carboxylic acid end groups, which could interact with the positive charges of the encapsulated protein, altering or even blocking its release. This exposure of the therapeutic protein to an acidic pH could induce its aggregation or affect its activity [196, 199]. Diverse stabilizer agents, such as pluronic F68, trehalose, sodium bicarbonate, among others, have also been tested to increase protein stability [200, 201].

II.2.2.4 PLGA-based nanoparticles for inflammatory bowel disease targeting

In order to avoid serious side effects resulting from systemic application and long-term treatment, a local delivery of anti-inflammatory drugs might be an interesting approach. PLGA nanoparticles were shown to be able to enhance drug localization in target site and to release sustainably in the entrapped compound [202].

After their systemic administration, PLGA-based drug delivery systems are preferentially taken up by the RES and present a high and selective uptake in inflamed areas. This phenomenon might be explained by increased presence of immune-related cells like macrophages, lymphocytes or DCs and by disruption of epithelium in these inflamed sites, resulting in a preferential accumulation of these nanoparticles. These characteristics look like the well-known “enhanced permeability” from the cancer field [203].

The surface of nanoparticles can also be modified in order to receive inflamed specific-targeting moieties. Antigens, receptors on cells or tissues, overexpressed in inflamed areas, which are not or poorly expressed in healthy areas (such as integrin $\alpha_v\beta_3$, ICAM-1 or E-selectin), can be recognized by grafted molecules as antibodies, specific adhesion molecules or specific ligands [204].

Oral administration of rolipram-loaded PLGA nanoparticles to rats suffering from TNBS-induced colitis led to a decrease of clinical activity score as compared to administration of rolipram in solution. Moreover, although control group of animal showed a strong relapse after 5 days without treatment, rolipram-loaded PLGA nanoparticles continuously reduced clinical activity scores. This could be explained by PLGA nanoparticles accumulation in inflamed regions of the colon associated with biodegradability of PLGA polymer allowing a sustained release of the entrapped drug. The reduction of neurotropic effects was observed after rolipram-loaded PLGA nanoparticles administration [160].

PLGA nanoparticles encapsulating tacrolimus were administered in two different rat colitis models, either by oral or rectal routes. While free tacrolimus was found in high concentrations in healthy tissues, tacrolimus-loaded PLGA nanoparticles increased drug amounts in inflamed areas. PLGA nanoparticles protected tacrolimus from its mucosal metabolism and P-gp efflux [159]. When Y. Meissner *et al.* compared therapeutic effects of oral administration of tacrolimus-loaded PLGA or Eudragit P-4135F nanoparticles in a dextran sulfate colitis model in mice, a selective accumulation of PLGA nanoparticles was

observed leading to higher drug concentration inside the inflamed tissue even if a lower total amount of drug reached inflamed sites [133].

II.2.3 Trimethylchitosan: A mucoadhesive polymer

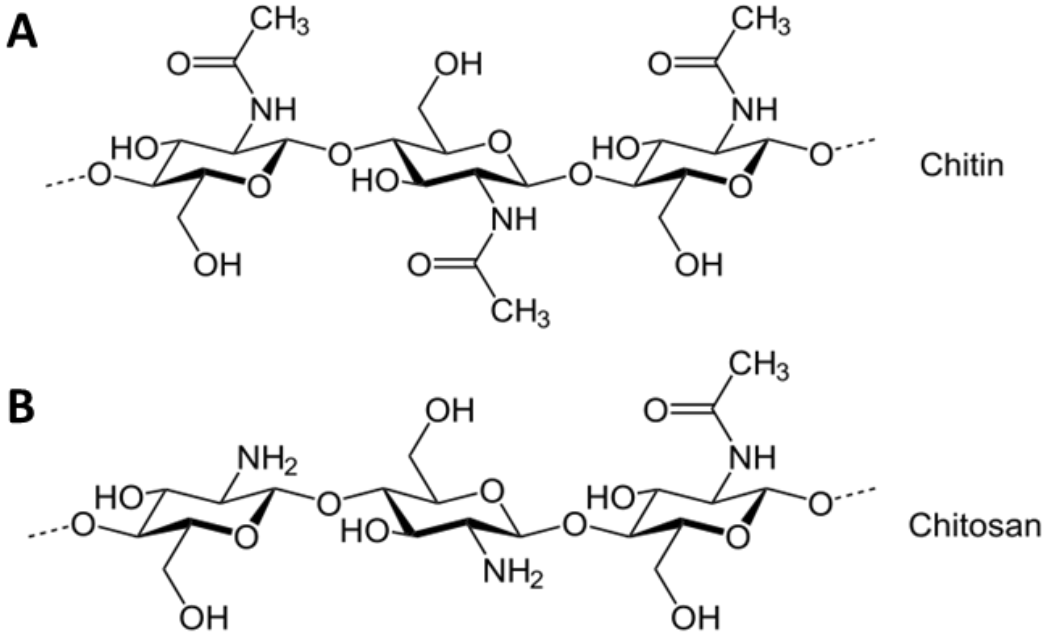


Figure 22: Chemical structures of chitin and chitosan

Among all the non-toxic and biodegradable polymers, natural polymers are the most used for biomedical applications [205]. Chitosan, a polysaccharidic one, has been studied for some decades as a promising drug vehicle. Chitosan is the derivative of the second most abundant natural polysaccharide, chitin. Chitin can be obtained from several natural sources, especially in exoskeletons of insects and crustaceans or mushrooms. Chitin is an aminoglucopyran composed of two units, N-acetyl glucosamine and glucosamine, which are linearly and randomly distributed. Incomplete deacetylation of the N-acetyl glucosamine units of chitin, generally obtained by hydrolysis under alkali conditions at high temperature, transforms chitin in chitosan when the acetylation degree get below 60% (Figure 22) [147]. Molecular weight ranges varies from 2,000 Da to 2 x 10^6 Da [206]. Sectors such as pharmaceutical, biomedical, agricultural or even textile ones are extensively exploring chitosan for applications [207]. Chitosan prepared from non-animal source is considered to be safer for bio-applications.

Contrarily to chitin that is insoluble in most solvents, chitosan is soluble in water, but only when the pH is below 7. With a pKa of 6.5, in acidic medium, protonation of primary amines of the chitosan skeleton occurrs, leading to a positive charge density profile in these

conditions. A consequent repulsion between the polymer chains results in an enhanced solubilization process [147, 208].

The wide use of chitosan as new drug delivery vehicle results from its interesting structure activity relation. First of all, because of its polysaccharidic structure, chitosan is biocompatible and biodegradable. Due to this polycationic structure, chitosan presents a positive charge density, resulting in interesting adhesive properties to negatively charged mucus. Moreover, chitosan is known to open reversibly tight junctions of membranes. Depending on the degree of acetylation and the pH, charge density of chitosan allows also electrostatic interactions with negatively charged macromolecules such as nucleic acids or peptides/proteins. All these characteristics contribute to the absorption/permeation enhancement effect, resulting in the promotion of paracellular transport of hydrophilic compounds [209, 210]. However, the protonated form of chitosan influences strongly this effect and thus the more basic the surrounding environment is, less optimal chitosan to open of tight junctions. In consequence, at the basic lumen from small intestine, large intestine and colon, chitosan is less susceptible to enhance the absorption of drugs. This is a major limitation for colonic delivery.

As luminal pH of the colon is above 7, the use of chitosan in colonic delivery is limited. Therefore, there is a need to provide new properties to chitosan, while maintaining the intrinsic ones. Thus, chemical modifications of the chitosan have been investigated.

II.2.3.1 Trimethylchitosan: A quaternized chitosan derivative

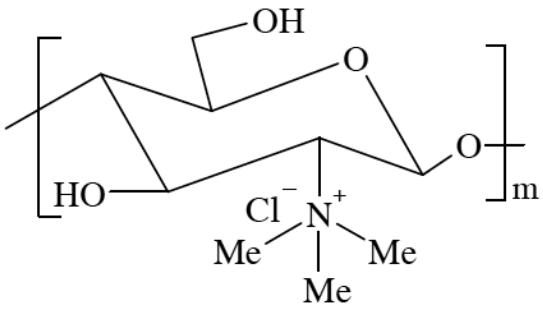


Figure 23: Chemical structure of trimethylchitosan (TMC) monomer

On chitosan, three reactive sites are available for chemical modifications: one primary amine and two hydroxyl groups (primary or secondary) by glucosamine units. Grafting of small molecules or polymer chains are some of the several chemical modifications that have been

investigated [208]. The significance of the intact presence of the primary amine of the chitosan for transfection efficiency is one of the various examples showing that structure-activity relationships for chitosan are relevant.

To increase the solubility of chitosan and maintain absorption enhancing properties in more basic environment, focus has been put on the preservation of the positive charge even in alkaline environment [211, 212]. Quaternization of the amino groups consists in the graft of an alkyl group on amino groups in chitosan. Thus, *N,N,N*-trimethyl chitosan (TMC) results from the switch of the primary amino group on the C-2 position of chitosan with a quaternary amino group, full of the simplest alkyl group, the methyl one (Figure 23). Different methods of quaternization of methyl group (methylation) have been reported [208]. The most well-known strategy use methyl iodide at elevated temperature in a strong alkaline environment. Basic pH avoids thus the protonation of the unreacted primary amino groups. Degree of quaternization reflects the charge density of positive charges available on the molecule and even if it is lower than 10%, it increases solubility of TMC compared to chitosan's solubility. Solubility of TMC was found high either in acidic, neutral or basic pH levels, with a peak obtained with the degree of quaternization of 40% [213].

TMC is known to be less mucoadhesive than native chitosan. It has been reported that as the degree of quaternization increases, and thus the presence of fixed positive charges, TMC is less mucoadhesive [214]. The explanation may be that the increased presence of the positive charged quaternary amino groups leads to changes in the conformation of TMC and thus a decrease in the flexibility of the polymer. Moreover, steric effects from the attached methyl groups occurred, causing screening effect and consequently the hideout of the fixed positive charges. Due to both these outcomes, the relation between the negatively charged sialic groups of the mucus and the positively charged quaternary amino groups of TMC polymers may change, leading to a decrease in the mucus penetration [208].

Permeation enhancement effect is another characteristic of the TMC-based drug delivery. The polymer, leading to the opening of the tight junctions positioned between epithelial cells. A mechanism has been recently proposed for the opening of tight junctions by chitosan: contact between chitosan and the tight junction activates integrin receptors on cell membranes, triggers the intracellular redistribution of the tight junction protein claudin-4 and its subsequent degradation in lysosomes. Cytoskeletal F-actin is then modified, resulting in the opening of the tight junctions [215, 216]. Thus, the paracellular route is then promoted and both *in vitro* and *in vivo* transport of various compounds such as small hydrophilic drugs, macromolecules or peptides through the epithelium have been successfully investigated

[217, 218]. As far as that goes, TMC carriers were able to transfect nucleic acids into cells [219].

In summary, methylation of amino groups of chitosan gave TMC, which presents the same properties as his native polymer (permeation and absorption enhancement, mucoadhesion, particle formulation, etc) while being it soluble in water, even at basic pH.

II.2.3.2 TMC based nano-sized delivery systems

To prepare TMC nanoparticles suitable for drug delivery, physical methods have been widely preferred to chemical ones due to the absence of use of organic solvents, vigorous agitation, sonication, high temperature and toxic crosslinkers that may be harmful to compounds such as small drugs, proteins, peptides or nucleic acids (Table 6). Ionotropic gelation and polyelectrolyte complexation, the most widely used formulation methods to prepare TMC nanoparticles, are both ionic crosslinking methods. Their principle is based on the electrostatic interactions of oppositely charged molecules. The negative charge of the macromolecule of interest is a key criterion for the choice of the method [220].

Ionotropic gelation is based on electronic interactions between polycationic TMC, polyanionic macromolecules and low molecular weight polyanionic crosslinkers such as tripolyphosphate (TPP). In this method, the drug is entrapped in a matrix created by the strong interaction existing between the positive amino groups of TMC with the negative groups of the crosslinker (phosphate groups of TPP for instance). The recent use of the self-assembled polyelectrolyte complexation method has shown that low molecular weight polyanionic crosslinkers are not required to obtain successful nanocarriers. Indeed, polyelectrolyte complexation occurred when negatively charged macromolecules such as nucleic acids or proteins self-interact with the permanent positively charged TMC, leading to the formulation of homogenous and stable nano-delivery systems. Thus, there is a direct interaction existing between positively charged TMC and the negatively charged macromolecules involved [221].

By using insulin as model drug, Sadeghi et al. found after comparison of both ionotropic gelation and polyelectrolyte complexation to produce insulin loaded nanoparticles, the ones obtained after polyelectrolyte complexation present higher insulin loading efficiently and zeta potential than the ones prepared with ionotropic gelation method, probably due to the direct interaction existing between TMC and insulin. Another interesting point was that when comparing chitosan- and TMC-based nanoparticles prepared with polyelectrolyte complexation method in terms of insulin loading efficiency, chitosan ones were found with higher values, probably due to better accessibility of N^+ atoms in the chitosan compared to

ones of TMC surrounded by methyl groups. Nevertheless, size and stability of nanoparticles were not found significantly different, depending on the method of formulation [222].

Gene transfection has also been investigated with TMC as delivery systems of compounds such as RNA, DNA or plasmids [223]. However, some drawbacks have appeared for the use of TMC as gene transfection systems. For example, TMC/DNA complexes are so strongly electrostatically fixed that, inside cells, the release of nucleic acids is obstructed, leading to a lower presentation of the DNA to the RNA polymerase and thus lower gene expression level [224]. Moreover, high doses of cationic polymers such as TMC are known to be toxic to cells, probably due to the interactions with the plasma membrane, its negatively charged components or the molecular weight of the polymers [223]. N/P ratio, which is defined as the ratios of moles of amines groups of cationic polymers to those of the phosphate ones of DNA, is a key criterion for the elaboration of polyelectrolyte complexes [225]. Therefore, TMC has to be optimized in order to provide an efficient gene silencing carrier.

With qualities such as a charge profile independent from gastro-intestinal pH, mucoadhesive and permeation enhancement properties, TMC is a good candidate for colonic delivery systems. Moreover, as a chitosan derivative, TMC is not digested in the upper part of the gastro-intestinal tract whereas colonic bacterial glycosidases degrade it by hydrolysis of its glycosidic linkages. These enzymes are not produced by the human body but mostly by colonic anaerobic bacteria species such as bacteroides and bifidobacteria [226, 227]. TMC was functionalized with galactose and thiol in order to obtain an inflamed colon specific delivery system for a mitogen-activated protein kinase 4 siRNA (siMap4k4). Galactosylation enhances the targeting of the activated macrophages presenting the macrophage galactose-type lectin (MGL) receptor whereas increase of bioadhesion was obtained by thiolation. TPP was shown as a better anionic crosslinker than HA, as the particles showed smaller particle size, lower PDI, and higher binding efficiency with siRNA of NPs. *In vitro* studies with LPS-activated macrophages showed that galactosylated TMC/TPP loaded with si*Map4k4* nanoparticles exhibited higher cell binding affinity, cell uptake and TNF-α suppression, mainly due to the preferential MGL receptor-mediated endocytosis. Orally delivered to mice with DSS-induced colitis, galactosylated TMC/TPP nanoparticles loaded with si*Map4k4 showed better in vivo efficacy*. All these results support colonic inflammation-focused targeting, accumulation and activity of the optimized TMC-based formulations compared to the controls [228].

Table 6 : Examples of TMC based nanocarriers

Type	Encapsulated Compound	Processes	DQ (%)	Size (nm)	Pdi	Encapsulation Efficiency (%)	Applications/Models	Ref
Small Drugs	Dextran	Ionotropic gelation	4;35;90	580-1100		± 87	In vitro & ex vivo intestinal penetration enhancement studies	[217]
	Cisplatin	Cisplatin–alginate complexation	85	150-300	0.43		Cancer targeting Growth inhibition & Apoptosis assay	[229]
	Vitamins B9, B12 & C	Electrostatic interaction Ionotropic gelation with TPP		220-540			Vitamin Carriers Physico-chemical characterization	[230]
	Lactosyl-norcantharidin	Ionic cross-linkage	65	120.6 ± 1.7	< 0.3	69.29 ± 0.76	Liver cancer therapy (In vitro & In vivo)	[231, 232]
Nucleic Acids	SiRNA eGFP	Polyelectrolyte complexation	25;27;45	120-160		95 at least	Cancer therapy In vitro cytotoxicity Transfection efficiency	[233]
	SiRNA Map4k4	Galactosylated conjugation Ionotropic gelation with TPP or HA	30	140-160	0.10-0.25		Oral administration Ulcerative colitis Targeted gene delivery	[228]
	SiRNA RhoA	Polyelectrolyte complexation with MAA	22-33	110-250		95 at least	Gene silencing	[219]
	SiRNA Interleukin-6	Ionotropic gelation with TPP or HA	34	150-180 170-290	0.03-0.250		Oral delivery Gene silencing Biodistribution	[234]
	DNA	Polyelectrolyte complexation	33	520 ± 41	0.25 ± 0.02	100	Evaluation of the influence of N/P ratio, [DNA] and presence of M cells on transfection efficiency	[209]
	Plasmid	Conjugation with histidine and folate-PEG		196			Gene delivery Active targeting Cell uptake	[235]
	Plasmid encoding eGFP	Conjugation with cysteine Polyelectrolyte complexation	15; 30	200			Gene delivery Cell uptake Transfection	[236]

Peptides & Proteins	Ovalbumin	Ionotropic gelation with TPP or HA or unmethylated CpG DNA		250–350	0.25 ± 0.03	52 ± 7	Ex vivo Horizontal Diffusion Chamber In vivo immunization studies Nasal & Intradermal vaccination	[211, 237-239]
	BSA	Folate-PEG grafting Ionotropic gelation with TPP	39				Intracellular transport	[240]
	BSA	Ionotropic gelation with mix of TPP and alginate	37	180-300	0.13-0.23	94.08 ± 1.88 99.56 ± 0.23	Effect of alginate on in vitro permeability studies	[241]
	Urease	Ionotropic gelation with TPP	37	326 ± 6	0.31 ± 0.04	81.57 ± 1.25	In vivo immunization studies	[241]
	Anti-neuroexcitation peptide	Ionotropic gelation with TPP	36;86	255		80.63	Brain targeting and delivery In vivo tissue distribution	[191]
	Insulin	Conjugation with cysteine or with targeting peptide Polyelectrolyte complexation	15;30	100–200		90	Oral delivery Mucoadhesion Permeation enhancement	[220, 242-244]
	Hepatitis B surface antigen	Polyelectrolyte complexation	24	80-100	0.3-0.4	80 at least	Mucosal immunization	[245, 246]
	Whole inactivated influenza virus vaccine	Polyelectrolyte complexation	25-45	120-210	0.05-0.35	95 at least	Gene therapy RNA interference	[247]

Abbreviations: Bovine Serum Albumin (BSA); Enhanced green fluorescence protein (eGFP); Hyaluronic acid (HA); methacrylic acid (MAA); Sodium Tripolyphosphate (TPP)

II.3 LIPID-BASED NANOCARRIERS OF INTEREST

It is a generally accepted fact that orally taken lipids enhance oral absorption of hydrophobic drugs. Indeed, in the gut, surface of lipid contents is enzymatically degraded into mono- or diglycerides. These lipid units detach from their previous lipid material and then form micelles. These formed micelles, which can contain the drug dissolved in the previous lipid content, are an important step in the absorption process. Furthermore, several drugs and lipids simultaneously administrated gave better results than drug and lipid given separately [248]. The use of lipid-based drug delivery systems has been highlighted, with as goal to improve the oral bioavailability of the poorly soluble drugs. One can combine this lipid absorption enhancing effect with the reproducible adherence property of the nanoparticles. For this purpose, self-nanoemulsifying drug delivery systems and nano-structured lipid carriers have been tested [249, 250].

II.3.1 Self-nanoemulsifying drug delivery systems

Self-nanoemulsifying drug delivery systems (SNEDDS) are defined as clear isotropic mixtures of oils (pure triglyceride oils and mixed glycerides), water-soluble surfactants and optionally hydrophilic co-solvents. In gastrointestinal fluids, they spontaneously generated oil-in-water colloidal nanoemulsion, with a size range generally between 50 nm and 300 nm [90]. This behavior allows a greater surface area of interaction between the formulation and the gastro-intestinal fluids, resulting in a better drug solubilization and increased membrane permeability [250]. Lymphatic transport seems also to play a relevant role [251].

Very specific excipient combinations trigger self-emulsification. Criteria such as nature, concentration or ratio of the excipients have to be rigorously monitored. Oils are considered as the most important excipients for SNEDDS. They simplify self-emulsification, solubilize the lipophilic drug and enhance the fraction of lipophilic drug transported via the intestinal lymphatic system. Modified or hydrolyzed vegetable oils are rather used as they present formulative, biocompatible and physiological advantages. The best surfactants suitable for the formulation of SNEDDS are non-ionic surfactants with a relatively high hydrophilic−lipophilic balance (Tween 80 for instance). They offer good compromise between self-emulsification capacity and toxicity, compared to the other types of surfactants. Co-solvents allow the marked amounts of surfactants to be decreased. Use of alcohol co-solvents as ethanol or

PEG is limited as they can evaporate in the final dosage forms and lead to drug precipitation [252].

SNEDDS are generally used to improve solubility of poorly water-soluble drugs and can be manufactured in gelatin capsules, tablets, pellets or granules [90]. Cyclosporin (Sandimmune Neoral®), ritonavir (Norvir®) and saquinavir Fortovase® are some of the successfully marketed SNEDDS-based medicines [252].

II.3.2 Nano-structured Lipid Carriers (NLC)

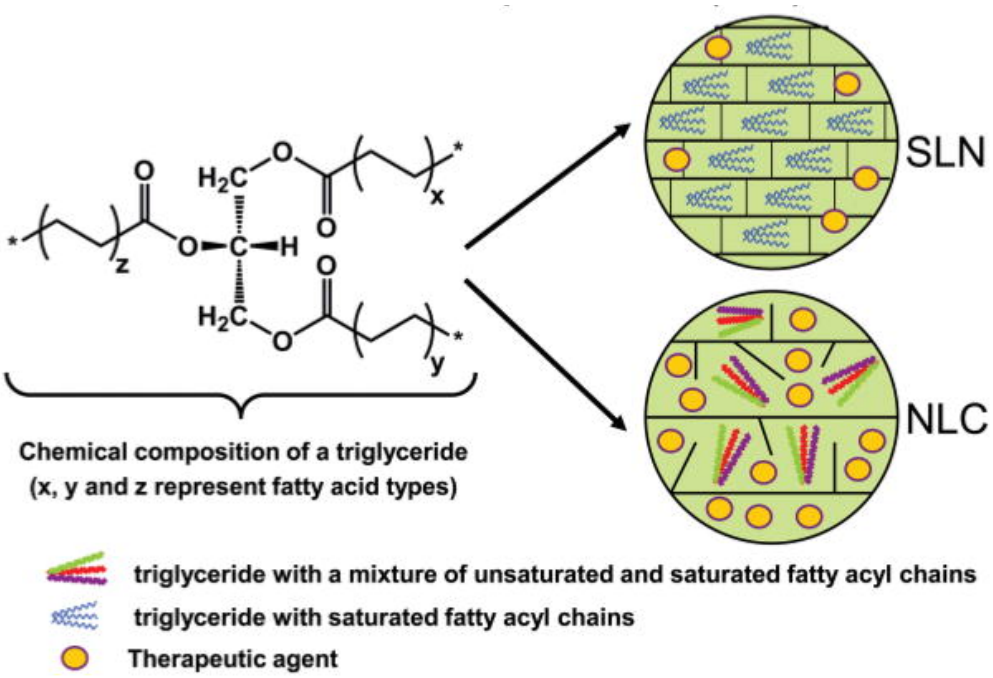


Figure 24: Solid lipid nanoparticles (SLN) and nanostructured lipid carriers (NLC)

First developed by Müller et al. in the 1990s, solid lipid nanoparticles (Figure 24) are colloidal systems with a solid matrix, especially useful for the encapsulation of lipophilic drugs. Easily produced, these physically stable systems suffer however from low drug loading capacity and potential drug expulsion during storage [253]. Their use in topical delivery of IBD drugs seems paradoxical as they are used rather to improve oral absorption and systemic bioavailability of poorly soluble drugs and proteins. Furthermore, once orally administrated, SLN adhere to the mucosa of the upper part of the gut, releasing their content by enzymatic cleavage mechanisms [96].

In order to deal with all these limitations, a 2nd generation of solid lipid nanoparticles, nanostructured lipid carriers (NLC) have been created (Figure 24). Unlike the lipid particle matrix of the SLNs, the matrix of the NLCs is made with solid and liquid lipids. This mix allows the control of the nanostructure of the particle. Indeed, the limitations of the SLNs were mainly due to the fact that their more or less perfect crystalline structure prevents the incorporation of drugs. With this combination of liquid and solid lipids, the matrix of NLCs is full of imperfections, leading to better drug loading capacity and lower drug expulsion during storage [254]. The drug can be incorporated in the matrix homogenously, preferentially in the shell or in the core. Defined as the amount of drug incorporated in the total lipidic mass, the loading capacity of NLCs depends on the solubility of the encapsulated drug in the lipid blend.

High-pressure homogenization is one of the main production methods of NLCs. In a working temperature approximately 5-10°C above the melting point of the lipid blend, the drug is dissolved in a melted mixture of both solid and liquid lipids. Then, by high-speed stirring, the whole mixture is dispersed in a surfactant solution, resulting in an aqueous oil-in-water “pre-emulsion”. Afterwards, homogenization of the pre-emulsion is made with a temperature-controlled high-pressure homogenizer. Finally, by decreasing the working temperature, crystallization occurred, providing stable and homogenous NLCs [255].

III. REFERENCES

[1] M. Cornaggia, M. Leutner, C. Mescoli, G.C. Sturniolo, R. Gullotta, D. Gruppo Italiano Patologi Apparato, I.d. Societa Italiana di Anatomia Patologica e Citopatologia Diagnostica/International Academy of Pathology, Chronic idiopathic inflammatory bowel diseases: the histology report, Dig Liver Dis, 43 Suppl 4 (2011) S293-303.
[2] J. Cosnes, C. Gower-Rousseau, P. Seksik, A. Cortot, Epidemiology and natural history of inflammatory bowel diseases, Gastroenterology, 140 (2011) 1785-1794.
[3] T.S. Hansen, T. Jess, I. Vind, M. Elkjaer, M.F. Nielsen, M. Gamborg, P. Munkholm, Environmental factors in inflammatory bowel disease: a case-control study based on a Danish inception cohort, J Crohns Colitis, 5 (2011) 577-584.
[4] E.V. Loftus, Jr., Clinical epidemiology of inflammatory bowel disease: Incidence, prevalence, and environmental influences, Gastroenterology, 126 (2004) 1504-1517.
[5] M.G. Neuman, R.M. Nanau, Inflammatory bowel disease: role of diet, microbiota, life style, Translational research : the journal of laboratory and clinical medicine, 160 (2012) 29-44.
[6] R.S. Sandler, J.E. Everhart, M. Donowitz, E. Adams, K. Cronin, C. Goodman, E. Gemmen, S. Shah, A. Avdic, R. Rubin, The burden of selected digestive diseases in the United States, Gastroenterology, 122 (2002) 1500-1511.
[7] J. Burisch, T. Jess, M. Martinato, P.L. Lakatos, E. EpiCom, The burden of inflammatory bowel disease in Europe, J Crohns Colitis, 7 (2013) 322-337.
[8] H.M. Malaty, J.K. Hou, S. Thirumurthi, Epidemiology of inflammatory bowel disease among an indigent multi-ethnic population in the United States, Clin Exp Gastroenterol, 3 (2010) 165-170.
[9] J.H. Kurata, S. Kantor-Fish, H. Frankl, P. Godby, C.M. Vadheim, Crohn's disease among ethnic groups in a large health maintenance organization, Gastroenterology, 102 (1992) 1940-1948.
[10] L. Halme, P. Paavola-Sakki, U. Turunen, M. Lappalainen, M. Farkkila, K. Kontula, Family and twin studies in inflammatory bowel disease, World J Gastroenterol, 12 (2006) 3668-3672.
[11] A. Kaser, S. Zeissig, R.S. Blumberg, Inflammatory bowel disease, Annu Rev Immunol, 28 (2010) 573-621.
[12] E.V. Loftus, Jr., M.D. Silverstein, W.J. Sandborn, W.J. Tremaine, W.S. Harmsen, A.R. Zinsmeister, Ulcerative colitis in Olmsted County, Minnesota, 1940-1993: incidence, prevalence, and survival, Gut, 46 (2000) 336-343.
[13] V. Chouraki, G. Savoye, L. Dauchet, G. Vernier-Massouille, J.L. Dupas, V. Merle, J.E. Laberenne, J.L. Salomez, E. Lerebours, D. Turck, A. Cortot, C. Gower-Rousseau, J.F. Colombel, The changing pattern of Crohn's disease incidence in northern France: a continuing increase in the 10- to 19-year-old age bracket (1988-2007), Aliment Pharmacol Ther, 33 (2011) 1133-1142.
[14] P. Turunen, K.L. Kolho, A. Auvinen, S. Iltanen, H. Huhtala, M. Ashorn, Incidence of inflammatory bowel disease in Finnish children, 1987-2003, Inflamm Bowel Dis, 12 (2006) 677-683.
[15] S. Auvin, F. Molinie, C. Gower-Rousseau, F. Brazier, V. Merle, B. Grandbastien, R. Marti, E. Lerebours, J.L. Dupas, J.F. Colombel, J.L. Salomez, A. Cortot, D. Turck, Incidence, clinical presentation and location at diagnosis of pediatric inflammatory bowel disease: a prospective population-based study in northern France (1988-1999), J Pediatr Gastroenterol Nutr, 41 (2005) 49-55.
[16] V. Binder, Epidemiology of IBD during the twentieth century: an integrated view, Best Pract Res Clin Gastroenterol, 18 (2004) 463-479.
[17] I. Vind, L. Riis, C. Jespersgaard, T. Jess, E. Knudsen, N. Pedersen, M. Elkjaere, T.S. Hansen, I.B. Andersen, A. Paerregaard, S. Bondesen, H. Locht, S.O. Larsen, F.

Moesgaard, F. Bendtsen, P.S. Andersen, P. Munkholm, D.s.g. on behalf of the, Genetic and environmental factors as predictors of disease severity and extent at time of diagnosis in an inception cohort of inflammatory bowel disease, Copenhagen County and City 2003-2005, J Crohns Colitis, 2 (2008) 162-169.
[18] J. Mate-Jimenez, J.A. Correa-Estan, M. Perez-Miranda, A. Gomez-Cedenilla, J.M. Pajares, R. Moreno-Otero, Tonsillectomy and inflammatory bowel disease location, Eur J Gastroenterol Hepatol, 8 (1996) 1185-1188.
[19] J.F. Mayberry, J. Rhodes, R. Allan, R.G. Newcombe, G.M. Regan, L.M. Chamberlain, K.G. Wragg, Diet in Crohn's disease two studies of current and previous habits in newly diagnosed patients, Dig Dis Sci, 26 (1981) 444-448.
[20] G. Bastida, B. Beltran, Ulcerative colitis in smokers, non-smokers and ex-smokers, World J Gastroenterol, 17 (2011) 2740-2747.
[21] O. Rom, K. Avezov, D. Aizenbud, A.Z. Reznick, Cigarette smoking and inflammation revisited, Respiratory Physiology & Neurobiology, 187 (2013) 5-10.
[22] J. Cosnes, Tobacco and IBD: relevance in the understanding of disease mechanisms and clinical practice, Best Pract Res Clin Gastroenterol, 18 (2004) 481-496.
[23] I.E. Koutroubakis, I.G. Vlachonikolis, E.A. Kouroumalis, Role of appendicitis and appendectomy in the pathogenesis of ulcerative colitis: a critical review, Inflamm Bowel Dis, 8 (2002) 277-286.
[24] G.L. Radford-Smith, J.E. Edwards, D.M. Purdie, N. Pandeya, M. Watson, N.G. Martin, A. Green, B. Newman, T.H. Florin, Protective role of appendicectomy on onset and severity of ulcerative colitis and Crohn's disease, Gut, 51 (2002) 808-813.
[25] D.C. Baumgart, S.R. Carding, Inflammatory bowel disease: cause and immunobiology, Lancet, 369 (2007) 1627-1640.
[26] C. Abraham, J.H. Cho, Inflammatory bowel disease, N Engl J Med, 361 (2009) 2066-2078.
[27] R.B. Sartor, Mechanisms of disease: pathogenesis of Crohn's disease and ulcerative colitis, Nat Clin Pract Gastroenterol Hepatol, 3 (2006) 390-407.
[28] J.G. Hyun, L. Mayer, Mechanisms underlying inflammatory bowel disease, Drug Discovery Today: Disease Mechanisms, 3 (2006) 457-462.
[29] B. Khor, A. Gardet, R.J. Xavier, Genetics and pathogenesis of inflammatory bowel disease, Nature, 474 (2011) 307-317.
[30] J.H. Cho, S.R. Brant, Recent insights into the genetics of inflammatory bowel disease, Gastroenterology, 140 (2011) 1704-1712.
[31] G. Reid, F.A. Carey, Pathology of idiopathic inflammatory bowel disease, Surgery (Oxford), 29 (2011) 362-365.
[32] P. Seksik, [Gut microbiota and IBD], Gastroenterol Clin Biol, 34 Suppl 1 (2010) S44-51.
[33] A. Darfeuille-Michaud, J. Boudeau, P. Bulois, C. Neut, A.L. Glasser, N. Barnich, M.A. Bringer, A. Swidsinski, L. Beaugerie, J.F. Colombel, High prevalence of adherent-invasive Escherichia coli associated with ileal mucosa in Crohn's disease, Gastroenterology, 127 (2004) 412-421.
[34] N. Barnich, F.A. Carvalho, A.L. Glasser, C. Darcha, P. Jantscheff, M. Allez, H. Peeters, G. Bommelaer, P. Desreumaux, J.F. Colombel, A. Darfeuille-Michaud, CEACAM6 acts as a receptor for adherent-invasive E. coli, supporting ileal mucosa colonization in Crohn disease, J Clin Invest, 117 (2007) 1566-1574.
[35] A. Suau, R. Bonnet, M. Sutren, J.J. Godon, G.R. Gibson, M.D. Collins, J. Dore, Direct analysis of genes encoding 16S rRNA from complex communities reveals many novel molecular species within the human gut, Appl Environ Microbiol, 65 (1999) 4799-4807.
[36] P. Seksik, L. Rigottier-Gois, G. Gramet, M. Sutren, P. Pochart, P. Marteau, R. Jian, J. Dore, Alterations of the dominant faecal bacterial groups in patients with Crohn's disease of the colon, Gut, 52 (2003) 237-242.

[37] P.D. Scanlan, F. Shanahan, C. O'Mahony, J.R. Marchesi, Culture-independent analyses of temporal variation of the dominant fecal microbiota and targeted bacterial subgroups in Crohn's disease, J Clin Microbiol, 44 (2006) 3980-3988.
[38] H. Sokol, P. Seksik, L. Rigottier-Gois, C. Lay, P. Lepage, I. Podglajen, P. Marteau, J. Dore, Specificities of the fecal microbiota in inflammatory bowel disease, Inflamm Bowel Dis, 12 (2006) 106-111.
[39] J.M. Peloquin, D.D. Nguyen, The microbiota and inflammatory bowel disease: Insights from animal models, Anaerobe, (2013).
[40] C. Manichanh, N. Borruel, F. Casellas, F. Guarner, The gut microbiota in IBD, Nat Rev Gastroenterol Hepatol, 9 (2012) 599-608.
[41] K.R. Groschwitz, S.P. Hogan, Intestinal barrier function: molecular regulation and disease pathogenesis, J Allergy Clin Immunol, 124 (2009) 3-20; quiz 21-22.
[42] E.J. Irvine, J.K. Marshall, Increased intestinal permeability precedes the onset of Crohn's disease in a subject with familial risk, Gastroenterology, 119 (2000) 1740-1744.
[43] S. Vermeire, M. Peeters, R. Vlietinck, S. Joossens, E. Den Hond, V. Bulteel, X. Bossuyt, B. Geypens, P. Rutgeerts, Anti-Saccharomyces cerevisiae antibodies (ASCA), phenotypes of IBD, and intestinal permeability: a study in IBD families, Inflamm Bowel Dis, 7 (2001) 8-15.
[44] S. Wirtz, M.F. Neurath, Mouse models of inflammatory bowel disease, Adv Drug Deliv Rev, 59 (2007) 1073-1083.
[45] J.J. Liu, K. Wong, A.L. Thiesen, S.J. Mah, L.A. Dieleman, B. Claggett, J.R. Saltzman, R.N. Fedorak, Increased epithelial gaps in the small intestines of patients with inflammatory bowel disease: density matters, Gastrointest Endosc, 73 (2011) 1174-1180.
[46] S. Rakoff-Nahoum, J. Paglino, F. Eslami-Varzaneh, S. Edberg, R. Medzhitov, Recognition of commensal microflora by toll-like receptors is required for intestinal homeostasis, Cell, 118 (2004) 229-241.
[47] S.H. Rhee, E. Im, M. Riegler, E. Kokkotou, M. O'Brien, C. Pothoulakis, Pathophysiological role of Toll-like receptor 5 engagement by bacterial flagellin in colonic inflammation, Proc Natl Acad Sci U S A, 102 (2005) 13610-13615.
[48] G. Hardenberg, T.S. Steiner, M.K. Levings, Environmental influences on T regulatory cells in inflammatory bowel disease, Semin Immunol, 23 (2011) 130-138.
[49] S.M. Cruickshank, L.D. McVay, D.C. Baumgart, P.J. Felsburg, S.R. Carding, Colonic epithelial cell mediated suppression of CD4 T cell activation, Gut, 53 (2004) 678-684.
[50] A. Hokama, E. Mizoguchi, K. Sugimoto, Y. Shimomura, Y. Tanaka, M. Yoshida, S.T. Rietdijk, Y.P. de Jong, S.B. Snapper, C. Terhorst, R.S. Blumberg, A. Mizoguchi, Induced reactivity of intestinal CD4(+) T cells with an epithelial cell lectin, galectin-4, contributes to exacerbation of intestinal inflammation, Immunity, 20 (2004) 681-693.
[51] A.L. Hart, H.O. Al-Hassi, R.J. Rigby, S.J. Bell, A.V. Emmanuel, S.C. Knight, M.A. Kamm, A.J. Stagg, Characteristics of intestinal dendritic cells in inflammatory bowel diseases, Gastroenterology, 129 (2005) 50-65.
[52] I. Ordas, L. Eckmann, M. Talamini, D.C. Baumgart, W.J. Sandborn, Ulcerative colitis, Lancet, 380 (2012) 1606-1619.
[53] Q.H. Yu, Q. Yang, Diversity of tight junctions (TJs) between gastrointestinal epithelial cells and their function in maintaining the mucosal barrier, Cell Biol Int, 33 (2009) 78-82.
[54] J. Zhu, H. Yamane, W.E. Paul, Differentiation of effector CD4 T cell populations (*), Annu Rev Immunol, 28 (2010) 445-489.
[55] P. Cobelens, A. Lucas, J. Langhorst, G. Dobos, A. Kavelaars, C.J. Heijnen, M. Schedlowski, S. Elsenbruch, Disturbed in vivo and in vitro stress responsiveness in inflammatory bowel diseases (IBD) in remission, Brain, Behavior, and Immunity, 20 (2006) 11.

[56] D.R. Clayburgh, L. Shen, J.R. Turner, A porous defense: the leaky epithelial barrier in intestinal disease, Lab Invest, 84 (2004) 282-291.
[57] N.A. Braus, D.E. Elliott, Advances in the pathogenesis and treatment of IBD, Clin Immunol, 132 (2009) 1-9.
[58] R.A. Taylor, M.C. Leonard, Curcumin for inflammatory bowel disease: a review of human studies, Altern Med Rev, 16 (2011) 152-156.
[59] E. Langholz, Current trends in inflammatory bowel disease: the natural history, Therap Adv Gastroenterol, 3 (2010) 77-86.
[60] M. Fatahzadeh, Inflammatory bowel disease, Oral Surg Oral Med Oral Pathol Oral Radiol Endod, 108 (2009) e1-10.
[61] J. Terzic, S. Grivennikov, E. Karin, M. Karin, Inflammation and colon cancer, Gastroenterology, 138 (2010) 2101-2114 e2105.
[62] P. Ak, Mark Feldman, Lawrence S Fredman, Lawrence J Brant,Editors, ,Sleisenger and Fordtran's Gastrointestinal and Liver Disease: pathophysiology, diagnosis, management Eighth edition (2006) Saunders Elsevier,1600 John F Kennedy Blvd Ste 1800 Philadelphia, PA 19103-2899 Pages-2890, Volume 1, ISBN-9996002551, Volume 2 ISBN 9996002616, Medical Journal Armed Forces India, 63 (2007) 205.
[63] K. Ephgrave, Extra-intestinal manifestations of Crohn's disease, Surg Clin North Am, 87 (2007) 673-680.
[64] F.D. Ghanchi, B.J. Rembacken, Inflammatory bowel disease and the eye, Surv Ophthalmol, 48 (2003) 663-676.
[65] J. Levy, N. Levy-Carrick, Pulmonary Complications of Gastrointestinal Disorders, Paediatric Respiratory Reviews.
[66] C. Mottet, J.P. Vader, C. Felley, F. Froehlich, J.J. Gonvers, P. Juillerat, R. Stockbrugger, E. Angelucci, F. Seibold, P. Michetti, V. Pittet, E.I.I.S.G. the, Appropriate management of special situations in Crohn's disease (upper gastro-intestinal; extra-intestinal manifestations; drug safety during pregnancy and breastfeeding): Results of a multidisciplinary international expert panel-EPACT II, J Crohns Colitis, 3 (2009) 257-263.
[67] F. Grimpen, P. Pavli, Advances in the management of inflammatory bowel disease, Intern Med J, 40 (2010) 258-264.
[68] G. Pineton de Chambrun, L. Peyrin-Biroulet, M. Lemann, J.F. Colombel, Clinical implications of mucosal healing for the management of IBD, Nat Rev Gastroenterol Hepatol, 7 (2010) 15-29.
[69] D. Burger, S. Travis, Conventional medical management of inflammatory bowel disease, Gastroenterology, 140 (2011) 1827-1837 e1822.
[70] G.R. Lichtenstein, S.B. Hanauer, W.J. Sandborn, G. Practice Parameters Committee of American College of, Management of Crohn's disease in adults, Am J Gastroenterol, 104 (2009) 465-483; quiz 464, 484.
[71] Y.X. Yang, G.R. Lichtenstein, Corticosteroids in Crohn's disease, Am J Gastroenterol, 97 (2002) 803-823.
[72] M.F. Fredin, E. Ulfhammer, M. Rhedin, S. Melgar, B. Mellgard, A. Peterson, Anti-inflammatory effects of budesonide in intestinal epithelial cells, Pharmacol Res, 52 (2005) 422-428.
[73] C. Randall, J. Vizuete, G. Wendorf, B. Ayyar, G. Constantine, Current and emerging strategies in the management of Crohn's disease, Best Pract Res Clin Gastroenterol, 26 (2012) 601-610.
[74] J.R. Korzenik, D.K. Podolsky, Evolving knowledge and therapy of inflammatory bowel disease, Nat Rev Drug Discov, 5 (2006) 197-209.
[75] P.C. Taylor, Pharmacology of TNF blockade in rheumatoid arthritis and other chronic inflammatory diseases, Current opinion in pharmacology, 10 (2010) 308-315.
[76] M. Allez, K. Karmiris, E. Louis, G. Van Assche, S. Ben-Horin, A. Klein, J. Van der Woude, F. Baert, R. Eliakim, K. Katsanos, J. Brynskov, F. Steinwurz, S. Danese, S. Vermeire, J.L. Teillaud, M. Lemann, Y. Chowers, Report of the ECCO

pathogenesis workshop on anti-TNF therapy failures in inflammatory bowel diseases: definitions, frequency and pharmacological aspects, J Crohns Colitis, 4 (2010) 355-366.
[77] Y. Chowers, A. Sturm, M. Sans, K. Papadakis, M. Gazouli, M. Harbord, J. Jahnel, G.J. Mantzaris, J. Meier, C. Mottet, L. Peyrin-Biroulet, M. Allez, Report of the ECCO workshop on anti-TNF therapy failures in inflammatory bowel diseases: Biological roles and effects of TNF and TNF antagonists, Journal of Crohn's and Colitis, 4 (2010) 367-376.
[78] J.E. Gudjonsson, A. Johnston, C.N. Ellis, Novel systemic drugs under investigation for the treatment of psoriasis, J Am Acad Dermatol, 67 (2012) 139-147.
[79] L. Dinesen, S. Travis, Targeting nanomedicines in the treatment of Crohn's disease: focus on certolizumab pegol (CDP870), Int J Nanomedicine, 2 (2007) 39-47.
[80] A. Stallmach, S. Hagel, T. Bruns, Adverse effects of biologics used for treating IBD, Best Pract Res Clin Gastroenterol, 24 (2010) 167-182.
[81] S. de Silva, S. Devlin, R. Panaccione, Optimizing the safety of biologic therapy for IBD, Nat Rev Gastroenterol Hepatol, 7 (2010) 93-101.
[82] B.B. Aggarwal, K.B. Harikumar, Potential therapeutic effects of curcumin, the anti-inflammatory agent, against neurodegenerative, cardiovascular, pulmonary, metabolic, autoimmune and neoplastic diseases, Int J Biochem Cell Biol, 41 (2009) 40-59.
[83] H.M. Arafa, R.A. Hemeida, A.I. El-Bahrawy, F.M. Hamada, Prophylactic role of curcumin in dextran sulfate sodium (DSS)-induced ulcerative colitis murine model, Food Chem Toxicol, 47 (2009) 1311-1317.
[84] A. Ukil, S. Maity, S. Karmakar, N. Datta, J.R. Vedasiromoni, P.K. Das, Curcumin, the major component of food flavour turmeric, reduces mucosal injury in trinitrobenzene sulphonic acid-induced colitis, Br J Pharmacol, 139 (2003) 209-218.
[85] B. Salh, K. Assi, V. Templeman, K. Parhar, D. Owen, A. Gomez-Munoz, K. Jacobson, Curcumin attenuates DNB-induced murine colitis, Am J Physiol Gastrointest Liver Physiol, 285 (2003) G235-243.
[86] S. Kumar, V. Ahuja, M.J. Sankar, A. Kumar, A.C. Moss, Curcumin for maintenance of remission in ulcerative colitis, Cochrane Database Syst Rev, 10 (2012) CD008424.
[87] M.M. Yallapu, M. Jaggi, S.C. Chauhan, Curcumin nanoformulations: a future nanomedicine for cancer, Drug Discov Today, 17 (2012) 71-80.
[88] C. Buzea, Pacheco, II, K. Robbie, Nanomaterials and nanoparticles: sources and toxicity, Biointerphases, 2 (2007) MR17-71.
[89] L. Plapied, N. Duhem, A. des Rieux, V.r. Pr√©at, Fate of polymeric nanocarriers for oral drug delivery, Current Opinion in Colloid & Interface Science, 16 (2011) 228-237.
[90] A. Bernkop-Schnurch, Nanocarrier systems for oral drug delivery: Do we really need them?, Eur J Pharm Sci, 49 (2013) 272-277.
[91] O. Kammona, C. Kiparissides, Recent advances in nanocarrier-based mucosal delivery of biomolecules, Journal of Controlled Release, 161 (2012) 781-794.
[92] F. Danhier, E. Ansorena, J.M. Silva, R. Coco, A. Le Breton, V. Préat, PLGA-based nanoparticles: An overview of biomedical applications, Journal of Controlled Release, 161 (2012) 505-522.
[93] S.B. Lim, A. Banerjee, H. Onyuksel, Improvement of drug safety by the use of lipid-based nanocarriers, J Control Release, 163 (2012) 34-45.
[94] A.W. Basit, Advances in colonic drug delivery, Drugs, 65 (2005) 1991-2007.
[95] U. Klotz, M. Schwab, Topical delivery of therapeutic agents in the treatment of inflammatory bowel disease, Adv Drug Deliv Rev, 57 (2005) 267-279.
[96] E.M. Collnot, H. Ali, C.M. Lehr, Nano- and microparticulate drug carriers for targeting of the inflamed intestinal mucosa, J Control Release, 161 (2012) 235-246.

[97] F. Borrelli, I. Fasolino, B. Romano, R. Capasso, F. Maiello, D. Coppola, P. Orlando, G. Battista, E. Pagano, V. Di Marzo, A.A. Izzo, Beneficial effect of the non-psychotropic plant cannabinoid cannabigerol on experimental inflammatory bowel disease, Biochem Pharmacol, 85 (2013) 1306-1316.
[98] N. Kannan, C. Guruvayoorappan, Protective effect of Bauhinia tomentosa on acetic acid induced ulcerative colitis by regulating antioxidant and inflammatory mediators, Int Immunopharmacol, 16 (2013) 57-66.
[99] D. Pertuit, B. Moulari, T. Betz, A. Nadaradjane, D. Neumann, L. Ismaili, B. Refouvelet, Y. Pellequer, A. Lamprecht, 5-amino salicylic acid bound nanoparticles for the therapy of inflammatory bowel disease, J Control Release, 123 (2007) 211-218.
[100] S.G. Nugent, D. Kumar, D.S. Rampton, D.F. Evans, Intestinal luminal pH in inflammatory bowel disease: possible determinants and implications for therapy with aminosalicylates and other drugs, Gut, 48 (2001) 571-577.
[101] Y. Sasaki, R. Hada, H. Nakajima, S. Fukuda, A. Munakata, Improved localizing method of radiopill in measurement of entire gastrointestinal pH profiles: colonic luminal pH in normal subjects and patients with Crohn's disease, Am J Gastroenterol, 92 (1997) 114-118.
[102] L.F. Asghar, S. Chandran, Multiparticulate formulation approach to colon specific drug delivery: current perspectives, J Pharm Pharm Sci, 9 (2006) 327-338.
[103] M.K. Chourasia, S.K. Jain, Pharmaceutical approaches to colon targeted drug delivery systems, J Pharm Pharm Sci, 6 (2003) 33-66.
[104] E.L. McConnell, H.M. Fadda, A.W. Basit, Gut instincts: explorations in intestinal physiology and drug delivery, Int J Pharm, 364 (2008) 213-226.
[105] L. Holm, M. Phillipson, Assessment of Mucus Thickness and Production In Situ, in: M.A. McGuckin, D.J. Thornton (Eds.) Mucins, Humana Press, 2012, pp. 217-227.
[106] L.M. Ensign, R. Cone, J. Hanes, Oral drug delivery with polymeric nanoparticles: the gastrointestinal mucus barriers, Adv Drug Deliv Rev, 64 (2012) 557-570.
[107] H. Schneider, A. Braun, J. Fullekrug, W. Stremmel, R. Ehehalt, Lipid based therapy for ulcerative colitis-modulation of intestinal mucus membrane phospholipids as a tool to influence inflammation, Int J Mol Sci, 11 (2010) 4149-4164.
[108] R.A. Cone, Barrier properties of mucus, Adv Drug Deliv Rev, 61 (2009) 75-85.
[109] A.M. Dvorak, G.R. Dickersin, Crohn's disease: transmission electron microscopic studies. I. Barrier function. Possible changes related to alterations of cell coat, mucous coat, epithelial cells, and Paneth cells, Hum Pathol, 11 (1980) 561-571.
[110] J. Van De Walle, A. Hendrickx, B. Romier, Y. Larondelle, Y.J. Schneider, Inflammatory parameters in Caco-2 cells: effect of stimuli nature, concentration, combination and cell differentiation, Toxicol In Vitro, 24 (2010) 1441-1449.
[111] A. Mizoguchi, E. Mizoguchi, Animal models of IBD: linkage to human disease, Current opinion in pharmacology, 10 (2010) 578-587.
[112] M. Garinot, V. Fievez, V. Pourcelle, F. Stoffelbach, A. des Rieux, L. Plapied, I. Theate, H. Freichels, C. Jerome, J. Marchand-Brynaert, Y.J. Schneider, V. Preat, PEGylated PLGA-based nanoparticles targeting M cells for oral vaccination, J Control Release, 120 (2007) 195-204.
[113] A. Lamprecht, N. Ubrich, H. Yamamoto, U. Schafer, H. Takeuchi, C.M. Lehr, P. Maincent, Y. Kawashima, Design of rolipram-loaded nanoparticles: comparison of two preparation methods, J Control Release, 71 (2001) 297-306.
[114] A. Makhlof, Y. Tozuka, H. Takeuchi, pH-Sensitive nanospheres for colon-specific drug delivery in experimentally induced colitis rat model, Eur J Pharm Biopharm, 72 (2009) 1-8.
[115] M. Vertzoni, A. Diakidou, M. Chatzilias, E. Soderlind, B. Abrahamsson, J.B. Dressman, C. Reppas, Biorelevant media to simulate fluids in the ascending colon of humans and their usefulness in predicting intracolonic drug solubility, Pharm Res, 27 (2010) 2187-2196.

[116] M. Vertzoni, K. Goumas, E. Soderlind, B. Abrahamsson, J.B. Dressman, A. Poulou, C. Reppas, Characterization of the ascending colon fluids in ulcerative colitis, Pharm Res, 27 (2010) 1620-1626.
[117] S. Simon, R. Schubert, Inhibitory effect of phospholipids on P-glycoprotein: cellular studies in Caco-2, MDCKII mdr1 and MDCKII wildtype cells and P-gp ATPase activity measurements, Biochim Biophys Acta, 1821 (2012) 1211-1223.
[118] K. Tahara, S. Samura, K. Tsuji, H. Yamamoto, Y. Tsukada, Y. Bando, H. Tsujimoto, R. Morishita, Y. Kawashima, Oral nuclear factor-kappaB decoy oligonucleotides delivery system with chitosan modified poly(D,L-lactide-co-glycolide) nanospheres for inflammatory bowel disease, Biomaterials, 32 (2011) 870-878.
[119] M.J. O'Neill, L. Bourre, S. Melgar, C.M. O'Driscoll, Intestinal delivery of non-viral gene therapeutics: physiological barriers and preclinical models, Drug Discov Today, 16 (2011) 203-218.
[120] E. Le Ferrec, C. Chesne, P. Artusson, D. Brayden, G. Fabre, P. Gires, F. Guillou, M. Rousset, W. Rubas, M.L. Scarino, In vitro models of the intestinal barrier. The report and recommendations of ECVAM Workshop 46. European Centre for the Validation of Alternative methods, Alternatives to laboratory animals : ATLA, 29 (2001) 649-668.
[121] A. des Rieux, E.G. Ragnarsson, E. Gullberg, V. Preat, Y.J. Schneider, P. Artursson, Transport of nanoparticles across an in vitro model of the human intestinal follicle associated epithelium, Eur J Pharm Sci, 25 (2005) 455-465.
[122] G. Bisping, N. Lugering, S. Lutke-Brintrup, H.G. Pauels, G. Schurmann, W. Domschke, T. Kucharzik, Patients with inflammatory bowel disease (IBD) reveal increased induction capacity of intracellular interferon-gamma (IFN-gamma) in peripheral CD8+ lymphocytes co-cultured with intestinal epithelial cells, Clin Exp Immunol, 123 (2001) 15-22.
[123] F. Leonard, E.M. Collnot, C.M. Lehr, A three-dimensional coculture of enterocytes, monocytes and dendritic cells to model inflamed intestinal mucosa in vitro, Mol Pharm, 7 (2010) 2103-2119.
[124] F. Leonard, H. Ali, E.M. Collnot, B.J. Crielaard, T. Lammers, G. Storm, C.M. Lehr, Screening of budesonide nanoformulations for treatment of inflammatory bowel disease in an inflamed 3D cell-culture model, Altex, 29 (2012) 275-285.
[125] S. Tedelind, F. Westberg, M. Kjerrulf, A. Vidal, Anti-inflammatory properties of the short-chain fatty acids acetate and propionate: a study with relevance to inflammatory bowel disease, World J Gastroenterol, 13 (2007) 2826-2832.
[126] J. Soni, A.W. Baird, L.M. O'Brien, M. McElroy, J.J. Callanan, H.F. Bassett, D. Campion, D.J. Brayden, Rat, ovine and bovine Peyer's patches mounted in horizontal diffusion chambers display sampling function, J Control Release, 115 (2006) 68-77.
[127] M. Fritsch Fredin, A. Vidal, H. Utkovic, Y.Y. Gotlind, R. Willen, L. Jansson, E. Hultgren Hornquist, S. Melgar, The application and relevance of ex vivo culture systems for assessment of IBD treatment in murine models of colitis, Pharmacol Res, 58 (2008) 222-231.
[128] G. Dothel, V. Vasina, G. Barbara, F. De Ponti, Animal models of chemically induced intestinal inflammation: Predictivity and ethical issues, Pharmacol Ther, (2013).
[129] A.R. Jurjus, N.N. Khoury, J.M. Reimund, Animal models of inflammatory bowel disease, Journal of pharmacological and toxicological methods, 50 (2004) 81-92.
[130] A.A. te Velde, F. de Kort, E. Sterrenburg, I. Pronk, F.J. ten Kate, D.W. Hommes, S.J. van Deventer, Comparative analysis of colonic gene expression of three experimental colitis models mimicking inflammatory bowel disease, Inflamm Bowel Dis, 13 (2007) 325-330.
[131] Y. Araki, A. Andoh, Y. Fujiyama, K. Hata, J. Makino, T. Okuno, F. Nakanura, T. Bamba, Application of 2-aminopyridine fluorescence labeling in the analysis of in vivo and in vitro metabolism of dextran sulfate sodium by size-exclusion high-

performance liquid chromatography, Journal of chromatography. B, Biomedical sciences and applications, 753 (2001) 209-215.
[132] H. Laroui, G. Dalmasso, H.T. Nguyen, Y. Yan, S.V. Sitaraman, D. Merlin, Drug-loaded nanoparticles targeted to the colon with polysaccharide hydrogel reduce colitis in a mouse model, Gastroenterology, 138 (2010) 843-853 e841-842.
[133] Y. Meissner, Y. Pellequer, A. Lamprecht, Nanoparticles in inflammatory bowel disease: particle targeting versus pH-sensitive delivery, Int J Pharm, 316 (2006) 138-143.
[134] D.S. Wilson, G. Dalmasso, L. Wang, S.V. Sitaraman, D. Merlin, N. Murthy, Orally delivered thioketal nanoparticles loaded with TNF-alpha-siRNA target inflammation and inhibit gene expression in the intestines, Nature materials, 9 (2010) 923-928.
[135] Y. Yan, V. Kolachala, G. Dalmasso, H. Nguyen, H. Laroui, S.V. Sitaraman, D. Merlin, Temporal and spatial analysis of clinical and molecular parameters in dextran sodium sulfate induced colitis, PLoS One, 4 (2009) e6073.
[136] C.O. Elson, R.B. Sartor, G.S. Tennyson, R.H. Riddell, Experimental models of inflammatory bowel disease, Gastroenterology, 109 (1995) 1344-1367.
[137] S. Melgar, A. Karlsson, E. Michaelsson, Acute colitis induced by dextran sulfate sodium progresses to chronicity in C57BL/6 but not in BALB/c mice: correlation between symptoms and inflammation, Am J Physiol Gastrointest Liver Physiol, 288 (2005) G1328-1338.
[138] A. Mizoguchi, Animal models of inflammatory bowel disease, Progress in molecular biology and translational science, 105 (2012) 263-320.
[139] L. Yang, J.S. Chu, J.A. Fix, Colon-specific drug delivery: new approaches and in vitro/in vivo evaluation, Int J Pharm, 235 (2002) 1-15.
[140] C. Schmidt, C. Lautenschlaeger, E.-M. Collnot, M. Schumann, C. Bojarski, J.-D. Schulzke, C.-M. Lehr, A. Stallmach, Nano- and microscaled particles for drug targeting to inflamed intestinal mucosa—A first in vivo study in human patients, Journal of Controlled Release, 165 (2013) 139-145.
[141] A. Lamprecht, U. Schafer, C.M. Lehr, Size-dependent bioadhesion of micro- and nanoparticulate carriers to the inflamed colonic mucosa, Pharm Res, 18 (2001) 788-793.
[142] T.T. Jubeh, Y. Barenholz, A. Rubinstein, Differential adhesion of normal and inflamed rat colonic mucosa by charged liposomes, Pharm Res, 21 (2004) 447-453.
[143] S.K. Lai, Y.Y. Wang, J. Hanes, Mucus-penetrating nanoparticles for drug and gene delivery to mucosal tissues, Adv Drug Deliv Rev, 61 (2009) 158-171.
[144] V. Fievez, L. Plapied, A. des Rieux, V. Pourcelle, H. Freichels, V. Wascotte, M.L. Vanderhaeghen, C. Jerome, A. Vanderplasschen, J. Marchand-Brynaert, Y.J. Schneider, V. Preat, Targeting nanoparticles to M cells with non-peptidic ligands for oral vaccination, Eur J Pharm Biopharm, 73 (2009) 16-24.
[145] E. Harel, A. Rubinstein, A. Nissan, E. Khazanov, M. Nadler Milbauer, Y. Barenholz, B. Tirosh, Enhanced transferrin receptor expression by proinflammatory cytokines in enterocytes as a means for local delivery of drugs to inflamed gut mucosa, PLoS One, 6 (2011) e24202.
[146] L.M. Ensign, C. Schneider, J.S. Suk, R. Cone, J. Hanes, Mucus penetrating nanoparticles: biophysical tool and method of drug and gene delivery, Adv Mater, 24 (2012) 3887-3894.
[147] R. Riva, H. Ragelle, A. Rieux, N. Duhem, C. Jérôme, V. Préat, Chitosan and Chitosan Derivatives in Drug Delivery and Tissue Engineering, in: R. Jayakumar, M. Prabaharan, R.A.A. Muzzarelli (Eds.) Chitosan for Biomaterials II, Springer Berlin Heidelberg, 2011, pp. 19-44.
[148] M.K. Chourasia, S.K. Jain, Polysaccharides for colon targeted drug delivery, Drug Deliv, 11 (2004) 129-148.
[149] T. Kean, M. Thanou, Biodegradation, biodistribution and toxicity of chitosan, Adv Drug Deliv Rev, 62 (2010) 3-11.

[150] D.R. Friend, New oral delivery systems for treatment of inflammatory bowel disease, Adv Drug Deliv Rev, 57 (2005) 247-265.
[151] P.B. Memvanga, V. Preat, Formulation design and in vivo antimalarial evaluation of lipid-based drug delivery systems for oral delivery of beta-arteether, Eur J Pharm Biopharm, 82 (2012) 112-119.
[152] Y.V. Ramshankar, S. Suresh, K. Devi, Novel Self-emulsifying Formulation of Curcumin with Improved Dissolution, Antiangiogenic and Anti-inflammatory Activity, Clinical Research and Regulatory Affairs, 25 (2008) 213-234.
[153] P. Severino, T. Andreani, A.S. Macedo, J.F. Fangueiro, M.H. Santana, A.M. Silva, E.B. Souto, Current State-of-Art and New Trends on Lipid Nanoparticles (SLN and NLC) for Oral Drug Delivery, Journal of drug delivery, 2012 (2012) 750891.
[154] H. Laroui, S.V. Sitaraman, D. Merlin, Gastrointestinal delivery of anti-inflammatory nanoparticles, Methods Enzymol, 509 (2012) 101-125.
[155] A. Lamprecht, H. Yamamoto, H. Takeuchi, Y. Kawashima, A pH-sensitive microsphere system for the colon delivery of tacrolimus containing nanoparticles, J Control Release, 104 (2005) 337-346.
[156] D. Kietzmann, B. Moulari, A. BÈduneau, Y. Pellequer, A. Lamprecht, Colonic delivery of carboxyfluorescein by pH-sensitive microspheres in experimental colitis, European Journal of Pharmaceutics and Biopharmaceutics, 76 (2010) 290-295.
[157] D. Chang, J. Lei, H. Cui, N. Lu, Y. Sun, X. Zhang, C. Gao, H. Zheng, Y. Yin, Disulfide cross-linked nanospheres from sodium alginate derivative for inflammatory bowel disease: Preparation, characterization, and in vitro drug release behavior, Carbohydrate Polymers, 88 (2012) 663-669.
[158] D. Hu, L. Liu, W. Chen, S. Li, Y. Zhao, A novel preparation method for 5-aminosalicylic Acid loaded eudragit s100 nanoparticles, Int J Mol Sci, 13 (2012) 6454-6468.
[159] A. Lamprecht, H. Yamamoto, H. Takeuchi, Y. Kawashima, Nanoparticles enhance therapeutic efficiency by selectively increased local drug dose in experimental colitis in rats, J Pharmacol Exp Ther, 315 (2005) 196-202.
[160] A. Lamprecht, N. Ubrich, H. Yamamoto, U. Schafer, H. Takeuchi, P. Maincent, Y. Kawashima, C.M. Lehr, Biodegradable nanoparticles for targeted drug delivery in treatment of inflammatory bowel disease, J Pharmacol Exp Ther, 299 (2001) 775-781.
[161] W. Niebel, K. Walkenbach, A. Beduneau, Y. Pellequer, A. Lamprecht, Nanoparticle-based clodronate delivery mitigates murine experimental colitis, J Control Release, 160 (2012) 659-665.
[162] H. Laroui, A.L. Theiss, Y. Yan, G. Dalmasso, H.T.T. Nguyen, S.V. Sitaraman, D. Merlin, Functional TNF[alpha] gene silencing mediated by polyethyleneimine/TNF[alpha] siRNA nanocomplexes in inflamed colon, Biomaterials, 32 (2011) 1218-1228.
[163] G.R. Veerappan, J. Betteridge, P.E. Young, Probiotics for the treatment of inflammatory bowel disease, Curr Gastroenterol Rep, 14 (2012) 324-333.
[164] P. Aureli, L. Capurso, A.M. Castellazzi, M. Clerici, M. Giovannini, L. Morelli, A. Poli, F. Pregliasco, F. Salvini, G.V. Zuccotti, Probiotics and health: an evidence-based review, Pharmacol Res, 63 (2011) 366-376.
[165] R.N. Fedorak, K.L. Madsen, Probiotics and the management of inflammatory bowel disease, Inflamm Bowel Dis, 10 (2004) 286-299.
[166] A. Saadatzadeh, F. Atyabi, M.R. Fazeli, R. Dinarvand, H. Jamalifar, A.H. Abdolghaffari, P. Mahdaviani, M. Mahbod, M. Baeeri, A. Baghaei, A. Mohammadirad, M. Abdollahi, Biochemical and pathological evidences on the benefit of a new biodegradable nanoparticles of probiotic extract in murine colitis, Fundamental & clinical pharmacology, 26 (2012) 589-598.
[167] W.K.P. Hong, Polymethacrylates, Polymer For Bioadhesive Controlled Release Systems, Oral Controlled Release Formulation Design and Drug Delivery: Theory to Practice, (2011) 81.

[168] J.G.-S. Wang, I. , Aqueous polymeric Dispersion as Film Formers, 3 135-136.
[169] P. Potesta, Eudragit FS 30 D: a new pH-sensitive polymer covering for mesalamine, European review for medical and pharmacological sciences, 5 (2001) 30.
[170] M.W. Rudolph, S. Klein, T.E. Beckert, H. Petereit, J.B. Dressman, A new 5-aminosalicylic acid multi-unit dosage form for the therapy of ulcerative colitis, Eur J Pharm Biopharm, 51 (2001) 183-190.
[171] L. Zimova, D. Vetchy, J. Muselik, J. Stembirek, The development and in vivo evaluation of a colon drug delivery system using human volunteers, Drug Deliv, 19 (2012) 81-89.
[172] S.U. Kucera, J.C. DiNunzio, N. Kaneko, J.W. McGinity, Evaluation of Ceolus microcrystalline cellulose grades for the direct compression of enteric-coated pellets, Drug Dev Ind Pharm, 38 (2012) 341-350.
[173] S.J. Kshirsagar, M.R. Bhalekar, R.P. Pawar, In vitro drug release and in vivo human X-ray studies of ileo-cecal targeting budesonide fast disintegrating tablet, Drug Dev Ind Pharm, 35 (2009) 788-795.
[174] S.J. Kshirsagar, M.R. Bhalekar, R.R. Umap, Design, development and in vitro-in vivo study of a colon-specific fast disintegrating tablet, Pharm Dev Technol, 16 (2011) 449-456.
[175] C. Gao, J. Huang, Y. Jiao, L. Shan, Y. Liu, Y. Li, X. Mei, In vitro release and in vivo absorption in beagle dogs of meloxicam from Eudragit FS 30 D-coated pellets, Int J Pharm, 322 (2006) 104-112.
[176] D. Prajakta, J. Ratnesh, K. Chandan, S. Suresh, S. Grace, V. Meera, P. Vandana, Curcumin loaded pH-sensitive nanoparticles for the treatment of colon cancer, J Biomed Nanotechnol, 5 (2009) 445-455.
[177] M. Sharma, V. Sharma, A.K. Panda, D.K. Majumdar, Development of enteric submicron particle formulation of papain for oral delivery, Int J Nanomedicine, 6 (2011) 2097-2111.
[178] M. Ahuja, A.S. Dhake, S.K. Sharma, D.K. Majumdar, Diclofenac-loaded Eudragit S100 nanosuspension for ophthalmic delivery, J Microencapsul, 28 (2011) 37-45.
[179] S.J. Kshirsagar, M.R. Bhalekar, J.N. Patel, S.K. Mohapatra, N.S. Shewale, Preparation and characterization of nanocapsules for colon-targeted drug delivery system, Pharm Dev Technol, 17 (2012) 607-613.
[180] J.W. Yoo, N. Giri, C.H. Lee, pH-sensitive Eudragit nanoparticles for mucosal drug delivery, Int J Pharm, 403 (2011) 262-267.
[181] J. Dai, T. Nagai, X. Wang, T. Zhang, M. Meng, Q. Zhang, pH-sensitive nanoparticles for improving the oral bioavailability of cyclosporine A, Int J Pharm, 280 (2004) 229-240.
[182] X.Q. Wang, J.M. Fan, Y.O. Liu, B. Zhao, Z.R. Jia, Q. Zhang, Bioavailability and pharmacokinetics of sorafenib suspension, nanoparticles and nanomatrix for oral administration to rat, Int J Pharm, 419 (2011) 339-346.
[183] A.P. Zheng, J.C. Wang, W.L. Lu, X. Zhang, H. Zhang, X.Q. Wang, Q. Zhang, Thymopentin-loaded pH-sensitive chitosan nanoparticles for oral administration: preparation, characterization, and pharmacodynamics, J Nanosci Nanotechnol, 6 (2006) 2936-2944.
[184] A.H. El-Kamel, M.S. Sokar, S.S. Al Gamal, V.F. Naggar, Preparation and evaluation of ketoprofen floating oral delivery system, Int J Pharm, 220 (2001) 13-21.
[185] A. Kumari, S.K. Yadav, S.C. Yadav, Biodegradable polymeric nanoparticles based drug delivery systems, Colloids Surf B Biointerfaces, 75 (2010) 1-18.
[186] A. Prokop, J.M. Davidson, Nanovehicular intracellular delivery systems, J Pharm Sci, 97 (2008) 3518-3590.
[187] M. Vert, J. Mauduit, S. Li, Biodegradation of PLA/GA polymers: increasing complexity, Biomaterials, 15 (1994) 1209-1213.

[188] D.E. Owens, 3rd, N.A. Peppas, Opsonization, biodistribution, and pharmacokinetics of polymeric nanoparticles, Int J Pharm, 307 (2006) 93-102.
[189] M.L. Hans, A.M. Lowman, Biodegradable nanoparticles for drug delivery and targeting, Current Opinion in Solid State and Materials Science, 6 (2002) 319-327.
[190] T. Betancourt, J.D. Byrne, N. Sunaryo, S.W. Crowder, M. Kadapakkam, S. Patel, S. Casciato, L. Brannon-Peppas, PEGylation strategies for active targeting of PLA/PLGA nanoparticles, J Biomed Mater Res A, 91 (2009) 263-276.
[191] S. Wang, T. Jiang, M. Ma, Y. Hu, J. Zhang, Preparation and evaluation of anti-neuroexcitation peptide (ANEP) loaded N-trimethyl chitosan chloride nanoparticles for brain-targeting, International Journal of Pharmaceutics, 386 (2010) 249-255.
[192] F. Danhier, O. Feron, V. Preat, To exploit the tumor microenvironment: Passive and active tumor targeting of nanocarriers for anti-cancer drug delivery, J Control Release, 148 (2010) 135-146.
[193] K. Tahara, T. Sakai, H. Yamamoto, H. Takeuchi, N. Hirashima, Y. Kawashima, Improved cellular uptake of chitosan-modified PLGA nanospheres by A549 cells, Int J Pharm, 382 (2009) 198-204.
[194] K.S. Soppimath, T.M. Aminabhavi, A.R. Kulkarni, W.E. Rudzinski, Biodegradable polymeric nanoparticles as drug delivery devices, J Control Release, 70 (2001) 1-20.
[195] H. Fessi, F. Puisieux, J.P. Devissaguet, N. Ammoury, S. Benita, Nanocapsule formation by interfacial polymer deposition following solvent displacement, International Journal of Pharmaceutics, 55 (1989) R1-R4.
[196] M. van de Weert, W.E. Hennink, W. Jiskoot, Protein instability in poly(lactic-co-glycolic acid) microparticles, Pharm Res, 17 (2000) 1159-1167.
[197] A. Giteau, M.C. Venier-Julienne, S. Marchal, J.L. Courthaudon, M. Sergent, C. Montero-Menei, J.M. Verdier, J.P. Benoit, Reversible protein precipitation to ensure stability during encapsulation within PLGA microspheres, Eur J Pharm Biopharm, 70 (2008) 127-136.
[198] J.L. Cleland, M.F. Powell, S.J. Shire, The development of stable protein formulations: a close look at protein aggregation, deamidation, and oxidation, Crit Rev Ther Drug Carrier Syst, 10 (1993) 307-377.
[199] G. Zhu, S.R. Mallery, S.P. Schwendeman, Stabilization of proteins encapsulated in injectable poly (lactide- co-glycolide), Nat Biotechnol, 18 (2000) 52-57.
[200] P.S. Kumar, S. Ramakrishna, T.R. Saini, P.V. Diwan, Influence of microencapsulation method and peptide loading on formulation of poly(lactide-co-glycolide) insulin nanoparticles, Pharmazie, 61 (2006) 613-617.
[201] P.S. Kumar, T.R. Saini, D. Chandrasekar, V.K. Yellepeddi, S. Ramakrishna, P.V. Diwan, Novel approach for delivery of insulin loaded poly(lactide-co-glycolide) nanoparticles using a combination of stabilizers, Drug Deliv, 14 (2007) 517-523.
[202] R. Gref, Y. Minamitake, M.T. Peracchia, V. Trubetskoy, V. Torchilin, R. Langer, Biodegradable long-circulating polymeric nanospheres, Science, 263 (1994) 1600-1603.
[203] W. Ulbrich, A. Lamprecht, Targeted drug-delivery approaches by nanoparticulate carriers in the therapy of inflammatory diseases, J R Soc Interface, 7 Suppl 1 (2010) S55-66.
[204] E. Simone, B.S. Ding, V. Muzykantov, Targeted delivery of therapeutics to endothelium, Cell Tissue Res, 335 (2009) 283-300.
[205] P.B. Malafaya, G.A. Silva, R.L. Reis, Natural-origin polymers as carriers and scaffolds for biomolecules and cell delivery in tissue engineering applications, Adv Drug Deliv Rev, 59 (2007) 207-233.
[206] J. Brugnerotto, J. Lizardi, F.M. Goycoolea, W. Argüelles-Monal, J. Desbrières, M. Rinaudo, An infrared investigation in relation with chitin and chitosan characterization, Polymer, 42 (2001) 3569-3580.

[207] V.K. Mourya, N.N. Inamdar, Chitosan-modifications and applications: Opportunities galore, Reactive and Functional Polymers, 68 (2008) 1013-1051.
[208] V.K. Mourya, N.N. Inamdar, Trimethyl chitosan and its applications in drug delivery, J Mater Sci Mater Med, 20 (2009) 1057-1079.
[209] L. Plapied, G. Vandermeulen, B. Vroman, V. Preat, A. des Rieux, Bioadhesive nanoparticles of fungal chitosan for oral DNA delivery, Int J Pharm, 398 (2010) 210-218.
[210] M. Dash, F. Chiellini, R.M. Ottenbrite, E. Chiellini, Chitosan—A versatile semi-synthetic polymer in biomedical applications, Progress in Polymer Science, 36 (2011) 981-1014.
[211] A.F. Kotze, H.L. Luessen, A.G. de Boer, J.C. Verhoef, H.E. Junginger, Chitosan for enhanced intestinal permeability: prospects for derivatives soluble in neutral and basic environments, Eur J Pharm Sci, 7 (1999) 145-151.
[212] A.F. Kotze, H.L. Luessen, B.J. de Leeuw, B.G. de Boer, J.C. Verhoef, H.E. Junginger, N-trimethyl chitosan chloride as a potential absorption enhancer across mucosal surfaces: in vitro evaluation in intestinal epithelial cells (Caco-2), Pharm Res, 14 (1997) 1197-1202.
[213] A. Jintapattanakit, S. Mao, T. Kissel, V.B. Junyaprasert, Physicochemical properties and biocompatibility of N-trimethyl chitosan: effect of quaternization and dimethylation, Eur J Pharm Biopharm, 70 (2008) 563-571.
[214] D. Snyman, J.H. Hamman, A.F. Kotze, Evaluation of the mucoadhesive properties of N-trimethyl chitosan chloride, Drug Dev Ind Pharm, 29 (2003) 61-69.
[215] L.W. Hsu, P.L. Lee, C.T. Chen, F.L. Mi, J.H. Juang, S.M. Hwang, Y.C. Ho, H.W. Sung, Elucidating the signaling mechanism of an epithelial tight-junction opening induced by chitosan, Biomaterials, 33 (2012) 6254-6263.
[216] T.H. Yeh, L.W. Hsu, M.T. Tseng, P.L. Lee, K. Sonjae, Y.C. Ho, H.W. Sung, Mechanism and consequence of chitosan-mediated reversible epithelial tight junction opening, Biomaterials, 32 (2011) 6164-6173.
[217] G. Sandri, M.C. Bonferoni, S. Rossi, F. Ferrari, S. Gibin, Y. Zambito, G. Di Colo, C. Caramella, Nanoparticles based on N-trimethylchitosan: evaluation of absorption properties using in vitro (Caco-2 cells) and ex vivo (excised rat jejunum) models, Eur J Pharm Biopharm, 65 (2007) 68-77.
[218] Y. Zambito, C. Zaino, G. Di Colo, Effects of N-trimethylchitosan on transcellular and paracellular transcorneal drug transport, Eur J Pharm Biopharm, 64 (2006) 16-25.
[219] V. Dehousse, N. Garbacki, A. Colige, B. Evrard, Development of pH-responsive nanocarriers using trimethylchitosans and methacrylic acid copolymer for siRNA delivery, Biomaterials, 31 (2010) 1839-1849.
[220] P. Mukhopadhyay, R. Mishra, D. Rana, P.P. Kundu, Strategies for effective oral insulin delivery with modified chitosan nanoparticles: A review, Progress in Polymer Science, 37 (2012) 1457-1475.
[221] M. Amidi, E. Mastrobattista, W. Jiskoot, W.E. Hennink, Chitosan-based delivery systems for protein therapeutics and antigens, Adv Drug Deliv Rev, 62 (2010) 59-82.
[222] A.M. Sadeghi, F.A. Dorkoosh, M.R. Avadi, P. Saadat, M. Rafiee-Tehrani, H.E. Junginger, Preparation, characterization and antibacterial activities of chitosan, N-trimethyl chitosan (TMC) and N-diethylmethyl chitosan (DEMC) nanoparticles loaded with insulin using both the ionotropic gelation and polyelectrolyte complexation methods, Int J Pharm, 355 (2008) 299-306.
[223] T. Kean, S. Roth, M. Thanou, Trimethylated chitosans as non-viral gene delivery vectors: Cytotoxicity and transfection efficiency, Journal of Controlled Release, 103 (2005) 643-653.
[224] Z. Mao, L. Ma, J. Yan, M. Yan, C. Gao, J. Shen, The gene transfection efficiency of thermoresponsive N,N,N-trimethyl chitosan chloride-g-poly(N-isopropylacrylamide) copolymer, Biomaterials, 28 (2007) 4488-4500.

[225] Q.Q. Zhao, J.L. Chen, T.F. Lv, C.X. He, G.P. Tang, W.Q. Liang, Y. Tabata, J.Q. Gao, N/P ratio significantly influences the transfection efficiency and cytotoxicity of a polyethylenimine/chitosan/DNA complex, Biol Pharm Bull, 32 (2009) 706-710.
[226] H. Zhang, I.A. Alsarra, S.H. Neau, An in vitro evaluation of a chitosan-containing multiparticulate system for macromolecule delivery to the colon, Int J Pharm, 239 (2002) 197-205.
[227] H. Zhang, S.H. Neau, In vitro degradation of chitosan by bacterial enzymes from rat cecal and colonic contents, Biomaterials, 23 (2002) 2761-2766.
[228] J. Zhang, C. Tang, C. Yin, Galactosylated trimethyl chitosan–cysteine nanoparticles loaded with Map4k4 siRNA for targeting activated macrophages, Biomaterials.
[229] S. Cafaggi, E. Russo, R. Stefani, R. Leardi, G. Caviglioli, B. Parodi, G. Bignardi, D. De Totero, C. Aiello, M. Viale, Preparation and evaluation of nanoparticles made of chitosan or N-trimethyl chitosan and a cisplatin-alginate complex, J Control Release, 121 (2007) 110-123.
[230] D. de Britto, M.R. de Moura, F.A. Aouada, L.H.C. Mattoso, O.B.G. Assis, N,N,N-trimethyl chitosan nanoparticles as a vitamin carrier system, Food Hydrocolloids, 27 (2012) 487-493.
[231] M. Guan, Y. Zhou, Q.-L. Zhu, Y. Liu, Y.-Y. Bei, X.-N. Zhang, Q. Zhang, N-trimethyl chitosan nanoparticle-encapsulated lactosyl-norcantharidin for liver cancer therapy with high targeting efficacy, Nanomedicine: Nanotechnology, Biology and Medicine, 8 (2012) 1172-1181.
[232] M. Guan, Q.L. Zhu, Y. Liu, Y.Y. Bei, Z.L. Gu, X.N. Zhang, Q. Zhang, Uptake and transport of a novel anticancer drug-delivery system: lactosyl-norcantharidin-associated N-trimethyl chitosan nanoparticles across intestinal Caco-2 cell monolayers, Int J Nanomedicine, 7 (2012) 1921-1930.
[233] V. Dehousse, N. Garbacki, S. Jaspart, D. Castagne, G. Piel, A. Colige, B. Evrard, Comparison of chitosan/siRNA and trimethylchitosan/siRNA complexes behaviour in vitro, Int J Biol Macromol, 46 (2010) 342-349.
[234] J. Zhang, C. He, C. Tang, C. Yin, Ternary Polymeric Nanoparticles for Oral siRNA Delivery, Pharm Res, (2013).
[235] V.B. Morris, C.P. Sharma, Folate mediated histidine derivative of quaternised chitosan as a gene delivery vector, International Journal of Pharmaceutics, 389 (2010) 176-185.
[236] X. Zhao, L. Yin, J. Ding, C. Tang, S. Gu, C. Yin, Y. Mao, Thiolated trimethyl chitosan nanocomplexes as gene carriers with high in vitro and in vivo transfection efficiency, Journal of Controlled Release, 144 (2010) 46-54.
[237] B. Slutter, L. Plapied, V. Fievez, M.A. Sande, A. des Rieux, Y.J. Schneider, E. Van Riet, W. Jiskoot, V. Preat, Mechanistic study of the adjuvant effect of biodegradable nanoparticles in mucosal vaccination, J Control Release, 138 (2009) 113-121.
[238] B. Slutter, S. Bal, C. Keijzer, R. Mallants, N. Hagenaars, I. Que, E. Kaijzel, W. van Eden, P. Augustijns, C. Lowik, J. Bouwstra, F. Broere, W. Jiskoot, Nasal vaccination with N-trimethyl chitosan and PLGA based nanoparticles: nanoparticle characteristics determine quality and strength of the antibody response in mice against the encapsulated antigen, Vaccine, 28 (2010) 6282-6291.
[239] R.J. Verheul, B. Slütter, S.M. Bal, J.A. Bouwstra, W. Jiskoot, W.E. Hennink, Covalently stabilized trimethyl chitosan-hyaluronic acid nanoparticles for nasal and intradermal vaccination, Journal of Controlled Release, 156 (2011) 46-52.
[240] Y. Zheng, X. Song, M. Darby, Y. Liang, L. He, Z. Cai, Q. Chen, Y. Bi, X. Yang, J. Xu, Y. Li, Y. Sun, R.J. Lee, S. Hou, Preparation and characterization of folate-poly(ethylene glycol)-grafted-trimethylchitosan for intracellular transport of protein through folate receptor-mediated endocytosis, J Biotechnol, 145 (2010) 47-53.

[241] F. Chen, Z.R. Zhang, F. Yuan, X. Qin, M. Wang, Y. Huang, In vitro and in vivo study of N-trimethyl chitosan nanoparticles for oral protein delivery, Int J Pharm, 349 (2008) 226-233.
[242] L. Yin, J. Ding, C. He, L. Cui, C. Tang, C. Yin, Drug permeability and mucoadhesion properties of thiolated trimethyl chitosan nanoparticles in oral insulin delivery, Biomaterials, 30 (2009) 5691-5700.
[243] S. Mao, U. Bakowsky, A. Jintapattanakit, T. Kissel, Self-assembled polyelectrolyte nanocomplexes between chitosan derivatives and insulin, J Pharm Sci, 95 (2006) 1035-1048.
[244] Y. Jin, Y. Song, X. Zhu, D. Zhou, C. Chen, Z. Zhang, Y. Huang, Goblet cell-targeting nanoparticles for oral insulin delivery and the influence of mucus on insulin transport, Biomaterials, 33 (2012) 1573-1582.
[245] M. Tafaghodi, V. Saluja, G.F. Kersten, H. Kraan, B. Slutter, J.P. Amorij, W. Jiskoot, Hepatitis B surface antigen nanoparticles coated with chitosan and trimethyl chitosan: Impact of formulation on physicochemical and immunological characteristics, Vaccine, 30 (2012) 5341-5348.
[246] R. Subbiah, P. Ramalingam, S. Ramasundaram, D.Y. Kim, K. Park, M.K. Ramasamy, K.J. Choi, N,N,N-Trimethyl chitosan nanoparticles for controlled intranasal delivery of HBV surface antigen, Carbohydrate Polymers, 89 (2012) 1289-1297.
[247] R.J. Verheul, N. Hagenaars, T. van Es, E.V. van Gaal, P.H. de Jong, S. Bruijns, E. Mastrobattista, B. Slutter, I. Que, J.G. Heldens, H. van den Bosch, H.L. Glansbeek, W.E. Hennink, W. Jiskoot, A step-by-step approach to study the influence of N-acetylation on the adjuvanticity of N,N,N-trimethyl chitosan (TMC) in an intranasal nanoparticulate influenza virus vaccine, Eur J Pharm Sci, 45 (2012) 467-474.
[248] W.N. Charman, Lipids, lipophilic drugs, and oral drug delivery-some emerging concepts, J Pharm Sci, 89 (2000) 967-978.
[249] C.J. Porter, K.M. Wasan, P. Constantinides, Lipid-based systems for the enhanced delivery of poorly water soluble drugs, Adv Drug Deliv Rev, 60 (2008) 615-616.
[250] C.J. Porter, C.W. Pouton, J.F. Cuine, W.N. Charman, Enhancing intestinal drug solubilisation using lipid-based delivery systems, Adv Drug Deliv Rev, 60 (2008) 673-691.
[251] J.B. Jeevana, K. Sreelakshmi, Design and evaluation of self-nanoemulsifying drug delivery system of flutamide, Journal of young pharmacists : JYP, 3 (2011) 4-8.
[252] R.N. Gursoy, S. Benita, Self-emulsifying drug delivery systems (SEDDS) for improved oral delivery of lipophilic drugs, Biomedicine & pharmacotherapy = Biomedecine & pharmacotherapie, 58 (2004) 173-182.
[253] M. Muchow, P. Maincent, R.H. Muller, Lipid nanoparticles with a solid matrix (SLN, NLC, LDC) for oral drug delivery, Drug Dev Ind Pharm, 34 (2008) 1394-1405.
[254] A. Beloqui, M.A. Solinis, A.R. Gascon, A. Del Pozo-Rodriguez, A. des Rieux, V. Preat, Mechanism of transport of saquinavir-loaded nanostructured lipid carriers across the intestinal barrier, J Control Release, 166 (2012) 115-123.
[255] S. Das, A. Chaudhury, Recent advances in lipid nanoparticle formulations with solid matrix for oral drug delivery, AAPS PharmSciTech, 12 (2011) 62-76.

CHAPTER II.

Aim of the thesis

Conventional anti-inflammatory drugs for IBD suffer from poor pharmacokinetic profile and systemic delivery after oral administration, leading to serious systemic side effects. As they show preferential uptake in inflamed colonic areas, use of nanocarriers for IBD delivery should lead to higher local drug concentrations and maintain therapeutic efficacy while enhancing safety by decreasing unspecific delivery.

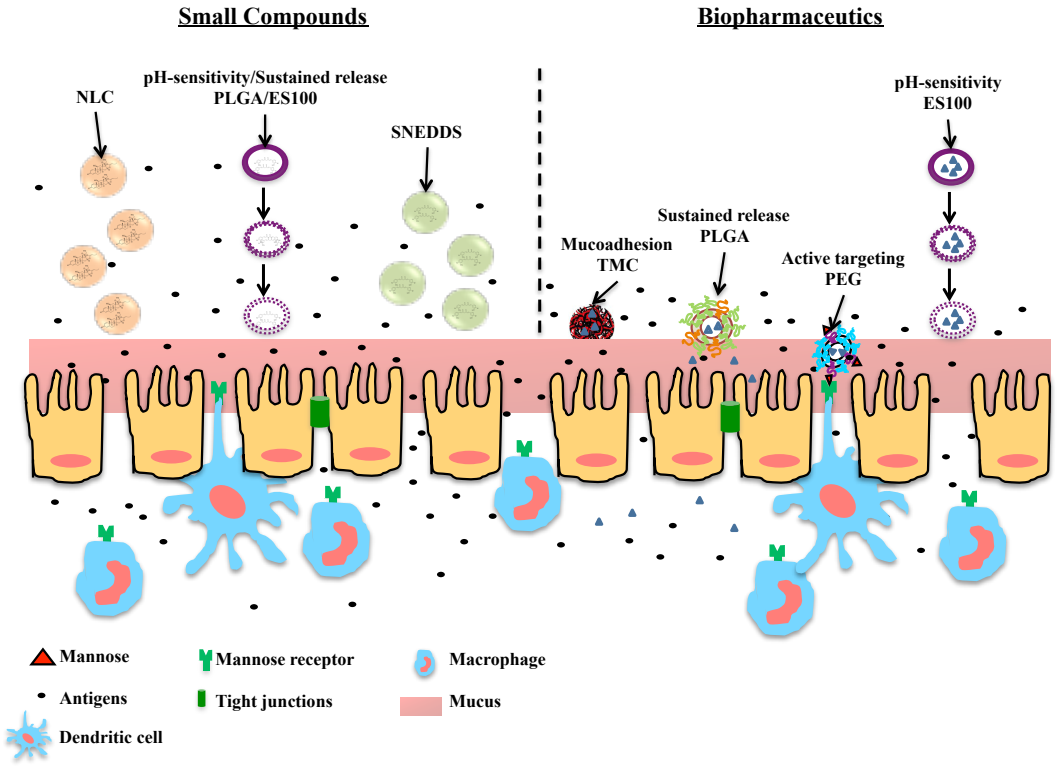


Figure 1: Nanocarriers-based topical delivery of small and biopharmaceutical anti-inflammatory drug for the treatment of IBD

The aim of the thesis was to deliver topically several anti-inflammatory drugs to IBD-induced inflamed colon with nanocarriers: polymeric nanoparticles or lipid-based nanocarriers. Choice of the polymer and the lipid-based nanocarriers enables to use various delivery strategies:

- pH-sensitivity (ES100): Luminal pH varies from acidic values in the stomach to neutral of slightly alkaline values in the colon
- Mucoadhesion (TMC): Colon is the gastro-intestinal part with the thickest mucus layer
- Sustained release (PLGA): Colon is the last part of the GIT
- Active targeting (PEG-grafting): Some specific patterns of the inflamed mucosa (inflammatory profile of the epithelium, overexpression of immune-related cells) can be targeted by the graft of ligands on the nanoparticles' surface

- Lipid-based delivery (SNEDDS and NLCs): They protect sensitive drugs from the outer environment, they enhance the solubility of poorly water soluble drugs, their production can be easily scaled up and there are experimental evidence of the immunomodulatory effects of lipids in IBD therapy.

The encapsulated anti-inflammatory compounds were either small active compounds (budesonide and curcumin) or biopharmaceutics (ovalbumin as model protein and anti-TNF-α Fab).

For each strategy, nanocarriers were formulated, optimized and characterized. Their potential for inflamed colon-specific topical targeting and delivery was evaluated in *in vitro*, *ex vivo* and *in vivo* models.

Chapter III and IV are dedicated to the topical delivery of anti-inflammatory small active compounds. Chapter III evaluates *in vitro* and *in vivo* the topical delivery and therapeutic activity of budesonide loaded nano-structured lipid carriers. Chapter IV assesses topical delivery of curcumin using two nanoscale delivery strategies: one using pH-sensitive and sustained release nanoparticles and one using SNEDDS. Chapter V and VI are dedicated to the topical delivery of biopharmaceutics. Chapter V compares different delivery strategies using ovalbumin as model protein and polymeric nanoparticles as nanocarriers. Chapter VI presents the selection of optimal polymeric nanoparticle suitable for the topical delivery of an active anti-TNF-α fragment antibody.

CHAPTER III.
Budesonide-loaded NLC reduce inflammation in murine colitis

Budesonide-loaded nanostructured lipid carriers reduce inflammation in murine DSS-induced colitis

Beloqui A.[a], Coco R.[a], Alhouayek M., Solinís M.A., Alicia Rodríguez-Gascón A., Muccioli G.G., Préat V.

International Journal of Pharmaceutics, doi: 10.1016/j.ijpharm.2013.05.017

[a]These two authors contributed equally to the study.

ABSTRACT

The challenge for the treatment of inflammatory bowel disease (IBD) is the delivery of the drug to the site of inflammation. Because nanoparticles have the ability to accumulate in inflamed regions, the aim of the present study was to evaluate nanostructured lipid carriers (NLCs) as nanoparticulate drug delivery systems for the treatment of IBD. Budesonide (BDS) was chosen as a candidate anti-inflammatory drug. BDS-loaded NLCs (BDS-NLC) produced by high-pressure homogenization had a size of 200 nm and a negative zeta potential. BDS-NLCs reduced the TNF-α secretion by activated macrophages (J774 cells). BDS-NLCs were more active in a murine model of dextran sulfate-induced colitis when compared with Blank-NLCs or a BDS suspension: BDS-NLCs decreased neutrophil infiltration, decreased the levels of the pro-inflammatory cytokines IL-1ß and TNF-α in the colon and improved the histological scores of the colons. These data suggest that NLCs could be a promising alternative to polymeric nanoparticles as a targeted drug delivery system for IBD treatment.

KEYWORDS

Nanostructured lipid carriers, macrophages, colonic delivery, inflammatory bowel disease, budesonide

TABLE OF CONTENTS

I. Introduction 97

Materials and methods 99

I.1 Materials 99

I.1.1 Chemicals 99

I.1.2 Cell culture 99

I.2 Preparation of the formulations 99

I.2.1 NLC preparation 99

I.2.2 BDS suspension 100

I.3 NLC characterization 100

I.3.1 Size and zeta potential measurements 100

I.3.2 Encapsulation efficiency 100

I.3.3 Determination of BDS by HPLC 101

I.4 In vitro studies 101

I.4.1 Cell culture 101

I.4.2 Effect of NLCs on cell viability 101

I.4.3 Inhibition of TNF-a production from J774 macrophages by BDS-NLCs 102

I.5 In vivo efficacy of BDS-loaded formulations 102

I.5.1 Clinical activity scoring 103

I.5.2 Colon weight/colon length ratio 103

I.5.3 Histological assessment of colonic inflammation 103

I.5.4 Myeloperoxidase activity (MPO) 103

I.5.5 Tissue cytokine quantitation by ELISA 104

I.6 In vivo localization of coumarin-6-NLCs in the gastrointestinal tract 104

I.7 Statistical analyses 105

II. Results 106

II.1 NLC characterization 106

II.2 In vitro studies with J774 cells 106

II.2.1 Assessment of the cytotoxicity of the nanoparticles on J774 cells 106

II.2.2 Inhibition of TNF-a production from J774 cells 106

II.3 In vivo effects of BDS-NLCs on murine colitis 107

II.3.1 Inflammatory clinical activity and histological scoring 107

II.3.2 MPO activity and pro-inflammatory cytokines (IL-1ß and TNF-α) in the colon 109

II.3.3 In vivo localization of coumarin-6-NLCs 110

III. Discussion 112

IV. Conclusion 115

V. References 116

I. INTRODUCTION

Inflammatory bowel diseases (IBD) are chronic and relapsing inflammatory disorders of the gastrointestinal tract (GIT). The two major forms, ulcerative colitis and Crohn's disease, present a colonic-specific or a widespread repartition of inflamed lesions, respectively [1-3]. Patients with IBD require life-long anti-inflammatory and immunosuppressive therapy. Although most of the drugs can be administered by the oral route for IBD treatment, high daily doses are required to obtain a therapeutic effect [4-6]. Furthermore, systemic absorption is observed, leading to serious adverse effects [7, 8].

Considering the colonic location of these diseases as well as the systemic side effects of absorbed drugs, the specific targeted delivery of anti-inflammatory drugs to the inflamed colonic areas should lead to higher local concentrations and maintain therapeutic efficacy while enhancing safety by decreasing absorption. Different delivery strategies to target the inflamed colon have been studied [9]. Sustained drug release devices, pH-sensitive formulations, rectal formulations and pro-drugs are some of the strategies that have been developed during the past several decades to obtain efficient colonic drug delivery. However, the inefficient control of drug release, patient sensitivity to IBD symptoms (e.g., diarrhea, modified colonic environment) or the inability to reach the inflamed areas are some of the observed drawbacks that cause decreased efficacy.

Because nanoparticulate drug delivery systems have the ability to accumulate in the inflamed regions of the gut, they offer a new targeting approach in IBD [9, 10]. Size is a critical factor in the design of drug delivery systems for the inflamed colon. During active IBD, the luminal content undergoes a decrease in its transit time due to diarrhea, the most frequent symptom of IBD. In animal models of experimental colitis and in human patients [11], a preferential uptake of nano-sized particles was observed in the inflamed colonic mucosa. It is apparent that the pathophysiological changes associated with mucosal inflammation, such as (i) a disrupted intestinal barrier due to the presence of mucosal surface alterations, crypt distortions and ulcers, (ii) increased mucus production and (iii) the infiltration of immune-related cells such as macrophages, lymphocytes or dendritic cells, provide an environment favorable for the preferential accumulation of nanoparticles in the inflamed colonic regions [12]. Therefore, nano- and microparticulate drug carriers have been widely studied for targeting the inflamed intestinal mucosa. Liposomes [13], polymeric nanoparticles [11, 14, 15] and drug-loaded nanoparticles in combination with polysaccharide hydrogels [16], among others, have been widely studied for effective drug targeting and release in the inflamed colonic mucosa. Most of these strategies are based on pH-, enzyme- or transit time-dependent systems [10, 16, 17]. Therefore, these delivery systems encounter inter- and

intra-individual variability in terms of the gut pH and microflora, which may evoke early release of the drug with subsequent decrease in therapeutic efficacy.

Among the wide variety of currently available nanocarriers, solid lipid nanoparticles (SLNs) are promising delivery vectors for the treatment of inflammatory diseases due to the following reasons: (i) SLNs can be prepared on a large scale without organic solvent [18]; (ii) SLNs are stable in the gastrointestinal tract compared with other lipid-based nanoparticles such as liposomes; and (iii) the ability of lipid-based nanoparticles to modulate the immune system and induce anti-inflammatory effects has been previously described [19, 20]. SLNs that are usually used for parental and topical formulations have been recently proposed for colonic delivery. Sodium butyrate-loaded SLNs displayed better anti-adhesive effects than butyrate alone on the *in vitro* adhesion of polymorphonuclear cells to human umbilical vein endothelial cells, as this step is critical in the recruitment and infiltration of immune-related cells into inflamed tissues during active IBD [21]. Furthermore, in a human inflammatory bowel disease whole-blood model, after 24 h of lipopolysaccharide exposure, a significant decrease in pro-inflammatory cytokines (IL-1β and TNF-α) secretion was observed following administration of dexamethasone- or butyrate-loaded SLNs, when compared with dexamethasone or butyrate alone [22]. However, to date, no *in vivo* studies of SLNs targeting the inflamed colonic mucosa have been published.

Budesonide (BDS) is a corticosteroid with high topical efficacy and minimal systemic activity [17, 23]. This steroid exhibits low oral bioavailability and an extensive hepatic first pass effect, as 10-15% of the drug reaches systemic circulation [24]. These characteristics give BDS a better adverse effect profile than the conventional steroids and thus make it the first choice for the induction of remission in IBD. Enemas and controlled-release formulations such as Budenofalk® or Entocort® have been used in clinical practice for the topical delivery of BDS. However, due to the long-term side effect profile inherent to the corticosteroid class, BDS cannot be used for the maintenance of remission [25, 26]. Specific mucosal targeting and delivery of BDS could reduce the inflammation in lesions while maintaining a good safety profile.

The aim of the present study was to evaluate nanostructured lipid carriers (NLCs), a second generation of SLNs with a higher stability and drug loading capacity, as nanoparticulate drug delivery systems for IBD treatment. BDS was chosen as a candidate anti-inflammatory drug for entrapment into NLCs. The evaluation of BDS-loaded NLCs (BDS-NLC) was performed (i) *in vitro,* by evaluating their anti-inflammatory potential in reducing TNF-α secretion from activated macrophages (J774 cells) and (ii) *in vivo,* in a murine dextran-sulfate (DSS)-induced colitis model, by quantitating neutrophil infiltration and the concentrations of the pro-inflammatory cytokines IL-1ß and TNF-α and by histological evaluation of inflammation severity in excised colons.

MATERIALS AND METHODS

I.1 MATERIALS

I.1.1 Chemicals

BDS, coumarin-6, *O*-dianisidine, HTAB (hexadecyltrimethylammonium bromide), 3-(4,5-dimethylthiazol-2-yl)-2,5-diphenyltetrazolium bromide (MTT), hematoxylin, eosin and hydrogen peroxide (30%) were purchased from Sigma-Aldrich (St. Louis, MO, USA). Precirol ATO®5 was kindly provided by Gattefossé (Madrid, ES). Polysorbate 80 (Tween 80) was purchased from Vencaser (Bilbao, SP). Poloxamer 188 was a gift from BASF (Madrid, ES). Miglyol 812 N/F was purchased from Sasol (Hamburg, GE). Potassium dihydrogen phosphate (KH_2PO_4), disodium hydrogen phosphate (Na_2HPO_4) and dimethylsulfoxide (DMSO) were obtained from Merck (Darmstadt, DE). Acetonitrile (gradient HPLC grade) and ethanol were purchased from VWR (Leuven, BE). Dulbecco's Phosphate-Buffered Saline (PBS) and Hank´s Balanced Salt Solution (HBSS) were purchased from Gibco™ Invitrogen Corporation (Paisley, UK). Dextran sodium sulfate (DSS) was purchased from TdB Consultancy (Uppsala, SE). Complete protease inhibitor cocktail tablets were purchased from Roche Diagnostics (Vilvoorde, BE). Paraffin was provided by Sakura Finetek (Torrance, CA).

I.1.2 Cell culture

Roswell Park Memorial Institute (RPMI) 1640 medium, fetal bovine serum (FBS), trypsin (0.05%) with EDTA was purchased from Gibco™ Invitrogen Corporation (Paisley, UK). Lipopolysaccharide (LPS, Escherichia coli O111:B4) was purchased from Sigma-Aldrich (St. Louis, MO, USA).

I.2 PREPARATION OF THE FORMULATIONS

I.2.1 NLC preparation

BDS-NLCs were prepared using the high-pressure homogenization technique [18, 27]. Briefly, Precirol ATO®5 (5 g) and Miglyol 812 (0.5 ml) were melted at 75ºC until a uniform and clear oil phase was obtained and BDS (4 mg) (melting point above 200 °C) was homogenously dispersed in the mentioned solution. The aqueous phase was prepared by dispersing Tween 80 (2%) (w/v) and poloxamer 188 (1%) (w/v) in water (50 ml) and heating to the same temperature as the lipid phase. The hot aqueous phase was then added to the

oil phase, and the mixture was sonicated for 15 s to form a hot pre-emulsion, which was subsequently homogenized at 80°C and 500 bar using a Stansted nG12500 homogenizer (SFP, Essex, UK) for ten homogenization cycles. A batch of blank nanoparticles was also prepared without BDS (Blank-NLCs).

For the *in vivo* localization study, the NLCs were labeled with the fluorescent dye coumarin-6. Briefly, 5 mg of coumarin-6 was incorporated into the lipid phase of the formulation in place of BDS, and the NLCs were prepared according to the aforementioned protocol (coumarin-6-NLCs).

I.2.2 BDS suspension

A BDS suspension (BDS sus) was prepared as a control. BDS (4 mg) was dispersed in PBS (50 ml). The primary volume median particle diameter of the BDS suspension was measured by laser diffraction (HELOS, Sympatec, Clausthal-Zellerfeld, DE). Before sizing, the suspension was homogenized in a 50 ml flask by sonication (30-60 s) with the internal probe powered at 60 W while magnetically stirring at 1000 rpm.

I.3 NLC CHARACTERIZATION

I.3.1 Size and zeta potential measurements

The size of the NLCs was determined using photon correlation spectroscopy (PCS), and the zeta potential was measured using Laser Doppler Velocimetry (LDV) with a Malvern Zetasizer Nano ZS (Malvern Instruments Ltd., Worcestershire, UK). Samples were diluted in ultra-pure water (Arium 611 VF, Sartorius AG Gottingen, Germany) before measurement.

I.3.2 Encapsulation efficiency

Untrapped BDS was quantified by ultrafiltration using Millipore (Madrid, ES) Amicon® ultracentrifugal filters (molecular weight cutoff, MWCO, 100,000 Da) (1,500 g, 20 min). The free BDS present in the filtrate was then measured by HPLC and was found to be below the limit of quantification (LOQ<1µg/mL).

The drug content within BDS-NLCs was calculated by dissolving the samples (1 ml) in a solvent mixture of methanol/chloroform (1:1 v/v) (1:10 dilution) and filtering through a 0.2 µm filter. The resulting solution was analyzed by HPLC. The encapsulation efficiency, determined in triplicate, was calculated as the percentage of the amount of BDS present in the NLCs (drug content – free drug) to the initial amount of BDS incorporated into the NLCs, as follows:

$$encapsulation\ efficiency(\%) = \frac{Amount\ of\ BDS\ in\ NLCs}{Initial\ amount\ of\ BDS} x100$$

Coumarin-6 (λ_{Ex}= 460 nm, λ_{Em}= 505 nm) encapsulation was assessed by ultracentrifuging the coumarin-6-loaded NLC suspension as described for BDS. The free coumarin-6 present in the filtrate was then measured using fluorimetry (SFM 25 fluorometer, Kontron Instruments, Basel, SW).

I.3.3 Determination of BDS by HPLC

HPLC was performed to determine the BDS concentration using a Waters 1525 HPLC Binary Pump (Waters Corp., Milford, USA). The UV-detector was a Waters 2487. The system was controlled by the Breeze software (Waters, UK). A Nucleodur 100-5 C18 5 µm (4 mm x 125 mm) column was used at room temperature. The mobile phase contained 55% (v/v) acetonitrile and 45% (v/v) of 0.025 M KH_2PO_4 adjusted to pH 3.2 with phosphoric acid, as previously reported by Gupta et al. [28]. BDS was detected at 244 nm using an ultraviolet detector. The flow rate was set to 1.1 ml/min for isocratic elution, and the injected sample volume was 50 µl. The assay was linear over the BDS concentration range of 1-30 µg/ml. The intra- and inter-day coefficients of variation were both within ± 5%. The limits of detection (LOD) and of quantitation (LOQ) of BDS were 0.05 µg/ml and 1 µg/ml, respectively. No interfering peaks were detected in the assay.

I.4 IN VITRO STUDIES

I.4.1 Cell culture

The J774 murine macrophage cell line was kindly donated by Pr. Marie-Paule Mingeot (Université catholique de Louvain, LDRI, BE). The J774 macrophage cell line was maintained in RPMI 1640 supplemented with 10% fetal bovine serum. Cells were grown in 75 cm^2 flasks (Corning, Lowell, MA, USA) in an atmosphere of 5% CO_2/95% air (v/v) at 37°C.

I.4.2 Effect of NLCs on cell viability

The cytotoxicity of the NLCs on J774 cells was evaluated using the MTT method. Briefly, J774 cells (20,000/well) were seeded in 96-well plates (Nunc, Roskilde, DK) and maintained for 24 h at 37°C and 5% CO_2. After 4 h of exposure at different NLC concentrations, the cells were washed 3 times with HBSS and incubated for 3 h with 0.5 mg/ml MTT in RPMI. The medium was then removed, and the purple formazan crystals were dissolved in 100 µl of DMSO. The absorbance was measured at 570 nm using a MultiSkan Ex plate reader

(Thermo Fisher Scientific, Waltham, MA, USA). The IC_{50}s for the different formulations were calculated using the GraphPad Prism 5 program (CA, USA). All MTT assays were repeated in triplicate.

I.4.3 Inhibition of TNF-α production from J774 macrophages by BDS-NLCs

The J774 cells were seeded in 12-well plates and allowed to adhere for 24 h. The cells were exposed for 4 h to the following formulations: (i) BDS-NLCs (0.4 mg/ml containing 0.29 µg/ml BDS, (ii) Blank-NLCs (0.4 mg/ml) or (iii) BDS suspension (0.29 µg/ml). The incubation medium was then collected for the lactate dehydrogenase release assay and replaced with fresh medium supplemented with 0.1 µg/ml of LPS to activate macrophages [29, 30]. Cell-free supernatants were harvested 24 h later and stored at -20°C for cytokine quantitation. TNF-α was assayed using a DuoSet® ELISA kit (R&D Systems, Minneapolis, MN, USA). During these experiments, the absence of cytotoxicity of the different formulations on macrophages was also assessed in the cell culture media after 4 h of incubation by measuring the activity of lactate dehydrogenase. A cytotoxicity detection kit (Roche Diagnostics GmbH, Mannheim, DE) was used according to the manufacturer's instructions. The results were expressed as a percentage of the positive control, which consisted of cells exposed to 1% (v/v) Triton X-100.

I.5 IN VIVO EFFICACY OF BDS-LOADED FORMULATIONS

An *in vivo* study was performed in C57BL/6 female mice (18-20 g, 6 weeks; Janvier Laboratories, FR). Animals were housed under standard conditions and supplied with food and tap water *ad libitum*. Protocols were approved by the *Université catholique de Louvain* animal committee (UCL/MD/2009-001). Colitis was induced by administration of drinking water containing 3% (w/v) DSS for 5 consecutive days, and colonic inflammation was assessed 7 days after the beginning of DSS treatment [16, 31]. The animals were divided into the following five groups (8 mice per group): untreated control group (healthy mice), untreated DSS group, DSS+BDS-NLCs group, DSS+Blank-NLCs group and DSS+BDS suspension group (0.4 mg of BDS/kg; 550 mg/kg NLCs). Food (but not water) was withdrawn 12 h prior to the administration of the treatment. One hundred microliters of each formulation were administered by gavage at days 1, 3 and 5; the untreated control group and the DSS control group received PBS instead of the formulation. At day 7, the animals were sacrificed, and colon samples were collected for evaluation of the severity of colitis.

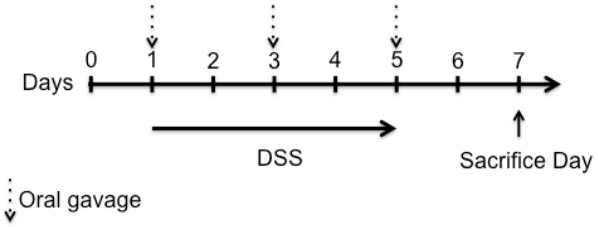


Figure 1: Schematic presentation of the *in vivo* experimental procedure

I.5.1 Clinical activity scoring

The clinical activity score for weight loss, stool consistency and rectal bleeding was calculated as described by Melgar et al. [32]. Inflammation was scored on a scale of 0-4.

I.5.2 Colon weight/colon length ratio

At the time of sacrifice, 7 days after colitis induction, the excised colons were measured and weighed (after rinsing the luminal contents), and the colon weight/colon length ratio was determined. This ratio is considered a reliable and sensitive indicator of the severity and extent of the inflammatory response in colitis [33, 34].

I.5.3 Histological assessment of colonic inflammation

For histological scoring, small segments of the colon were fixed in 4% buffered formalin overnight, washed with 70% ethanol and subsequently embedded in paraffin. Two sets of 3 serial sections (10 µm) were cut 100 µm apart, and 6 sections were evaluated for each mouse. Sections were stained with hematoxylin-eosin, and histological scores were determined in a blind manner according to a scoring procedure for colitis reported by Geboes et al. [35], with slight modifications. Briefly, a five-grade classification system for inflammation was employed. Inflammation was graded semiquantitatively from 0 to 4 as follows: 0, no structural change; 1, inflammation visible; 2, leukocytes present in the lamina propria; 3, leukocytes present in the epithelium (3.1 <5% crypts involved, 3.2 <50% crypts involved, 3.3 >50% crypts involved); and 4, crypt destruction visible. Mice were scored individually. Each score represented the mean of six sections.

I.5.4 Myeloperoxidase activity (MPO)

The tissue-associated MPO assay was performed to quantitate the degree of inflammatory infiltration, which correlates with the severity of colitis [36]. Briefly, colon specimens from both the proximal and the distal portion of the colon together (~25 mg) were snap frozen in liquid N_2 at the time of sacrifice and stored for later assessment. For determination of MPO activity, tissue was placed in HTAB buffer (0.5% HTAB in 50 mM potassium phosphate buffer, pH 6)

on ice and gently homogenized. The homogenate was centrifuged (Allegra X-15R, Beckman Coulter, CA) at 2,000 g for 10 min and subsequently ultracentrifuged (Biofuge 15 R, Heraeus Sepatech, Chandler, Arizona, USA) at 18,393 g for 20 min at 4ºC. The supernatant (7 µl) was added to 96-well plates (Nunc, Roskilde, DK) together with 200 µl of a 50 mM potassium phosphate buffer containing 0.167 mg/ml *O*-dianisidine and 500 ppm hydrogen peroxide. Samples were analyzed in duplicate. MPO activity in the supernatant was measured spectrophotometrically (Spectophotometer Spectramax M2e & program SoftMax Pro, Molecular Devices, LLC, USA) at 460 nm for 30 min. The results were expressed as MPO units per gram of tissue, and one unit of MPO activity was defined as the amount that degrades 1 mmol/min of hydrogen peroxide at 25ºC [34].

I.5.5 Tissue cytokine quantitation by ELISA

The concentrations of pro-inflammatory cytokines (IL-1ß and TNF-α) in the colon were determined by a sandwich-type ELISA technique using the Ready-Set-Go! Kit (eBioscience, Vienna, AU) following the manufacturer's instructions [34]. Colon homogenates were directly prepared from frozen tissue samples. Briefly, colonic tissue samples were homogenized in 1 ml of extraction buffer (PBS with 1% SDS and 1 tablet of complete protease inhibitor cocktail (Roche Diagnostics, Vilvoorde, BE), per 10 ml of solution) with an UltraTurrax (IKA T18 Basic, Staufen, Germany) and centrifuged first at 900 g for 10 min at 4°C and then for 15 min at 7,000 g at 4°C. The supernatants were collected and stored at -80°C for later assessment. The total protein concentration was determined using the Lowry method protein assay.

I.6 IN VIVO LOCALIZATION OF COUMARIN-6-NLCS IN THE GASTROINTESTINAL TRACT

The localization of coumarin-6-NLCs in the gastrointestinal tract (GIT) *in vivo* was studied quantitatively by fluorophotometry and qualitatively by fluorescence microscopy. Inflammatory colitis was induced in mice as previously described in section I.5. After 7 days, mice received by gavage 100 µl of coumarin-6-NLCs. Food (but not water) was withdrawn 12 h prior to the administration of the treatment. Mice were sacrificed 3, 8 or 12 h after administration, and the whole GIT (including the luminal content) was then collected. The samples were divided into four sections: stomach, small intestine, colon and cecum. The different samples were homogenized in 1 ml of PBS, and the homogenate was subsequently extracted with a methanol/chloroform mixture as described by Makhlof et al. [17]. Coumarin-6 content was quantitated by fluorophotometry. Specimens excised from the non-treated mice were homogenized as mentioned above and used as blanks. Samples emitting less than double the blank´s signal were discarded and not included for the quantitation. Amount of coumarin-6 in the organ was calculated using the following equation:

$$Amount\ of\ C6\ in\ the\ organ = \frac{Signal\ of\ organ}{Signal\ of\ stock\ solution}\ x\ \frac{1}{Organ\ weight\ (g)}$$

For fluorescence microscopy, colon specimens were embedded in Tissue-Tek® O.C.T. compound (Sakura Finetek, Torrance, CA) and frozen at -80°C for subsequent experiments. Sections were then cut at a thickness of 10 µm using a cryostat (Leica Microsystems, Wetzlar, GE), and images were captured using a fluorescence microscope (Carl Zeiss® Axio Observer) equipped with a structured illumination module (ApoTome).

I.7 STATISTICAL ANALYSES

Statistical analyses were performed using the GraphPad Prism 5.0 program for Windows (GraphPad Software Inc., San Diego, CA, USA). The normal distribution was assessed by the Shapiro-Wilk normality test. The one-way ANOVA test of multiple comparisons followed by Bonferroni's *post-hoc* test was applied according to the result of Bartlett's test of homogeneity of variances for the protein concentration comparisons. All other analyses were performed using *S*tudent´s *t*-test. Differences were considered statistically significant at $*p<0.05$. The results are expressed as the means ± SD (SD: standard deviation).

II. RESULTS

II.1 NLC CHARACTERIZATION

The particle characterization of Blank-NLCs, BDS-NLCs and coumarin-6-NLCs is summarized in Table 1. Their sizes were approximately 200 nm and all presented a negative zeta potential. The mean particle diameter of the BDS suspension was 41 ± 3 µm. BDS was completely encapsulated in the NLCs.

Table 1. Summary of the formulation particle size, zeta potential, polydispersity index (PdI) and entrapment efficiency (E.E.) of each formulation (n=3; data are expressed as the mean ± SD).

	Size (nm)	Zeta Potential (mV)	PdI	Entrapment Efficiency (%)
Blank-NLCs	244 ± 12	-40 ± 7	0.25 ± 0.02	-
BDS-NLCs	204 ± 9	-42 ± 7	0.21 ± 0.02	96 ± 2
Coumarin-6-NLCs	197 ± 12	-43 ± 7	0.18 ± 0.01	~100

II.2 IN VITRO STUDIES WITH J774 CELLS

II.2.1 Assessment of the cytotoxicity of the nanoparticles on J774 cells

To select a non-toxic concentration, the cell viability of the BDS-NLCs was measured using the MTT assay on proliferating J774 cells. The IC_{50}s of Blank-NLCs and BDS-NLCs were 1.74 and 1.59 mg/ml, respectively. Blank-NLCs and BDS-NLCs did not affect the metabolic activity of J774 cells (~100% of cell viability) at concentrations below 0.4 mg/ml. The absence of toxicity of these three formulations on J774 cells was corroborated by the lactate dehydrogenase release assay (lactate dehydrogenase release < 10% after 4h incubation at 0.4 mg/ml, data not shown).

II.2.2 Inhibition of TNF-α production from J774 cells

The inhibition of TNF-α secretion by J774 macrophages was evaluated by comparing BDS-NLCs with blank-NLCs and free BDS. While the BDS suspension did not exhibit any significant difference in the TNF-α levels (measured by ELISA) when compared with the control medium, no TNF-α secretion was observed from J774 macrophages treated with blank NLCs nor BDS-NLCs (Figure 2) (***$p<0.001$).

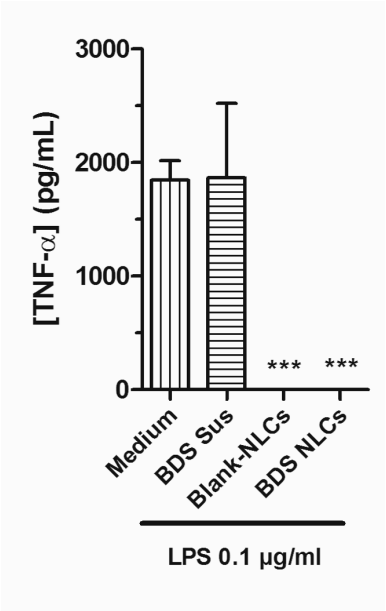


Figure 2. Comparison of the anti-inflammatory activity of the formulations assessed by measuring LPS-stimulated TNF-α secretion in J774 macrophages. The following formulations were tested: control medium; suspension of BDS (0.29 µg/ml); Blank NLCs (0.4 mg/ml); BDS-NLCs (BDS 0.29 µg/ml, NLC 0.4 mg/ml). The results were expressed as the absolute (mean ± SD; n=4) TNF-α levels (pg/ml) and were compared to medium-treated cells (*** p<0.001 *vs.* medium)**.**

II.3 IN VIVO EFFECTS OF BDS-NLCS ON MURINE COLITIS

II.3.1 Inflammatory clinical activity and histological scoring

At day 7, mice were sacrificed, and the severity of inflammation was characterized by clinical activity scoring (Figure 3A) and colon structure and histology (Figures 3B and 4, respectively). As shown in Figure 3B, the colon weight/length ratio was increased in the Blank-NLCs-treated and BDS-sus-treated DSS groups when compared with both the control and the PBS-treated DSS group, but no significant differences were observed for the BDS-NLCs group.

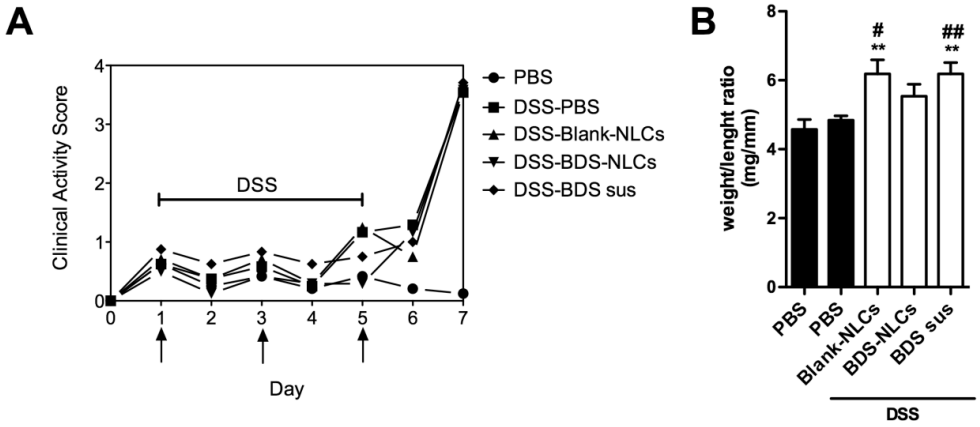


Figure 3. A) Clinical activity scoring after 7 days B) Colon weight/length ratio for control (PBS) (n=8), PBS-treated DSS group (n=8), Blank-NLCs-treated DSS group (n=8), BDS-NLCs-treated DSS group (n=7) and BDS-sus-treated DSS group (n=8). Values are means ± SD. **p<0.01 *vs.* control; $^{\#}$p<0.05, $^{\#\#}$p<0.01 *vs.* PBS-treated DSS group.

Histological scoring (Figure 4) demonstrated a decrease in inflammation for the BDS-sus group (**p<0.01), the BDS-NLCs group (***p<0.001) and the Blank-NLCs-treated group (*p<0.05) when compared with the PBS group. Moreover, the decrease in inflammation was significantly higher in the BDS-NLCs group (*p<0.05) than in the Blank-NLCs-treated and the BDS-sus groups. As shown Figures 4B and 4E, the inflammation observed in the colon was strongly reduced in the BDS-NLCs-treated group, and the mucosal architecture was maintained.

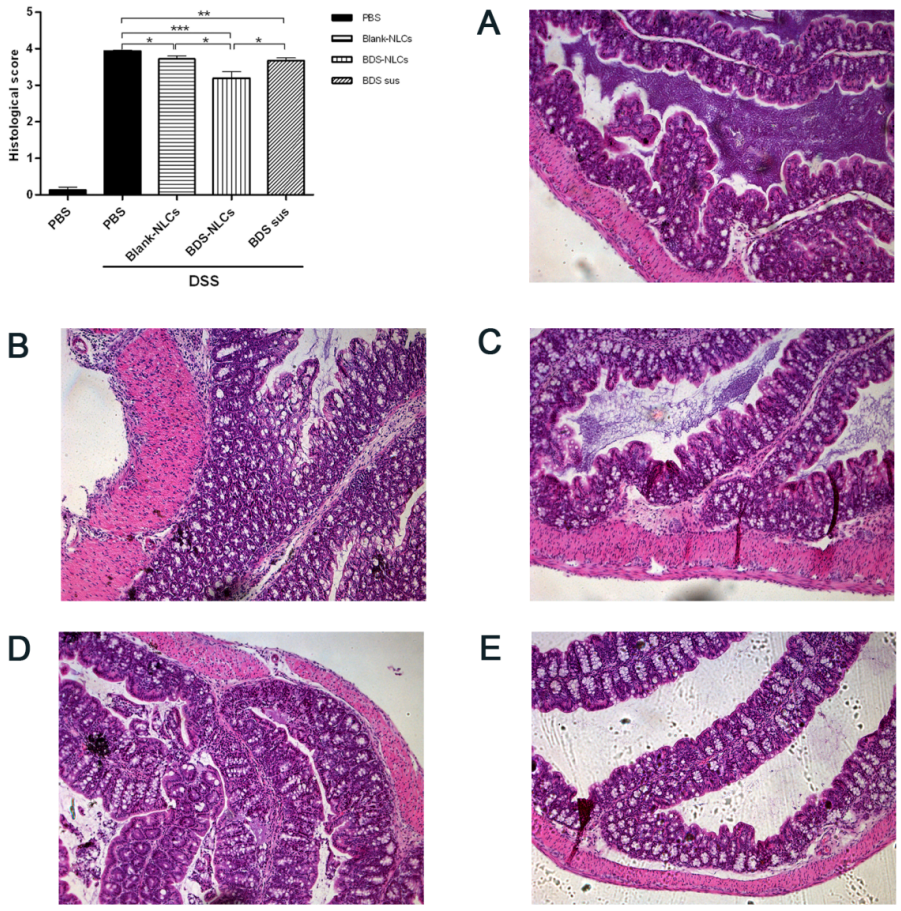


Figure 4. Histological scoring of colonic inflammation in DSS-induced colitis (top left). Values are the means ± SD. *p<0.05, **p<0.01, ***p<0.001 *vs.* PBS-treated DSS group. Histological sections of the colon stained with hematoxylin-eosin. A) PBS-treated control, B) PBS-treated DSS group, C) BDS sus-treated DSS group, D) Blank-NLCs-treated DSS group and E) BDS-NLCs-treated DSS group.

II.3.2 MPO activity and pro-inflammatory cytokines (IL-1ß and TNF-α) in the colon

MPO activity, which is a measure of neutrophil infiltration, and the concentrations of the pro-inflammatory cytokines IL-1ß and TNF-α in the colon are shown in Figure 5. It is noteworthy that MPO activity and cytokine concentrations for the BDS-NLCs-treated DSS group were decreased in all cases when compared with the PBS-treated DSS group (*p<0.05). No significant differences were observed when mice were treated with control, Blank-NLCs, or free BDS sus.

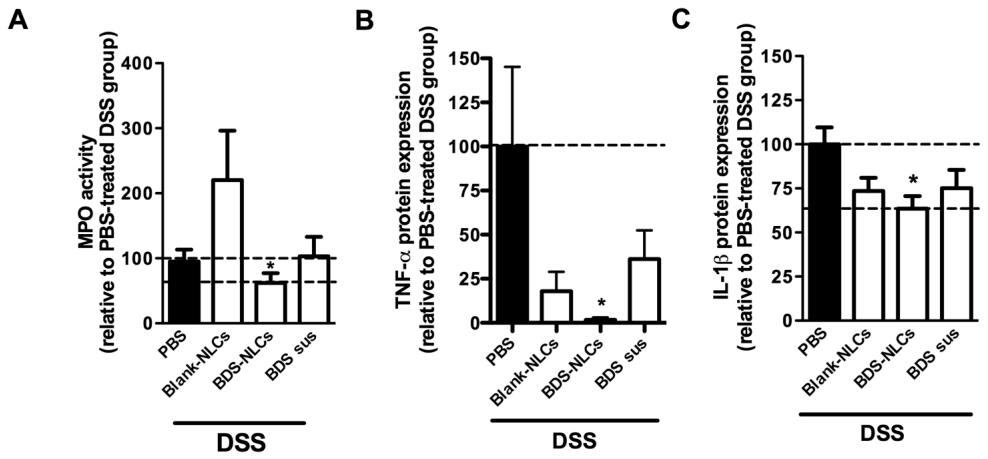


Figure 5. Reduction of inflammation in DSS-induced colitis. The BDS-NLCs-treated group showed a significant reduction in MPO activity (A) and in the expression of TNF-α (B) and IL-1ß (C) in the colon as measured by an ELISA assay when compared with the PBS-treated DSS group. *p<0.05 *vs.* PBS-treated DSS group.

II.3.3 In vivo localization of coumarin-6-NLCs

To evaluate the localization of the NLCs in the gastrointestinal tract, coumarin-6-NLCs were administered, and the amounts were quantitated in the stomach, the small intestine, the cecum and the colon. Figure 6 shows the amounts of coumarin-6 per organ (% dose/g organ) in control and DSS-treated mice 3, 8 and 12 h after the oral administration of coumarin-6-NLCs. Healthy mice exhibited a higher amount of coumarin-6 in the cecum and the colon 3 h after NLC administration compared to 12 h after. In the cecum and colon, the amount of coumarin-6 found in the DSS-treated group was lower than the one found in the control group 3 h after NLC administration. However, compared to control group, the amount of coumarin-6 found in the cecum and the colon of the DSS-treated group stayed stable over time. In control mice, the NLCs appeared to accumulate at the surface of the villi. In DSS-treated rats, the NLCs penetrated the mucosae (data not shown).

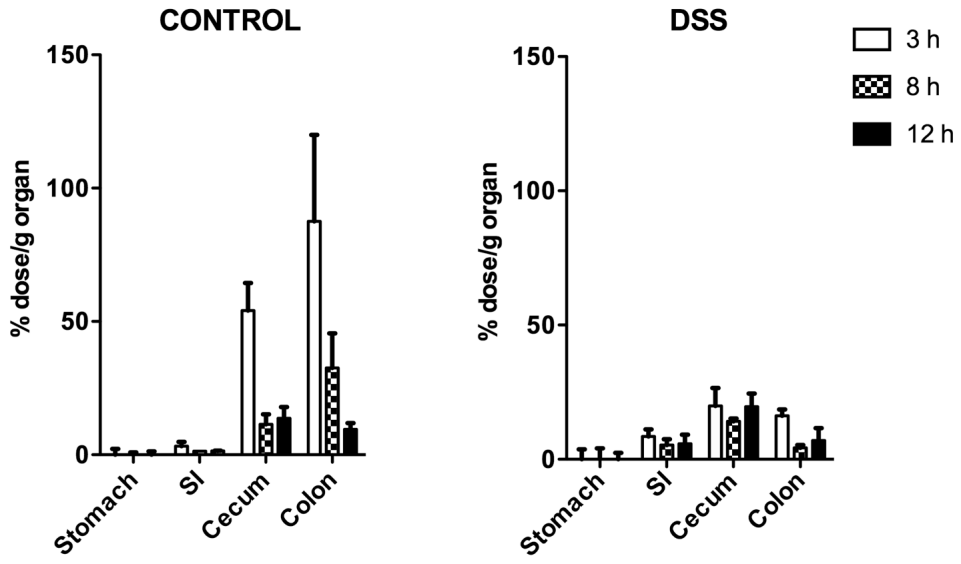


Figure 6. Amount of coumarin-NLCs in the stomach, small intestine, cecum and colon 3 h, 8h and 12 h post administration in control and DSS mice. (3 mice/condition)

III. DISCUSSION

Currently, strategies for targeting the inflamed mucosa in IBD using polymeric nano- and microparticulate drug carriers are particularly promising [9, 11, 37, 38]. In this study, a nanoparticulate system was developed based on NLCs loaded with BDS and tested it *in vitro* and *in vivo* to evaluate its potential for IBD treatment.

The BDS-NLC formulation obtained using the high-pressure homogenization technique exhibited physico-chemical characteristics suitable for delivery to the inflamed colonic mucosa, as they exhibited a mean size distribution in the range of 200 nm and a fairly monodispersed (PdI < 0.30) population (Table 1). With an encapsulation efficiency close to 95%, BDS was efficiently incorporated into NLCs, most likely due to their solid lipid matrix which was mixed with liquid oil (Precirol ATO®5 and Miglyol 812). Negatively charged BDS-NLCs (zeta potential -40 mV) may also exhibit a strong attraction to the positively charged proteins in ulcerated tissues. Moreover, high absolute potential zeta values suggest that BDS-NLC formulations should not aggregate because of the high repulsive effect occurring between the charged particles [39, 40]. BDS is a poorly water-soluble drug. When suspended in PBS, 41 µm-sized crystals were found in the suspension. In this conformation, BDS displays poor absorption characteristics and poor targeting to the inflamed mucosa, as there is a preferential uptake of nano-sized particles [12].

The idea of the central role of innate immunity in IBD has progressively emerged from studies of IBD pathogenesis. The accumulation of experimental evidence from *in vitro* and animal models, the genetic knowledge of IBD genetic and the emergence of biological therapy support this concept [41]. Thus, this study was focused on the contribution of the innate immune system in IBD pathogenesis. As nano-sized particles are taken up more easily by increased immune-related cells in active inflammation [12], the anti-inflammatory potential of NLCs was evaluated *in vitro*. A reduction in TNF-α secretion by activated macrophages (J774 cells) was observed (Figure 2). It is a well-accepted fact that BDS and steroids have an inhibitory effect on the production of most cytokines by macrophages [8]. Interestingly, the pretreatment of J774 cells with Blank-NLCs or BDS-NLCs for 4 h was found to reduce LPS-induced TNF-α levels, but no difference was observed when cells were pretreated with BDS suspension. These results are in line with Serpe et al. [22], who also observed a significantly reduced production of IL-1ß and TNF-α *in vitro* after 4 h and 24 h of co-incubation of solid lipid nanoparticles (SLNs) in a human inflammatory bowel disease whole-blood model. Furthermore, the immunomodulatory ability of lipid-based nanoparticles has been discussed elsewhere [42, 43]. The nature of the NLCs could contribute to the ability of both BDS-NLCs and Blank-NLCs to reduce TNF-α secretion by LPS-activated macrophages.

The acute DSS colitis model has been shown to be a good mouse model for the study of the innate immune aspect of colitis, as it does not involve the entire adaptive immune system [44]. The infiltration of leukocytes is one of the early steps of the innate response occurring during the active intestinal inflammation. The increased number of leukocytes in the active inflamed mucosa leads to the recrudescence of reactive oxygen species [45]. MPO, the most abundant protein in neutrophils, is used as a standard test in animal models of IBD and also as a biological marker in clinical practice, as it can be detected in the feces of IBD patients [46]. In the murine DSS-induced colitis model, the MPO level is significantly higher at all stages of DSS treatment and even after DSS withdrawal [47]. At day 7, after a 3-day treatment, only BDS-NLC DSS-treated mice exhibited a reduction in MPO activity when compared with the non-treated-DSS group (Figure 5). Interestingly, no difference was observed from the control group when mice were treated with either Blank-NLCs or the BDS-suspension, suggesting that the encapsulation of BDS in NLCs induces a reduction in the inflammation of DSS-induced colitis in mice. In the active inflamed area, the activation of macrophages leads to the secretion of the pro-inflammatory cytokines TNF-a and IL-1β. The quantitation of pro-inflammatory cytokines in the colon by ELISA showed a significant reduction in the expression of both TNF-α and IL-1ß in the colon for the BDS-NLCs DSS-treated group compared with the PBS-treated DSS group. Although BDS is known to suppress TNF-α production by macrophages, only BDS-NLCs were effective *in vivo*, highlighting the contribution of the NLCs to the effect of BDS. A histological evaluation of the severity of inflammation in the treated groups was performed. DSS-induced colitis changed the structure of the colon, with a loss in the protective epithelial layer and extensive infiltration of immune cells. For the BDS-NLC treatment group, a colonic architecture similar to the control group was observed. The *in vivo* data demonstrate that in a DSS-colitis model, 3 administrations of BDS-NLC reduce the cellular infiltration, the levels of inflammatory cytokines and maintain the mucosal architecture similar to the control group.

By reducing the diameter of the particles, it is possible to avoid rapid carrier elimination by diarrhea, which is a common symptom in IBD and to allow the preferential uptake of the nano-sized particles by immune-related cells [12]. The decrease in size is believed to increase the residence time of the formulation in the large intestine. Coumarin-6 was still observed in the colon 12 h after the administration of coumarin-6-loaded NLCs to DSS-treated mice (Figure 6). As these mice are subjected to serious diarrhea, these results suggest that a more sustained release of coumarin-6 was obtained by NLCs in an inflamed context compared to an healthy one. Recently, an *in vivo* study in human patients based on nano- and microscaled particles for drug targeting to the inflamed mucosa has been

published, highlighting the importance of particle size on colon targeting and indicating promising results for the potential application of these formulations [11].

IV. CONCLUSION

To our knowledge, this is the first study showing an indirect evidence of the local delivery of NLCs to the inflamed mucosa in a murine model of induced colitis. *In vitro*, NLCs and BDS-NLCs reduced TNF-α secretion by activated macrophages by ~100%. *In vivo,* we demonstrated the sustained presence of NLCs in the colon over 12 h and more importantly their efficacy in reducing inflammation in DSS-induced colitis after a 3-day dosage, as observed by a reduction in MPO activity, a reduction in the pro-inflammatory cytokines IL-1ß and TNF-α in the colon and by an improved histological score of the colon.

V. REFERENCES

[1] D.C. Baumgart, S.R. Carding, Inflammatory bowel disease: cause and immunobiology, Lancet, 369 (2007) 1627-1640.
[2] B. Khor, A. Gardet, R.J. Xavier, Genetics and pathogenesis of inflammatory bowel disease, Nature, 474 (2011) 307-317.
[3] R.B. Sartor, Mechanisms of disease: pathogenesis of Crohn's disease and ulcerative colitis, Nat Clin Pract Gastroenterol Hepatol, 3 (2006) 390-407.
[4] D.C. Baumgart, W.J. Sandborn, Inflammatory bowel disease: clinical aspects and established and evolving therapies, Lancet, 369 (2007) 1641-1657.
[5] M. Fatahzadeh, Inflammatory bowel disease, Oral Surg Oral Med Oral Pathol Oral Radiol Endod, 108 (2009) e1-10.
[6] C. Mowat, A. Cole, A. Windsor, T. Ahmad, I. Arnott, R. Driscoll, S. Mitton, T. Orchard, M. Rutter, L. Younge, C. Lees, G.T. Ho, J. Satsangi, S. Bloom, Guidelines for the management of inflammatory bowel disease in adults, Gut, 60 (2011) 571-607.
[7] M.K. Chourasia, S.K. Jain, Pharmaceutical approaches to colon targeted drug delivery systems, J Pharm Pharm Sci, 6 (2003) 33-66.
[8] D.R. Friend, New oral delivery systems for treatment of inflammatory bowel disease, Adv Drug Deliv Rev, 57 (2005) 247-265.
[9] E.M. Collnot, H. Ali, C.M. Lehr, Nano- and microparticulate drug carriers for targeting of the inflamed intestinal mucosa, J Control Release, 161 (2012) 235-246.
[10] W. Ulbrich, A. Lamprecht, Targeted drug-delivery approaches by nanoparticulate carriers in the therapy of inflammatory diseases, J R Soc Interface, 7 Suppl 1 (2010) S55-66.
[11] C. Schmidt, C. Lautenschlaeger, E.M. Collnot, M. Schumann, C. Bojarski, J.D. Schulzke, C.M. Lehr, A. Stallmach, Nano- and microscaled particles for drug targeting to inflamed intestinal mucosa-A first in vivo study in human patients, J Control Release, 165 (2013) 139-145.
[12] A. Lamprecht, U. Schafer, C.M. Lehr, Size-dependent bioadhesion of micro- and nanoparticulate carriers to the inflamed colonic mucosa, Pharm Res, 18 (2001) 788-793.
[13] T.T. Jubeh, M. Nadler-Milbauer, Y. Barenholz, A. Rubinstein, Local treatment of experimental colitis in the rat by negatively charged liposomes of catalase, TMN and SOD, J Drug Target, 14 (2006) 155-163.
[14] L.B. Vong, T. Tomita, T. Yoshitomi, H. Matsui, Y. Nagasaki, An orally administered redox nanoparticle that accumulates in the colonic mucosa and reduces colitis in mice, Gastroenterology, 143 (2012) 1027-1036 e1023.
[15] A. Lamprecht, H. Yamamoto, H. Takeuchi, Y. Kawashima, A pH-sensitive microsphere system for the colon delivery of tacrolimus containing nanoparticles, J Control Release, 104 (2005) 337-346.
[16] H. Laroui, G. Dalmasso, H.T. Nguyen, Y. Yan, S.V. Sitaraman, D. Merlin, Drug-loaded nanoparticles targeted to the colon with polysaccharide hydrogel reduce colitis in a mouse model, Gastroenterology, 138 (2010) 843-853 e841-842.
[17] A. Makhlof, Y. Tozuka, H. Takeuchi, pH-Sensitive nanospheres for colon-specific drug delivery in experimentally induced colitis rat model, Eur J Pharm Biopharm, 72 (2009) 1-8.
[18] R.H. Muller, K. Mader, S. Gohla, Solid lipid nanoparticles (SLN) for controlled drug delivery - a review of the state of the art, Eur J Pharm Biopharm, 50 (2000) 161-177.
[19] T. Harel-Adar, T. Ben Mordechai, Y. Amsalem, M.S. Feinberg, J. Leor, S. Cohen, Modulation of cardiac macrophages by phosphatidylserine-presenting liposomes improves infarct repair, Proc Natl Acad Sci U S A, 108 (2011) 1827-1832.
[20] M.L. Bondi, G. Montana, E.F. Craparo, R. Di Gesu, G. Giammona, A. Bonura, P. Colombo, Lipid nanoparticles as delivery vehicles for the Parietaria judaica major allergen Par j 2, Int J Nanomedicine, 6 (2011) 2953-2962.
[21] C. Dianzani, R. Cavalli, G.P. Zara, M. Gallicchio, G. Lombardi, M.R. Gasco, P. Panzanelli, R. Fantozzi, Cholesteryl butyrate solid lipid nanoparticles inhibit adhesion of human neutrophils to endothelial cells, Br J Pharmacol, 148 (2006) 648-656.

[22] L. Serpe, R. Canaparo, M. Daperno, R. Sostegni, G. Martinasso, E. Muntoni, L. Ippolito, N. Vivenza, A. Pera, M. Eandi, M.R. Gasco, G.P. Zara, Solid lipid nanoparticles as anti-inflammatory drug delivery system in a human inflammatory bowel disease whole-blood model, Eur J Pharm Sci, 39 (2010) 428-436.
[23] A. Chopra, D.S. Pardi, E.V. Loftus, Jr., W.J. Tremaine, L.J. Egan, W.A. Faubion, K.A. Hanson, T.A. Johnson, W.J. Sandborn, Budesonide in the treatment of inflammatory bowel disease: the first year of experience in clinical practice, Inflamm Bowel Dis, 12 (2006) 29-32.
[24] R. Lofberg, P. Rutgeerts, H. Malchow, C. Lamers, A. Danielsson, G. Olaison, D. Jewell, O. Ostergaard Thomsen, H. Lorenz-Meyer, H. Goebell, H. Hodgson, T. Persson, C. Seidegard, Budesonide prolongs time to relapse in ileal and ileocaecal Crohn's disease. A placebo controlled one year study, Gut, 39 (1996) 82-86.
[25] U. Klotz, M. Schwab, Topical delivery of therapeutic agents in the treatment of inflammatory bowel disease, Adv Drug Deliv Rev, 57 (2005) 267-279.
[26] Y.X. Yang, G.R. Lichtenstein, Corticosteroids in Crohn's disease, Am J Gastroenterol, 97 (2002) 803-823.
[27] A. Beloqui, M.A. Solinis, A.R. Gascon, A. Del Pozo-Rodriguez, A. des Rieux, V. Preat, Mechanism of transport of saquinavir-loaded nanostructured lipid carriers across the intestinal barrier, J Control Release, 166 (2012) 115-123.
[28] M. Gupta, H.N. Bhargava, Development and validation of a high-performance liquid chromatographic method for the analysis of budesonide, J Pharm Biomed Anal, 40 (2006) 423-428.
[29] C.A. Fernandes, L. Fievez, A.M. Neyrinck, N.M. Delzenne, F. Bureau, R. Vanbever, Sirtuin inhibition attenuates the production of inflammatory cytokines in lipopolysaccharide-stimulated macrophages, Biochem Biophys Res Commun, 420 (2012) 857-861.
[30] H. Kitamura, M. Ito, T. Yuasa, C. Kikuguchi, A. Hijikata, M. Takayama, Y. Kimura, R. Yokoyama, T. Kaji, O. Ohara, Genome-wide identification and characterization of transcripts translationally regulated by bacterial lipopolysaccharide in macrophage-like J774.1 cells, Physiol Genomics, 33 (2008) 121-132.
[31] R. Coco, L. Plapied, V. Pourcelle, C. Jérôme, D.J. Brayden, Y.-J. Schneider, V. Préat, Drug delivery to inflamed colon by nanoparticles: comparison of different strategies, International Journal of Pharmaceutics.
[32] S. Melgar, A. Karlsson, E. Michaelsson, Acute colitis induced by dextran sulfate sodium progresses to chronicity in C57BL/6 but not in BALB/c mice: correlation between symptoms and inflammation, Am J Physiol Gastrointest Liver Physiol, 288 (2005) G1328-1338.
[33] J. Galvez, M. Garrido, M. Merlos, M.I. Torres, A. Zarzuelo, Intestinal anti-inflammatory activity of UR-12746, a novel 5-ASA conjugate, on acute and chronic experimental colitis in the rat, Br J Pharmacol, 130 (2000) 1949-1959.
[34] M. Alhouayek, D.M. Lambert, N.M. Delzenne, P.D. Cani, G.G. Muccioli, Increasing endogenous 2-arachidonoylglycerol levels counteracts colitis and related systemic inflammation, FASEB J, 25 (2011) 2711-2721.
[35] K. Geboes, R. Riddell, A. Ost, B. Jensfelt, T. Persson, R. Lofberg, A reproducible grading scale for histological assessment of inflammation in ulcerative colitis, Gut, 47 (2000) 404-409.
[36] J.E. Krawisz, P. Sharon, W.F. Stenson, Quantitative assay for acute intestinal inflammation based on myeloperoxidase activity. Assessment of inflammation in rat and hamster models, Gastroenterology, 87 (1984) 1344-1350.
[37] H. Laroui, D.S. Wilson, G. Dalmasso, K. Salaita, N. Murthy, S.V. Sitaraman, D. Merlin, Nanomedicine in GI, Am J Physiol Gastrointest Liver Physiol, 300 (2011) G371-383.
[38] H. Laroui, S.V. Sitaraman, D. Merlin, Gastrointestinal delivery of anti-inflammatory nanoparticles, Methods Enzymol, 509 (2012) 101-125.
[39] C. Freitas, R.H. Mullera, Spray-drying of solid lipid nanoparticles (SLN TM), Eur J Pharm Biopharm, 46 (1998) 145-151.
[40] B. Heurtault, P. Saulnier, B. Pech, J.E. Proust, J.P. Benoit, Physico-chemical stability of colloidal lipid particles, Biomaterials, 24 (2003) 4283-4300.

[41] A. Kaser, S. Zeissig, R.S. Blumberg, Inflammatory bowel disease, Annu Rev Immunol, 28 (2010) 573-621.
[42] D. Landesman-Milo, D. Peer, Altering the immune response with lipid-based nanoparticles, J Control Release, 161 (2012) 600-608.
[43] D. Peer, Immunotoxicity derived from manipulating leukocytes with lipid-based nanoparticles, Adv Drug Deliv Rev, 64 (2012) 1738-1748.
[44] S. Wirtz, M.F. Neurath, Mouse models of inflammatory bowel disease, Adv Drug Deliv Rev, 59 (2007) 1073-1083.
[45] R. Holma, P. Salmenpera, A. Riutta, I. Virtanen, R. Korpela, H. Vapaatalo, Acute effects of the cys-leukotriene-1 receptor antagonist, montelukast, on experimental colitis in rats, Eur J Pharmacol, 429 (2001) 309-318.
[46] J.L. Mendoza, M.T. Abreu, Biological markers in inflammatory bowel disease: practical consideration for clinicians, Gastroenterol Clin Biol, 33 Suppl 3 (2009) S158-173.
[47] Y. Yan, V. Kolachala, G. Dalmasso, H. Nguyen, H. Laroui, S.V. Sitaraman, D. Merlin, Temporal and spatial analysis of clinical and molecular parameters in dextran sodium sulfate induced colitis, PLoS One, 4 (2009) e6073.

CHAPTER IV.
Design of curcumin-loaded nanocarriers for the treatment of inflammatory bowel disease

Design of curcumin-loaded nanocarriers for the treatment of inflammatory bowel disease

Coco R.; Memvanga P.B.; Ucakar B.; Préat V.

ABSTRACT

Topical delivery of drugs in the inflamed area is a hot topic for inflammatory bowel disease (IBD) treatment. Nano-scaled particles have been found to preferentially accumulate in inflamed regions. Curcumin (CC) is an anti-inflammatory topical agent, which presents poor ADME features. Hence, we investigated and compared *in vitro* and *in vivo* the local delivery of CC using pH-sensitive polymeric nanoparticles and self-(nano)emulsifying drug delivery systems (SNEDDS) as nanoparticulate drug delivery systems for the treatment of IBD. CC-loaded nanocarriers present submicronic size. Compared to suspension and SNEDDS, a higher transport of CC was obtained by NPs accross a Caco-2 epithelial barrier model. Confocal microscope images showed a higher uptake of CC-loaded SNEDDS in Caco-2 cells. TNF-α secretion by activated macrophages (J774 cells) was reduced by both CC-loaded nanocarriers. In a murine model of dextran sulfate-induced colitis, CC-Nps decreased neutrophil infiltration and showed similar mucosal pattern to control group. These data suggest that contrarily to SNEDDS, polymeric nanoparticles provide an effective topical delivery of CC, leading in therapeutic efficacy of CC in IBD treatment.

TABLE OF CONTENTS

I. Introduction 125

II. Materials & Methods 127

II.1 Materials 127

II.1.1 Chemicals 127

II.1.2 Cell culture 127

II.2 Preparation and characterization of the pH-sensitive nanoparticles 127

II.2.1 pH-sensitive nanoparticles preparation 127

II.2.2 Physico-chemical measurements and drug encapsulation efficiency 128

II.3 Preparation and characterization of the SNEDDS 128

II.3.1 SNEDDS preparation 128

II.3.2 Self-emulsification of CC-SNEDDS in gastrointestinal and transport media 128

II.4 CC suspension 129

II.5 CC analysis by HPLC 129

II.6 pH-dependent release profile of Cur-Nps 129

II.7 In vitro studies 129

II.7.1 Cell culture 129

II.7.2 Effect of formulations on cell viability 130

II.7.3 Permeation studies of CC-loaded formulations across intestinal in vitro Caco-2 model 130

II.7.4 In vitro localization of curcumin in the cell monolayer 131

II.7.5 Inhibition of TNF-a production from J774 macrophages by CC-loaded formulations 131

II.8 In vivo efficacy of CC-loaded formulations 132

II.8.1 Daily monitoring of weight loss 132

II.8.2 Myeloperoxidase activity (MPO) 132

II.8.3 Histological assessment of colonic inflammation 133

II.9 Statistical analyses 133

III. Results 134

III.1 Physico-chemical characterization of nanocarriers 134

III.2 Release profile of CC-Nps 135

III.3 In vitro studies 135

III.3.1 Assessment of the cytotoxicity of the CC-loaded nanocarriers 135

III.3.2 Transport of CC-loaded formulations across Caco-2 cell monolayers 136

III.3.3 Localization of CC-loaded formulations in intestinal barrier model 137
III.3.4 Inhibition of TNF-a secretion from LPS-activated J774 macrophage cells 138
III.4 In vivo therapeutic activity of the CC-loaded formulations 139
III.4.1 Weight monitoring 139
III.4.2 MPO activity 140
III.4.3 Histological assessment of colonic inflammation 141
IV. Discussion 143
V. Conclusion 146
VI. References 147

I. INTRODUCTION

Ulcerative colitis and Crohn's disease are the most representative diseases of the inflammatory bowel diseases (IBD). IBD can be described as chronic but relapsing inflammatory disorders of the gastrointestinal tract. Abdominal pain, diarrhea, rectal bleeding and weight loss are some of the frequent symptoms that patients with active IBD suffered from. The etiology of these diseases is still unknown but it seems that the mucosal inflammation is maintained by the deregulated presence of pro-inflammatory cytokines such as TNF-α or IFN-β [1, 2].

For over four decades, conventional treatment of IBD has consisted of anti-inflammatory medications, such as corticosteroids, aminosalicylates, immunosuppressants and biologic agents such as anti-TNF-amonoclonal antibodies. However, due to several weaknesses related among all to the unspecific administration, these drugs present several side adverse effects. So an approach in improving IBD therapy should be to target specifically inflamed colonic areas in order to decrease side effects and ameliorate the therapeutic efficacy [3].

Among all the vehicles available for small drugs, nano-sized drug delivery systems are promising for IBD delivery and targeting, mostly due to the fact that they accumulate in in the inflamed regions of the gut [4, 5]. A size close to 100 nm was found to give to PLGA nanoparticles a preferential uptake in the inflamed colonic mucosa from animal models and human patients [6]. Increased mucus production, mucosal surface alterations, crypt distortions and ulcers responsible of disrupted intestinal barrier, and infiltration of immune-related cells such as macrophages, lymphocytes or dendritic cells are some of the pathophysiological changes leading to the superior accumulation of nanoparticles in the inflamed colonic regions compared to the healthy ones regions [7].

Extracted from the turmeric pigment of *Curcuma longa*, curcumin (CC) is known for decades for its pleiotropic effects: anti-inflammatory, antioxidant, anticarcinogenic, antimicrobial, hepatoprotective, antihyperlipidemic and anti-angiogenic. Anti-inflammatory effects of CC have been reported in several diseases such as Alzheimer's disease, Parkinson's disease, multiple sclerosis, epilepsy or cerebral injury. CC has also been shown to downregulate the expression of various chemokines such as TNF-a, IL-6 or IL-1b [8]. In a murine DSS-induced colitis model, a prophylactic role of CC was highlighted and explained by its beneficial role in regulation of oxidant/anti-oxidant balance and modulation of the release of some inflammatory mediators, namely TNF-a and NO [9]. In a double-blind human trial, CC at a dose of 1 g/day had better clinical efficacy over placebo in the prevention of relapse of UC and was well-tolerated [10]. However, CC presents several limiting factors as low solubility in water (i.e. 0.4 µg/mL at pH 7.3) and instability at neutral pH values, which results in its low oral bioavailability. So an optimal and IBD-specific CC delivery system should improve its

topical delivery by protecting CC from fast degradation and target specifically the inflamed colon.

CC has been encapsulated in several nanoparticulate drug delivery systems: self-assembly, polymeric conjugates, nanogels, micelles or magnetic, polymeric, solid or lipid nanoparticles [11]. For instance, derivative chitosan-based nanoparticles were used to encapsulate CC [12-14]. CC-loaded pH-sensitive nanoparticles were used for the treatment of colon cancer [15].

Two nanocarriers were chosen. First, polymeric nanoparticles composed of 2 polymers were made: pH-sensitive Eudragit S 100 (ES100) and sustained release poly(lactic-co-glycolic) acid (PLGA). pH-sensitivity has been considered as a one of the main colonic drug delivery strategy as luminal pH varies along the GIT until it reaches in the colon value superior to 7, which is the dissolution pH of ES100 polymer [15, 16]. Furthermore, the joint use of PLGA provides a controlled-release phase in the distal part of the GI tract [17]. The second choice was a lipid-based carrier, the self-nanoemulsifying drug delivery system (SNEDDS). Clear isotropic mixtures of oils, water-soluble surfactants and optionally hydrophilic co-solvents, spontaneously generate oil-in-water colloidal nanoemulsions in gastrointestinal fluids. They are generally used to improve solubility of poorly water-soluble drugs [18]. CC-self-emulsifying drug delivery systems were evaluated successfully as IBD therapeutic alternative [19]. SNEDDS were then used as CC drug delivery system to combine this lipid-based strategy with a nanoscale and to potentialize the efficacy of CC.

The aim of the present study was to compare these nanoparticulate CC delivery for IBD treatment. CC-loaded nanocarriers were compared (i) based on their physico-chemical behavior, (ii) *in vitro,* by evaluating the reduction of TNF-α secretion from activated macrophages (J774 cells) and the passage through an intestinal epithelium model and (iii) *in vivo,* in a murine dextran-sulfate sodium (DSS)-induced colitis model, by monitoring mice weight loss, by quantitating neutrophil infiltration and by histological evaluation of inflammation severity in excised colons.

II. MATERIALS & METHODS

II.1 MATERIALS

II.1.1 Chemicals

Curcumin (80% curcumin and 20% other curcuminoids), *O*-dianisidine, HTAB (hexadecyltrimethylammonium bromide), poly(lactic-co-glycolic) acid (PLGA, L:G 50:50, average Mw 7000–17,000, acid terminated), hydrogen peroxide (30%) and polyvinyl alcohol (PVA average 13,000–23,000) were purchased from Sigma–Aldrich (St. Louis, MO, USA). Eudragit® S100 was a gift from Evonik RÖHM GmbH (Darmstadt, DE). Potassium dihydrogen phosphate and disodium hydrogen phosphate were obtained from Merck (Darmstadt, DE). Dextran sodium sulfate (DSS) was purchased from TdB Consultancy (Uppsala, SE). Complete protease inhibitor cocktail tablets were purchased from Roche Diagnostics (Vilvoorde, BE).

II.1.2 Cell culture

The J774 murine macrophage cell line was kindly donated by Pr. Marie-Paule Mingeot (Université catholique de Louvain, LDRI, BE). Caco-2 cells (clone 1) obtained from the University of Milano-Bicocca, Italy, were used [20].

Roswell Park Memorial Institute (RPMI) 1640 medium, fetal bovine serum (FBS), trypsin (0.05%) with EDTA was purchased from Gibco™ Invitrogen Corporation (Paisley, UK). Lipopolysaccharide (LPS, Escherichia coli O111:B4) was purchased from Sigma-Aldrich.

II.2 PREPARATION AND CHARACTERIZATION OF THE PH-SENSITIVE NANOPARTICLES

II.2.1 pH-sensitive nanoparticles preparation

pH-sensitive nanoparticles were prepared by an adaption of the modified spontaneous emulsification solvent diffusion (SESD) [17]. Briefly, 45 mg of PLGA, 45 mg of Eudragit S100 or 10 mg of CC were dissolved in 1 mL of a mix of acetone/methanol (2:1). These 3 mL were then pooled and added dropwise in 20 mL of 0.5% (w/v) PVA under magnetic stirring. The whole mixture was immediately centrifuged at 4°C at 45,000 x g for 30 min. The nanoparticles suspension was then washed twice in distilled water. Supernatants were collected to evaluate encapsulation efficiency of CC, using HPLC.

II.2.2 Physico-chemical measurements and drug encapsulation efficiency

Particle size distribution was determined by means of dynamic light scattering (DLS) using a NanoSizer Zeta Series (Malvern Instruments, Malvern, UK). The zeta potential of the particles was measured in 1 mM KCl with the NanoSizer ZS by laser Doppler velocimetry. The encapsulation efficiency of CC in pH-sensitive nanoparticles was calculated by measuring by HPLC non-encapsulated CC in supernatants. The encapsulation efficiency of CC-NPs, determined in triplicate, was expressed in percentage of the amount of encapsulated CC compared to the amount of CC used to form the nanoparticles. Drug loading was expressed as the ratio of the amount of encapsulated CC compared to the amount of polymer used for the formulation.

II.3 PREPARATION AND CHARACTERIZATION OF THE SNEDDS

II.3.1 SNEDDS preparation

The CC-SNEDDS were prepared by mixing under agitation (400 rpm, 30 min, 20°C) the appropriate quantities of excipients (Table 1). Thirty milligrams of CC was then added in 1 g of each SNEDDS preconcentrate (drug loading = 30 mg/g) and mixed for dissolution under agitation (400 rpm, 120 min, 20°C), protected from light [21]. Two CC-SNEDDSs were developed. Compared to SNEDDS A, SNEDDS B contains in its composition Transcutol HP, a solubilizer [22].

Table 1: Composition of selected CC-SNEDDSs

Composition (mg)	**SNEDDS A**	**SNEDDS B**
Labrafil	300	400
Labrasol	300	400
Cremophor EL	300	400
Transcutol HP	-	200
CC (mg/g excipient)	30	30

II.3.2 Self-emulsification of CC-SNEDDS in gastrointestinal and transport media

The size of droplets of CC-loaded SNEDDS in gastric (FaSSGF), intestinal (FaSSIF), lipolysis and transport (HBSS) media were assessed as previously described [23]. Briefly, 1.03 g of CC-SNEDDS was gently stirred with 1000 mL of gastro-intestinal and transport media at 37°C. After 20 min, samples were removed for particle size analysis by photon correlation spectroscopy (Malvern, UK). To evaluate the solubility and the stability of CC, samples or supernatants from centrifugation (5,000×g, 15 min, 37°C) were diluted twice in mixture of methanol-3.6% glacial acetic acid (73:27, v/v). The quantity of CC present in

solution in the various media with or without centrifugation was assayed by HPLC analysis. All measurements were performed in triplicate.

II.4 CC SUSPENSION

A CC suspension (CC Sus) was prepared as a control. CC (125 mg) was dispersed in PBS (10 mL). The primary volume median particle diameter of the CC suspension was measured by laser diffraction (HELOS, Sympatec, Clausthal-Zellerfeld, DE). Before sizing, the suspension was homogenized in a 50 mL flask by sonication (30-60 s) at a power of 60 W while magnetically stirring at 1000 rpm.

II.5 CC ANALYSIS BY HPLC

An Agilent 1100 Series HPLC system with a diode array and multiple wavelength detector was used for these experiments. The column was an EC 250/2 Nucleodur 100-5 C18 ec (Macherey-Nagel, DE). The sample (50 µL) was eluted with the mobile phase composed of methanol and 3.6% glacial acetic acid (73:27, v/v) [24]. The different samples were analyzed after appropriate dilution in the mobile phase. The system was run isocratically at a flow rate of 0.2 mL/min and sample detection was achieved at 428 nm. The retention time of CC was approximately 6 min under these conditions. The limits of detection (LOD) and of quantification (LOQ) of CC were 5 ng/mL and 15 ng/mL, respectively. The coefficients of variation (CV) for intra- and inter-assay were all within 5%.

II.6 PH-DEPENDENT RELEASE PROFILE OF CUR-NPS

In vitro release characteristics of the pH-sensitive nanoparticles were evaluated by using pH-changing system (pH 1.2, 4.5 and 7.2), as described in the European Pharmacopeia [25]. 22.5 mg of CC loaded PLGA/ES100 nanoparticles were suspended in 50 mL of the release medium and incubated into a shaking water bath (60 rpm, 37 ◦C). After predetermined durations, samples were centrifuged at 45,000 × g for 30 min in order to analyze by HPLC the free CC in the supernatant.

II.7 IN VITRO STUDIES

II.7.1 Cell culture

Caco-2 cells were maintained in Dulbecco's Modified Eagle's Minimal Essential Medium (DMEM) supplemented with 10% (v/v) heat inactivated fetal bovine serum (Hyclone®, UK), 1% (v/v) L-glutamine and 1% (v/v) non-essential amino-acids at 37°C in an atmosphere of 10% CO_2. Caco-2 cells were used between passages x+17 and x+30 [20, 23].

The J774 macrophage cell line was maintained in RPMI 1640 supplemented with 10% fetal bovine serum. Cells were grown in 75 cm^2 flasks (Corning, Lowell, MA, USA) in an atmosphere of 5% CO_2/95% air (v/v) at 37°C.

II.7.2 Effect of formulations on cell viability

The cytotoxicity of the formulations on J774 cells and Caco-2 cells was evaluated using the MTT method. Briefly, 20.000 cells/well were seeded in 96-well plates (Nunc, Roskilde, DK) and maintained for 24 h at 37°C and 5% CO_2. After exposure to 100 µL of unloaded formulations dispersed in the culture medium, the cells were washed 3 times with HBSS and incubated for 3 h with 0.5 mg/mL MTT in RPMI. The medium was then removed, and the purple formazan crystals were dissolved in 100 µL of DMSO. The absorbance was measured at 570 nm using a MultiSkan Ex plate reader (Thermo Fisher Scientific, Waltham, MA, USA). The IC_{50}s for the different formulations were calculated using the GraphPad Prism 5 program (CA, USA). All MTT assays were repeated in triplicate.

II.7.3 Permeation studies of CC-loaded formulations across intestinal in vitro Caco-2 model

5 × 10^5 Caco-2 cells were seeded on 12-well cell culture inserts (1 µm pore diameter, 0.9 cm² area) (Corning Costar®, NY, USA) and were grown in supplemented DMEM + 1% PEST for 21 days [20, 23, 26]. The culture medium was changed every 2 days. Only Caco-2 cell monolayers with initial transepithelial electrical resistance (TEER) values higher than 400 Ω cm2, respectively, were used.

Apical to basolateral transport experiments across Caco-2 monolayers were studies. 0.5 mL of CC-SNEDDS (1.03 mg/ml) or CC-NPS (1 mg/mL) dispersed in HBSS was added on the apical compartment of the inserts. This corresponds to 30 and 74 µg/mL of CC respectively. 0.5 mL of CC suspension at a concentration of 150 µg/ml of CC was used as control. The basolateral compartment was filled out with 1.2 mL of HBSS + 10 mM HEPES + 1% BSA. After 2h, sampling of the basolateral was done to determine the permeation of CC in suspension or loaded in SNEDDS or NPs. The amount of CC that had crossed the Caco-2 monolayers was determined by HPLC.

CC apparent permeability coefficient (Papp) was calculated according to the following equation:

$$P_{app} = \frac{dQ}{dt} \times \frac{1}{C_o\ A}$$

where dQ/dt (transport rate) is the amount of CC (µg) appearing per time unit (s) in the receiver compartment, Co is the initial concentration in the donor compartment (µg/mL) and A is the surface area of the monolayer (A= 0.9 cm^2).

Integrity of cell monolayers after 2 h exposure with the CC-SNEDDSs was assessed by TEER measurements using an electrode connected to an EVOM® volt-ohmmeter (World Precision Instruments, USA).

II.7.4 In vitro localization of curcumin in the cell monolayer

For the confocal microscopy study, inserts obtained from transport studies were fixed in 2% (v/v) buffered paraformaldehyde (pH 7.4; 30 min) and washed twice in PBS. To reveal cell borders, actin was stained with 250 µL of rhodamine–phalloidine (4U/mL) (Molecular Probes, OR, USA) in PBS for 30 min in the dark. After washing in PBS, the inserts were cut and mounted on glass slides with 4',6'-diamidino-2-phenylindole (DAPI) (1:20) to reveal cell nuclei [27]. Images were captured using a Carl Zeiss™ confocal microscope equipped with a multi-Argon laser for excitation at 405, 488, 594 and 605 nm. The fluorescence of CC was detected at 488 nm [28]. Data were analyzed by the Axio Vision software (version 4.8) to obtain *y–z*, *x–z* and *x–y* views of the cell monolayers.

II.7.5 Inhibition of TNF-a production from J774 macrophages by CC-loaded formulations

One hundred thousands J774 cells/well were seeded in 12-well plates and allowed to adhere for 24 h. The cells were exposed for 4 h to the following formulations: (i) CC-SNEDDSs (0.3 mg/mL), (ii) Blank-SNEDDSs (0.3 mg/mL), (iii) CC-NPs (0.122 mg/mL) or (iv) CC-Sus (9 µg/mL). These concentrations were chosen based on the cytotoxic studies. The incubation medium was then collected for the LDH release assay and replaced with fresh medium supplemented with 0.1 µg/mL of LPS to activate macrophages [29, 30]. Cell-free supernatants were harvested 24 h later and stored at -20°C for cytokine quantitation. TNF-a was assayed using a DuoSet® ELISA kit (R&D Systems, Minneapolis, MN, USA).

The absence of cytotoxicity of the different formulations on macrophages was also assessed in the cell culture media after 4 h incubation by measuring the activity of lactate dehydrogenase (LDH). A cytotoxicity detection kit (Roche Diagnostics GmbH, Mannheim, DE) was used according to the manufacturer's instructions. The results were expressed as a percentage of the positive control, which consisted of cells exposed to 1% (v/v) Triton X-100.

II.8 IN VIVO EFFICACY OF CC-LOADED FORMULATIONS

An *in vivo* study was performed in C57BL/6 female mice (18-20 g, 8 weeks; Janvier Laboratories, FR). Animals were housed under standard conditions and supplied with food and tap water *ad libitum*. Protocols were approved by the *Université catholique de Louvain* animal committee (UCL/MD/2009-001). Colitis was induced by administration of drinking water containing 3% (w/v) DSS for 5 consecutive days, and colonic inflammation was assessed 8 days after the beginning of DSS treatment [27, 31]. The animals were divided into the following nine groups (8 mice per group): untreated control group (healthy mice), untreated DSS group, DSS+Blank-NPs, DSS+Blank SNEDDSs A, DSS+Blank SNEDDSs B, DSS+CC-NPs, DSS+CC-SNEDDSs A, DSS+CC-SNEDDSs B and DSS+CC Sus. 15 mg/kg was chosen as CC dose for all CC-treated groups. Food (but not water) was withdrawn 12 h prior to the administration of the treatment. One hundred microliters of each formulation were administered daily by oral gavage during the 5 days of DSS administration; the untreated control group and the DSS control group received PBS instead of the formulation. At day 8, the animals were sacrificed, and colon samples were collected for evaluation of the severity of colitis.

II.8.1 Daily monitoring of weight loss

Daily changes in body weight of C57BL/6 mice were evaluated during the treatment period. Body weight loss was calculated by dividing body weight on the specified day by body weight at day 0 (starting body weight) and expressed in percentage.

II.8.2 Myeloperoxidase activity (MPO)

The tissue-associated MPO assay was performed to quantitate the degree of inflammatory infiltration, which correlates with the severity of colitis [32]. Briefly, colon specimens from both the proximal and the distal portion of the colon together (~25 mg) were snap frozen in liquid N_2 at the time of sacrifice and stored for later assessment. For determination of MPO activity, tissue was placed in HTAB buffer (0.5% HTAB in 50 mM potassium phosphate buffer, pH 6) on ice and gently homogenized. The homogenate was centrifuged at 2,000 g for 10 min and subsequently ultracentrifuged (15,000 g, 20 min at 4ºC). The supernatant (7 µL) was added to 96-well plates (Nunc, Roskilde, DK) together with 200 µL of a 50 mM potassium phosphate buffer containing 0.167 mg/mL *O*-dianisidine and hydrogen peroxide (500 ppm). Samples were analyzed in duplicate. MPO activity in the supernatant was measured spectrophotometrically (Spectophotometer Spectramax M2e & program SoftMax Pro, Molecular Devices, LLC, USA) at 460 nm for 30 min. The results were expressed as MPO

units per gram of tissue, and one unit of MPO activity was defined as the amount that degrades 1 mmol/min of hydrogen peroxide at 25ºC [33].

II.8.3 Histological assessment of colonic inflammation

For histological scoring, small segments of the colon were fixed in 4% buffered formalin overnight, washed with 70% ethanol and subsequently embedded in paraffin. Two sets of 3 serial sections (10 µm) were cut 100 µm apart, and 6 sections were evaluated for each mouse. Sections were stained with hematoxylin-eosin, and histological scores were determined according to a scoring procedure for colitis reported by Beloqui et al. [33]. Mice were scored individually. Briefly, a five-grade classification system for inflammation was employed. Inflammation was graded semi-quantitatively from 0 to 4 as follows: 0, no structural change; 1, inflammation visible; 2, leukocytes present in the lamina propria; 3, leukocytes present in the epithelium (3.1 <5% crypts involved, 3.2 <50% crypts involved, 3.3 >50% crypts involved); and 4, crypt destruction visible. Mice were scored individually. Each score represented the mean of five sections.

II.9 STATISTICAL ANALYSES

Statistical analyses were performed using the GraphPad Prism 5.0 program for Windows (GraphPad Software Inc., San Diego, CA, USA). The normal distribution was assessed by the Shapiro-Wilk normality test. An one-way ANOVA test of multiple comparisons followed by Bonferroni's *post-hoc* test was applied. All other analyses were performed using *S*tudent´s *t*-test. Differences were considered statistically significant at $*p<0.05$. The results are expressed as the means ± SD (SD: standard deviation).

III. RESULTS

III.1 PHYSICO-CHEMICAL CHARACTERIZATION OF NANOCARRIERS

Table 2: Summary of the NPs particle size, zeta potential (ζ), polydispersity index (PdI) and encapsulation efficiency (E.E.), drug loading of each formulation (n=3; data are expressed as the mean ± SD).

	Size (nm)	ζ (mV)	PdI	EE (%)	Drug Loading (µgCC/mgP)
Empty Nps	122 ± 5	-39.8 ± 0.5	0.244 ± 0.04	-	-
CC-Nps	116 ± 3	-40.4 ± 0.6	0.261 ± 0.03	67 ± 8	74 ± 9

The particle characterization of nanoparticles loaded or not with CC is summarized in Table 2. A fairly monodisperse (PdI < 0.300) population of about 100 nm-sized particles was obtained. These PLGA/ES100 nanoparticles were negatively charged. Encapsulation efficiency was good (>50%).

Table 3: *Droplet size in nm and Polydispersity index* [a] of selected CC-SNEDDSs

Droplet size (nm), Polydispersity index	SNEDDS A	SNEDDS B
FaSSGF[b]	38.0 ± 3.1 (0.27)	42.0 ± 2.7 (0.29)
FaSSIF pH 6.8[b]	49.2 ± 1.2 (0.17)	56.4 ± 0.5 (0.31)
HBSS[b]	32.1 ± 0.1 (0.03)	29.5 ± 0.3 (0.09)

[a] Polydispersity index (PdI) are given in the parentheses.
[b] The size of the droplets (nm) was determined in 100 mL of medium (HBSS, FaSSGF or FaSSIF pH 6.8).
(n=3)

To check whether the CC-loaded SNEDDSs could self-emulsify in the gastrointestinal tract, the size of the droplets was assessed. In gastrointestinal medium, SNEDDS A and SNEDDS B dispersed spontaneously to form nanoemulsions with size of 30-40 nm (PdI < 0.25). The incorporation of CC in the self-emulsifying systems did not change significantly the size and the polydispersity index of droplets compared to unloaded-SNEDDS ($p < 0.05$, Table 3).

The mean particle diameter of the CC suspension was 9.83 ± 0.13 µm.

III.2 RELEASE PROFILE OF CC-NPS

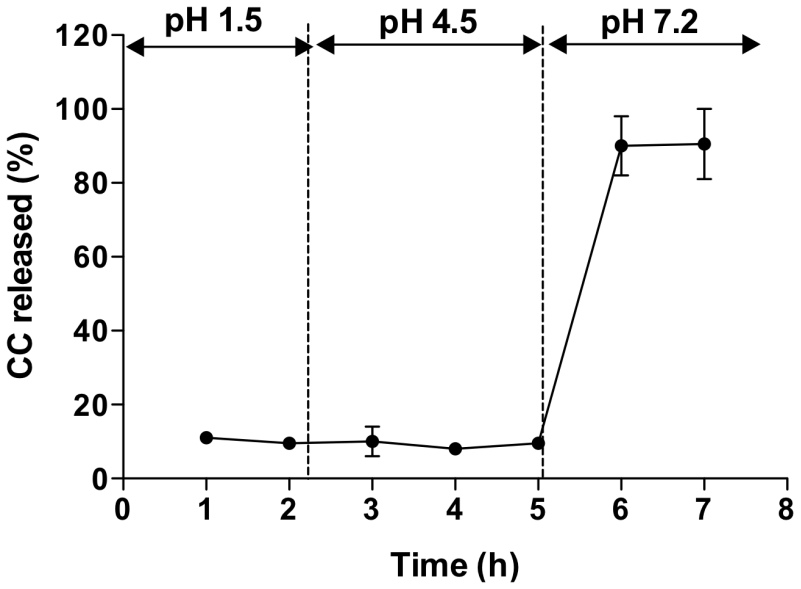


Figure 1: In vitro release profile of CC from PLGA/ES100 nanoparticles in gradually pH-changing buffers **(n=3)**

In vitro pH-dependent release profile of CC from the pH-sensitive nanocarriers was investigated in a gradually pH-changing buffer in order to assess protection of the content from the acidity and effective delivery in neutral pH values [17]. Low amounts of CC were released in the medium from the CC-Nps when the pH was 1.2 and 4.5 with less than 15 % of CC present in the release medium (Figure 1). Once the pH reached neutral values, CC was rapidly released and found in more amounts in the medium.

III.3 IN VITRO STUDIES

III.3.1 Assessment of the cytotoxicity of the CC-loaded nanocarriers

MTT test was used to evaluate the cytotoxicity of the nanocarriers and then select the range of concentrations used for the Caco-2 permeation and J774 TNF-a inhibition studies.

For Caco-2 cells, IC_{50} ranged between 2.0 and 3.0 mg/mL for all nanocarriers (data not shown). After exposure of cells with 3 mg/mL of SNEDDSs, less than 20 % of LDH was released (data not shown).

For J774 cytotoxic studies, IC_{50} ranged between 0.40 and 0.70 mg/mL for SNEDDS A and B and close to 0,5 mg/mL for NPs.

III.3.2 Transport of CC-loaded formulations across Caco-2 cell monolayers

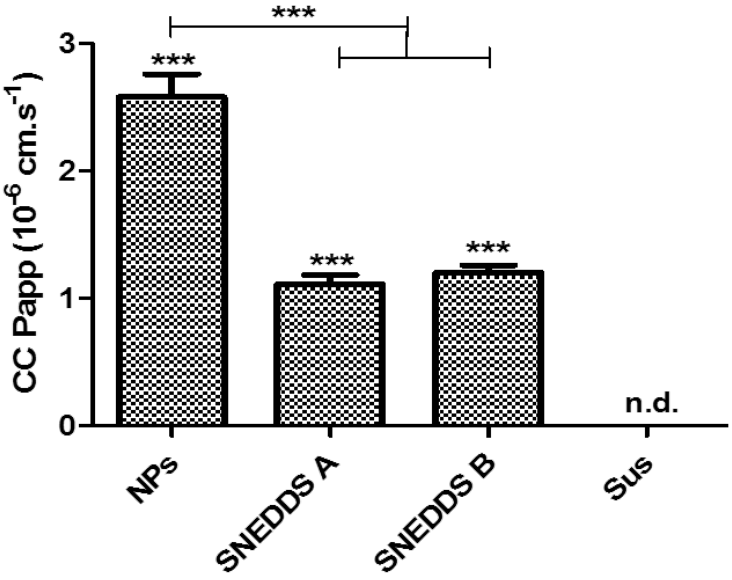


Figure 2: Apparent permeabilities of CC (CC Papp) from different formulations. pH-sensitive nanoparticles (NPs,1 mg/mL), SNEDDS A (1.03 mg/mL), SNEDDS B (1.03 mg/mL), Sus (150 µg/mL of CC). CC from Sus was non detectable (n.d.) (N=3; n=3)

To evaluate the apparent permeability (Papp) of CC from the CC-loaded formulations, absorptive transport across Caco-2 cell monolayers were performed for 120 min (Figure 2). To improve the recovery of CC by the enhancement of its solubility and its stability, a solution of 1% BSA in HBSS + 10 mM HEPES was used as receiver medium [34, 35]. Based on cytotoxicity studies, Caco-2 monolayers were incubated for 120 min at 37°C with 1.03 of CC-SNEDDS and 1 mg/mL of CC-NPs corresponding to respective CC concentration of 30 and 74 µg/mL. CC-Sus at 150 µg/mL was incubated on the apical compartment. Transport of CC across Caco-2 monolayers did not significantly increase with the solubilizer Transcutol employed in SNEDDS B when comparing the transport of both SNEDDS ($p > 0.05$). In these conditions, highest Papp of CC was obtained by the NPs. CC Papp of CC-Sus was not possible to evaluate as CC from the Sus present in the basolateral compartment was not detectable.

III.3.3 Localization of CC-loaded formulations in intestinal barrier model

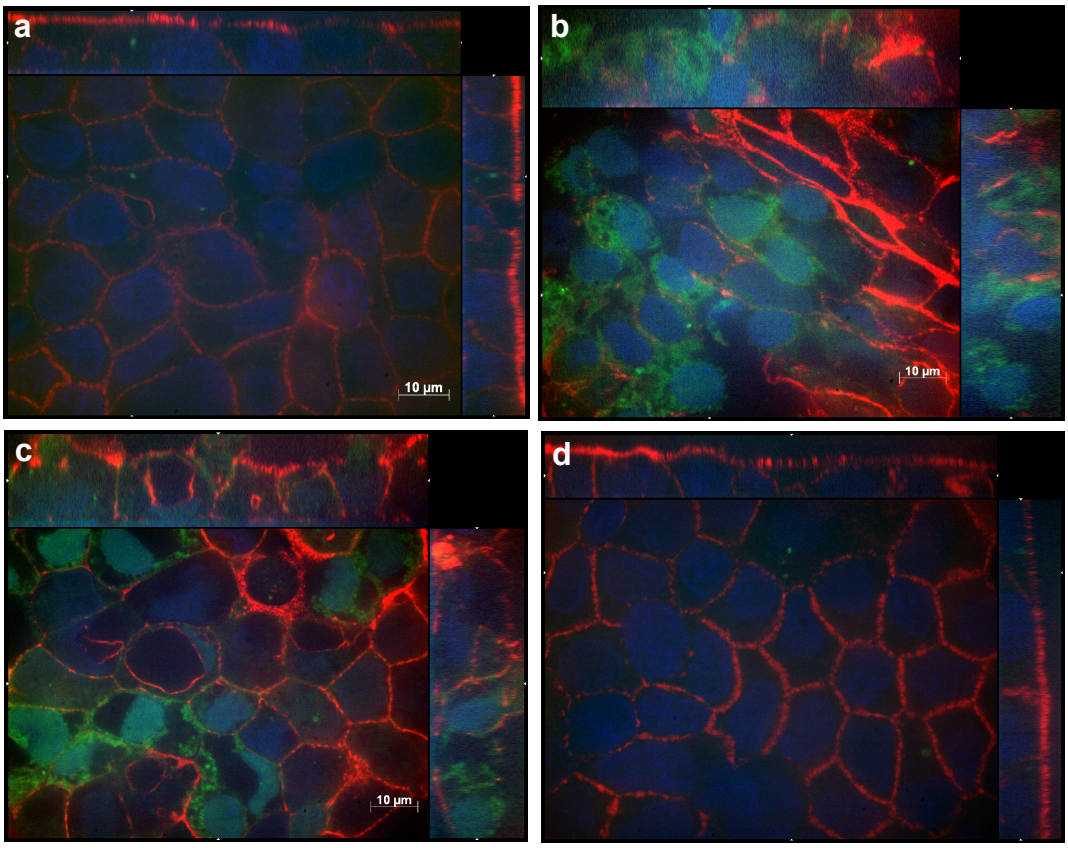


Figure 3: Representative confocal microscopy images of Caco-2 cells from in vitro intestinal barrier model fixed after 2 h of exposure to CC-loaded formulations: a) suspension, b) SNEDDS A, c) SNEEDS B and d) nanoparticles. Inserts were formaldehyde fixed for 30 min and incubated with PBS containing rhodamine-phalloidin (4 U/mL) for 30 min to stain cell membranes. To reveal the nuclei, inserts were put on glass slides with an UltraCruz® mounting medium that contains DAPI.

Figure 3 shows the confocal microscopy images corresponding to the cellular uptake of CC in Caco-2 cells. CC is a fluorescent molecule and exhibits green fluorescence. Rhodamine-phalloidin makes membranes appear red whereas DAPI stained the nuclei in blue. CC loaded in SNEDDS exhibited higher fluorescence intensity than CC in suspension and loaded in nanoparticles. Whatever the formulation, CC showed an intracellular localization. CC from CC-loaded SNEDDS (Figure 3b and 3c) showed a higher presence in the cytoplasm than CC from CC-Sus and CC-NPs (Figure 3a and 3d).

III.3.4 Inhibition of TNF-a secretion from LPS-activated J774 macrophage cells

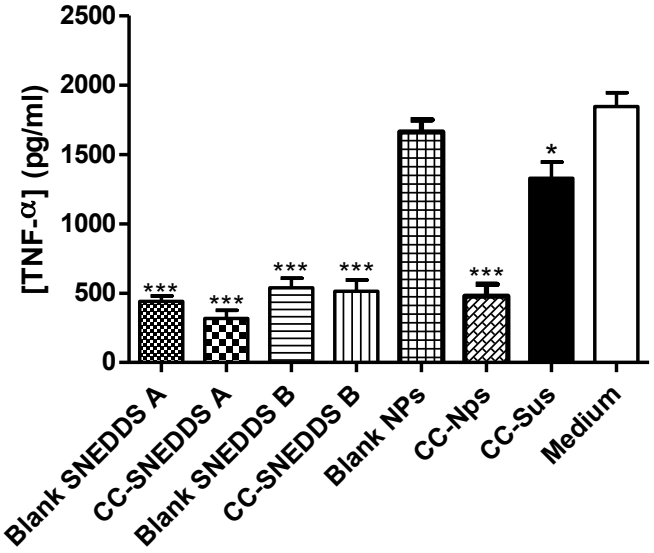


Figure 4: Comparison of the anti-inflammatory activity of the formulations assessed by measuring LPS-stimulated TNF-a secretion in J774 macrophages. The following formulations were tested: Empty SNEDDS A (0.3 mg/mL); CC-SNEDDS A (0.3 mg/mL); Empty SNEDDS B (0.3 mg/mL); CC-SNEDDS B (0.3 mg/mL); Blank NPs (0.122 mg/mL); CC-NPs (0.122 mg/mL); suspension of CC (9 µg/mL); control medium. The results were expressed as the absolute (mean ± SD; n=4). TNF-α levels (pg/mL) and were compared to medium-treated cells ((* p<0.05 vs. medium; *** p<0.001 vs. medium).

The inhibition of TNF-α secretion by J774 macrophages was evaluated by comparing the different formulations, with or without CC. CC suspension exhibited significant difference in the TNF-a levels (measured by ELISA) when compared with the control medium (*p<0.05). However, TNF-a secretion from J774 macrophages was more reduced by Blank-SNEDDS, CC-SNEDDS and CC-NPs. No differences were obtained between the CC-loaded formulations (***p <0.001).

III.4 IN VIVO THERAPEUTIC ACTIVITY OF THE CC-LOADED FORMULATIONS

III.4.1 Weight monitoring

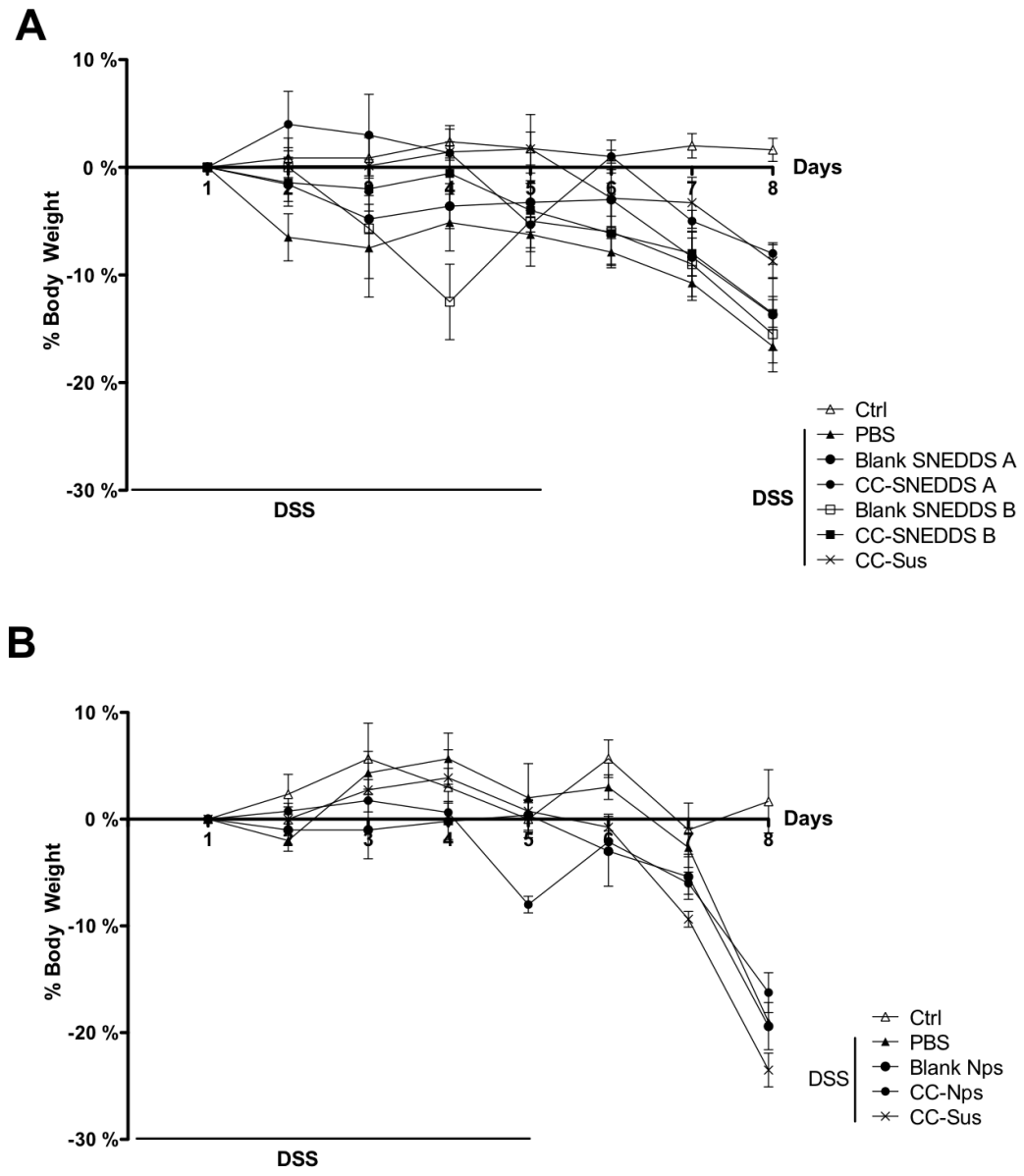


Figure 5: Daily changes in body weight in colitis-induced mice. A) SNEDDSs compared to controls. B) NPs compared to controls (n=7-8)

Body weight loss is a significant symptom of IBD. Thus, body weight was monitored during the 8 consecutive days. Compared to the control group, a decrease in all DSS groups (with or without treatment) was observed, showing that colitis was effectively induced. Neither NPs-treated nor SNEDDS-treated DSS groups were found significantly different than the DSS group.

III.4.2 MPO activity

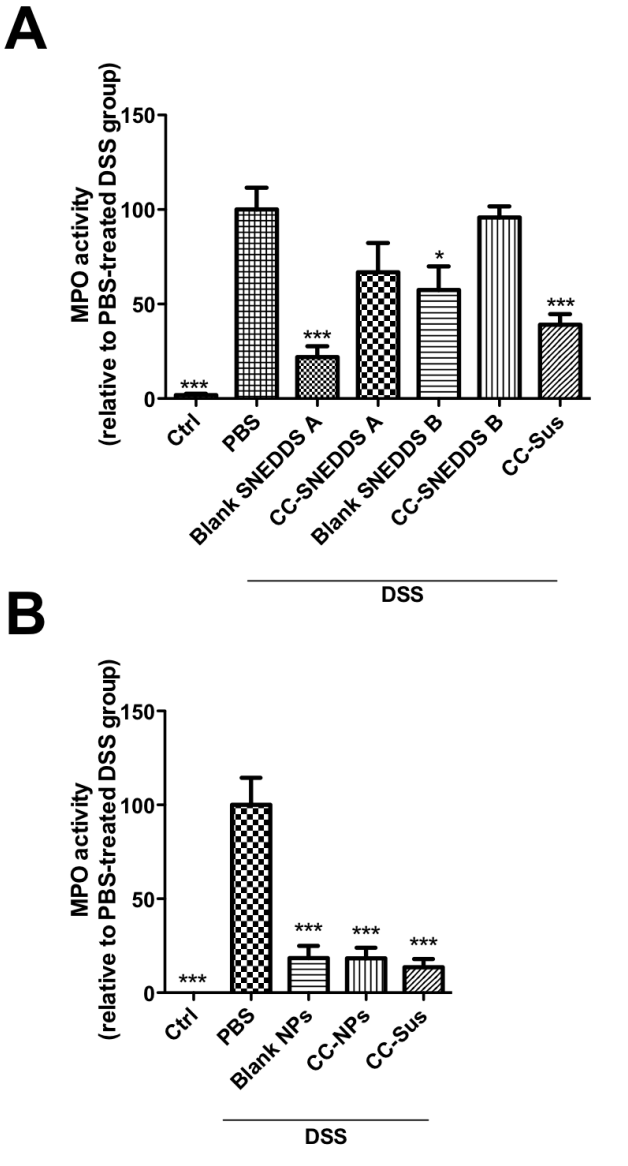


Figure 6: Assessment of inflammation in DSS-induced colitis. A) SNEDDSs compared to PBS-treated DSS group. B) NPs compared to PBS-treated DSS group. (n=6)

Colonic MPO activity, which is a measure of neutrophil infiltration, has been investigated (Figure 6.A and B). Compared with the PBS-treated DSS group, significant differences were observed when mice were treated with untreated group, CC-Sus-treated DSS group, Blank NPs-treated DSS group and Blank SNEDDS A-treated DSS group (*p<0.0001) but also with Blank SNEDDS-treated DSS group (*p<0.05).

III.4.3 Histological assessment of colonic inflammation

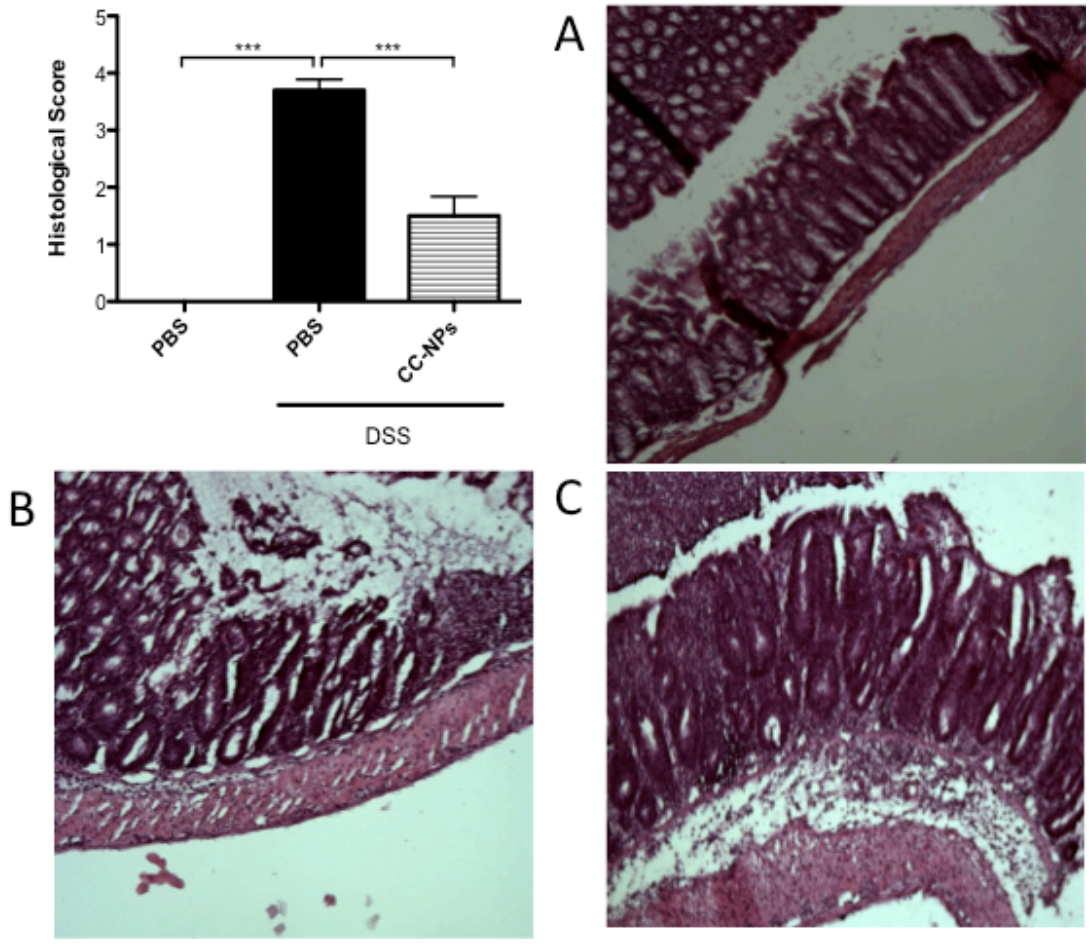


Figure 7: Histological scoring of colonic inflammation in DSS-induced colitis. Values are the means ± SEM. ***p<0.001 *vs.* PBS-treated DSS group. Histological sections of the colon stained with hematoxylin-eosin. A) PBS-treated control, B) PBS-treated DSS group and C) CC-NPs-treated DSS group. Compared to PBS-treated DSS group, CC-NPs-treated DSS group showed a reduction in histological scoring.

At day 8, mice were sacrificed, and the severity of inflammation was characterized by colon histology scoring (Figure 7). CC-NPs-treated DSS group showed a decrease in inflammation,

when compared to PBS-treated DSS group (***p<0.001). Figures 7B and 7C showed CC-NPs decreased the colonic inflammation and maintained the mucosal architecture.

IV. DISCUSSION

Target the inflamed mucosa in IBD using nano-sized drug delivery systems is a promising topic [4, 6, 36, 37]. In this study, two nanoparticulate systems, polymeric pH-sensitive nanoparticles and lipid-based nanocarriers SNEDDS were developed, loaded with CC and compared *in vitro* and *in vivo* to assess their potential for IBD treatment. The CC-NPs formulation obtained using the SESD technique displayed a mean size distribution in the range of 100 nm and a fairly monodispersed (PdI < 0.30) population (Table 2). Their zeta potential was found negative, probably due to the presence at the nanoparticle surface of the anionic carboxylate of the PLGA chain ends and the ionized carboxylic functional groups of the ES100 polymer. This feature may allow them to be attracted to positively charged ulcerated tissues [38]. With an encapsulation efficiency close to 70%, CC was efficiently incorporated into the pH-sensitive NPs. pH-sensitive profile of CC-Nps was consistent with the desired oral administration. Thereby, in more acidic pH values, a low amount of CC was released from the nanoparticles and found in the medium. This effect is probably due to the hydrogen bonding between the hydroxyl groups of the carboxylic moiety and the carbonyl oxygen of ester groups. However, as pH of the aqueous medium shifted to 7.4, carboxylic function groups of ES100 polymer started to be de-protonated. ES100 start then to dissolve and to swell, leading to the release of the encapsulated CC from pH-sensitive nanoparticles [39]. CC-Nps can withstand the CC release at expected gastric and ileal pH, but CC was released from the delivery system at expected higher colonic pH values. The other nanocarriers, the SNEDDS, showed a fairly monodisperse population of particles with a size around 30 nm (Table 3). Due to their emulsion forming capability, Cremophor EL and Labrasol were selected as surfactants. Labrafil M2125CS was also chosen due to its good miscibility with Cremophor EL and Labrasol. After lipolysis, Labrafil M2125CS could also release linolenic and oleic acid, contributing to the anti-inflammatory activity [40, 41]. Transcutol HP was selected as a solubilizer. Both type of formulations (NPs and SNEDDSs) exhibited physico-chemical characteristics suitable for delivery to the inflamed colonic mucosa, as a preferential uptake of nano-sized particles is found in the inflamed mucosa [7]. On the contrary, when solubilized in PBS, 10 µm-sized crystals of CC confer to CC-Sus poor targeting to the inflamed mucosa.

For IBD treatment, topical delivery of anti-inflammatory drugs such as CC is of high interest. Indeed, they present specific features such as intracellular activity, poor solubility and low absorption. Thus, we focused on the passage of CC-loaded formulations through the epithelial barrier. A significant difference was observed between both Papp of CC-nanoparticles and CC-SNEDDS (p<0.05). CC is known to be retained in enterocytes [42]. It seems that CC delivered by nanocarriers pass better through the epithelial barrier compared

to free CC. However, even if a better passage of CC through the epithelial barrier is obtained by CC-nanoparticles, CC-SNEDDS present a better cellular uptake. Indeed, confocal microscopy images confirm an increased uptake of CC from SNEDDS in Caco-2 cells.

Indeed, accumulation of experimental evidence from *in vitro* and animal models, increasing genetic knowledge of IBD genetic and emergence of biological therapy push forward the idea of a central role of innate immunity in IBD pathogenesis [2]. CC possessed anti-inflammatory properties but however poor pharmacokinetic profile. As nano-sized particles are taken up more easily by increased immune-related cells in active inflammation [7], use of CC-loaded nanocarriers against IBD may be of great interest. Thus, anti-inflammatory potential of the latters were evaluated *in vitro*. A decrease in TNF-α production by LPS-activated macrophages (J774 cells) was observed (Figure 4). CC is known to suppress inflammation via multiple pathways like inhibiting production of various pro-inflammatory cytokines (TNF-a, IL-1b or IL-8) [8]. J774 cells pretreated with CC suspension showed a decrease in LPS-induced TNF-α production (p<0.05). Interestingly, a more significant reduction of LPS-induced TNF-α secretion from J774 cells pretreated with CC-NPs but also with Blank- or CC-SNEDDSs for 4 h were observed. Lipid-based nanoparticles may present immunomodulatory effects [43-45]. Similar results about TNF-a reduction by CC-loaded SNEDDS was observed in an *in vivo* diabetes model [46]. Reduction of TNF-α secretion from LPS-activated macrophages by both CC-SNEDDSs and Blank-SNEDDSs could be due to the combination of anti-inflammatory property of CC and lipid nature of the SNEDDS.

Pleiotropic effects of CC are counterbalanced by its poor water solubility and low oral bioavaibility. Encapsulation of CC in nanocarriers may improve these drawbacks and provide topical delivery in inflamed colon. Lamprecht et al. showed an enhanced uptake of 100 nm-sized particles [7]. Intense particle uptake inside the colitis tissue is the result of pathophysiological changes: i) elevated levels of mucus production and ii) presence of a highly increased number of immune-related cells. Once CC encapsulated in well-characterized nanoformulations, topical delivery of CC-loaded nanocarriers in the inflamed colon was evaluated *in vivo*. The choice of acute DSS colitis model has been driven by the fact that this murine model present similar characteristics to the human ulcerative colitis [47]. DSS produced symptoms as bloody stool, loose feces and weight loss. Following the latter, monitoring of body weight loss showed us that no treatment was able to interfere with the DSS-related weight loss. During the first steps of active intestinal inflammation, an increasing number of leukocytes infiltrate the active inflamed mucosa, resulting in the recrudescence of reactive oxygen species [48]. MPO is one of the most abundant proteins in neutrophils. MPO level is used as an index of inflammation in clinical practice, animal models of IBD and especially in the murine DSS-induced colitis model, where it is found significantly higher at all stages of DSS treatment and even after DSS withdrawal [49, 50]. At day 8, several groups

exhibited a reduction in MPO activity when compared with the non-treated-DSS group (Figure 6). Mice treated with CC-Sus group found their MPO level decreased, showing the ability of CC to reduce inflammation of DSS-induced colitis in mice. Considering the SNEDDS groups, only Blank SNEDDS A and B groups present a difference when compared to the control group. As said earlier, the lipid nature of SNEDDS may provide a protective effect on colitis to the cargo. However, a therapeutic inefficiency was also associated to CC-SNEDDS A and B. The combination between CC and SNEDDS do not provide any therapeutic effects. One could say that CC from SNEDDS is retained in the enterocytes as showed on confocal microscope images (Figure 3). Thus, CC is not delivered in the main cell targets namely the immune-related cells overexpressed in the inflamed mucosa and by this way cannot provide its anti-inflammatory effect. This result also highlights the strong correlation that exists between the encapsulated drug and the carrier. Considering the NPs groups, difference was observed from the control group for both Blank-NPs and CC-NPs. CC-NPs was able to induce a reduction in the inflammation of DSS-induced colitis in mice, suggesting that these NPs provide a topical delivery. The severity of inflammation in the treated groups was also performed using histological scoring (Figure 7). Due to the DSS-induced colitis, loss in the protective epithelial layer and extensive infiltration of immune cells modified the structure of the colon. CC-NPs were able to decrease the inflammation induced by DSS compared to the control group (PBS).

T yh!h n;bnRecently, nano- and microscaled PLGA particles have been assessed during an *in vivo* study in human patients for drug targeting to the inflamed mucosa. This publication highlights how particle size on colon targeting may give promising results for the potential application of these formulations [6]. Indeed, in IBD human patients, an enhanced accumulation of microparticles was found whereas nanoparticles were detectable only in traces in mucosal surfaces. At the same extent, our nanoscaled CC-loaded SNEDDS were not found effective in IBD therapy whereas CC-loaded self-emulsifying drug delivery systems with a bigger size present therapeutic efficacy against IBD [19]. However, the mechanism of action associated to these results is still unclear and questions still need to be addressed. Due to the pH-sensitive property, CC from NPs is released since the carriers reached the colonic luminal compartment. CC can thus reach the activated immune cells and decrease the production of a central inflammatory mediator, TNF-a, leading to a decrease of inflammation in the colonic inflamed areas.

V. CONCLUSION

For a topical delivery in the inflamed mucosa, CC was encapsulated in two nanoparticulate systems, polymeric pH-sensitive nanoparticles and lipid-based nanocarriers SNEDDS. Both type of formulations exhibited physico-chemical characteristics suitable for colonic delivery. *In vitro* results showed that compared to CC suspension, CC encapsulated in nanocarriers passed better through the epithelial barrier. Confocal microscopy images highlight that higher intracellular concentration of CC was achieved by SNEDDS. Furthermore, CC-loaded formulations reduced TNF-α secretion by *in vitro* activated macrophages. *In vivo*, CC-loaded pH-sensitive nanoparticles showed a reduction in MPO activity and similar structural colonic pattern to untreated one. Compared to CC-SNEDDS, CC-NPs present an efficient *in vivo* delivery of CC, resulting in therapeutic efficacy of CC-loaded NPs in IBD treatment.

VI. REFERENCES

[1] C. Abraham, J.H. Cho, Inflammatory bowel disease, N Engl J Med, 361 (2009) 2066-2078.
[2] A. Kaser, S. Zeissig, R.S. Blumberg, Inflammatory bowel disease, Annu Rev Immunol, 28 (2010) 573-621.
[3] F. Grimpen, P. Pavli, Advances in the management of inflammatory bowel disease, Intern Med J, 40 (2010) 258-264.
[4] E.M. Collnot, H. Ali, C.M. Lehr, Nano- and microparticulate drug carriers for targeting of the inflamed intestinal mucosa, J Control Release, 161 (2012) 235-246.
[5] W. Ulbrich, A. Lamprecht, Targeted drug-delivery approaches by nanoparticulate carriers in the therapy of inflammatory diseases, J R Soc Interface, 7 Suppl 1 (2010) S55-66.
[6] C. Schmidt, C. Lautenschlaeger, E.-M. Collnot, M. Schumann, C. Bojarski, J.-D. Schulzke, C.-M. Lehr, A. Stallmach, Nano- and microscaled particles for drug targeting to inflamed intestinal mucosa—A first in vivo study in human patients, Journal of Controlled Release, 165 (2013) 139-145.
[7] A. Lamprecht, U. Schafer, C.M. Lehr, Size-dependent bioadhesion of micro- and nanoparticulate carriers to the inflamed colonic mucosa, Pharm Res, 18 (2001) 788-793.
[8] B.B. Aggarwal, K.B. Harikumar, Potential therapeutic effects of curcumin, the anti-inflammatory agent, against neurodegenerative, cardiovascular, pulmonary, metabolic, autoimmune and neoplastic diseases, Int J Biochem Cell Biol, 41 (2009) 40-59.
[9] H.M. Arafa, R.A. Hemeida, A.I. El-Bahrawy, F.M. Hamada, Prophylactic role of curcumin in dextran sulfate sodium (DSS)-induced ulcerative colitis murine model, Food Chem Toxicol, 47 (2009) 1311-1317.
[10] R.A. Taylor, M.C. Leonard, Curcumin for inflammatory bowel disease: a review of human studies, Altern Med Rev, 16 (2011) 152-156.
[11] M.M. Yallapu, M. Jaggi, S.C. Chauhan, Curcumin nanoformulations: a future nanomedicine for cancer, Drug Discov Today, 17 (2012) 71-80.
[12] A. Anitha, S. Maya, N. Deepa, K.P. Chennazhi, S.V. Nair, R. Jayakumar, Curcumin-Loaded N,O-Carboxymethyl Chitosan Nanoparticles for Cancer Drug Delivery, J Biomater Sci Polym Ed, (2011).
[13] A. Anitha, V.G. Deepagan, V.V. Divya Rani, D. Menon, S.V. Nair, R. Jayakumar, Preparation, characterization, in vitro drug release and biological studies of curcumin loaded dextran sulphate,Äìchitosan nanoparticles, Carbohydrate Polymers, 84 (2011) 1158-1164.
[14] R.K. Das, N. Kasoju, U. Bora, Encapsulation of curcumin in alginate-chitosan-pluronic composite nanoparticles for delivery to cancer cells, Nanomedicine, 6 (2010) 153-160.
[15] D. Prajakta, J. Ratnesh, K. Chandan, S. Suresh, S. Grace, V. Meera, P. Vandana, Curcumin loaded pH-sensitive nanoparticles for the treatment of colon cancer, J Biomed Nanotechnol, 5 (2009) 445-455.
[16] D.R. Friend, New oral delivery systems for treatment of inflammatory bowel disease, Adv Drug Deliv Rev, 57 (2005) 247-265.
[17] A. Makhlof, Y. Tozuka, H. Takeuchi, pH-Sensitive nanospheres for colon-specific drug delivery in experimentally induced colitis rat model, Eur J Pharm Biopharm, 72 (2009) 1-8.
[18] A. Bernkop-Schnurch, Nanocarrier systems for oral drug delivery: Do we really need them?, Eur J Pharm Sci, 49 (2013) 272-277.
[19] Y.V. Ramshankar, S. Suresh, K. Devi, Novel Self-emulsifying Formulation of Curcumin with Improved Dissolution, Antiangiogenic and Anti-inflammatory Activity, Clinical Research and Regulatory Affairs, 25 (2008) 213-234.
[20] A. des Rieux, E.G. Ragnarsson, E. Gullberg, V. Preat, Y.J. Schneider, P. Artursson, Transport of nanoparticles across an in vitro model of the human intestinal follicle associated epithelium, Eur J Pharm Sci, 25 (2005) 455-465.
[21] P.B. Memvanga, R. Coco, P. V., An oral malaria therapy: curcumin-loaded lipid-based drug delivery systems combined with b-arteether, Journal of Controlled Release, (Submitted).

[22] L. Li, T. Yi, C.W. Lam, Effects of spray-drying and choice of solid carriers on concentrations of Labrasol(R) and Transcutol(R) in solid self-microemulsifying drug delivery systems (SMEDDS), Molecules, 18 (2013) 545-560.
[23] P.B. Memvanga, V. Preat, Formulation design and in vivo antimalarial evaluation of lipid-based drug delivery systems for oral delivery of beta-arteether, Eur J Pharm Biopharm, 82 (2012) 112-119.
[24] J. Cui, B. Yu, Y. Zhao, W. Zhu, H. Li, H. Lou, G. Zhai, Enhancement of oral absorption of curcumin by self-microemulsifying drug delivery systems, Int J Pharm, 371 (2009) 148-155.
[25] European Pharmacopeia 7.0 (2010), 5.17.1, Recommandations on dissolution testing:p.666.
[26] P.B. Memvanga, P. Eloy, E.M. Gaigneaux, V. Preat, In Vitro Lipolysis and Intestinal Transport of beta-Arteether-Loaded Lipid-Based Drug Delivery Systems, Pharm Res, (2013).
[27] R. Coco, L. Plapied, V. Pourcelle, C. Jerome, D.J. Brayden, Y.J. Schneider, V. Preat, Drug delivery to inflamed colon by nanoparticles: comparison of different strategies, Int J Pharm, 440 (2013) 3-12.
[28] A. Kunwar, A. Barik, R. Pandey, K.I. Priyadarsini, Transport of liposomal and albumin loaded curcumin to living cells: an absorption and fluorescence spectroscopic study, Biochim Biophys Acta, 1760 (2006) 1513-1520.
[29] C.A. Fernandes, L. Fievez, A.M. Neyrinck, N.M. Delzenne, F. Bureau, R. Vanbever, Sirtuin inhibition attenuates the production of inflammatory cytokines in lipopolysaccharide-stimulated macrophages, Biochem Biophys Res Commun, 420 (2012) 857-861.
[30] H. Kitamura, M. Ito, T. Yuasa, C. Kikuguchi, A. Hijikata, M. Takayama, Y. Kimura, R. Yokoyama, T. Kaji, O. Ohara, Genome-wide identification and characterization of transcripts translationally regulated by bacterial lipopolysaccharide in macrophage-like J774.1 cells, Physiol Genomics, 33 (2008) 121-132.
[31] H. Laroui, G. Dalmasso, H.T. Nguyen, Y. Yan, S.V. Sitaraman, D. Merlin, Drug-loaded nanoparticles targeted to the colon with polysaccharide hydrogel reduce colitis in a mouse model, Gastroenterology, 138 (2010) 843-853 e841-842.
[32] J.E. Krawisz, P. Sharon, W.F. Stenson, Quantitative assay for acute intestinal inflammation based on myeloperoxidase activity. Assessment of inflammation in rat and hamster models, Gastroenterology, 87 (1984) 1344-1350.
[33] A. Beloqui, R. Coco, M. Alhouayek, M.A. Solinis, A. Rodriguez-Gascon, G.G. Muccioli, V. Preat, Budesonide-loaded nanostructured lipid carriers reduce inflammation in murine DSS-induced colitis, Int J Pharm, (2013).
[34] M.H. Leung, T.W. Kee, Effective stabilization of curcumin by association to plasma proteins: human serum albumin and fibrinogen, Langmuir, 25 (2009) 5773-5777.
[35] G. Krishna, K. Chen, C. Lin, A.A. Nomeir, Permeability of lipophilic compounds in drug discovery using in-vitro human absorption model, Caco-2, Int J Pharm, 222 (2001) 77-89.
[36] H. Laroui, D.S. Wilson, G. Dalmasso, K. Salaita, N. Murthy, S.V. Sitaraman, D. Merlin, Nanomedicine in GI, Am J Physiol Gastrointest Liver Physiol, 300 (2011) G371-383.
[37] H. Laroui, S.V. Sitaraman, D. Merlin, Gastrointestinal delivery of anti-inflammatory nanoparticles, Methods Enzymol, 509 (2012) 101-125.
[38] T.T. Jubeh, Y. Barenholz, A. Rubinstein, Differential adhesion of normal and inflamed rat colonic mucosa by charged liposomes, Pharm Res, 21 (2004) 447-453.
[39] A.H. El-Kamel, M.S. Sokar, S.S. Al Gamal, V.F. Naggar, Preparation and evaluation of ketoprofen floating oral delivery system, Int J Pharm, 220 (2001) 13-21.
[40] J. Bassaganya-Riera, R. Hontecillas, Dietary conjugated linoleic acid and n-3 polyunsaturated fatty acids in inflammatory bowel disease, Current opinion in clinical nutrition and metabolic care, 13 (2010) 569-573.
[41] S. Borniquel, E.A. Jansson, M.P. Cole, B.A. Freeman, J.O. Lundberg, Nitrated oleic acid up-regulates PPARgamma and attenuates experimental inflammatory bowel disease, Free Radic Biol Med, 48 (2010) 499-505.
[42] B. Wahlang, Y.B. Pawar, A.K. Bansal, Identification of permeability-related hurdles in oral delivery of curcumin using the Caco-2 cell model, Eur J Pharm Biopharm, 77 (2011) 275-282.

[43] D. Landesman-Milo, D. Peer, Altering the immune response with lipid-based nanoparticles, J Control Release, 161 (2012) 600-608.
[44] D. Peer, Immunotoxicity derived from manipulating leukocytes with lipid-based nanoparticles, Adv Drug Deliv Rev, 64 (2012) 1738-1748.
[45] L. Serpe, R. Canaparo, M. Daperno, R. Sostegni, G. Martinasso, E. Muntoni, L. Ippolito, N. Vivenza, A. Pera, M. Eandi, M.R. Gasco, G.P. Zara, Solid lipid nanoparticles as anti-inflammatory drug delivery system in a human inflammatory bowel disease whole-blood model, Eur J Pharm Sci, 39 (2010) 428-436.
[46] R.P. Joshi, G. Negi, A. Kumar, Y.B. Pawar, B. Munjal, A.K. Bansal, S.S. Sharma, SNEDDS curcumin formulation leads to enhanced protection from pain and functional deficits associated with diabetic neuropathy: An insight into its mechanism for neuroprotection, Nanomedicine, (2013).
[47] S. Wirtz, M.F. Neurath, Mouse models of inflammatory bowel disease, Adv Drug Deliv Rev, 59 (2007) 1073-1083.
[48] R. Holma, P. Salmenpera, A. Riutta, I. Virtanen, R. Korpela, H. Vapaatalo, Acute effects of the cys-leukotriene-1 receptor antagonist, montelukast, on experimental colitis in rats, Eur J Pharmacol, 429 (2001) 309-318.
[49] J.L. Mendoza, M.T. Abreu, Biological markers in inflammatory bowel disease: practical consideration for clinicians, Gastroenterol Clin Biol, 33 Suppl 3 (2009) S158-173.
[50] Y. Yan, V. Kolachala, G. Dalmasso, H. Nguyen, H. Laroui, S.V. Sitaraman, D. Merlin, Temporal and spatial analysis of clinical and molecular parameters in dextran sodium sulfate induced colitis, PLoS One, 4 (2009) e6073.

CHAPTER V.
Protein delivery to inflamed colon by nanoparticles

Protein delivery to inflamed colon by nanoparticles: comparison of different strategies

Coco R., Plapied L., Pourcelle V., Jérôme C., Brayden D.J., Schneider Y.J., Préat V.

Adapted from International Journal of Pharmaceutics, 2013, 440(1):3-12

ABSTRACT

For inflammatory bowel disease (IBD) treatment, local delivery of molecules loaded in nanoparticles to the inflamed colon could be a promising strategy. The aim of this study was to investigate how drug-loaded polymeric nanoparticles target the site of inflammation and to analyse the influence of different colon-specific delivery strategies. Three different polymeric nanoparticles were formulated using ovalbumin (OVA) as a model drug. pH-sensitive nanoparticles were made with Eudragit S100 (ES100). Mucoadhesive nanoparticles were created with trimethylchitosan (TMC). A mix of polymers, PLGA, PEG-PLGA and PEG-PCL, were used to obtain a sustained drug delivery. Furthermore, ligands targeting immune cells (i.e. mannose) or the inflamed colon (i.e. a specific peptide) were grafted on the PEG chain of PCL. Interaction of nanoparticles with the intestinal epithelium was explored using Caco-2 monolayers designed to mimic an inflamed epithelium and then visualized using confocal laser microscopy. TMC nanoparticles had the highest apparent permeability for OVA in the untreated model. However, in the inflamed model, there were no difference between TMC, PLGA-based and ES100 nanoparticles. The uptake of nanoparticles in the inflamed mouse colon was assessed in a horizontal diffusion chamber. Mannose-grafted PLGA nanoparticles showed the highest accumulation of OVA in inflamed colon. Based on these results, active targeting of macrophages and dendritic cells may be a promising approach for targeting the colon in IBD.

KEYWORDS

Nanoparticles, intestinal barrier, colonic delivery, intestinal inflammation, trimethylchitosan, PLGA, Eudragit®

TABLE OF CONTENTS

I. Introduction 157

II. Materials & methods 159

II.1 Materials 159

II.1.1 Cell lines 159

II.1.2 Cell culture 159

II.1.3 Chemicals 159

II.1.4 Radio-labelling of ovalbumin 160

II.2 Ligands 160

II.2.1 Grafting of GSQSHPRH on PCL-PEG 160

II.2.2 Grafting of mannose on PCL-PEG 161

II.3 Preparation and characterization of nanoparticles 161

II.3.1 Preparation of PLGA-based nanoparticles 161

II.3.2 Preparation of bio-adhesive nanoparticles 161

II.3.3 Preparation of pH-sensitive nanoparticles 162

II.3.4 Characterization of the formulations 162

II.4 In vitro release of ovalbumin from nanoparticles 162

II.5 Transport studies on Caco-2 cells 163

II.5.1 Cell culture 163

II.5.2 Effect of polymers on cell viability 163

II.5.3 Ovalbumin transport mediated by nanoparticles across the Caco-2 monolayers untreated or exposed to pro-inflammatory cytokines 163

II.5.4 Assessment of cytotoxicity during transport studies 164

II.5.5 In vitro localization of ovalbumin and/or nanoparticles in the cell monolayer 165

II.6 Ex vivo studies in horizontal diffusion chambers 165

II.6.1 Induction of acute colitis using dextran sodium sulphate (DSS) in mice 165

II.6.2 Horizontal diffusion chambers 166

II.7 Statistical analysis 166

III. Results and discussion 167

III.1 Physico-chemical characterization of nanoparticles 167

III.2 Release of OVA in simulated intestinal media 169

III.2.1 In vitro release of pH-sensitive nanoparticles 169

III.2.2 Nanoparticles stability in colonic medium 169

III.3 In vitro studies with Caco-2 cells 170

III.3.1 Assessment of the cytotoxicity of the nanoparticles on Caco-2 cells 170
III.3.2 Assessment of monolayer integrity 171
III.3.3 Ovalbumin transport across Caco-2 monolayers 172
III.3.4 Localization of nanoparticles and OVA in intestinal barrier model 174

III.4 Uptake of nanoparticles in ex vivo colon 175

IV. Conclusion 177

V. References 178

I. INTRODUCTION

Ulcerative colitis (UC) and Crohn's disease (CD), two of the major inflammatory bowel diseases (IBD), are relapsing and chronic inflammatory disorders of the intestinal mucosa, with an organ-susceptibility for the colon [1]. Conventional therapy has been extensively used during five decades to treat IBD with, however, serious adverse effects [2, 3]. Thus, in the last 15 years, alternative biological therapies have been developed to treat IBD. In this context, tumor necrosis factor alpha (TNFα) antibodies have been widely used with success. However, these biopharmaceutics are administered systemically and several side effects and complications are associated with their use [4, 5].

A targeted colonic carrier of these biopharmaceutical drugs could be a major advance to treat such diseases by delivering the drug locally in the colon and reaching the specific site of inflammation. Different strategies have been used in the literature to target the inflamed colon after oral administration. Pro-drugs, exploitation of higher colonic pH values, enzymatic activity of colonic microflora, intestinal transit time or colonic pressure have been investigated as specific colonic drug delivery strategies the last decades [6, 7]. However, the overall dimensions of the delivery system significantly influence the targeting of the inflamed colon. Size-dependency of particles impacts their epithelial uptake and a preferential accumulation in the inflamed colon has been found for 100 nm-sized particles. Indeed, it has been demonstrated in experimental colitis that nanosized particles are taken up more readily by immune-related cells such as macrophages or dendritic cells in the area of active inflammation. They can also better attach to mucus layers due to their easier penetration and their relatively small mass [8]. Furthermore, it seems that pathophysiological changes due to mucosal inflammation are involved in this preferential uptake: i) disrupted intestinal barrier due to the presence of mucosal surface alterations, crypt distortions and ulcers, ii) infiltration of immune related cells as macrophages, lymphocytes or dendritic cells and iii) higher mucus production [9, 10]. This accumulation of nano-sized drug delivery systems should locally deliver higher amounts of entrapped drugs to the inflamed areas, thus leading to a better therapeutic efficacy and a decrease in systemic side effects.

An initial approach to target inflamed areas of the colon was to combine specific colonic drug delivery strategies with nanocarriers. Polymeric nanoparticles were chosen as carriers able to fulfil such criteria. Based on the literature, three colonic delivery strategies for nanocarriers were selected. In the gastro-intestinal tract, from the stomach to the colon, intraluminal pH varies progressively up to 7. In order to obtain pH-sensitive nanoparticles, ES100, a polymer of methacrylic acid and methyl methacrylate, which dissolves when the pH is above 7, was used to release the entrapped drug [11, 12]. N,N,N-trimethylchitosan chloride (TMC) was

used to prepare mucoadhesive nanoparticles. TMC, which is the result of the partial quaternization of chitosan, is characterized by fixed positive charges irrespective of pH, making it soluble at a colonic pH (>7), unlike chitosan. Similar to chitosan, TMC opens tight junctions between epithelial cells, leading to an increase of paracellular permeability. It has also a special characteristic to adhere to the mucosal surface because this cationic polymer is attracted by negatively charged intestinal mucosa [13]. Furthermore, chitosan and its derivatives are not degraded in the upper gastrointestinal tract, but undergo enzymatic hydrolysis by colonic microbiota [14, 15]. Biodegradable nanoparticles were made using a mix of three polymers: poly(lactic-co-glycolic) acid (PLGA), poly(lactic-co-glycolic) acid-block-polyethyleneglycol (PLGA-PEG) and poly-ε-caprolactone-block-polyethyleneglycol (PCL-PEG) to get sustained release of the entrapped drug [16] and to compare active from passive targeting by the grafting of specific ligands on the PEG [17]. PLGA nanoparticles have been shown to accumulate in ulcerous lesions of IBD in human [18]. A peptidic sequence identified by phage display as well as a mannose derivative were selected as ligands, to target the inflamed colon and immune-related cells respectively [19, 20].

The aim of this study was to compare different strategies to locally deliver biopharmaceutical drugs to inflamed colonic tissue using oral administration of nanoparticles. Therefore, a model protein, ovalbumin (OVA) was encapsulated in (i) bioadhesive TMC nanoparticles, (ii) pH-sensitive nanoparticles made with ES100 and (iii) PLGA-based nanoparticles to obtain a sustained delivery. The features of these different nanoparticles including size, potential zeta, encapsulation efficiency and drug loading were examined. The epithelial cell viability upon exposure to the nanoparticles was determined. The transepithelial transport of the different nanoparticles was investigated using Caco-2 monolayers mimicking the inflamed colon and visualized using confocal laser microscopy. In an inflamed colonic murine tissue, the uptake of these different nanoparticles was evaluated in horizontal diffusion chambers ex vivo.

II. MATERIALS & METHODS

II.1 MATERIALS

II.1.1 Cell lines

Human colon carcinoma Caco-2 line (clone 1), obtained from Dr. Maria Rescigno, University of Milano-Bicocca, Milano, Italy, was used [21].

II.1.2 Cell culture

Dulbecco's modified Eagle minimal essential medium (DMEM, 4.5 g/L D-glucose), non-essential amino acids, L-glutamine and penicillin-streptomycin (PenStrep) were purchased from Gibco™ Invitrogen Corporation (Paisley, UK). HyClone® fetal bovine serum (FBS) from South America was purchased from Thermo Fisher Scientific (Waltham, MA). Trypsin 0.05% with EDTA was purchased from Gibco™ Invitrogen Corporation. Dulbecco's PBS without $CaCl_2$ and $MgCl_2$ (D-PBS) and Hank's Balanced Salt Solution (HBSS) were purchased from Gibco™ Invitrogen Corporation.

Rhodamine-phalloidin was obtained from Molecular Probes (Eugene, OR). UltraCruz mounting medium was obtained from Santa Cruz (Delaware, CA). Triton X-100, 3-(4,5-Dimethylthiazol-2-yl)-2,5-diphenyltetrazolium bromide (MTT) and dimethyl sulfoxide (DMSO) were purchased from Sigma-Aldrich (St-Louis, MO). Transwell® polyethylene terephthalate (PET) filters were purchased from Corning (Lowell,MA). Inserts were coated with Matrigel™ Basement Membrane Matrix (Becton Dickinson) before cells seeding. IL-1β, TNF-α and LPS were obtained from Sigma-Aldrich. IFN-γ was purchased from Chemicon-Millipore (Billerica, MA).

II.1.3 Chemicals

N,N,N-trimethylchitosan chloride (TMC) (Degree of acetylation: 22.3 mol%; Degree of quaternization: 33 mol%) was a gift from KitoZyme (Herstal, Belgium). Pentasodium tripolyphosphate (TPP), dichloromethane, ovalbumin (OVA) grade V, polyvinyl alcohol (PVA) and sodium cholate were obtained from Sigma-Aldrich (St-Louis, MO). FITC-ovalbumin (FITC-OVA) was purchased from Molecular Probes (Eugene, OR). ES100 was a gift from Evonik RÖHM GmbH (Darmstadt, DE). Poly(lactic-co-glycolic) acid (PLGA) (L:G 50:50, average Mw 7000–17000) was obtained from Boehringer Ingelheim GmbH (Ingelheim am Rhein, Germany). PEGylated poly(lactic-co-glycolic) acid (PLGA-PEG average Mw 16500-4600) was synthesized by ring opening polymerization as previously described [22, 23]. PCL-

PEG (12000-6000 g/mol) were synthesized. The molecular clip (i.e. O-succinimidyl-4-(1-azi-2,2,2-trifluoroethyl) benzoate) was synthesized as described elsewhere [24].

II.1.4 Radio-labelling of ovalbumin

Sodium boro[^{3}H]hydride (100 mCi) was supplied by Perkin Elmer (Boston, MA). Radiolabelling of OVA (Sigma) was performed by reductive alkylation of amino groups [25]. The [^{3}H]-ovalbumin specific activity was obtained by measuring the total protein concentration by a microBCA protein assay Kit (Pierce, Rockford, IL, USA) according to the manufacturer's instructions, and the radioactivity by liquid scintillation. The peptide integrity after labelling was evaluated by SDS-PAGE and ELISA analysis according to standards protocols (data not shown) [17].

II.2 LIGANDS

The ligands grafted on PCL-PEG were the following:

- Gly-Ser-Gln-Ser-His-Pro-Arg-His (GSQSHPRH) octapeptide, identified by phage display as specific to murine inflamed colon [19], was purchased from Eurogentec (Seraing, Belgium).
- Man: Mannose derivative, i.e. 2-aminoethyl-α-D-mannopyroside (MannOH–NH_2), was synthesized as previously described [26].

II.2.1 Grafting of GSQSHPRH on PCL-PEG

PCL-PEG was dissolved in CH_3CN (20 mL/g) with the desired amount of the molecular clip (65 µmol/g of polymer) and the solution was cast on clean glass plates. Films formed by solvent evaporation were dried *in vacuo*, removed from the plates as shavings, and irradiated (3x8W BLB Lamps, 360 nm, 4.5 cm) in a homemade reactor (rotating quartz flask of 15 mL) under argon atmosphere for 20 min. Samples were then washed in a mixture of isopropanol:ethyl acetate (19:1) and vacuum dried. They were then incubated in 5 ml of a 2 mM solution of GSQSHPRH in PB:CH_3CN (1/1, v/v) at pH 8 and shacked for 24 h at room temperature. The samples were filtered, washed with a slightly acidic (pH 5-6) solution, deionised water (5 times) and dried by azeotropic distillation of dry CH_3CN. Finally, samples were dissolved in a minimum of CH_2Cl_2 (≤ 1 ml/g), slowly added to ten volumes of iPr_2O (precipitation), and the suspension was sonicated for 15 min. The iPr_2O phase was removed and the treatment was twice repeated. The grafting rate of the peptidic ligand was found to be 0.44 - 0.2 peptide GSQSHPRH per PCL-PEG chain (i.e. 44 - 20 % of grafted chains) by comparison of grafted and non-grafted PCL-PEG samples functionalized with a tritiated probe as described elsewhere [24, 26].

II.2.2 Grafting of mannose on PCL-PEG

Synthesis of the mannosylated diblock copolymer was done as previously reported [27]. Briefly, diethylacetal-poly(ethylene glycol)-b-poly(ε-caprolactone) (acetal-PEG-b-PCL) was synthesized by anionic polymerization of ethylene oxide initiated from 3,3-diethoxy-1-propanyl, followed by the ring opening polymerization of ε-caprolactone catalyzed with stannous octoate. 2-Aminoethyl-α-D-mannopyroside was then coupled on acetal-PEO-b-PCL after deprotection of the aldehyde followed by reductive amination. The end functionalization of the copolymer by mannose determined by the phenol/sulphuric assay was 30% [27].

II.3 PREPARATION AND CHARACTERIZATION OF NANOPARTICLES

II.3.1 Preparation of PLGA-based nanoparticles

PLGA nanoparticles were prepared by a "water-in-oil-in-water" solvent evaporation method [17]. Briefly, 30 mg, 7.5 mg and 7.5 mg of PLGA, PLGA-PEG and either PCL-PEG or mannose-grafted PCL-PEG or peptidic ligand-grafted PCL-PEG ligand respectively were dissolved in 1 ml of dichloromethane. 50 µl of either 10 mg/ml OVA or FITC-OVA or ^{3}H-OVA in distilled water was added to the organic phase. An ultrasonic processor was used for 15 s at 70 W to make the first emulsion. The emulsion was emulsified again with 2 ml of 1% (w/v) sodium cholate in water. The double emulsion was then poured into 100 ml of a 0.3% sodium cholate aqueous solution and stirred at 37°C for 1 h. The nanoparticles suspension was then washed twice in distilled water by centrifugation at 22000 g for 45 min. Supernatants were collected to evaluate encapsulation efficiency of ovalbumin. Empty nanoparticles were prepared by adding 50 µl of distilled water instead of the ovalbumin solution during the preparation of formulations.

II.3.2 Preparation of bio-adhesive nanoparticles

TMC nanoparticles were prepared by ionic complexation/gelation method [28]. Briefly, TPP as well as OVA or FITC-OVA or ^{3}H-OVA solution were dissolved in distilled water at a concentration of respectively 1 mg/ml and 5 mg/ml. These solutions were then added under continuous stirring to a TMC solution (2 mg/ml) in order to obtain a weight ratio TMC:TPP:OVA of 10:1.8:1. Nanoparticles were collected by centrifugation (30 min, 15000 g) on a glycerol bed, to avoid aggregation. Supernatants were collected to evaluate encapsulation efficiency. Empty nanoparticles were prepared by adding distilled water instead of the ovalbumin solution during the preparation of formulations.

II.3.3 Preparation of pH-sensitive nanoparticles

ES100 nanoparticles were prepared by a "water-in-oil-in-water" method [11, 12, 29]. Briefly, 1 ml of OVA (10 mg/ml) or ^{3}H-OVA or a mix of OVA/FITC-OVA 75:15 was emulsified with 10 ml of a mix of acetone/methanol 2:1 containing 125 mg of ES100 with an ultrasonic processor for 30 s at 70 W. The secondary emulsion was prepared by adding the first emulsion in 40 ml of PVA 0.1 % before ultrasonication for 1 min at 70 W. The nanoparticles suspension was then washed twice in distilled water by centrifugation at 45000 g for 20 min. Supernatants were collected to evaluate encapsulation efficiency of OVA. Empty nanoparticles were prepared by adding 1 ml of distilled water instead of the ovalbumin solution during the preparation of formulations.

II.3.4 Characterization of the formulations

Particle size distribution was determined by means of dynamic light scattering (DLS) using a NanoSizer Zeta Series (Malvern Instruments, Malvern UK). The zeta potential of the particles was measured in 1mM KCl with the NanoSizer ZS by laser Doppler velocimetry.

Supernatants and pellets were used to measure the non-encapsulated OVA. For ES100 nanoparticles, ^{3}H-OVA was quantified by liquid scintillation counting. Briefly, 4 ml of Ready Safe® scintillation cocktail (Beckman Coulter, Suarlée, BE) were added to the samples and ^{3}H-OVA was measured using a TriCarb 2900TR liquid scintillation analyzer (Perkin Elmer, Waltham, MA). For TMC and PLGA nanoparticles, OVA was quantified using a microBCA protein assay kit (Pierce, Rockford, IL) according to the manufacturer's instructions. The encapsulation efficiency was expressed in percentage as the amount of OVA encapsulated compared to the amount of OVA used to form the nanoparticles.

Drug loading was expressed as the ratio of the amount of OVA encapsulated compared to the amount of polymer used for the formulation.

Integrity of OVA after encapsulation in nanoparticles was checked by SDS-PAGE and ELISA analysis after release from nanoparticles.

II.4 IN VITRO RELEASE OF OVALBUMIN FROM NANOPARTICLES

In vitro release characteristics of the pH-sensitive nanoparticles were evaluated by using pH-changing system (pH 1.2, 4.5 and 7.2), as described in the European pharmacopoeia[30] [30]. 10 mg of ^{3}H-OVA loaded ES100 nanoparticles were suspended in 50 ml of the release medium and incubated into a shaking water bath (60 rpm, 37°C). After predetermined durations, samples were centrifuged at 45000 g for 30 min in order to obtain the free OVA in the supernatant. 4 mL of Ready Safe® liquid scintillation cocktail were added to the

supernatants and the concentration of free OVA in the supernatant was measured using liquid scintillation analyzer Tri-Carb 2900TR (Perkin Elmer, Waltham, MA).

^{3}H-OVA-loaded nanoparticles were added in one vial per time point at the following final concentration: 500 µg/ml of polymer for TMC nanoparticles and 2.5 mg/ml of polymer for PLGA nanoparticles. They were then suspended in HBSS, pH = 7.4, under gentle mechanic stirring (750 rpm) for various durations. . After the predetermined time intervals, vials were centrifuged at 15000 rpm for 20 min and nanoparticle size and release of ^{3}H-radiolabelled OVA were investigated. Liquid scintillation counting, described before, was used to measure the amounts of released ^{3}H-OVA from supernatant and nanoparticles [17].

II.5 TRANSPORT STUDIES ON CACO-2 CELLS

II.5.1 Cell culture

Human Caco-2 cell line (clone 1) was used between passages 20 and 40 and cultured in DMEM supplemented with 10% (v/v) FBS, 1% (v/v) L-glutamine 200 mM and 1% (v/v) non-essential amino acids. Cells were grown on 175 cm^2 flasks (Sarstedt, Numbrecht, DE) in an atmosphere of 10% CO_2/90% air (v/v) at 37°C. Caco-2 cells were grown on inserts in the same medium further supplemented with 1% (v/v) Pen-Strep.

II.5.2 Effect of polymers on cell viability

Cytotoxicity of the formulations on Caco-2 cells was evaluated using the MTT method. Briefly, Caco-2 cells (20000/well) were seeded in a 96-well plate (Nunc, Roskilde, DK) and maintained for 24 hours at 37°C and 10% CO_2. After 90 minutes exposure to the desired concentration of the various delivery systems, the cells were washed 3 times with HBSS and incubated for 3 h with 0.5 mg/ml MTT in DMEM. Medium was then removed and the purple formazan crystal was dissolved in 100 µL DMSO. Absorbance at 570 nm was measured using a MultiSkan Ex plate reader (Thermo Fisher Scientific, Waltham, MA).

II.5.3 Ovalbumin transport mediated by nanoparticles across the Caco-2 monolayers untreated or exposed to pro-inflammatory cytokines

For transport experiments, cells were cultivated on bicameral inserts Transwell® following standards protocols [17]. Briefly, the cells were seeded at a density of 500 x 10^3 cells/well on Matrigel® (Beckton Dickinson, Franklin Lakes, NJ) basement precoated 12-well plates and cultured in standard medium supplemented with 1% Pen-Strep. After 20 days, half of the inserts were exposed to a pro-inflammatory cocktail in order to obtain a model of an inflamed intestinal epithelial barrier. The pro-inflammatory cocktail, consisted of the inflammatory

mediators IL-1β, TNF-α, INF-γ and LPS at 25, 50, 50 and 1000 ng/ml respectively, was added into the basolateral side during 24 hours [31]. Inserts without pro-inflammatory cocktail were also made in order to obtain an untreated intestinal barrier model.

To demonstrate of the presence of inflammation induction in the *in vitro* model, the extracellular media, from the apical and basolateral side were collected from inflamed and untreated model on day 21 after seeding and centrifuged at 16 $x10^3$ g for 10 min. IL-8 secretion was evaluated using a sandwich ELISA (BD Biosciences Pharmingen, San Diego, CA) and quantified in pg/ml using the standard provided with the kit, with sensitivity limits of 0.8 pg/ml. Results were subsequently expressed in absolute terms [31].

Transport experiments were run in HBSS at 37°C. Nanoparticles encapsulating ^{3}H-radiolabelled OVA were used for these experiments. The nanoparticle concentration was adjusted at 1 mg/ml for PLGA and ES100 nanoparticles and 0.5 mg/ml for TMC nanoparticles by diluting the stock solution in HBSS. Controls were: free OVA at the same concentration than those of the OVA-loaded nanoparticles (5 µg/ml for PLGA; 60 µg/ml for TMC and ES100); free OVA with empty nanoparticles; free OVA with free soluble TMC polymer. After equilibration in HBSS at 37°C, the apical medium of the cell monolayers was replaced by a formulation (400 µL) at the desired concentration and inserts were incubated at 37°C for 90 min. Basolateral solutions were then sampled and the quantity of ^{3}H-ovalbumin from the basolateral solutions was measured using a liquid scintillation analyser. Results are expressed as apparent permeability coefficient (Papp) (mean ± standard error of the mean (SEM)).

The apparent permeability, Papp (cm/s), is defined by the following equation:

$$Papp = \frac{dQ}{dtAC_0}$$

where dQ/dt is the quantity of ^{3}H-ovalbumin (mg) present in the basal compartment as a function of time (s); A, the area of the Transwell (cm^2); and C_0, the initial concentration of ^{3}H-OVA in apical compartment (mg/mL).

II.5.4 Assessment of cytotoxicity during transport studies

The absence of cytotoxicity of the different formulations was assessed after transport experiment by measuring activity of the lactate dehydrogenase (LDH) released from the cytosol of damaged cells into the apical medium. A cytotoxicity detection kit (Roche Diagnostics GmbH, Mannheim, DE) was used according to manufacturer's instructions.

Results were expressed as a percentage of the positive control, consisting of cells exposed to 1% (v/v) Triton-X-100.

Integrity of the monolayer was assessed by TEER measurements, using an epithelial voltohmmeter (World Precision Instruments, Sarasota, FL). The TEER was measured before exposure to the proinflammatory cocktail (considered as 100%), before transport experiments and after incubation with the nanoparticles for 90 min.

II.5.5 In vitro localization of ovalbumin and/or nanoparticles in the cell monolayer

Fluorescent formulations were obtained by encapsulating FITC-OVA in PLGA, TMC or ES100 nanoparticles. Free FITC-OVA was used as control. After transport experiments, inserts were washed three times with PBS. Inserts were then fixed in 2% (v/v) buffered formaldehyde (pH 7.4; 30 min) at room temperature. The inserts were then washed three times with PBS, and let at 4°C overnight. The inserts were then washed three times with 1% Triton X-100 then washed three times again. In order to reveal cell borders, actin was stained with 250 µl of rhodamin-phalloidin (4 U/ml) in PBS for 30 minutes at ambient temperature. Inserts were washed in PBS, cut and mounted on glass slides with an UltraCruz® mounting medium that contains DAPI so as to reveal nuclei. Nanoparticle position in the cell monolayer was observed with a Carl Zeiss™ Cell Observer® Spinning Disk confocal microscope.

II.6 EX VIVO STUDIES IN HORIZONTAL DIFFUSION CHAMBERS

II.6.1 Induction of acute colitis using dextran sodium sulphate (DSS) in mice

Specific pathogen-free female C57Bl/6 mice, 7 weeks at the beginning were purchased from JANVIER (Le Genest-Saint-Isle, FR). The mice were kept in hanging wire cages with 12:12-h light dark cycles and allowed access to food and drink *ad libitum*. Mice were fasted the day before ex vivo studies. The ethical committee for animal care of the Health Science Sector of the Université Catholique de Louvain (Brussels, BE) approved all the experiments. The mice were exposed to dextran sulphate sodium (DSS) solution (3% w/v in tap water) for 5 days. Untreated control animals received tap water only. The presence of colitis was confirmed histologically by hematoxylin-eosin staining (data not shown).

Mice were sacrificed at day 12 by cervical dislocation. After a mid-ventral abdominal incision, colon was removed and immediately immersed in freshly prepared oxygenated Krebs-Ringer (KR) solution at room temperature. Colon was opened longitudinally along the mesenteric border and rinsed with KR to remove intestinal contents. An average of 3 chambers was made per mice.

II.6.2 Horizontal diffusion chambers

A horizontal diffusion chamber was used as described [32]. Briefly, within 15 min after death the sample of colon was mounted between the two tapered fitted halves of the chamber, which comprised an Eppendorf tube and its cap with an internal window area of 0.35 cm^2. The internal mucosal-side volume contained 0.2 ml in the inner chamber of the Eppendorf® tube. The receiver compartment was filled with KR solution and gassed with 95% O_2: 5% CO_2 during all the experiment. No gas inlet was provided in the apical side in order to mimic the low oxygen environment in the luminal side of the colon. A water bath maintained temperature of the system at 37°C. The apical side of chamber was filled with 200 µl of KR solution at 37°C for 30 min. It was then cleaned and filled with 200 µl of formulation containing 10 µg of OVA. After 1 hour, the apical side of the chamber was washed three times with KR solution. Colonic samples were removed and 500 µl of Solvable tissue solubilizer (Perkin Elmer, Waltham, MA) were added at room temperature overnight. 50 µl of 35% hydrogen peroxide were then added during 30 min. 4 mL of Ultima Gold scintillation cocktail (Perkin Elmer, Waltham, MA) were added to these samples and the resulting mixture was counted for radioactivity using a Tricarb 2900TR liquid scintillation analyzer (Perkin Elmer, Waltham, MA) [33]. The percent accumulated dose per cm^2 (% AD/cm^2) values were calculated using the following equation:

$$\%AD/cm^2 = \frac{^3H\text{-OVA in colon x internal window area x } 100}{^3H\text{-OVA in donor compartment}}$$

II.7 STATISTICAL ANALYSIS

Data analysis was achieved using a software program GraphPad Prism®. Statistical analysis of *in vitro* transport and *ex vivo* uptake studies were calculated using ANOVA parametric tests using a significance level of $p < 0.05$.

III. RESULTS AND DISCUSSION

III.1 PHYSICO-CHEMICAL CHARACTERIZATION OF NANOPARTICLES

PLGA and TMC nanoparticles showed a mean size distribution in the range of 200-300 nm which is appropriate for uptake of nanoparticles in inflamed colonic mucosa [8]. ES100 nanoparticles (620 nm) showed the highest mean hydrodynamic diameter. As the dissolution of these particles will start in the luminal side, their size was not a key criterion for this delivery system. OVA was efficiently encapsulated into monodisperse (PdI<0.15) PLGA nanoparticles and fairly monodisperse (PdI<0.30) TMC and ES100 nanoparticles (Table 1).

Table 1: Characteristics of OVA loaded PLGA-based, TMC and ES100 nanoparticles

	Size (nm)[c]	Polydispersity Index[c]	Zeta potential (mV) [c]	Loading Efficiency (BCA ;%)[d]	Loading Efficiency (LSC;%)[d]	Drug loading (µgOVA/mgP)
PLGA	182±8	0.121±0.01	-14±4	55±1	54±4	5±1
PLGA-Pep[a]	213±12	0.197±0.01	-11±3	-	67+6	7±2
PLGA-Man[b]	212±8	0.177±0.01	-7±2	-	59+5	6+1
TMC	343±46	0.249±0.03	27±12	54±2	57±3	115±5
ES100	619±45	0.285±0.01	-33±2	-	76±16	61±13

[a] PLGA-Pep, peptidic ligand grafted PLGA nanoparticles.
[b] PLGA-Man, mannosylated PLGA nanoparticles.
[c] Data represent the mean of 6 independently prepared batches ± standard deviation. Size measurements were performed in distilled water and zeta potential measurements in KCl (1 mM).
[d] Loading efficiencies were measured by liquid scintillation counting (LSC) and/or microBCA assay (BCA) when nanoparticles were loaded respectively with 3H-OVA and OVA.
[e] Microgram ovalbumin/ milligram polymers.
(n=6)

With a positive zeta potential (+27±12 mV), TMC nanoparticles carried a positive charge on their surface due to the protonated methyl functions, enabling bioadhesive properties to negative mucins of the intestinal mucosa. PLGA nanoparticles showed a zeta potential close to neutrality (-14±4 mV) probably due to the presence of PEG chains partly shielding negative charges of the anionic carboxylate of the PLGA chain ends present at the

nanoparticle surface. ES100 nanoparticles carried a negative charge due to ionized carboxylic functional groups present on the polymer.

All OVA-loaded formulations showed good loading efficiency (>50%). However, OVA was more efficiently encapsulated into E^{S100} nanoparticles (76%) than PLGA and TMC nanoparticles (loading efficiency 54% and 57% respectively). Drug loading, expressed as µg of OVA per mg of polymer, was much lower for PLGA nanoparticles than the others formulations while TMC nanoparticles showed 20 fold higher drug loading than PLGA ones (Table 1).

TMC nanoparticles were made by ionic complexation/ionotropic gelation. The result of the interactions between the negative groups of TPP and OVA and the positive amino groups of TMC is a spontaneously self-assembled matrix system in the aqueous phase. As factors such as organic solvents or heat can potentially degrade the entrapped proteins, this method has an advantage over the others methods [34]. OVA-loaded PLGA/PLGA-PEG/PCL-PEG nanoparticles were manufactured by water-in-oil-in-water ($w_1/o/w_2$) double emulsion/solvent extraction method. PEGylation offers several advantages to nanoparticles. They are less subject to aggregation due to the steric repulsion. In addition, PEG chains can be found towards the inner surface of the aqueous phase containing the protein, the PEG barrier can protect protein from the denaturing effect of organic solvent/water interface [35]. Double emulsion method was also used to form pH-sensitive nanoparticles with ES100 polymer. As the harsh gastro-intestinal environment is a major obstacle for oral protein delivery, double emulsion is considered as one of the most appropriate methods to incorporate proteins in the nanoparticles, leading to a better protection than a simple adsorption on the surface of nanoparticles. However, emulsification of the aqueous protein solution in an organic solvent such as methylene chloride (for the PLGA nanoparticles) or acetone and methanol (for the pH-sensitive nanoparticles) can be a deleterious step in the encapsulation processes of proteins and peptides by exposing proteins to heat, shear and organic solvents. In addition, several parameters such as speed and time of both homogenizations, interaction of the protein molecule with organic solvent or polymer residuals dissolved in the organic solvent have to be studied to optimize the entrapment efficiency [36, 37]. PLGA-based nanoparticles grafted with mannose or peptidic ligand showed size in the same range than the ungrafted particles and their OVA loading was similar (Table 1).

Integrity of OVA after encapsulation in the nanoparticles was investigated by SDS-PAGE and ELISA analysis. As profile of OVA nanoencapsulated was similar to control OVA, integrity of OVA released from the nanoparticles was considered as unaltered (data not shown) [17].

III.2 RELEASE OF OVA IN SIMULATED INTESTINAL MEDIA

III.2.1 In vitro release of pH-sensitive nanoparticles

To check if ES100 nanoparticles could resist at low pH and effectively release their content in the luminal side of the colon, the *in vitro* pH-dependent release pattern of OVA from the pH-sensitive nanoparticulate system was investigated in a gradually pH-changing buffer [12]. As expected, ES100 nanoparticles show a low release of the entrapped OVA when pH was 1.2 and 4.5 with less than 7 % of OVA present in the release medium (Figure 1). In this range of pH, pH-sensitive nanoparticles had low permeability due to the hydrogen bonding between the hydroxyl groups of the carboxylic moiety and the carbonyl oxygen of ester groups of the ES100 polymer. As the pH of the aqueous medium shifted to 7.4, carboxylic function groups started to be de-protonated and a combination of dissolution and swelling was responsible for the release of the encapsulated OVA from pH-sensitive nanoparticles [38]. *In vitro* release profile showed that OVA should be retained by the nanoparticles at expected gastric and ileal pH, but the protein should be rapidly released from particles at expected higher colonic pH values and thus reach the colon.

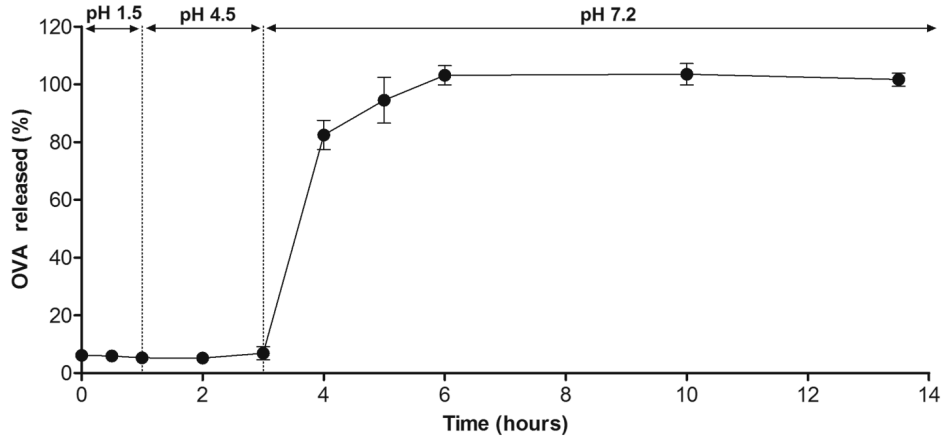


Figure 1: In vitro release profile of 3H-OVA from ES100 nanoparticles in gradually pH-changing buffers (N = 3; n = 3).

III.2.2 Nanoparticles stability in colonic medium

The stability of OVA-loaded PLGA and TMC nanoparticles was investigated to check if the nanocarriers could keep their content and remain intact in a colonic-like medium. As topical delivery in the colon is the objective, the formulations have to be stable even at neutral pH of the luminal side in the colonic region and not release the biopharmaceutical agent until it reaches the inflamed mucosa. Hence, HBSS was chosen as buffer to mimic the colonic pH

(Figure 2) [17]. The size of the OVA-loaded PLGA nanoparticles was not altered. A small release of [^{3}H] labelled OVA, approximately 10% during the 3 hours of incubation in HBSS, was observed. In the same conditions, TMC nanoparticles showed some variation in the size and 20% of ^{3}H-OVA were released during the first hour of incubation. Hence, as a significant relative quantity of OVA stays inside the nanoparticles in the colonic stimulated medium, the PLGA and TMC nanoparticles are promising formulations for the delivery of biopharmaceutics in the inflamed mucosa.

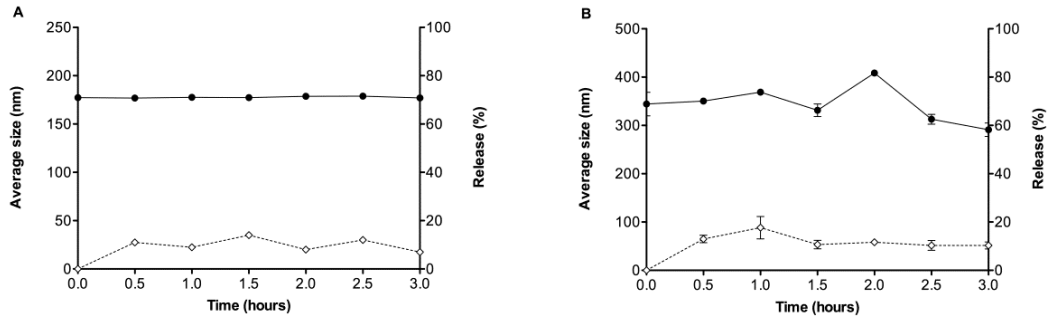


Figure 2: Evolution of the nanoparticle size (●) and OVA release (◊) during incubation in HBSS (pH 7.4) (A) PLGA nanoparticles (PLGA/PLGA-PEG/PCL-PEG 70:15:15) and (B) TMC nanoparticles (N=3; n=3).

III.3 IN VITRO STUDIES WITH CACO-2 CELLS

III.3.1 Assessment of the cytotoxicity of the nanoparticles on Caco-2 cells

Cell viability was investigated in order to choose the range of concentration used for the transport experiments. The cytotoxicity of the nanoparticles was measured with an MTT assay on proliferating Caco-2 cells.

ES100 and PLGA nanoparticles did not affect the metabolic activity at 1 mg/ml. TMC nanoparticles started to display cytotoxicity at 0.5 mg/ml (80 % of the metabolic activity of control cells) (Figure 3). The toxicity of TMC may be due to the fact that the positively charged polymer may interact strongly with the anionic cellular surface, leading to higher association [28, 34]. Based on these results, PLGA and ES100 nanoparticles were used at a concentration of 1 mg/ml of polymer while TMC nanoparticles were incubated at 0.5 mg/ml during transport experiments.

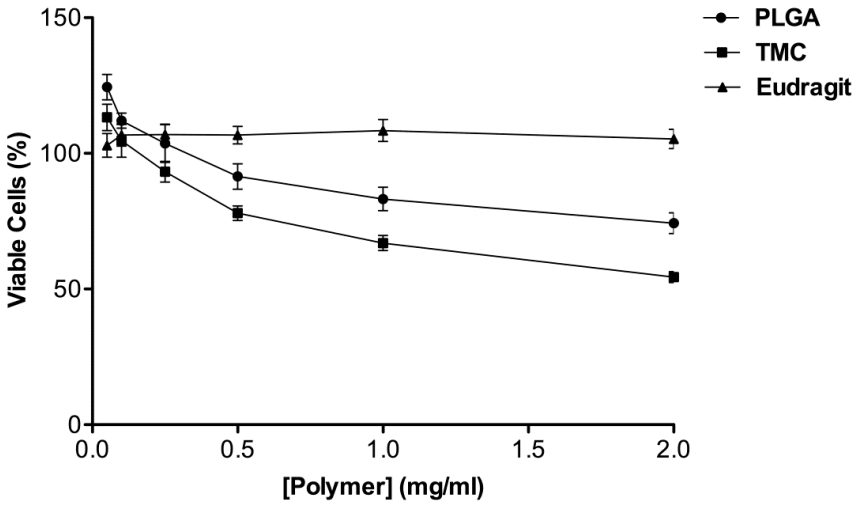


Figure 3 : Effect of OVA-loaded nanoparticles on Caco-2 cell metabolic activity upon 90 min of exposure to a range from 0.05 to 2 mg/ml. (●) PLGA nanoparticles; (■) TMC nanoparticles; (▲) ES100 nanoparticles. The metabolic activity was assessed by an MTT test. Results are expressed as percentage (mean ±SEM; n = 12) of the medium control (100%) (N = 3; n = 3).

III.3.2 Assessment of monolayer integrity

To compare the transport of OVA loaded nanoparticles through normal and inflammatory colon, Caco-2 monolayers either untreated or exposed to proinflammatory factors [31] were used. This model of inflammatory Caco-2 cells was validated by measuring the secretion of IL-8 [39]. Basal IL-8 secretion was 154 ± 19 pg/ml whereas IL-8 secretion in inflamed model was evaluated at 2057 ± 78 pg/ml confirming that the pro-inflammatory cocktail increased IL-8 secretion by 13.4–fold [31].

The cytotoxicity of formulations in these conditions was quantified by a LDH release test. For all exposures, less than 15 % of LDH were released showing that presence of inflammation and/or nanoparticles did not lead to a significant cellular necrosis (Figure 4d). The monolayer integrity was evaluated by monitoring TEER before cocktail incubation (100%), before and after transport experiments (Figures 4a, b and c). 24 hours post-exposure to proinflammatory factors, the TEER of activated Caco-2 monolayers decreased significantly ($p<0.05$) compared to untreated monolayers. After 90 minutes incubation with the different formulations, TEER was unchanged except for TMC formulations, which decreased TEER of control Caco-2 monolayers. This TMC-dependent decrease of TEER was observed for TMC nanoparticles and TMC soluble polymer. This phenomenon could be explained by the fact that TMC is known to open tight junctions [40, 41].

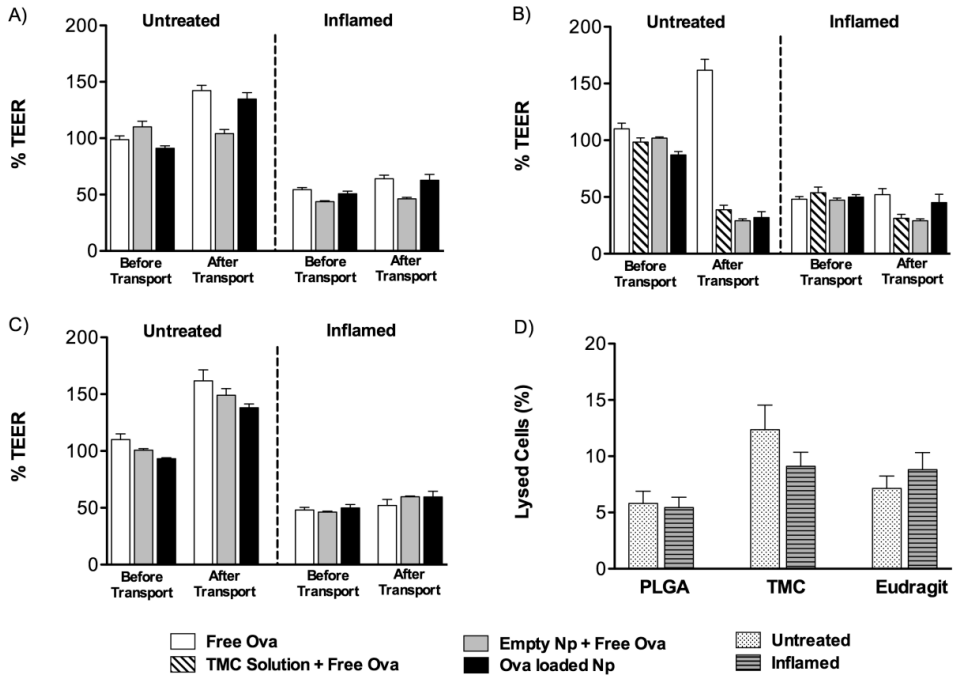


Figure 4: Monolayer integrity of Caco-2 monolayers (TEER) with/without pro-inflammatory factors and/or formulations during transport studies. The different formulations studied were free OVA (5 µg/ml for PLGA particles; 60 µg/ml for TMC and ES100 particles); Empty PLGA (0.5 mg/ml), TMC (1 mg/ml) or ES100 (1 mg/ml) nanoparticles (Np) with free OVA at a corresponding concentration; free soluble TMC polymer solution (1 mg/ml) with free OVA (60 µg/ml) and OVA-loaded PLGA, TMC or ES100 nanoparticles. Panel (A) PLGA formulations; panel (B) TMC formulations; panel (C) ES100 formulations. Monolayer integrity is expressed as percentage of transepithelial electric resistance (TEER). Panel (D) Caco-2 cell necrosis (release of LDH) (p-value <0.05) (N = 3, n = 3).

III.3.3 Ovalbumin transport across Caco-2 monolayers

OVA transport was investigated *in vitro* by comparing the apparent permeability (Papp; cm/s) of the formulations containing ^{3}H-OVA through inflamed and untreated Caco-2 monolayers after 90 minutes incubation [13, 42]. Free OVA was used as control at the same concentration than those of the OVA-loaded nanoparticles. None of the formulations showed a significant difference in terms of Papp between untreated and inflamed model.

In the untreated model, the apparent permeability of the OVA encapsulated in the TMC nanoparticles was higher than those of the OVA contained in PLGA and ES100 nanoparticles ($p<0.05$). However, in the inflamed monolayer, when the Papp of the 3 different OVA-loaded nanoparticles were compared together, no significant difference was observed (Figure 5). This higher transport of TMC nanoparticles could result from the decrease of the TEER and/or tight junction opening [43]. Papp of OVA included in the TMC nanoparticles and free OVA mixed to the empty TMC nanoparticles were significantly higher than the Papp of free OVA in both in vitro models ($p<0,05$). However, the TEER of inflamed Caco-2 monolayers was equivalent to the TEER of untreated Caco-2 cells exposed to TMC,

suggesting that TEER is not predictive for OVA transport across the monolayer. Furthermore, similar TMC nanoparticles transport through untreated and inflamed monolayers was found.

No significant differences were found between free OVA, free OVA associated with empty PLGA nanoparticles and nanoencapsulated OVA in PLGA particles in terms of Papp. The transport of OVA from GSQSHPRH-grafted and untargeted PLGA based nanoparticles was also investigated, but no significant difference was observed (data not shown).

Apparent permeability of free OVA, free OVA associated with empty ES100 nanoparticles and encapsulated OVA in ES100 nanoparticles were also found not significantly different. As expected, the fast dissolution of the ES100 particles at neutral pH shown in Figure 1 leads to the release of the peptide in the apical medium. The incorporation of OVA in ES100-based formulations did not interfere with its passage through the epithelial barrier. These results confirm that pH-triggered vehicles as ES100-based nanoparticles might be an interesting tool to deliver as is their content in the colonic lumen.

The transport of OVA from the 3 types of loaded nanoparticles through HT29 monolayers or a co-culture of HT29 and Caco-2 was not significantly different from their transport through Caco-2 monolayers, indicating that the secretion of mucus did not significantly influence the transport of OVA through the cell monolayers (data not shown).

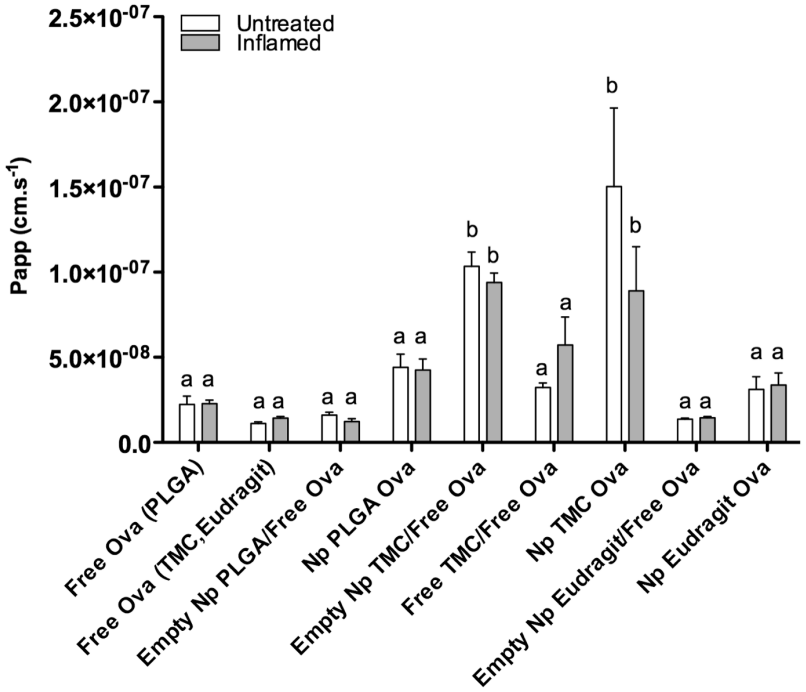


Figure 5: Comparisons of 3H-OVA formulations Papp between untreated Caco-2 monolayers and inflamed Caco-2 monolayers quantified by liquid scintillation counting. 3H-OVA transport is expressed as apparent permeability (Papp, cm/s). Columns were filled in white for untreated model and grey for inflamed model. The OVA formulations tested were: free OVA (5 g/ml for PLGA particles; 60 g/ml for TMC and ES100 particles); free OVA with empty PLGA (0.5 mg/ml), TMC (1 mg/ml) or **ES100** (1 mg/ml) nanoparticles (Np); free OVA (60 g/ml) with free soluble TMC polymer (1 mg/ml); OVA (5 g/ml for PLGA particles; 60 g/ml for TMC and **ES100** particles) encapsulated in PLGA, TMC or **ES100** nanoparticles. No significant differences in nanoparticles' transport between untreated and inflamed model was observed. Data are mean ± SEM. Data with different superscript letters are significantly different (p-value <0.05) (N = 3, n = 3).

III.3.4 Localization of nanoparticles and OVA in intestinal barrier model

In order to highlight how nanoparticles cross the intestinal barrier, whether in an inflamed or untreated state, FITC-OVA was encapsulated in the three types of nanoparticles and their association with Caco-2 cells was investigated by confocal microscopy images. Free FITC-OVA, was used as control.

FITC-OVA from PLGA nanoparticles was found in the intracellular compartment of the Caco-2 cell monolayer (Figures 6a and 6b). This finding is consistent with previous studies that showed intracellular penetration in Caco-2 cells [21] and clathrin- or receptor-mediated endocytosis as the main pathways of internalization of PEGylated PLGA nanoparticles in cells [44, 45].

FITC-OVA from TMC nanoparticles was found mainly associated with the cell membrane the apical side of the polarized monolayer, whatever the state of the barrier (Figures 6c and 6d). This results from the bioadhesivity of TMC [15]. The behavior of these nanoparticles was independent on the state of the epithelial monolayer.

No fluorescence was detected in the Caco-2 monolayers exposed to free OVA (data not shown). Similarly, confocal images of inserts exposed to FITC-OVA loaded ES100 nanoparticles did not allow the detection of nanoparticles (data not shown) as these nanoparticles are expected to dissolve and release their content in the medium.

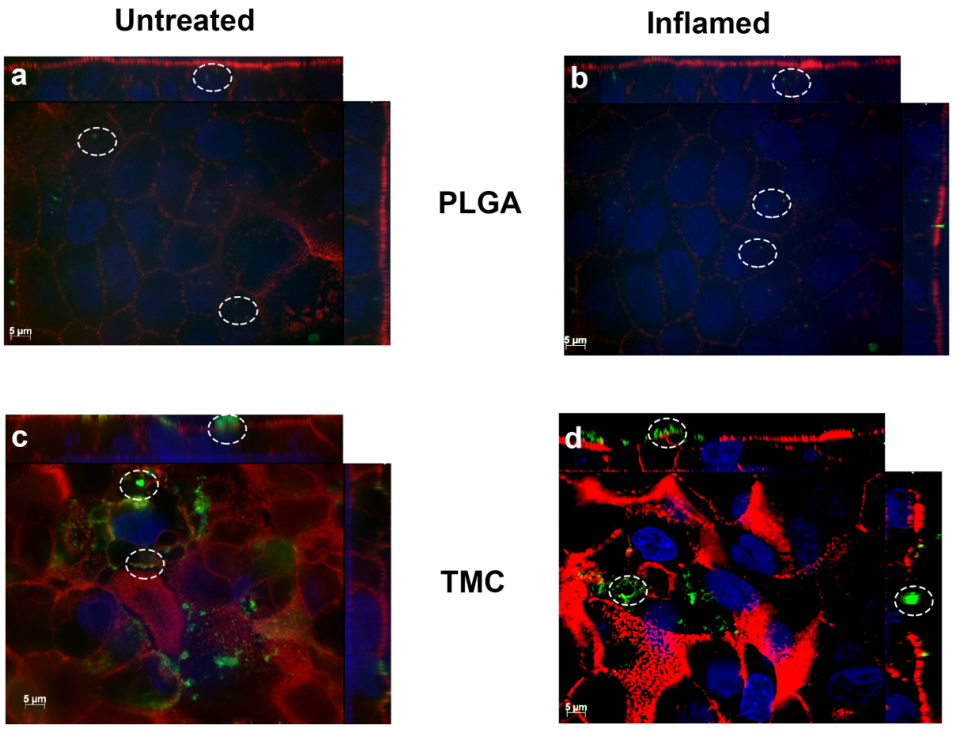


Figure 6: Representative confocal microscopy images of untreated (A and C) and inflamed (B and D) Caco-2 cells from in vitro intestinal barrier model fixed after 90 min exposure to (A and B) FITC-OVA-loaded PLGA nanoparticles at a polymer concentration of 1 mg/ml and FITC-OVA at 5 µg/ml and (C and D) FITC-OVA-loaded in TMC nanoparticles at a polymer concentration of 0.5 mg/ml TMC and FITC-OVA 60 µg/ml. Confocal microscope images A and B were centered at the same z-position (6 µm from the PET membrane) while images C and D were taken at the apical side. Inserts were formaldehyde fixed for 30 min and incubated with PBS containing rhodamine-phalloidin (4 U/ml) for 30 min to stain cell membranes. To reveal the nuclei, inserts were put on glass slides with an UltraCruz® mounting medium that contains DAPI.

III.4 UPTAKE OF NANOPARTICLES IN EX VIVO COLON

To study how the composition of the nanoparticles could influence their uptake in normal colon from healthy mice and inflamed colon from DSS-treated mice, the uptake of 10 µg of ^{3}H-OVA, loaded in nanoparticles was studied in horizontal diffusion chambers [32, 46]. After 60 min of incubation of the formulations, the accumulation of ^{3}H-OVA in inflamed colonic tissue had an increased trend as compared to the control group. PLGA-PEG-mannose nanoparticles, however, lead to a significant enhancement of accumulated ^{3}H-OVA (0.15 %/cm^{2}; $p < 0.05$) in the inflamed colon compared to the healthy one. Furthermore, ^{3}H-OVA-loaded PLGA-PEG-mannose nanoparticles were significantly accumulated in the inflamed

colonic samples than the others formulations, especially these with free OVA and OVA-loaded untargeted PLGA nanoparticles (Figure 7). As mannose present on the surface of the nanoparticles allows targeting immune-related cells presenting mannose receptor such as macrophages and dendritic cells, this increased uptake of ^{3}H-OVA-loaded PLGA-PEG-mannose nanoparticles can be explained by the infiltration of neutrophils into the mucosa and the lamina propria as the DSS-induced inflammation progressed [47-49]. The grafting of the peptidic ligand targeting murine inflamed colon did not increase the accumulation of ^{3}H-OVA in an inflamed colonic sample compared to a healthy one. The lack of targeting efficacy may be due to the fact that DSS-induced colitis does not present the same inflammatory profile than the intestinal ischemia model where the peptidic ligand was derived [19].

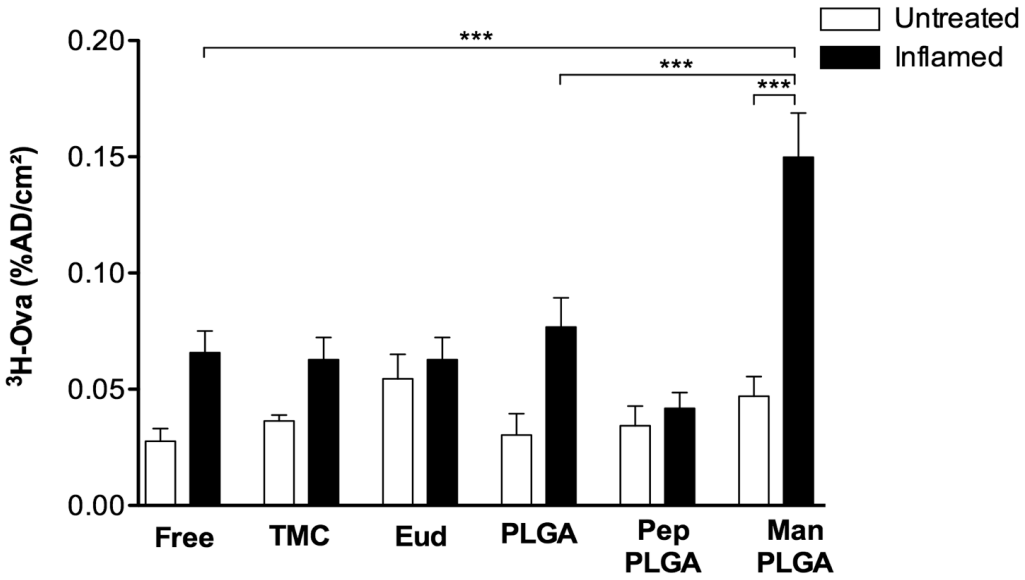


Figure 7: Accumulation of 3H-OVA in untreated or inflamed colonic samples (n = 7). Uptake of 10 g of 3H-OVA by untreated colonic samples (white bars) and inflamed colonic samples (black bars) was quantified by liquid scintillation counting. OVA formulations tested were free (ovalbumin solution); PLGA, Pep-PLGA (PLGA/PLGA-PEG/PCL-PEG-GSQSHPRH 70:15:15); Man-PLGA (PLGA/PLGA-PEG/PCL-PEG-Mannose 70:15:15); TMC; Eud (ES100). Uptake is expressed as percentage of administered dose per cm2 (%AD/cm2). Data are mean ± SEM. A significant difference in 3H-OVA uptake was observed when compared Man-PLGA nanoparticles in the inflamed colonic samples to other conditions (p-value <0.05).

IV. CONCLUSION

OVA was encapsulated in three different colon-specific polymeric nanoparticles that may target the inflamed colon in IBD. pH-sensitive formulations present a controlled release option that reach the colon without degradation in the upper part of the gut. As the goal is to pass through the epithelial barrier and deliver the encapsulated therapeutic agent within the mucosa, *in vitro* results particularly highlight TMC nanoparticles partly due to their interaction with tight junctions and bioadhesion. However, the major results were found ex vivo, where the highest accumulation of OVA in inflamed colonic tissue was obtained with PLGA-PEG-mannose nanoparticles, underlining the benefit of active targeting of immune-related cells in an inflamed context and suggesting that mannose could be used to achieve a targeted delivery to the site of inflammation in IBD.

Several delivery strategies have been investigated with varying degrees of success to deliver proteins locally in the inflamed colon after oral ingestion. The inflamed colon is an area difficult to target due to its various and complex features. Furthermore, biopharmaceutical drugs such anti-inflammatory peptides or antibodies present additional hurdles including stability and lack of permeation after oral ingestion. All these issues may be solved by the combination of the different colon specific approaches. This study is in line with this strategy by successfully consolidating the preferential uptake of nano-sized carriers with use of colon-specific polymers, in a polymeric nanoparticle construct. In the future, blending the different colon delivery strategies may provide a solution of an optimal carrier for protein drugs to reach the inflamed colon.

V. REFERENCES

[1] M.J. Carter, A.J. Lobo, S.P. Travis, B.S.o.G. Ibd Section, Guidelines for the management of inflammatory bowel disease in adults, Gut, 53 Suppl 5 (2004) V1-16.
[2] G. Rogler, Gastrointestinal and liver adverse effects of drugs used for treating IBD, Best Pract Res Clin Gastroenterol, 24 (2010) 157-165.
[3] F. Grimpen, P. Pavli, Advances in the management of inflammatory bowel disease, Intern Med J, 40 (2010) 258-264.
[4] A. Stallmach, S. Hagel, T. Bruns, Adverse effects of biologics used for treating IBD, Best Pract Res Clin Gastroenterol, 24 (2010) 167-182.
[5] S.E. Plevy, S.R. Targan, Future therapeutic approaches for inflammatory bowel diseases, Gastroenterology, 140 (2011) 1838-1846.
[6] Y. Meissner, A. Lamprecht, Alternative drug delivery approaches for the therapy of inflammatory bowel disease, J Pharm Sci, 97 (2008) 2878-2891.
[7] D.R. Friend, New oral delivery systems for treatment of inflammatory bowel disease, Adv Drug Deliv Rev, 57 (2005) 247-265.
[8] A. Lamprecht, U. Schafer, C.M. Lehr, Size-dependent bioadhesion of micro- and nanoparticulate carriers to the inflamed colonic mucosa, Pharm Res, 18 (2001) 788-793.
[9] M. Cornaggia, M. Leutner, C. Mescoli, G.C. Sturniolo, R. Gullotta, D. Gruppo Italiano Patologi Apparato, I.d. Societa Italiana di Anatomia Patologica e Citopatologia Diagnostica/International Academy of Pathology, Chronic idiopathic inflammatory bowel diseases: the histology report, Dig Liver Dis, 43 Suppl 4 (2011) S293-303.
[10] B. Moulari, D. Pertuit, Y. Pellequer, A. Lamprecht, The targeting of surface modified silica nanoparticles to inflamed tissue in experimental colitis, Biomaterials, 29 (2008) 4554-4560.
[11] C. Damge, M. Socha, N. Ubrich, P. Maincent, Poly(epsilon-caprolactone)/eudragit nanoparticles for oral delivery of aspart-insulin in the treatment of diabetes, J Pharm Sci, 99 (2010) 879-889.
[12] A. Makhlof, Y. Tozuka, H. Takeuchi, pH-Sensitive nanospheres for colon-specific drug delivery in experimentally induced colitis rat model, Eur J Pharm Biopharm, 72 (2009) 1-8.
[13] L. Plapied, G. Vandermeulen, B. Vroman, V. Preat, A. des Rieux, Bioadhesive nanoparticles of fungal chitosan for oral DNA delivery, Int J Pharm, 398 (2010) 210-218.
[14] A. Jain, Y. Gupta, S.K. Jain, Perspectives of biodegradable natural polysaccharides for site-specific drug delivery to the colon, J Pharm Pharm Sci, 10 (2007) 86-128.
[15] V.K. Mourya, N.N. Inamdar, Trimethyl chitosan and its applications in drug delivery, J Mater Sci Mater Med, 20 (2009) 1057-1079.
[16] S. Fredenberg, M. Wahlgren, M. Reslow, A. Axelsson, The mechanisms of drug release in poly(lactic-co-glycolic acid)-based drug delivery systems--a review, Int J Pharm, 415 (2011) 34-52.
[17] M. Garinot, V. Fievez, V. Pourcelle, F. Stoffelbach, A. des Rieux, L. Plapied, I. Theate, H. Freichels, C. Jerome, J. Marchand-Brynaert, Y.J. Schneider, V. Preat, PEGylated PLGA-based nanoparticles targeting M cells for oral vaccination, J Control Release, 120 (2007) 195-204.
[18] C. Schmidt, E.M. Collnot, C. Bojarski, M. Schumann, J.D. Schulzke, C.M. Lehr, A. Stallmach, W1266 Confocal Laser Endomicroscopy (CLE) Reveals Mucosal Accumulation of Plga-Nanoparticles in Ulcerous Lesions of Patients With Inflammatory Bowel Diseases, Gastroenterology, 138 (2010) S-687.
[19] T. Takagi, T. Arisawa, K. Yamamoto, I. Hirata, H. Nakano, M. Sawada, Identification of ligands binding specifically to inflammatory intestinal mucosa using phage display, Clin Exp Pharmacol Physiol, 34 (2007) 286-289.
[20] V. Fievez, L. Plapied, A. des Rieux, V. Pourcelle, H. Freichels, V. Wascotte, M.L. Vanderhaeghen, C. Jerome, A. Vanderplasschen, J. Marchand-Brynaert, Y.J. Schneider, V. Preat, Targeting nanoparticles to M cells with non-peptidic ligands for oral vaccination, Eur J Pharm Biopharm, 73 (2009) 16-24.

[21] A. des Rieux, V. Fievez, I. Theate, J. Mast, V. Preat, Y.J. Schneider, An improved in vitro model of human intestinal follicle-associated epithelium to study nanoparticle transport by M cells, Eur J Pharm Sci, 30 (2007) 380-391.
[22] M.L. Zweers, G.H. Engbers, D.W. Grijpma, J. Feijen, In vitro degradation of nanoparticles prepared from polymers based on DL-lactide, glycolide and poly(ethylene oxide), J Control Release, 100 (2004) 347-356.
[23] P. Vangeyte, B. Leyh, M. Heinrich, J. Grandjean, C. Bourgaux, R. Jerome, Self-assembly of poly(ethylene oxide)-b-poly(epsilon-caprolactone) copolymers in aqueous solution, Langmuir, 20 (2004) 8442-8451.
[24] V. Pourcelle, C.S. Le Duff, H. Freichels, C. Jérôme, J. Marchand-Brynaert, Clickable PEG conjugate obtained by "clip" photochemistry: Synthesis and characterization by quantitative 19F NMR, Journal of Fluorine Chemistry, (2012).
[25] G.E. Means, R.E. Feeney, Reductive alkylation of amino groups in proteins, Biochemistry, 7 (1968) 2192-2201.
[26] V. Pourcelle, H. Freichels, F. Stoffelbach, R. Auzély-Velty, C. Jérôme, J. Marchand-Brynaert, Light Induced Functionalization of PCL-PEG Block Copolymers for the Covalent Immobilization of Biomolecules, Biomacromolecules, 10 (2009) 966-974.
[27] H. Freichels, R. Auzely-Velty, P. Lecomte, C. Jerome, Easy functionalization of amphiphilic poly(ethylene oxide)-b-poly([varepsilon]-caprolactone) copolymer micelles with unprotected sugar: synthesis and recognition by lectins, Polymer Chemistry, 3 (2012) 1436-1445.
[28] B. Slutter, L. Plapied, V. Fievez, M.A. Sande, A. des Rieux, Y.J. Schneider, E. Van Riet, W. Jiskoot, V. Preat, Mechanistic study of the adjuvant effect of biodegradable nanoparticles in mucosal vaccination, J Control Release, 138 (2009) 113-121.
[29] D. Jain, A.K. Panda, D.K. Majumdar, Eudragit S100 entrapped insulin microspheres for oral delivery, AAPS PharmSciTech, 6 (2005) E100-107.
[30] European Pharmacopeia 7.0 (2010), 5.17.1, Recommandations on dissolution testing:p.666.
[31] J. Van De Walle, A. Hendrickx, B. Romier, Y. Larondelle, Y.J. Schneider, Inflammatory parameters in Caco-2 cells: effect of stimuli nature, concentration, combination and cell differentiation, Toxicol In Vitro, 24 (2010) 1441-1449.
[32] J. Soni, A.W. Baird, L.M. O'Brien, M. McElroy, J.J. Callanan, H.F. Bassett, D. Campion, D.J. Brayden, Rat, ovine and bovine Peyer's patches mounted in horizontal diffusion chambers display sampling function, J Control Release, 115 (2006) 68-77.
[33] C.J. Rijcken, C.J. Snel, R.M. Schiffelers, C.F. van Nostrum, W.E. Hennink, Hydrolysable core-crosslinked thermosensitive polymeric micelles: synthesis, characterisation and in vivo studies, Biomaterials, 28 (2007) 5581-5593.
[34] B. Sayin, S. Somavarapu, X.W. Li, D. Sesardic, S. Senel, O.H. Alpar, TMC-MCC (N-trimethyl chitosan-mono-N-carboxymethyl chitosan) nanocomplexes for mucosal delivery of vaccines, Eur J Pharm Sci, 38 (2009) 362-369.
[35] Y. Li, Y. Pei, X. Zhang, Z. Gu, Z. Zhou, W. Yuan, J. Zhou, J. Zhu, X. Gao, PEGylated PLGA nanoparticles as protein carriers: synthesis, preparation and biodistribution in rats, J Control Release, 71 (2001) 203-211.
[36] T. Feczko, J. Toth, G. Dosa, J. Gyenis, Influence of process conditions on the mean size of PLGA nanoparticles, Chemical Engineering and Processing: Process Intensification, 50 (2011) 846-853.
[37] T. Feczko, J. Toth, G. Dosa, J. Gyenis, Optimization of protein encapsulation in PLGA nanoparticles, Chemical Engineering and Processing: Process Intensification, 50 (2011) 757-765.
[38] A.H. El-Kamel, M.S. Sokar, S.S. Al Gamal, V.F. Naggar, Preparation and evaluation of ketoprofen floating oral delivery system, Int J Pharm, 220 (2001) 13-21.
[39] K. Liboni, N. Li, J. Neu, Mechanism of glutamine-mediated amelioration of lipopolysaccharide-induced IL-8 production in Caco-2 cells, Cytokine, 26 (2004) 57-65.

[40] T.H. Yeh, L.W. Hsu, M.T. Tseng, P.L. Lee, K. Sonjae, Y.C. Ho, H.W. Sung, Mechanism and consequence of chitosan-mediated reversible epithelial tight junction opening, Biomaterials, 32 (2011) 6164-6173.
[41] A.M. Sadeghi, F.A. Dorkoosh, M.R. Avadi, M. Weinhold, A. Bayat, F. Delie, R. Gurny, B. Larijani, M. Rafiee-Tehrani, H.E. Junginger, Permeation enhancer effect of chitosan and chitosan derivatives: comparison of formulations as soluble polymers and nanoparticulate systems on insulin absorption in Caco-2 cells, Eur J Pharm Biopharm, 70 (2008) 270-278.
[42] A. des Rieux, E.G. Ragnarsson, E. Gullberg, V. Preat, Y.J. Schneider, P. Artursson, Transport of nanoparticles across an in vitro model of the human intestinal follicle associated epithelium, Eur J Pharm Sci, 25 (2005) 455-465.
[43] Y. Zambito, C. Zaino, G. Di Colo, Effects of N-trimethylchitosan on transcellular and paracellular transcorneal drug transport, Eur J Pharm Biopharm, 64 (2006) 16-25.
[44] M.S. Cartiera, K.M. Johnson, V. Rajendran, M.J. Caplan, W.M. Saltzman, The uptake and intracellular fate of PLGA nanoparticles in epithelial cells, Biomaterials, 30 (2009) 2790-2798.
[45] M.S. Shive, J.M. Anderson, Biodegradation and biocompatibility of PLA and PLGA microspheres, Adv Drug Deliv Rev, 28 (1997) 5-24.
[46] K. Osth, L. Strindelius, A. Larhed, A. Ahlander, G.M. Roomans, I. Sjoholm, E. Bjork, Uptake of ovalbumin-conjugated starch microparticles by pig respiratory nasal mucosa in vitro, J Drug Target, 11 (2003) 75-82.
[47] S. Melgar, A. Karlsson, E. Michaelsson, Acute colitis induced by dextran sulfate sodium progresses to chronicity in C57BL/6 but not in BALB/c mice: correlation between symptoms and inflammation, Am J Physiol Gastrointest Liver Physiol, 288 (2005) G1328-1338.
[48] F. Ahsan, I.P. Rivas, M.A. Khan, A.I. Torres Suarez, Targeting to macrophages: role of physicochemical properties of particulate carriers--liposomes and microspheres--on the phagocytosis by macrophages, J Control Release, 79 (2002) 29-40.
[49] A. Jain, A. Agarwal, S. Majumder, N. Lariya, A. Khaya, H. Agrawal, S. Majumdar, G.P. Agrawal, Mannosylated solid lipid nanoparticles as vectors for site-specific delivery of an anti-cancer drug, Journal of Controlled Release, 148 (2010) 359-367.

CHAPTER VI. Design of anti-TNF-α Fab loaded nanoparticles for IBD treatment

Design of anti-TNF-α fab loaded nanoparticles for the treatment of inflammatory bowel disease

Coco R., Préat V.

ABSTRACT

For inflammatory bowel disease treatment, topical delivery of biopharmaceutics to the inflamed colon using nanoparticles could be of great interest. The aim of this study was to encapsulate an active biopharmaceutical drug, an anti-TNF-α Fab into various polymeric nanoparticles, to compare their physico-chemical parameters and, based on this, to select the more appropriate formulations for inflamed colon specific targeting. Several delivery strategies of anti-TNF-α Fab were evaluated. Eudragit S100 (ES100) was used as polymer to create pH-sensitive nanoparticles. Formulation of mucoadhesive nanoparticles was done using trimethylchitosan. PLGA-based nanoparticles were obtained with a mix of polymers, PLGA, PEG-PLGA and PEG-PCL. PLGA and ES100 were combined to get PLGA/ES100-based nanoparticles. Both anti-TNF-α Fab loaded PLGA- and ES100-based nanoparticles exhibited attractive properties for inflamed colon specific drug delivery.

TABLE OF CONTENTS

I. Introduction 184

II. Materials & Methods 186

II.1 Materials 186

II.2 Preparation and characterization of nanoparticles 186

II.2.1 Preparation of PLGA-based nanoparticles 186

II.2.2 Preparation of pH-sensitive nanoparticles 186

II.2.3 Preparation of PLGA/ES100-based nanoparticles 187

II.2.4 Preparation of TMC-based nanoparticles 187

II.2.5 Characterization of nanoparticles 187

III. Results of Physico-chemical characterization of nanoparticles 189

IV. DIscussion and Conclusion 191

V. Acknowledgements 191

VI. References 192

I. INTRODUCTION

Inflammatory bowel diseases (IBD) are inflammatory disorders of the gastro-intestinal tract. Crohn's disease and ulcerative colitis are the main representative of this group. The etiology of these diseases is still unknown but it seems that the mucosal inflammation is maintained by the dysregulated presence of pro-inflammatory cytokines such as tumor necrosis factor alpha (TNF-α) or interferon beta (IFN-β) [1, 2].

For over four decades, conventional treatment of IBD has consisted of anti-inflammatory medications, such as corticosteroids, aminosalicylates and immunosuppressants. However, their non-specific effects on the immune system and the need of high daily doses to obtain a therapeutic activity lead often to significant adverse effects [3]. Furthermore, significant inter- and intra-individual variations and apparition of refractory diseases make therapeutic efficacy and safety associated with these conventional drugs very limited [4]. A better understanding of the physiopathology of the IBD and biotechnology advances lead over the past two decades to the development of biologic agents such as monoclonal antibodies anti-TNF-α. Despite the fact that these biopharmaceutical therapies show a relevant efficacy on patient refractory to conventional treatment, their systemic administration (intravenous and subcutaneous injections) contributes to a lack of specificity of their action, resulting to serious systemic side effects [5].

Therefore, there is a need to develop a carrier system able to deliver the biopharmaceuticals specifically in the inflamed lesions and the ulcerated lesions of the colon, after oral administration. Polymeric nanoparticles appears to be a great interest in IBD therapy because mainly they accumulate preferentially in the inflamed areas [6, 7]. These following pathophysiological changes seem to play a significant role in the preferential accumulation: i) increased mucus production, ii) uptake from overexpressed immune-related cells and iii) loss of structure of intestinal epithelial with mucosal surface alterations, crypt distortions and ulcers.

Preclinical and clinical studies showed that topical delivery of biologic agents for IBD treatment might be of great interest. High doses of anti-TNF-α antibodies have been shown to treat experimental acute and chronic colitis in rats [8]. Local injections of low dose of infliximab (<60 mg) by endoscopies or after surgery were found feasible and safe and accounted for favorable clinical response [9, 10]. Furthermore, oral administration of *Lactococcus lactis* secreting interleukin-10 or anti-TNF-α nanobody or rectal administration of adenoviruses secreting interleukin-10 demonstrate efficacy in experimental colitis and in a phase 1 trial for Crohn's disease [11-13]. Hence, we hypothesize that biopharmaceutical drugs could be delivered locally for the treatment of IBD using polymeric nanoparticles as drug delivery systems.

Based on the literature and our previous studies, several nano-sized delivery strategies were selected. pH-sensitive nanoparticles were created using Eudragit® S100 (ES100), a polymer of methacrylic acid and methyl methacrylate, which dissolves when the intraluminal pH raises values above 7, that-is-to-say in the colonic lumen [14, 15]. Mucoadhesive nanoparticles were obtained using N,N,N-trimethylchitosan chloride (TMC) as polymer due to its solubility insensitive to pH, its resistance to the harsh conditions of the upper gastrointestinal tract, its paracellular permeability enhancing effect and its interaction with the intestinal mucosa [16]. PLGA nanoparticles have been shown to accumulate in ulcerous lesions of IBD in human [7, 17]. Using a mix of three polymers: poly(lactic-co-glycolic) acid (PLGA), poly(lactic-co-glycolic) acid-block-polyethyleneglycol (PLGA-PEG) and poly-ε-caprolactone-block-polyethyleneglycol (PCL-PEG), PLGA-based nanoparticles were made to get sustained release of the entrapped drug [18, 19]. In order to mix two delivery strategies (pH-sensitivity and sustained release) in one nanocarrier, nanoparticles made of ES100 and PLGA were formulated [15].

The aim of this study was to deliver topically a biopharmaceutical monoclonal antibody to treat IBD using polymeric nanoparticles. This dimer form of fragment antibody (Fab) is directed against the human TNF-α and consists in the non-PEGylated version of the certolizumab pegol. We encapsulated this anti-TNF-α Fab in several chosen nanoparticulate drug delivery systems and then compared them in terms of size, potential zeta, encapsulation efficiency and drug loading. The selected nanocarrier(s) should allow after oral administration the topical delivery of the biopharmaceutical anti-TNF-α to inflamed colonic tissue and thus will be evaluated *in vitro* and *in vivo* in further studies.

II. MATERIALS & METHODS

II.1 MATERIALS

N,N,N-trimethylchitosan chloride (TMC) (MW: 110 kDa; Degree of acetylation: 22.3 mol%; Degree of quaternization: 33 mol%) was a gift from KitoZyme (Herstal, Belgium). Pentasodium tripolyphosphate (TPP), dichloromethane, polyvinyl alcohol (PVA), dextran sulfate and sodium cholate were obtained from Sigma-Aldrich (St-Louis, MO). FITC-ovalbumin (FITC-OVA) was purchased from Molecular Probes (Eugene, OR). Eudragit® S100 was a gift from Evonik RÖHM GmbH (Darmstadt, DE). Poly(lactic-co-glycolic) acid (PLGA) (L:G 50:50, average Mw 7000–17000) was obtained from Boehringer Ingelheim GmbH (Ingelheim am Rhein, Germany). PEGylated poly(lactic-co-glycolic) acid (PLGA-PEG average Mw 16500-4600) was synthesized by ring opening polymerization as previously described [20, 21]. PCL-PEG (12000-6000 g/mol) was synthesized. PRONOVA® sodium alginate was obtained from Novamatrix FMC Biopolymer (Sandvika, Norway). Anti-TNF-α Fab was kindly gifted by UCB (Braine l'Alleud, Belgium). The dimer form of this Fab was suspended in 100 mM sodium phosphate, 1 mM EDTA pH6.0 buffer

II.2 PREPARATION AND CHARACTERIZATION OF NANOPARTICLES

II.2.1 Preparation of PLGA-based nanoparticles

PLGA nanoparticles were prepared by a "water-in-oil-in-water" solvent evaporation method [19, 22]. Briefly, 30 mg, 7.5 mg and 7.5 mg of PLGA, PLGA-PEG and PCL-PEG were dissolved in 1 ml of dichloromethane. 50 µl of either 20 mg/ml Fab in pH 6.0 buffer containing 100mM sodium phosphate and 1mM EDTA was added to the organic phase. An ultrasonic processor was used for 15 s at 70 W to make the first emulsion. The emulsion was emulsified again with 2 ml of 1% (w/v) sodium cholate in water. The double emulsion was then poured into 100 ml of a 0.3% sodium cholate aqueous solution and stirred at 37 ◦C for 1 h. The nanoparticles suspension was then washed twice in distilled water by centrifugation at 22,000 × g for 45 min. Supernatants were collected to evaluate encapsulation efficiency of Fab. Empty nanoparticles were prepared by adding 50 µl of distilled water instead of the Fab solution during the preparation of formulations.

II.2.2 Preparation of pH-sensitive nanoparticles

ES100 nanoparticles were prepared by a "water-in-oil-in-water" method [14, 15, 22, 23]. Briefly, 500 µl of anti-TNF-α Fab (20 mg/ml) was emulsified with 10 ml of a mix of acetone/methanol 2:1 containing 125 mg of ES100 with an ultrasonic processor for 30 s at

70 W. The secondary emulsion was prepared by adding the first emulsion in 40 ml of PVA 0.1 % before ultrasonication for 1 min at 70 W. The nanoparticles suspension was then washed twice in distilled water by centrifugation at 45000 g for 20 min. Supernatants were collected to evaluate encapsulation efficiency of anti-TNF-α Fab. Empty nanoparticles were prepared by adding 500 µl of distilled water instead of the anti-TNF-α Fab solution during the preparation of formulations.

II.2.3 Preparation of PLGA/ES100-based nanoparticles

Dual nanoparticles were prepared by an adaption of the modified spontaneous emulsification solvent diffusion (SESD) [15]. Briefly, 45 mg of PLGA, 45 mg of ES100 were respectively dissolved in 1 ml of a mix of acetone/methanol (2:1) and pooled. 500 µl of anti-TNF-α Fab (20 mg/ml) were then added to the organic solution and emulsified with an ultrasonic processor for 30 s at 70 W. The whole mixture was added dropwise in 20 ml of 0.5% (w/v) PVA under magnetic stirring and thus immediately centrifuged at 4°C at 45,000 x g for 30 minutes. The nanoparticles suspension was then washed twice in distilled water. Supernatants were collected to evaluate encapsulation efficiency of anti-TNF-α Fab.

II.2.4 Preparation of TMC-based nanoparticles

TMC nanoparticles were prepared by ionic complexation/gelation method [22, 24]. Briefly, anti-TNF-α Fab solution and the corresponding counter-ion (TPP, alginate or dextran sulfate) were dissolved in distilled water at the desired concentration. These solutions were then added under continuous stirring to a TMC solution (2 mg/ml) in order to obtain the desired weight ratio. Nanoparticles were collected by centrifugation (30 min, 15000 g) on a glycerol bed, to avoid aggregation. Supernatants were collected to evaluate encapsulation efficiency.

II.2.5 Characterization of nanoparticles

Particle size distribution was determined by means of dynamic light scattering (DLS) using a NanoSizer Zeta Series (Malvern Instruments, Malvern, UK). The zeta potential of the particles was measured in 1 mM KCl with the NanoSizer ZS by laser Doppler velocimetry. Supernatants and pellets were used to measure the non-encapsulated Fab. Fab was quantified using a microBCA protein assay kit (Pierce, Rockford, IL) according to the manufacturer's instructions. The encapsulation efficiency was expressed in percentage as the amount of Fab encapsulated compared to the amount of Fab used to form the nanoparticles. Drug loading was expressed as the ratio of the amount of Fab encapsulated compared to the amount of polymer used for the formulation. Integrity of Fab after

encapsulation in nanoparticles was checked by SDS-PAGE analysis after release from nanoparticles.

III. RESULTS OF PHYSICO-CHEMICAL CHARACTERIZATION OF NANOPARTICLES

Table 1: Characteristics of anti-TNF-α Fab loaded nanoparticles

Polymer	Content	Size (nm)[a]	Polydispersity index[a]	Zeta Potential (mV)[a]	Loading efficiency (%)	Drug Loading (µgFab/mgP)[b]
PLGA PLGA-PEG PCL-PEG	Fab-loaded	97±0.3	0.24 ± 0.0	-19±0.4	100	22
	Empty	85±0.2	0.11±0.03	-22±1.4	-	-
ES100	Fab-loaded	190±3	0.50±0.01	-	86±12	69
PLGA ES100	Fab-loaded	186±16	0.466±0.06	-42.9±0.6	21±12	2.3
	Empty	370±136	0.667±0.125	-35.3±0.8	-	-
TMC[c]	Fab TPP	203±4	0.22±0.02	-	0	-
	Fab Dextran	271±116	0.38±0.13	-	0	-
	Fab Alginate	150±13	0.33±0.19	-	0	-

[a] Data represent the mean of 3 independently prepared batches ± standard deviation. Size measurements were performed in distilled water and zeta potential measurements in KCl (1 mM).
[b] Microgram Fab/milligram polymers
[c] Only best results regarding the size and the polydispersity index were written on this table
n=3

To deliver topically in the inflamed colon, drug loaded nanocarriers must meet some criteria. First, as a size dependency has been associated with a preferential uptake in inflamed colonic areas, a size of the nanocarriers close to 100 nm is desired [6]. If an interaction with the mucosa occurs, the population is preferable to be homogenous and present a polydispersity index inferior to 0.3. Furthermore, loading efficiency must be as high as possible to consider the nanocarrier as a good anti-TNF-α Fab delivery system. Finally, the drug loading, which measures the amount of drug (µg) per amount of polymer (mg), should be as high as possible. The particle characterization of nanoparticles is summarized in Table 1. Based on these criteria and the physico-chemical characterization of the nanoparticles, ES100 and PLGA/PLGA-PEG/PCL-PEG nanoparticles were considered as the most promising nanocarriers for the delivery of anti-TNF-α Fab and its targeting towards the inflamed mucosa.

Using ES100 as polymer, pH-sensitive nanoparticles showed a size around 190 nm. They displayed a polydispersity index (PdI) superior to 0.3. However, this latter feature was not considered eliminatory as these nanoparticles are supposed to dissolve and liberate their encapsulated content into the colonic lumen, when the pH is above 7. Indeed, ES100-based

nanoparticles are able to withstand to low pH values and keep their content intact. Then, when neutral pH values are obtained as these from the colonic lumen, these nanoparticles dissolve and liberate their encapsulated content in the medium [15, 22]. This population of particles presents a good loading efficiency of 86%. Drug loading was the highest found.

PLGA/PLGA-PEG/PCL-PEG nanoparticles present the optimal size to preferentially accumulate in the inflamed colon. PLGA-based nanoparticles were found homogenous, as they possessed a good PdI (<0.3). All the anti-TNF-a Fab was encapsulated in the nanoparticles. Approved by the US Food and Drug Administration and the European Medicine Agency in drug delivery systems for parenteral administration, PLGA is biodegradable and biocompatible polymer widely available commercially with different molecular weights and copolymer compositions [25]. PEG grafts offers stealthness to the carrier by decreasing recognition by the reticulo-endothelial system and enhancing the penetration through the mucus [26]. Depending to the ratio of the two monomers, lactic acid and glycolic acid, degradation of these particles allows sustained release of the content. Fluorescent PLGA particles were found preferentially accumulated in the inflamed mucosa of human patients of IBD, showing the clinical relevance of these PLGA particles [7]. These PLGA-based nanoparticles exhibited attractive properties for inflamed colon specific drug delivery and offered possibilities of translation to clinical practice.

PLGA/ES100-based nanoparticles present unfortunately too high PdI and too low loading efficiency. Whatever the counter-ion, populations of mucoadhesive nanoparticles do not succeed to encapsulate the anti-TNF-a Fab. As electrical interactions are responsible of the formulation of these particles, their stability depends strongly on the electrical profile of the components. TMC is cationic and the counter-ion is chosen for among all its negative charge. Ovalbumin, the model protein used for the development of this formulation presents an isoelectric point (pI) of 4.6, meaning that at the desired pH, ovalbumin is negative [24, 27]. However, with a pI > 8.0, anti-TNF-α Fab presents a positive charge profile in the working pH, resulting in a disrupting change in the formulation. As high pH is deleterious for protein and peptides, increasing the working pH is not a viable option [28].

IV. DISCUSSION AND CONCLUSION

The encapsulation of an active anti-TNF-α Fab was investigated using several nanocarriers. ES100/PLGA- and PLGA-based nanoparticles were able to present physico-chemical features suitable for the IBD delivery and targeting. We were not able to do *in vivo* studies, as the murine version of anti-TNF-α Fab was not available.

V. ACKNOWLEDGEMENTS

We would like to thank UCB for the gift of the anti-TNF-α Fab.

VI. REFERENCES

[1] C. Abraham, J.H. Cho, Inflammatory bowel disease, N Engl J Med, 361 (2009) 2066-2078.
[2] A. Kaser, S. Zeissig, R.S. Blumberg, Inflammatory bowel disease, Annu Rev Immunol, 28 (2010) 573-621.
[3] F. Grimpen, P. Pavli, Advances in the management of inflammatory bowel disease, Intern Med J, 40 (2010) 258-264.
[4] N.A. Braus, D.E. Elliott, Advances in the pathogenesis and treatment of IBD, Clin Immunol, 132 (2009) 1-9.
[5] A. Stallmach, S. Hagel, T. Bruns, Adverse effects of biologics used for treating IBD, Best Pract Res Clin Gastroenterol, 24 (2010) 167-182.
[6] A. Lamprecht, U. Schafer, C.M. Lehr, Size-dependent bioadhesion of micro- and nanoparticulate carriers to the inflamed colonic mucosa, Pharm Res, 18 (2001) 788-793.
[7] C. Schmidt, C. Lautenschlaeger, E.-M. Collnot, M. Schumann, C. Bojarski, J.-D. Schulzke, C.-M. Lehr, A. Stallmach, Nano- and microscaled particles for drug targeting to inflamed intestinal mucosa—A first in vivo study in human patients, Journal of Controlled Release, 165 (2013) 139-145.
[8] K.L. Worledge, R. Godiska, T.A. Barrett, J.A. Kink, Oral administration of avian tumor necrosis factor antibodies effectively treats experimental colitis in rats, Dig Dis Sci, 45 (2000) 2298-2305.
[9] G. Poggioli, S. Laureti, F. Pierangeli, F. Rizzello, F. Ugolini, P. Gionchetti, M. Campieri, Local injection of Infliximab for the treatment of perianal Crohn's disease, Dis Colon Rectum, 48 (2005) 768-774.
[10] L. Biancone, M. Cretella, C. Tosti, G. Palmieri, C. Petruzziello, A. Geremia, E. Calabrese, F. Pallone, Local injection of infliximab in the postoperative recurrence of Crohn's disease, Gastrointest Endosc, 63 (2006) 486-492.
[11] L. Steidler, W. Hans, L. Schotte, S. Neirynck, F. Obermeier, W. Falk, W. Fiers, E. Remaut, Treatment of murine colitis by Lactococcus lactis secreting interleukin-10, Science, 289 (2000) 1352-1355.
[12] K. Vandenbroucke, H. de Haard, E. Beirnaert, T. Dreier, M. Lauwereys, L. Huyck, J. Van Huysse, P. Demetter, L. Steidler, E. Remaut, C. Cuvelier, P. Rottiers, Orally administered L. lactis secreting an anti-TNF Nanobody demonstrate efficacy in chronic colitis, Mucosal Immunol, 3 (2010) 49-56.
[13] J.F. Valentine, M.B. Grisham, Intramuscular injection of a recombinant adeno-associated virus (rAAV) vector containing interleukin-10 (IL-10) reduces proximal colonic inflammation in IL-10 deficient mice, Gastroenterology, 120 (2001) A689.
[14] C. Damge, M. Socha, N. Ubrich, P. Maincent, Poly(epsilon-caprolactone)/eudragit nanoparticles for oral delivery of aspart-insulin in the treatment of diabetes, J Pharm Sci, 99 (2010) 879-889.
[15] A. Makhlof, Y. Tozuka, H. Takeuchi, pH-Sensitive nanospheres for colon-specific drug delivery in experimentally induced colitis rat model, Eur J Pharm Biopharm, 72 (2009) 1-8.
[16] L. Plapied, G. Vandermeulen, B. Vroman, V. Preat, A. des Rieux, Bioadhesive nanoparticles of fungal chitosan for oral DNA delivery, Int J Pharm, 398 (2010) 210-218.
[17] C. Schmidt, E.M. Collnot, C. Bojarski, M. Schumann, J.D. Schulzke, C.M. Lehr, A. Stallmach, W1266 Confocal Laser Endomicroscopy (CLE) Reveals Mucosal Accumulation of Plga-Nanoparticles in Ulcerous Lesions of Patients With Inflammatory Bowel Diseases, Gastroenterology, 138 (2010) S-687.
[18] S. Fredenberg, M. Wahlgren, M. Reslow, A. Axelsson, The mechanisms of drug release in poly(lactic-co-glycolic acid)-based drug delivery systems--a review, Int J Pharm, 415 (2011) 34-52.
[19] M. Garinot, V. Fievez, V. Pourcelle, F. Stoffelbach, A. des Rieux, L. Plapied, I. Theate, H. Freichels, C. Jerome, J. Marchand-Brynaert, Y.J. Schneider, V. Preat, PEGylated PLGA-based nanoparticles targeting M cells for oral vaccination, J Control Release, 120 (2007) 195-204.

[20] M.L. Zweers, G.H. Engbers, D.W. Grijpma, J. Feijen, In vitro degradation of nanoparticles prepared from polymers based on DL-lactide, glycolide and poly(ethylene oxide), J Control Release, 100 (2004) 347-356.
[21] P. Vangeyte, B. Leyh, M. Heinrich, J. Grandjean, C. Bourgaux, R. Jerome, Self-assembly of poly(ethylene oxide)-b-poly(epsilon-caprolactone) copolymers in aqueous solution, Langmuir, 20 (2004) 8442-8451.
[22] R. Coco, L. Plapied, V. Pourcelle, C. Jerome, D.J. Brayden, Y.J. Schneider, V. Preat, Drug delivery to inflamed colon by nanoparticles: comparison of different strategies, Int J Pharm, 440 (2013) 3-12.
[23] D. Jain, A.K. Panda, D.K. Majumdar, Eudragit S100 entrapped insulin microspheres for oral delivery, AAPS PharmSciTech, 6 (2005) E100-107.
[24] B. Slutter, L. Plapied, V. Fievez, M.A. Sande, A. des Rieux, Y.J. Schneider, E. Van Riet, W. Jiskoot, V. Preat, Mechanistic study of the adjuvant effect of biodegradable nanoparticles in mucosal vaccination, J Control Release, 138 (2009) 113-121.
[25] F. Danhier, E. Ansorena, J.M. Silva, R. Coco, A. Le Breton, V. Preat, PLGA-based nanoparticles: an overview of biomedical applications, J Control Release, 161 (2012) 505-522.
[26] L.M. Ensign, R. Cone, J. Hanes, Oral drug delivery with polymeric nanoparticles: the gastrointestinal mucus barriers, Adv Drug Deliv Rev, 64 (2012) 557-570.
[27] S. Jarudilokkul, A. Tongthammachat, V. Boonamnuayvittaya, Preparation of chitosan nanoparticles for encapsulation and release of protein, Korean J. Chem. Eng., 28 (2011) 1247-1251.
[28] W. Wang, S. Singh, D.L. Zeng, K. King, S. Nema, Antibody structure, instability, and formulation, J Pharm Sci, 96 (2007) 1-26.

CHAPTER VII.
Discussion and Perspectives

TABLE OF CONTENTS

I. General discussion on drug-loaded nanocarriers for IBD treatment 199

I.1 Main objective of the thesis 199

I.2 Main findings of this work 199

II. Open questions 201

II.1 Which type of nanocarrier is more effective: polymeric nanoparticles or lipid-based nanocarriers? 201

II.2 What is the best delivery strategy? Topical delivery of small drug vs. topical delivery of biopharmaceutics 203

II.3 Is active targeting the most promising delivery strategy? 205

II.4 Are the chosen in vitro models relevant? 206

II.5 Is the choice of DSS-induced colitis model relevant? 207

III. Perspectives 209

III.1 Biopharmaceutics drugs 209

III.2 Combination of delivery strategies 209

IV. References 211

I. GENERAL DISCUSSION ON DRUG-LOADED NANOCARRIERS FOR IBD TREATMENT

I.1 MAIN OBJECTIVE OF THE THESIS

The oral delivery of the anti-inflammatory drugs to the site of inflammation is one of the main challenges in IBD therapy. However, as the colon is the target organ, this route of administration has to face the harsh conditions of the gastro-intestinal environment. Furthermore, IBD induce pathophysiological changes, resulting in the delivery of the drug in undesired areas. To overcome these problems, we encapsulated several anti-inflammatory drugs (small drugs or biopharmaceutics) in nanocarriers such as polymeric nanoparticles or lipid-based nanocarriers, because, as explained in the introduction, nanoparticles have the ability to accumulate in inflamed regions. Topical delivery of these drugs in colonic tissue by nanoparticles should lead to a specific targeting of intestinal inflamed lesions, promote accumulation and capture in ulcerated and inflamed areas, decrease the frequency and the severity of the associated side effects and enhance the therapeutic efficacy of the drugs. Oral delivery should also increase the compliance of the patient.

I.2 MAIN FINDINGS OF THIS WORK

Firstly, in this work, we have demonstrated the topical delivery of budesonide using NLCs. *In vitro*, budesonide-loaded NLCs reduced TNF-α secretion by activated macrophages (J774 cells). Interestingly, *in vivo* studies showed that BDS-NLCs decreased neutrophil infiltration and levels of the pro-inflammatory cytokines IL-1ß and TNF-α in the colon and improved the histological scores of the colons with better results when compared to blank-NLCs and BDS suspension. To our knowledge, it is the first study using NLCs as drug delivery system to target IBD.

Secondly, we compared the topical delivery of curcumin using two nanosized drug delivery systems: pH-sensitive nanoparticles and lipid-based SNEDDS. CC-loaded nanocarriers present physico-chemical characteristics suitable for colon delivery. Compared to suspension and SNEDDS, a higher transport of CC was obtained by pH-sensitive nanoparticles on a Caco-2 epithelial barrier model. Confocal microscope images showed a better uptake of CC-loaded SNEDDS on Caco-2 cells. TNF-α secretion by activated macrophages (J774 cells) was reduced by both types of CC-loaded nanocarriers. In a murine DSS-induced colitis model, CC-loaded nanoparticles decreased inflammation.

Thirdly, we investigated the topical delivery of biopharmaceutics in inflamed colonic mucosa by three different polymeric nanoparticles. We used ovalbumin (OVA) as a model drug in order to formulate: (i) pH-sensitive nanoparticles made with Eudragit® S100, (ii) mucoadhesive nanoparticles with trimethylchitosan (TMC), (iii) stealth nanoparticles able of sustained release using a mix of polymers PLGA, PEG-PLGA and PEG-PCL. Furthermore, the latter were able to accept grafted on the PEG chain of PCL ligands targeting immune cells (i.e. mannose) or the inflamed colon (i.e. a specific peptide). In an *in vitro* inflamed epithelium, TMC nanoparticles showed the highest apparent permeability for OVA in the untreated model. However, no difference between the nanoparticles was observed. In the *ex vivo* horizontal diffusion chamber model, mannose-grafted PLGA nanoparticles showed the highest uptake of OVA in inflamed colon. These results highlight active targeting of macrophages and dendritic cells as promising delivery and targeting strategy for IBD.

Finally, we developed an anti-TNF-α Fab-loaded polymeric nano-scaled drug delivery system. Several polymeric nanoparticles corresponding to several delivery strategies have been evaluated: pH-sensitive and mucoadhesive nanoparticles were obtained by using respectively ES100 and TMC as polymers. Stealth nanoparticles were obtained with a mix of polymers, PLGA, PEG-PLGA and PEG-PCL. At last, a mixed strategy between sustained release and pH-sensitivity was assessed using PLGA and Eudragit S100 as polymers. Anti-TNF-α Fab loaded stealth and pH-sensitive nanoparticles both exhibited attractive properties for inflamed colon specific drug delivery.

II. OPEN QUESTIONS

II.1 WHICH TYPE OF NANOCARRIER IS MORE EFFECTIVE: POLYMERIC NANOPARTICLES OR LIPID-BASED NANOCARRIERS?

The aim of this thesis was to investigate the topical delivery of drugs in the inflamed colonic mucosa. During the whole thesis, two types of nanocarriers were used: polymeric nanoparticles and lipid-based nanocarriers. But which type is more effective? Based on our results and on the literature, we can discuss about that question.

First of all, two types of drugs were evaluated: small drugs and biopharmaceutical drugs. Small drugs consisted in 2 compounds: BDS, a conventional drug extensively used in clinical practice and CC, a compound with anti-inflammatory effects and therapeutic potential against IBD [1, 2]. They are more likely to be absorbed after oral delivery but as CC and BDS, a lot of them suffered from poor solubility, leading to inefficient topical delivery. Biopharmaceutical drugs include large molecules as proteins, peptides or siRNA. For the oral delivery, vehicles for this type of drugs are more needed as they can be degraded in the GIT or not cross the epithelial barrier. OVA was selected as a biopharmaceutical model drug due to its cheapness, its inactivity and its labeling ability (radio- or fluorolabeling) [3].

Polymeric nanoparticles were chosen as they can be designed to match pathophysiological features of the inflamed colon (pH-sensitivity, mucoadhesion, immune infiltration, etc.). The immunomodulatory effects and the intrinsic affinity with lipophilic drugs were some of the criteria explaining the choice of lipid-based nanocarriers.

summarizes physico-chemical characters of each type of nanocarriers. All the carriers that we used present submicronic size. Most of them have a size between 100 nm and 400 nm. Only SNEDDS presented a size below 100 nm. Zeta potential of the nanocarriers, which represents the net surface charge, is also a discriminating criterion. Positively charged nanoparticles like TMC nanoparticles adhere to negative mucosal components: i) mucins, main proteins of the mucus and ii) negatively charged membranes of enterocytes. All the other polymeric nanoparticles present a negative net surface charge. Negative particles may be more attracted by ulcerated regions as the latter presented an abundance of positive proteins as eosinophil proteins [4]. Encapsulation efficiency and drug loading depend strongly on the encapsulated drug. Concerning the encapsulation efficiency, lipid-based carriers possessed a net advantage. Indeed, NLC and SNEDDS present encapsulation efficiency close to 100%. However, these rates cannot be explained by the correlation between the lipophilic nature of both encapsulated small drug and nanocarrier. A preliminary study of formulation of CC-loaded NLCs gave low encapsulation efficiency rates.

Encapsulation efficiency values of polymeric nanoparticles were less important but they were able to encapsulate hydrophilic and lipophilic compounds. However, absolute reading of the encapsulation efficiency can lead to misunderstandings since the starting drug amount is essential. What really matters is drug loading, which represents the amount of drug that can be presented by the vehicle. Thus, drug loading is really important for cytotoxicity, *in vivo* studies and scaling-up. Drug loading of our nanocarriers was variable but lipid-based nanocarriers presented worse values.

Cellular uptake of these nanocarriers was proved in different manners. In an *in vivo* localization study, after DSS treatment on mice, higher amounts of NLCs were observed in the colon 12 h after the administration of coumarin-6-loaded NLCs. In an *ex vivo* horizontal diffusion chamber, polymeric nanoparticles were compared in terms of uptake of OVA. Active targeted nanoparticles were found more retained in the inflamed colon than the other polymeric nanoformulations.

Finally, these nanocarriers can be compared from an *in vivo* point of view. In chapter IV, we investigated the topical delivery of CC by comparing PLGA/ES100 nanoparticles and SNEDDS. The lack of efficacy of SNEDDS lets us suppose that they were not an optimal choice for a topical delivery. CC-loaded PLGA nanoparticles were able to decrease inflammation. Unlike NLC and SNEDDS, some polymeric nanoparticles (and in this thesis especially PLGA-based particles) offer the possibility for an active targeting of IBD-related inflamed areas.

In my opinion, polymeric nanoparticles offered more possibilities of customization as choice of polymer(s) is associated with the chosen delivery strategy(ies). They also can encapsulate different types of contents (small drugs or biopharmaceutics). However, they are less easy to formulate than lipid-based carriers. Furthermore, they offer less possibilities of scaling up than lipid-based nanocarriers.

Table 1: Comparison between different properties of polymeric nanoparticles and lipid-based nanocarriers

	Stealth Active targeting	**Mucoadhesive**	**pH-sensitive**	**pH-sensitive Sustained release**	**SNEDDS**	**NLC**
Carrier Composition	PLGA PLGA-PEG PCL-PEG	TMC	Eudragit S100	Eudragit S100 PLGA	Labrafil Labrasol Cremophor EL Transcutol HP	Precirol ATO 5 Miglyol
Nature of encapsulated drug	OVA Anti-TNF-α Fab	OVA	OVA	CC	CC	BDS
Size (nm)	202	343	619	116	30	204
PdI	0.17	0.25	0.29	0.26	0.06	0.21
Zeta potential (mV)	11	27	-33	-40	-	-42
Drug loading (µgAS/mgP)	6	115	61	74	30	0.8
Facility of formulation	+	+	+	+	+++	++
Possibility of active targeting	+	+	-	-		
Topical colonic delivery	Yes	Yes	Yes	Yes	No	Yes

II.2 WHAT IS THE BEST DELIVERY STRATEGY? TOPICAL DELIVERY OF SMALL DRUG VS. TOPICAL DELIVERY OF BIOPHARMACEUTICS

The first part of the thesis focused on the topical delivery of two small drugs: budesonide (BDS) and curcumin (CC). Both have similar pharmacokinetic features: poor water solubility, intracellular action and poor oral bioavaibility. Topical delivery of BDS was assured by NLCs whereas SNEDDS and PLGA/ES100 were used to encapsulate and deliver topically CC. Studies showed that encapsulation in nanocarriers provide improvement in terms of stability, epithelial passage and/or *in vitro* activity. BDS-loaded NLCs and CC-loaded PLGA-/ES100 were found to decrease inflammation in a DSS-induced colitis.

The second part of the thesis was dedicated to the topical delivery of biopharmaceutics on IBD-inflamed colon using polymeric nanoparticles. We first elaborated several polymeric nanoformulations using different polymers and thus different colon-specific delivery strategies: pH-dependent release profile by Eudragit nanoparticles or bioadhesion by TMC nanoparticles. We used ovalbumin (OVA) as model biopharmaceutical drug. Hence, active targeting may be considered as being the most promising approach. But transfer of formulation procedures from OVA to anti-TNF-α Fab was not so obvious, mainly due to the electrochemical profile of the Fab (isoelectric potential). Furthermore, as activity of this Fab is

extracellular, active targeting was discarded as a potential approach. PLGA/PLGA-PEG/PCL-PEG nanoparticles give hence suitable results for colon delivery. Stealth ability of PEG against the reticulo-endothelial system and local sustained release ability of PLGA polymer can be used for this purpose.

Further, as previously reported in the introduction, targeting the inflamed colonic mucosa is quite different from targeting the healthy one. The lumen, entry compartment of the oral route administration, differs in terms of pH, transit time, microbiota, mucus production or lipid content. The mucosa in an inflamed state is itself altered with the abundance of gaps, immune-related cells and antigens. Thus, to increase the targeting properties, drug delivery systems may be designed using inflamed colon specific delivery strategies instead of conventional ones. We used several strategies to elaborate drug-loaded nanocarriers: mucoadhesion, pH-sensitivity, sustained release, active targeting and lipid-based nanocarriers.

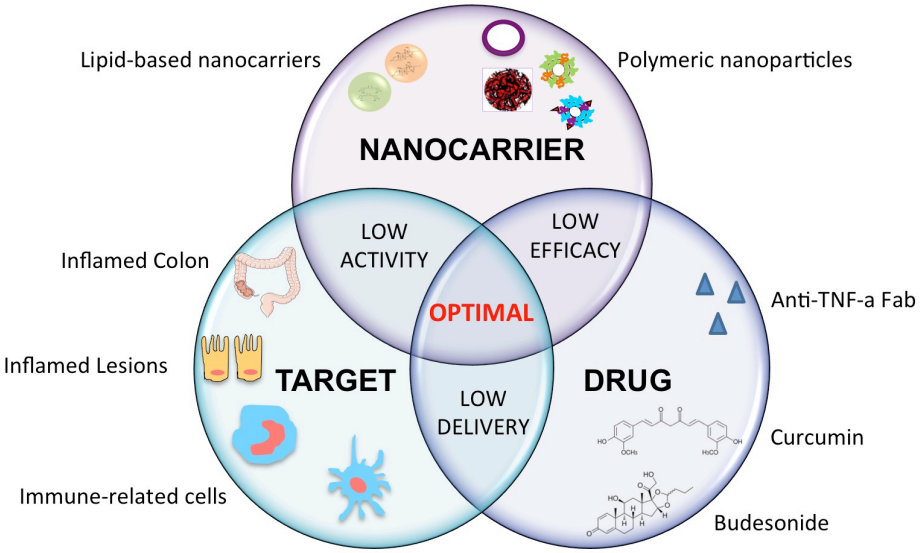


Figure 1: Key criteria for an optimal IBD nano-scaled specific drug delivery system. Target, nanocarrier and drug have all to be taken into consideration in order to avoid low activity, efficacy or delivery and get an optimal inflamed colon specific topical delivery.

From my point of view, it is difficult to generalize these results. Figure 1 represents the key criteria for an optimal IBD specific nano-scaled drug delivery system. Getting it depends strongly on the characteristics of the drug (small or biopharmaceutical drug, physico-chemical characteristics, intra- or extracellular activity), the characteristics of the nanocarrier (lipid- or polymeric-based, size, zeta potential, drug loading, encapsulation efficiency) and the relation between both. One nanocarrier cannot fit all the drugs and vice-versa. For instance, due to its hydrophilic nature, a biopharmaceutical drug such as anti-TNF-α Fab

may be difficult to encapsulate in lipid-based nanocarriers and may result in low efficacy against IBD. Comparison between the two types of nanocarriers might have ended differently if encapsulation of curcumin in NLC would have been investigated. But it seems that the characteristics of the target (organ or cellular targeting, intra- or extracellular localization,) or is also a key criterion. For instance, use a nanocarrier able to target actively the overexpressed immune-related cells for the delivery of the anti-TNF-α Fab is a no sense and will result in low delivery, efficacy and low activity. Only by giving the same importance to these the used nanocarrier, the desired target and the selected drug that: i) a "personalized nanocarrier", ii) an efficient encapsulation of the drug of interest and iii) and an effective targeting will be obtained. This will result in an optimal nano-formulation for IBD topical delivery and, finally, an enhanced therapeutic efficacy.

II.3 IS ACTIVE TARGETING THE MOST PROMISING DELIVERY STRATEGY?

One of the most significant data of this thesis showed the potential of active targeting for inflamed colon delivery. Inflamed colonic mucosa presents similarities with the tumor vasculature. Indeed, mannose-receptor presenting cells such as macrophages and dendritic cells are overexpressed in the inflamed mucosa. In order to target these immune-related cells, we decorated our nanoparticles with mannose and observed *ex vivo* the accumulation of these particles in the horizontal diffusion chamber model. A better uptake was observed by mannose-grafted nanoparticles compared to several other nanoformulations, demonstrating that active targeting of immune-related cells may be a promising approach for inflamed colon delivery. Active targeting has been found superior also in several inflammation-related publications [5-7] and other fields as cancer [8-10]. However, several elements still be brought into questions. First, active targeting is mainly associated with an intracellular drug delivery. Thus, therapeutic compounds with intracellular activity such as siRNA are good candidates. However, drug with extracellular activity such as pro-inflammatory cytokines (IL-10) or antibodies (anti-TNF-a Fab, anti-IL17, etc…) may be internalized and degraded without reaching their extracellular targets as they are not released in time by the nanocarrier. Second, mannose may not be the only ligand available to target the inflamed mucosa. We tried a peptidic ligand identified by phage display specific to inflamed mucosa [11] but it did not present targeting efficacy. This lack of targeting may be explained by the fact that this peptide ligand was found using an ischemic model or the peptide was degraded. This model may not present the same inflammatory pattern than a DSS-induced inflamed mucosa. In the same extent, a siRNA nanocarrier made with a mannosylated bioreducible polymer was able to reduce TNF-α level in colonic tissues [5]. Other ligands may be of great

interest. The associated receptor of an efficient ligand must be overexpressed in the inflamed colonic mucosa but low or not expressed in the healthy mucosa.

II.4 ARE THE CHOSEN IN VITRO MODELS RELEVANT?

As it has been previously reported, we are conscious that our *in vitro* monoculture models present some limitations. One may say that the use of coculture should be more appropriate as human IBD-induced inflamed mucosa is a complex and interactive cellular patchwork. However, our *in vitro* monoculture models are well characterized in the literature, highly reproducible, simple to induce and provided us the ability to study separately the behaviour of nanoparticles in different cell cultures. Our *in vitro* inflamed epithelial barrier model, consisting in a Caco-2 cell monoculture put in an inflamed state by a pro-inflammatory cocktail (IL-1ß, TNF-α, IFN-γ and LPS), helps us to study the passage of nanoparticles through an inflamed epithelium. In patients with IBD, an enhanced permeability occurs in the inflamed areas [12]. This event, which is one of the first steps of IBD-induced inflammation, plays a major role in the preferential uptake of the nanoparticles. Using TEER measurements, we showed that our *in vitro* model was able to display a reduction of the monolayer integrity. However, even if we found that there was no difference in the passage of OVA between untreated and inflamed model, it does not mean that the *in vitro* model does not work. It emphasizes the fact that immunocompetent cells may play a major role in the preferential accumulation of nanocarriers in the inflamed mucosa. Indeed, a preferential uptake of 50 nm-sized polystyrene nanoparticles by immunocompetent cells in a 3D model was found in contrast with a stimulated Caco-2 single cell culture [13]. Our model was also able to overexpress well-known pro-inflammatory markers such as IL-6 or IL-8 [14]. The crucial role of immune-related cells such as macrophages and dendritic cells in the pathogenesis of IBD cannot be omitted. In order to examine more attentively the interaction between our nanocarriers and these immune-related cells, therapeutic activity of CC- and BDS-loaded nanocarriers was evaluated by the reduction of TNF-α secretion from LPS-activated J774 macrophages. Activation of macrophages can be attempted by several ways: recognition of bacterial antigens such as LPS or recruitment via neutrophils produced inflammatory chemokines such as IL-1β or TNF-α [15]. To reproduce *in vitro* the inflamed state, it is primordial to activate the immune-related cells. In the same 3D model elaborated by Leonard et al., uptake into immune-competent cells was found stronger in the IL-1β-induced inflamed model than in the control one. Furthermore, compared to the non-stimulated control, inflamed 3D model presented immunocompetent cells closer to the apical side [13]. We used TNF-α secretion as marker to evaluate therapeutic activity because TNF-α is considered as a central mediator in pathogenesis of IBD. TNF-α is usually not detectable

in healthy individuals but is found in abundance in serum, tissue and feces of IBD patients [16]. Furthermore, TNF-α is mainly produced by activated macrophages and dendritic cells. By decreasing TNF-α production, our nanoformulations displayed promising data for IBD treatment.

II.5 IS THE CHOICE OF DSS-INDUCED COLITIS MODEL RELEVANT?

We are aware that several drawbacks related to the use of DSS murine colitis model have been highlighted. However, we still think that this chemically induced colitis model can provide remarkable data about the *in vivo* behavior of nanoformulations. DSS model is recognized to be highly reproducible, not expensive and easy to induce and mimic human IBD-related features [17, 18]. When rodents (mice, rats, rabbits and guinea pigs) are fed with DSS solution (2–5%) added to the drinking water for 5 up to 7 days, they developed symptoms as weight loss, bloody diarrhea and loose stools [19]. These macroscopic symptoms are similar to the ones in human patients with active IBD. In our *in vivo* studies, we were able to monitor these symptoms in mice by using a clinical inflammatory score. Microscopically, inflamed colonic mucosa in an active state is characterized by ulcerations, the loss of structural architecture and the infiltration of immune-related cells. This last element can be characterized by the MPO activity. This enzyme, overexpressed in immune-related cells such as macrophages and dendritic cells, can be used as an efficient inflammation index in clinical practice as well as in DSS-induced model [20]. Furthermore, results from *ex vivo* horizontal diffusion chambers highlight the overexpression of immune-related cells, as mannose-grafted PLGA-based nanoparticles showed the best accumulation on DSS-treated colonic samples. The disturbance of epithelial integrity has a central position in pathogenesis of IBD even we still do not know if this enhanced intestinal permeability is a primary event or a secondary phenomenon. Gut epithelial cells of the basal crypts are damaged by DSS, resulting in a disruption in the integrity of the mucosal barrier [21]. DSS damages trigger only the innate part of the immune system and thus allow focusing on this part. Immune response from acute DSS-induced inflammation is Th1-mediated with overexpression of pro-inflammatory cytokines such as TNF-α, IFNγ, IL-1β [22]. We use the latter as inflammatory markers in our *in vivo* studies with BDS-loaded NLCs. By not considering the disregulation of the adaptive immune system, DSS model allows us to have continuity and a correlation with our *in vitro* models Caco-2 and J774 models. Finally, the choice of this model was also driven by the numerous future possibilities that it allows us. Acute for most of the mice strains, DSS model can become chronic after repeated cycles of DSS for predisposed strains or spontaneously for C57Bl/6 strain mice [23]. Chronicity is an important characteristic of the human IBD-related inflammation. This chronic colitis model

can even become an inflammation-associated colorectal cancer if DSS is combined to genotoxic colon carcinogen azoxymethane. As colorectal cancer presented a high risk rate in IBD patients, this model may give useful data about the triggering of this complication.

III. PERSPECTIVES

III.1 BIOPHARMACEUTICS DRUGS

We have evaluated the topical delivery of biopharmaceutics using ovalbumin as a model drug. We used several nanocarriers and thus several delivery strategies. Anti-TNF-α Fab was successfully encapsulated in pH-sensitive stealth nanoparticles. The nanoformulations were physico-chemically characterized. Release studies in colonic simulated fluids should give us details about the stability of the formulations. By using fluorolabelled PLGA or Fab, *in vivo* localization studies should allow us to know the future of the nanoparticle and/or its content inside the colonic tissue. *In vivo* studies should be performed in a murine colitis model to assess the therapeutic activity of the active nano-scaled drug delivery system.

We should also use all the generated results to try to encapsulate other therapeutic biopharmaceutics of interest such as pro-inflammatory cytokine IL-10, anti-IL-17 antibody or anti-TNF-α siRNA or anti-NF-κB olgionucleotides. A preliminary study made with anti-TNF-α siRNA loaded TMC nanoparticles showed that they can get a size between 200 and 400 nm. Hence, in this case, as an intracellular delivery is needed for this compound and as immune-related cells are the most TNF-α secreting cells, active targeting may be an interesting approach. So an optimal drug delivery system for anti-TNF-α siRNA may be made with TMC-PEG-mannose or PLGA-PEG-mannose as polymers, resulting in a mix of delivery strategies. After the formulation process, these nanoformulations should be evaluated *in vitro* and *in vivo*.

III.2 COMBINATION OF DELIVERY STRATEGIES

We formulated several nanocarriers using delivery strategies one at the time. One idea might be the mix of several strategies in order to target the inflamed mucosa and to deliver to the site of inflammation. For instance, encapsulating nanocarriers in pH-sensitive microspheres should protect the structure of nanocarriers from the harsh conditions of the upper part of the gut [24]. As IBD colonic pH is variable, a combination of Eudragit polymers with different dissolution pH may provide better specificity of pH-dependent release profile. A mix of polymers also may result in a mix of delivery strategies. CC-loaded and anti-TNF-α Fab-loaded PLGA/EudragitS100 nanoparticles are good examples. As we proposed earlier with the topical delivery of anti-TNF-α siRNA, a combination of 2 delivery strategies, mucoadhesion and active targeting of immune related-cells, should be achieved by the graft of mannose on PEG-part of the PEGylated-TMC. Examples on the literature exist already.

KPV, an anti-inflammatory peptide was encapsulated in polylactic acid nanoparticles to achieve a sustained release. This formulation was thus incorporated into a colon targeting polysaccharide gel, consisting of a mix of chitosan and alginate [25].

IV. REFERENCES

[1] D. Burger, S. Travis, Conventional medical management of inflammatory bowel disease, Gastroenterology, 140 (2011) 1827-1837 e1822.
[2] R.A. Taylor, M.C. Leonard, Curcumin for inflammatory bowel disease: a review of human studies, Altern Med Rev, 16 (2011) 152-156.
[3] M. Garinot, V. Fievez, V. Pourcelle, F. Stoffelbach, A. des Rieux, L. Plapied, I. Theate, H. Freichels, C. Jerome, J. Marchand-Brynaert, Y.J. Schneider, V. Preat, PEGylated PLGA-based nanoparticles targeting M cells for oral vaccination, J Control Release, 120 (2007) 195-204.
[4] T.T. Jubeh, Y. Barenholz, A. Rubinstein, Differential adhesion of normal and inflamed rat colonic mucosa by charged liposomes, Pharm Res, 21 (2004) 447-453.
[5] B. Xiao, H. Laroui, S. Ayyadurai, E. Viennois, M.A. Charania, Y. Zhang, D. Merlin, Mannosylated bioreducible nanoparticle-mediated macrophage-specific TNF-alpha RNA interference for IBD therapy, Biomaterials, (2013).
[6] K. Hu, J. Li, Y. Shen, W. Lu, X. Gao, Q. Zhang, X. Jiang, Lactoferrin-conjugated PEG-PLA nanoparticles with improved brain delivery: in vitro and in vivo evaluations, J Control Release, 134 (2009) 55-61.
[7] K. Hu, Y. Shi, W. Jiang, J. Han, S. Huang, X. Jiang, Lactoferrin conjugated PEG-PLGA nanoparticles for brain delivery: Preparation, characterization and efficacy in Parkinson's disease, Int J Pharm, 415 (2011) 273-283.
[8] F. Danhier, V. Pourcelle, J. Marchand-Brynaert, C. Jerome, O. Feron, V. Preat, Targeting of tumor endothelium by RGD-grafted PLGA-nanoparticles, Methods Enzymol, 508 (2012) 157-175.
[9] F. Danhier, B. Ucakar, N. Magotteaux, M.E. Brewster, V. Preat, Active and passive tumor targeting of a novel poorly soluble cyclin dependent kinase inhibitor, JNJ-7706621, Int J Pharm, 392 (2010) 20-28.
[10] O.J. Kwon, E. Kang, J.W. Choi, S.W. Kim, C.O. Yun, Therapeutic targeting of chitosan-PEG-folate-complexed oncolytic adenovirus for active and systemic cancer gene therapy, J Control Release, 169 (2013) 257-265.
[11] T. Takagi, T. Arisawa, K. Yamamoto, I. Hirata, H. Nakano, M. Sawada, Identification of ligands binding specifically to inflammatory intestinal mucosa using phage display, Clin Exp Pharmacol Physiol, 34 (2007) 286-289.
[12] B. Khor, A. Gardet, R.J. Xavier, Genetics and pathogenesis of inflammatory bowel disease, Nature, 474 (2011) 307-317.
[13] F. Leonard, E.M. Collnot, C.M. Lehr, A three-dimensional coculture of enterocytes, monocytes and dendritic cells to model inflamed intestinal mucosa in vitro, Mol Pharm, 7 (2010) 2103-2119.
[14] J. Van De Walle, A. Hendrickx, B. Romier, Y. Larondelle, Y.J. Schneider, Inflammatory parameters in Caco-2 cells: effect of stimuli nature, concentration, combination and cell differentiation, Toxicol In Vitro, 24 (2010) 1441-1449.
[15] J.G. Hyun, L. Mayer, Mechanisms underlying inflammatory bowel disease, Drug Discovery Today: Disease Mechanisms, 3 (2006) 457-462.
[16] R. Al-Sadi, M. Boivin, T. Ma, Mechanism of cytokine modulation of epithelial tight junction barrier, Front Biosci, 14 (2009) 2765-2778.
[17] M.L. Clapper, H.S. Cooper, W.C. Chang, Dextran sulfate sodium-induced colitis-associated neoplasia: a promising model for the development of chemopreventive interventions, Acta Pharmacol Sin, 28 (2007) 1450-1459.
[18] M. Perse, A. Cerar, Dextran sodium sulphate colitis mouse model: traps and tricks, J Biomed Biotechnol, 2012 (2012) 718617.
[19] R. Ito, M. Kita, M. Shin-Ya, T. Kishida, A. Urano, R. Takada, J. Sakagami, J. Imanishi, Y. Iwakura, T. Okanoue, T. Yoshikawa, K. Kataoka, O. Mazda, Involvement of IL-17A in the pathogenesis of DSS-induced colitis in mice, Biochem Biophys Res Commun, 377 (2008) 12-16.

[20] J.L. Mendoza, M.T. Abreu, Biological markers in inflammatory bowel disease: practical consideration for clinicians, Gastroenterol Clin Biol, 33 Suppl 3 (2009) S158-173.
[21] S. Wirtz, M.F. Neurath, Mouse models of inflammatory bowel disease, Adv Drug Deliv Rev, 59 (2007) 1073-1083.
[22] G. Dothel, V. Vasina, G. Barbara, F. De Ponti, Animal models of chemically induced intestinal inflammation: Predictivity and ethical issues, Pharmacol Ther, (2013).
[23] S. Melgar, A. Karlsson, E. Michaelsson, Acute colitis induced by dextran sulfate sodium progresses to chronicity in C57BL/6 but not in BALB/c mice: correlation between symptoms and inflammation, Am J Physiol Gastrointest Liver Physiol, 288 (2005) G1328-1338.
[24] D. Kietzmann, B. Moulari, A. Beduneau, Y. Pellequer, A. Lamprecht, Colonic delivery of carboxyfluorescein by pH-sensitive microspheres in experimental colitis, Eur J Pharm Biopharm, 76 (2010) 290-295.
[25] H. Laroui, G. Dalmasso, H.T. Nguyen, Y. Yan, S.V. Sitaraman, D. Merlin, Drug-loaded nanoparticles targeted to the colon with polysaccharide hydrogel reduce colitis in a mouse model, Gastroenterology, 138 (2010) 843-853 e841-842.